DIARYLIODONIUM SALTS AS PRECURSORS TO ELECTRON-RICH [^{18}F]FLUOROARENES FOR USE IN THE MEDICAL IMAGING TECHNIQUE – POSITRON EMISSION TOMOGRAPHY

SATWINDER SINGH BHATT

Submitted in fulfilment of the requirements for the degree of Doctor of Philosophy.

Sir Bobby Robson Foundation PET Tracer Production Unit,
School of Chemistry, Newcastle University

January 2016

Contents

Acknowledgements

First and foremost I would like to thank the School of Chemistry at Newcastle University and EPSRC for funding this research project, as well as the Sir Bobby Robson Foundation for providing the radiochemistry facility and its equipment, which allowed me to work in this inspiring research area.

I would like to thank my supervisor Dr Michael A. Carroll for his continued guidance and counsel throughout this project. Similarly, I would like to thank my co-workers within the research group who provided me with both unrelenting support as well as endless comedy - an invaluable combination when handling a host of temperamental equipment and apathetic undergraduate project students.

I am also hugely appreciative of the academic, technical and administrative staff within the department, as well as the other doctoral students that have provided their support and assistance throughout my time at Newcastle University. I would also like to credit Prof. William McFarlane and Dr Corinne Y. Wills for their assistance with NMR spectroscopy, Dr Ross Harrington and Dr Ulrich Baisch for their help with x-ray crystallography, the EPSRC Mass Spectrometry Service in Swansea and Dr Stephen Boyer for elemental microanalysis. In addition, I would like to thank Dr Kerry Elgie and Asynt Ltd for providing their ReactoMate batch reactor system, as well as Dr Lindsay Fowler and Dr Christophe Lucatelli at the Clinical Research Imaging Centre, Edinburgh for the their contribution to [^{18}F]fluorination work on their GE TRACERlab FX FN system.

I would also like to thank my friends at QuantuMDx for their encouragement during my writing up period, as starting a new role in a dissimilar area of research whilst completing another is never an easy task. I have nothing but gratitude for Newcastle itself, for playing host to my life for the years of my PhD study, as well as before and after, without its numerous waterholes I would have fell foul to thirst a long time ago.

Finally I would like to thank my family and friends, far and near for their relentless love and support, in particular my mother for never doubting my capability and for supporting me every step of the way.

List of Abbreviations

AcOH	Acetic acid
Bq	Becquerel
^{13}C NMR	Carbon-13 NMR
°C	Degrees Celsius
Ci	Curie
d_3-MeCN	Deuterated acetonitrile
d_4-MeOH	Deuterated methanol
d_6-DMSO	Deuterated dimethylsulfoxide
d_7-DMF	Deuterated *N,N*-dimethylformamide
d	Doublet
decomp.	decomposition
DCM	Dichloromethane
DIPEA	*N,N*-Diisopropylethylamine
DMF	Dimethylformamide
DMTr	Dimethoxytrityl
dd	Double doublet
EIMS	Electron ionisation mass spectrometry
EMA	European Medicines Agency
Equiv.	Equivalents
Et	Ethyl
eV	Electron volt
FDA	Food and Drug Administration
[^{18}F]FDG	[^{18}F]2-deoxy-2-fluoro-D-glucose

FTIR	Fourier Transform Infra-Red
g	Grams
GC-MS	Gas chromatography mass spectrometry
GE	General Electric (Company)
h	Hours
HR-MS	High resolution Mass Spectrometry
Hz	Hertz
ID	Internal diameter
IR	Infra-Red
J	Coupling constant measured in Hz
K_{222}	K·4,7,13,16,21,24-hexaoxa-1,10 diazabicyclo[8.8.8]hexacosane
LDA	Lithium diisopropylamine
M	Molar
M+	Molecular ion peak
$[M+H^+]$	Molecular ion peak plus a proton
m	Multiplet
Me	Methyl
MeCN	Acetonitrile
mCPBA	*meta*-Chloroperoxybenzoic acid
min	Minute(s)
mL	Millilitre
mmol	Millimole
mp	Melting Point
m/z	Mass/Charge ratio
NMR	Nuclear magnetic resonance

NOESY	Nuclear Overhauser effect spectroscopy
NSAID	Nonsteroidal anti-inflammatory drug
Nu	Nucleophile
OAc	Acetate
OTf	Trifluoromethane sulfonate (triflate)
OTFA	Trifluoroacetate
OTs	*para*-tolylsulfonate (tosylate)
p	Pentet
Ph	Phenyl
ppm	Parts per million
q	Quartet
QC	Quality control
R&D	Research and development
Rb	Round bottom
RCY	Radiochemical yield
R_f	Retention factor
R_t	Retention time
RT	Room temperature
Rxn/RXN	Reaction
s	Singlet
SI unit	International System of Units
S_NAr	Nucleophilic aromatic substitution
SPE	Solid phase extraction
Sx	Sextet
t	Triplet

TFE	2,2,2-Trifluoroethanol
THF	Tetrahydrofuran
TLC	Thin Layer Chromatography
UV	Ultra-violate
w/v	Weight divided by volume
w/w	Weight divided by weight

1 Introduction

Non-invasive medical imaging has played a pivotal role in the diagnosis of disease, as well as the development of new drugs and treatments for decades. Techniques such as magnetic resonance imaging (MRI), ultrasound, computed tomography (CT) and X-ray typically provide detailed structural informational, exceptionally useful for the rapid diagnosis of many conditions in the clinical environment.[1,2,3] However, information regarding metabolic events and biological processes is much better achieved through the application of specific imaging probes. Imaging probes bearing positron (β^+) emitting radiolabels are proving to have increasingly essential roles in medical imaging, both for clinical and research applications; and are utilised in the techniques known as Positron Emission Tomography (PET) and Single Photon Emission Computed Tomography (SPECT).[4,5]

The uptake of PET into the medical world was initially relatively slow, largely due to the lack of cyclotrons to generate the required radioisotopes and the low number of facilities with the associated scanning capability, as well as the intrinsically high cost associated with the technology. However, growing clinical interest and developments in technology in PET have seen a substantial increase in the use of this imaging technique for clinical roles and a large number of pre-clinical studies.[6] The array of commercially available PET imaging agents is rapidly increasing, delivering more disease specific imaging probes; and the nationwide demand multi-modality imaging platforms such as PET-computed tomography (PET-CT) is also on the rise. Both factors are fuelling an ever increasing requirement for further research in PET chemistry and PET-healthcare integration.[7]

1.1 Positron Emission Tomography

PET is a non-invasive imaging technique that utilises *in vivo* emission of positrons (anti-electrons) from neutron-deficient (or proton-rich) radionuclides that have been used to label tracers, drugs or metabolic probes. Thus biochemical changes and

interactions can be mapped in real-time to deliver information on the pharmacokinetic profile of a radiolabelled species across a full body scan, thanks to the essentially unlimited depth of penetration offered by PET. Such information can be used to scope the metabolic pathway of an experimental drug; the severity of tumour metastasis in a patient suffering from cancer or the neurodegenerative effects of Alzheimer's disease to mention but a few.

PET can be characterised as a molecular imaging technique in that it is capable of targeting specific tissue or cell types using target-specific molecular probes. Although other modalities such as MRI, CT and ultrasound can be used for molecular imaging, they are markedly less sensitive, with their relative contrast agents being in the chemical concentration range of μM to nM. Whereas PET and SPECT are able to detect radiolabelled materials at the pM to nM level, giving them a distinctive detection advantage.[8]

The first use of positron-emitting isotope labelled imaging agents for medical applications was as early as 1951,[9,10] whilst the first human studies were undertaken in 1974.[11] However, it wasn't until 2000 that the integration of PET with computed tomography (CT) allowed for mainstream use of the imaging techniques, thanks to the inclusion of the structural detail offered by CT. Continued advancements in the field are on-ongoing and continue to drive PET imaging into new applications of medical imaging and drug bio-distribution understanding.

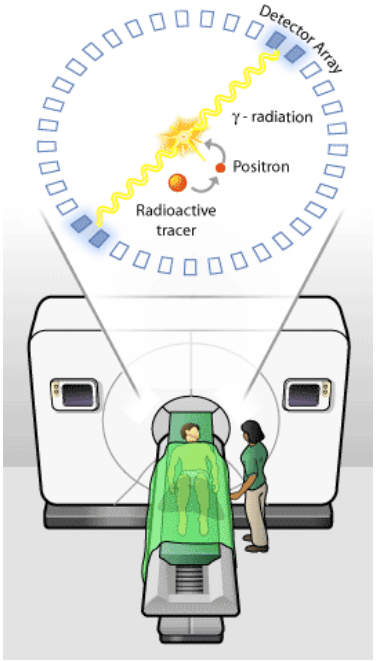

Figure 1: A graphic depicting the positron emission and subsequent annihilation event that occurs inside of a patient during a PET scan having been injected with an imaging agent bearing a PET radionuclide.[12]

The sequence of events that are responsible for the PET imaging process are summarised in the above representation (Figure 1). The patient is administered with the appropriate radiolabeled imaging agent (followed by a period of rest, typically 30–60 min for [^{18}F]FDG, allowing the imaging agent to localise at its target region) before the patient is moved into the scanner. As the radioisotope decays it emits positrons, which travel a short distance (1–2 mm) before encountering an electron, resulting in a matter–antimatter annihilation event.[13] This collision event results in the release of energy in the form of two gamma rays (or photons) of 511 keV in energy, proportional to the total mass of the electron and positron, in agreement with the mass–energy equivalence equation, $E = mc^2$. Crucially, these gamma rays are projected from the annihilation event simultaneously and at 180° to one another, allowing the PET scanner's computer to back-calculate where that annihilation event occurred and hence where the PET imaging agent is situated (within a small area of uncertainty), which results in the production of a PET image like that shown below (Figure 2).

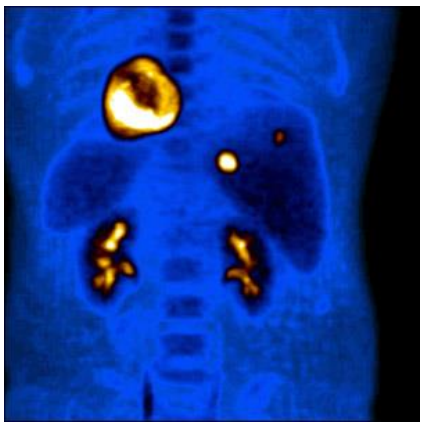

Figure 2: PET image showing colorectal cancer metastasis to the liver using [^{18}F]fluorodeoxyglucose (FDG). The heart and kidneys display normal high uptake of FDG, whereas the two foci of increased FDG uptake situated in the liver indicate tumorous lesions.[14]

PET imaging is reliant on the innate instability of proton-rich (or concurrently neutron-deficient) radioisotopes that decay by emitting positrons to regain nuclear stability. This process, termed as nuclear transmutation, involves the conversion of a proton into neutron whilst emitting a positron (β^+) and an electron neutrino (v_e); and is conventionally represented as:

$$\mathbf{p \ \ddagger \ n + v_e + \beta^+}$$

proton ‡ neutron + neutrino + positron

Where the overall nuclear transformation can be signified by:

$$^{A}_{Z}X_{N} \ \rightarrow \ ^{A}_{Z-1}X_{N+1}$$

Thus for commonly used PET radioisotopes such as carbon-11, oxygen-15 and fluorine-18, the following decay products are observed:

$$^{11}_{6}C_{5} \ \rightarrow \ ^{11}_{5}B_{6} \qquad ^{15}_{8}O_{7} \ \rightarrow \ ^{15}_{7}N_{8} \qquad ^{18}_{9}F_{9} \ \rightarrow \ ^{18}_{8}O_{10}$$

Although the mechanism of positron emission goes beyond the scope of this work, the process essentially involves a 'flavour' change of elemental particles known as quarks, whereby an 'up quark' is converted into a 'down quark', changing the physical make-up of the proton to yield a neutron.[15] However, there is an alternative route to stability available to proton-rich radionuclides, which is similarly isobaric in nature, known as electron–capture. Here, the proton-rich nuclide absorbs an inner shell electron, thus converting a proton into a neutron. This process occurs with

radioisotopes with insufficient energy to decay by positron emission and acts as a competing decay mode for heavier positron-emitting radioisotopes, as discussed further in Section 1.2. Unlike positron-emission, electron capture does not produce gamma rays and therefore cannot be detected by a PET scanner.[16]

Ultimately, the performance of a PET scanner or gamma camera is ruled by the properties of the detector array, which are composed of scintillating materials. Despite substantial research in the area of scintillators, only a handful materials have found their way into widespread use amongst PET imaging platforms, namely thallium-doped sodium iodide (NaI(Tl)), bismuth germinate (BGO) and cerium-doped or yttrium-doped lutetium oxyorthosilicate (L(Ce)SO and L(Y)SO).[17] Although scintillation materials have been developed as organic materials, liquids and even plastics; inorganic crystals such as the above are far more appropriate for PET, as their higher density allows for maximised photon capture and thereby improved detection efficiency. The key characteristic of a scintillating material is its ability to absorb ionising radiation and convert a small portion of that energy into a pulse of visible or UV light, within a very short amount of time (ns - μs) allowing a rapid return to the group state.[18]

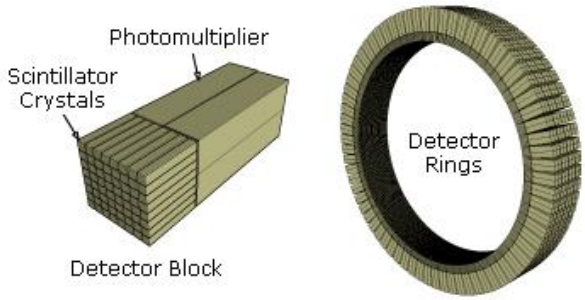

Figure 3: Simplified representation of a PET scanner detection ring and blocks comprised of scintillating crystals and photomultiplier tubes (PMTs)[19]

With the development of scintillation materials being a key starting point in producing the PET scanners of tomorrow, much focus is aimed towards producing scintillation crystals with higher γ-ray detection efficiencies, which results in reduced scan times and lower necessary dose to the patient.[20] Start-of-the-art PET scanners

usually employ LYSO based scintillators because of they offer increased γ-ray detection efficiency *versus* more traditional systems, as well as other related advantages including the possession of high scintillation light output, rapid decay time and practical considerations such as having a low hygroscopicity.[21] The further development of these faster and brighter scintillators has paved the way for new PET technologies with improved correction methods and superior resolution, with time-of-flight PET (TOF-PET) being a very successful example of such a technology.[22] TOF-PET utilises these high-speed detectors to capitalise on the minuscule time-of-flight difference of the generated gamma rays, allowing more accurate localisation of the positron-electron annihilation.[23]

After scintillation technology, the next area of continuing development in the PET image acquisition chain is the development of photomultipliers tubes (PMTs), which allow for the conversion of the photonic energy (produced by the scintillation array) into electrical pulses; a digital format more suitable for computed processing.[24] PMTs consist of an evacuated enclosure with a thin photo-cathode window, which release photo-electrons when exposed to a scintillation photon, which are in turn accelerated through the chamber towards a dynode in the presence of an applied electric field and the resulting collision emits secondary electrons. This acceleration-emission process is repeated multiple times, hence amplifying the effect of the original scintillation photon into a more easily detectable and more quantifiable electrical signal.

Traditional PET imaging relies on the above described analogue-type photomultiplier approach, however, more developed PET scanners employ the use of silicon solid-state photomultipliers such as avalanche photodiode detectors (APDs); the inclusion of which also has also aided the integration of PET into MR systems for PET/MRI scanners.[25,26] These semiconductor detectors exploit the photoelectric effect to convert light into electricity and are not only insensitive to magnetic fields but are also highly sensitive, more compact, relatively cheap and provide better timing properties than traditional means.[27] In essence, APDs operate by impact ionisation, whereby the release of electrons when the semiconductor material is struck with incoming photons results in the release of more electrons; they are then accelerated through the chamber with the application of an external reverse voltage, producing the so-called avalanche effect. Eventually the multiplied electrons will reach the

anode and result in an amplified electrical signal, however, this technology relies on a sequence of photons and electrons reaching target detectors the majority of the time to produce a true representation of the PET imaging result, although in practise such complete detection cannot be guaranteed.

In a PET scanner most gamma rays will not be detected by the array of detectors, but some will remain in the plane of the detection ring and two scintillating detectors will be hit. On photon impact each detector produces a timed electrical pulse, which are then combined in coincidence circuitry. If pulses are detected within a very short timeframe they are considered to be coincident, as depicted in the below diagram (Figure 4).[28]

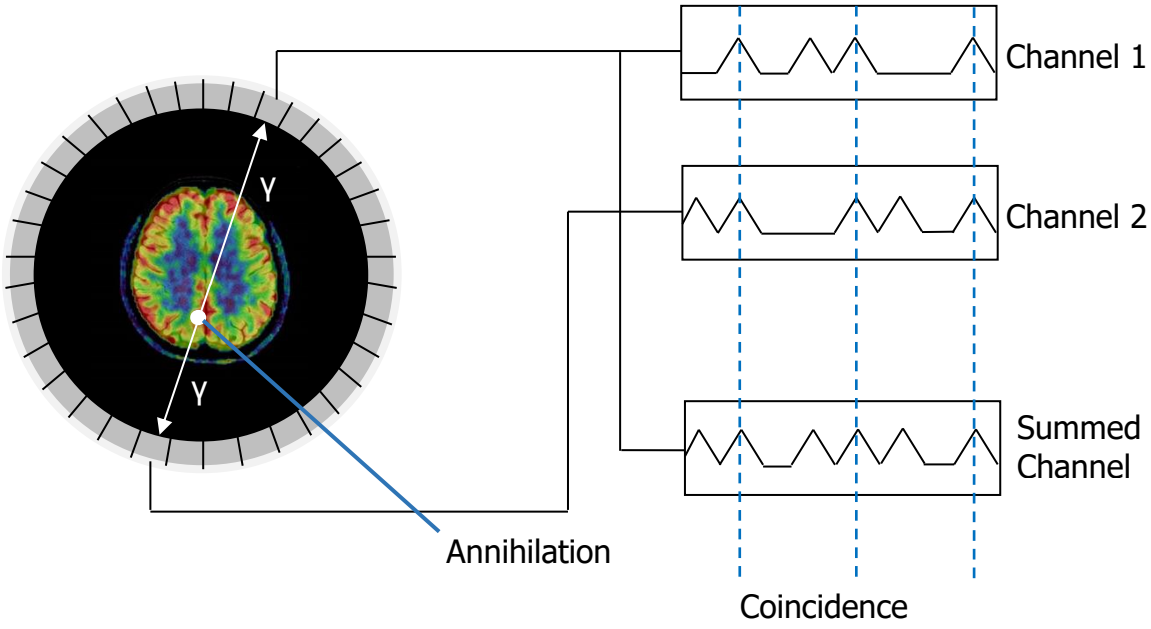

Figure 4: Coincidence detection in a PET scanner, PET image adapted from http://www3.gehealthcare.com/en/products/categories/magnetic_resonance_imaging/optima_mr360_advance

Each coincidence event is assigned a line of response (LOR), which provides the positional detail of the annihilation event by electronic collimation (without the need for physical collimation). The basis of PET relies on these coincidence events, which indicate that an annihilation event occurred at some point between the two detectors; this is referred to as a line of response (LOR).[29] The number of gamma rays that hit the PET scanner's detection array that successfully produce "true" LORs

is proportional to the resolution and quality of the PET image, making this a particularly important feature of PET imaging.

There are two key phenomena that can hinder or falsify the acquisition of the LOR, Compton scattering and photoelectric absorption; both of which are consequences of the interactions of PET photons and matter. Attenuation is a direct consequence of Compton scattering, whereby the flight path of a photon emitted by the annihilation event is altered when it collides with an electron in the outer shell of a nearby atom.[30] This results in loss of energy and crucially can cause the photon to be redirected, away from the PET scanner's detection array and is therefore not accounted for. It is seen that an increase in patient body mass will amplify this effect, meaning that for larger, more rotund subjects, attenuation increases as a result of increased Compton scattering, reducing the number of LORs and ultimately a poorer PET image.[31]

Photoelectric absorption sees the uptake of an emitted gamma photon by an atom with resulting ejection of an electron, an effect that increases with the increase of materials with high atomic number and density.[32] Again this loss of a photon's detection not only reduces the number of LORs and thereby attenuation, but also means the non-absorbed opposing photon contributes to background activity, reducing the signal to noise ratio (SNR). Given the electron-discharging nature of this occurrence, photoelectric absorption also has a considerable detrimental effect on PET-CT but can be corrected.[33] These effects can contribute to a number of commonly occurring coincidence events that can detract from true LORs, as shown in Figure 5.

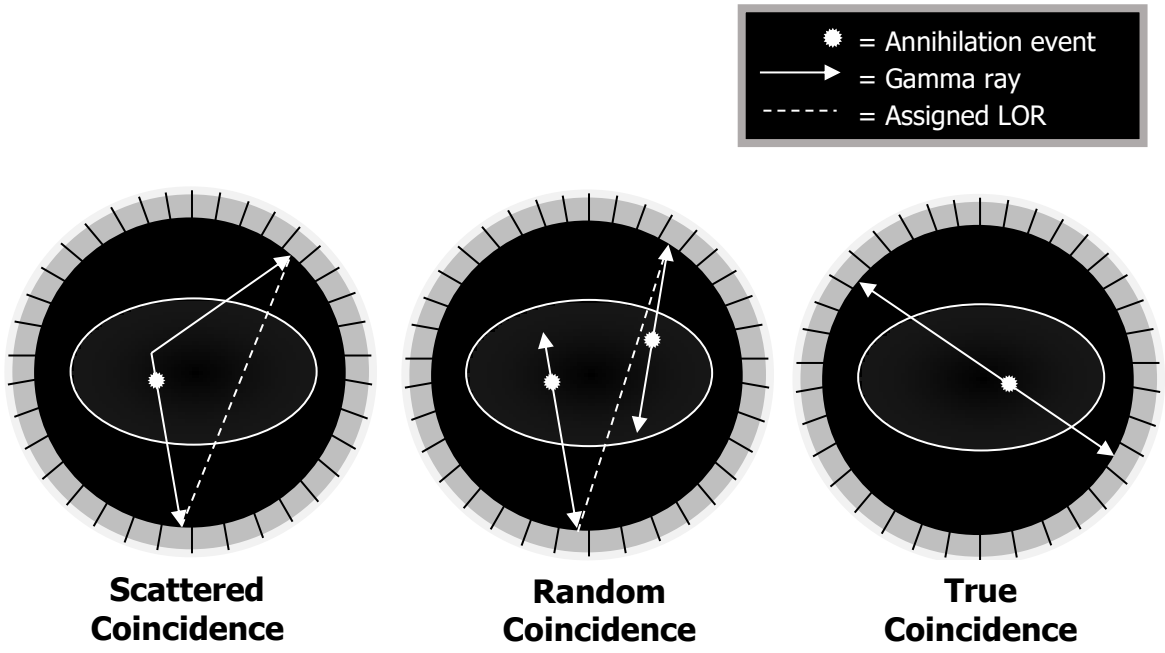

Figure 5: Types of potential coincidence from PET annihilation events

In essence, scattered and random coincidence events are results of two unpaired γ photons reaching the detector array within the coincidence timing window, a problem that is reduced as technology develops and the coincidence timing window is reduced.

1.2 Radioisotopes in PET Imaging

There are a number of commonly and less commonly exploited positron-emitting radioisotopes available for use in PET imaging (Table 1).[34] Also termed as radionuclides, each of these radioisotopes have their own associated biological activity and physical characteristics; and thereby advantages and disadvantages in their utility in PET. Although there are exceptions, typically the lighter radionuclides present reduced half-lives, are more frequently seen within biological molecules and decay by largely positron-emission; whereas the heavier PET radiolabels decay by a higher proportion of electron capture, have longer half-lives and can inconveniently yield radioactive decay products.

Radionuclide	$t_{1/2}$	Positron E_{MAX} (MeV)	Decay product	% Decay by β^+ emission	Production method
Carbon-11	20.4 min	0.959	Boron-11	100	Cyclotron
Nitrogen-13	9.97 min	1.190	Carbon-13	100	Cyclotron
Oxygen-15	2.04 min	1.732	Nitrogen-15	100	Cyclotron
Fluorine-18	109.7 min	0.634	Oxygen-18	97	Cyclotron
Copper-62	9.76 min	2.91	Zinc-62	98	Generator
Copper-64	12.8 h	0.656	Nickel-64	19	Cyclotron
Gallium-68	67.6 min	1.899	Zinc-68	89	Generator
Bromine-75	98 min	1.74	Selenium-75	76	Cyclotron
Rubidium-81	4.57 h	0.335	Krypton-81	96	Generator
Yttrium-86	17.7 h	3.15	Strontium-86	34	Cyclotron
Technetium-94m	53 min	2.47	Molybdenum-94	72	Cyclotron
Zirconium-89	78.41 h	0.897	yttrium-89	22	Cyclotron
Iodine-124	4.18 days	0.603	Tellurium-124	23	Cyclotron

Table 1: Some radionuclides utilised in PET with their corresponding production and decay characteristics[31]

A number of factors greatly influence the choice of positron-emitting isotope when targeting a specific PET imaging role; as preparation, lifetime, resolution, positron-energy, toxicity, safety and cost can vary hugely from one radionuclide to another and also have a monumental impact on the resulting PET image and the patient. Initially, the convenience of availability is integral to a radionuclides use and there are two major routes to radionuclides, cyclotron production and generator formulation. The former, used to prepare the more commonly used radionuclides ^{15}O, ^{13}N, ^{11}C and ^{18}F, involves the bombardment of a parent nuclide with high energy

charged species within a particle accelerator, yielding the daughter positron-emitting radionuclide. Alternatively, positron-emitting radionuclides can be obtained from a long-lived parent radioisotope as it readily decays to its daughter PET isotope, which are typically separated from one another *via* chromatographic methods making use of a mobile phase that allows for rapid elution of the metal-radionuclide as a ready-to-use reagent; the most commonly seen being copper-62 as [^{62}Cu]pyruvaldehyde-bis(*N*-4-methylthiosemicarbazone) (PTSM)[35] and Gallium-68 as [^{68}Ga]ethylene-diaminetetraacetic-acid ([^{68}Ga]EDTA) or [^{68}Ga]$GaCl_3$.[36]

The selection of generator-produced radionuclides is inherently based around their convenience, both in the application of such systems, but also in the labelling-chemistry of the resultant metal-radionuclide. *Versus* the expense of cyclotron acquisition, installation and service, the adoption of a bench-top generator system is drastically lower in cost and far simpler. Generators offer a continuous supply of radio-metals with practical half-lives, which can often be conveniently incorporated into imaging agents *via* chelating groups, making for a high yielding and rapid radiolabelling process. However, the integration of such a large radiolabel and obligatory chelator in to a small molecule imaging agent target can alter the pharmacokinetics of the imaging agent *versus* the unlabelled species, potentially reducing its bioavailability in the necessary location. However, in the case of biomacromolecule labelling this is less of a concern.

The alternative, cyclotron production of radionuclides, allows for the preparation of more biochemical compatible radionuclides, in particular ^{11}C and ^{18}F, which can be incorporated into small molecule imaging agents without a detrimental effect on the compound's biophysical properties. Although traditionally the associated costs of cyclotron produced radiolabels were a significant barrier to their application, recent development has been driven towards more cost- and space-effective solutions, allowing for economical dose-on-demand production of imaging agents, typically on-site or very near to a PET imaging centre.[37,38]

The half-life of a radionuclide is also a tremendously important feature to be considered. The majority of biological processes would be extremely difficult to imagine with very short-lived radionuclides like oxygen-15 or nitrogen-13, given the time required to produce, purify, formulate, transport and finally administer an imaging agent; although there are some circumstances where these are useful, such

as the use of oxygen-15 in cerebral blood flow imaging.[39] On the other hand, an imaging agent with an overly long half-life, for example iodine-124 ($t^{½}$ = 4.18 days) could result in the patient receiving a needlessly high radiation dose, that could be avoided by using a radiolabel with an intermediary half-life, such as ^{18}F or ^{68}Ga. Some prior understanding of the radioligand/radiotracer's biological route is required to forecast the PET scan timing and selection of radionuclide*, i.e.* sufficient time for the radionuclide to be produced, incorporated into a precursor molecule, administered and to bio accumulate in the desired location is necessary. Although all PET appropriate radionuclides decay by emitting positrons to produce gamma rays, there are distinct differences in the energy of that emitted positron which greatly influences the quality of the resulting PET image, as shown in Table 1. Ideally, the positron emitted should be of the lowest energy so that the resulting annihilation event is as close as possible to the imaging agent. Again, here ^{18}F makes for a very practical choice since it possesses one of the lowest position energies.[40]

In addition, fluorine-18 offers a decay mode that is largely positron-emission over alternative decay modes, whereas other radioisotopes such as ^{94m}Te, may decay by mixed decay modes, presenting needless additional radiation dosage to the patient, as well as an inefficient decay process. Another key consideration is the nature of the daughter nuclide, which can be toxic or radioactive (*e.g.* ^{75}Se) for some PET radionuclides, whilst ^{18}F produces an idyllic decay product in ^{18}O.

These points make ^{18}F an ideal candidate for the imaging of many biological processes and radiopharmaceuticals, providing a radioactive tag compatible with complex multi-step syntheses, whilst achieving high resolution with acceptably safe decay characteristics.

1.3 Fluorine in Pharmaceuticals

Although fluorine is the most abundant halogen found in the Earth's crust, its natural incorporation into organic molecules is surprisingly rare, with only 13 naturally occurring organo-fluorine compounds known to date, *versus* over 3000 natural products containing chlorine, bromine and/or iodine.[41] However, the occurrence of fluorine-containing compounds within the world of pharmaceuticals is far more

common.[42,43] Developed as early 1950s, 9α-fluorohydrocortisone – a synthetic mineralocorticoid with anti-inflammatory activity; and 5-fluorouracil – a potent thymidylate synthase inhibitor used in cancer treatment (Figure 6) represent two historically successful fluorine-bearing compounds, recognised as having innate qualities provided by the inclusion of fluorine.

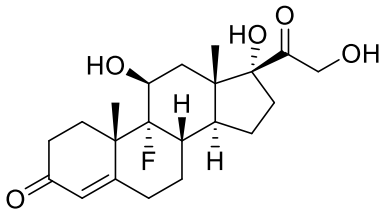

9-fluorohydrocortisone

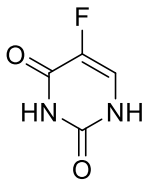

5-fluorouracil

Figure 6: Examples of fluorine containing pharmaceuticals

The success of such fluorine-containing drugs has driven research on the incorporation of fluorine into medicinal chemistry targets ever since, making the synthesis of fluoro-derivatives standard practice. With the incorporation of fluorine considered such a substantial driver for success, it's unsurprising that a considerable proportion (~20%) of new pharmaceuticals released, contain the element and can prove to be very profitable targets.[44,45,46] Examples of particularly high earning fluorine-contain drugs include Ciprofloxacin (Bayer AG) – a second generation fluoroquinolone;[47] Fluoxetine – the antidepressant more commonly known as Prozac[48]; Rosuvastatin (AstraZeneca/Shionogi) – for the treatment of high cholesterol;[49] and Celecoxib (Pfizer) – a COX-2 selective NSAID used to treat arthritis-related conditions;[50] as shown below in Figure 7.

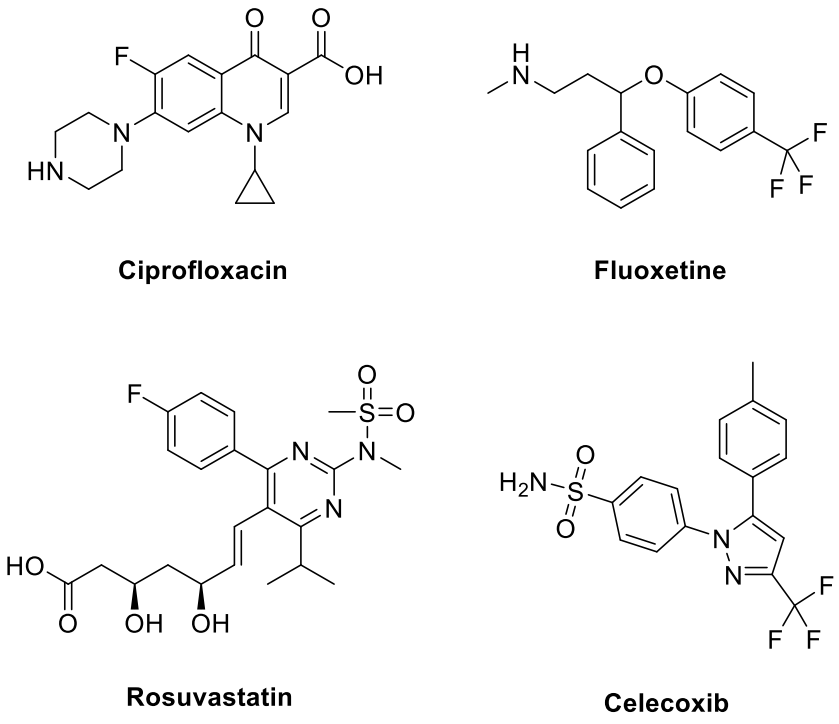

Figure 7: Some top-selling fluorine-containing drugs

Such drugs owe their much of their success to the native properties of fluorine and the distinctive interactions it creates *in vivo*. Firstly, the relatively strong bond it forms with carbon, particularly when installed on an aromatic ring, greatly reduces the risk of C-F cleavage during metabolism.[51] This C-H to C-F substitution, can prevent hydroxylation of the would-be C-H group, a common pathway in metabolism. This is known as the 'blocking effect' and is used to strategically improve the bioactive longevity of a molecule, an effect accounted for by the distinct difference in bond dissociation energy of H_3C-H (103.1 kcal/mol) *versus* H_3C-F (108.1 kcal/mol).[52] The incorporation of fluorine to reduce metabolic oxidation is a commonly used strategy, one such example includes work by Kath and co-workers,[53] whereby the addition of fluorine greatly improves the potency and metabolic stability of the CCR1 (CC-chemokine-1) antagonist drug candidate, (for the treatment of autoimmune diseases and organ transplant rejection), by hindering aliphatic metabolism at the positions shown in Scheme 1.

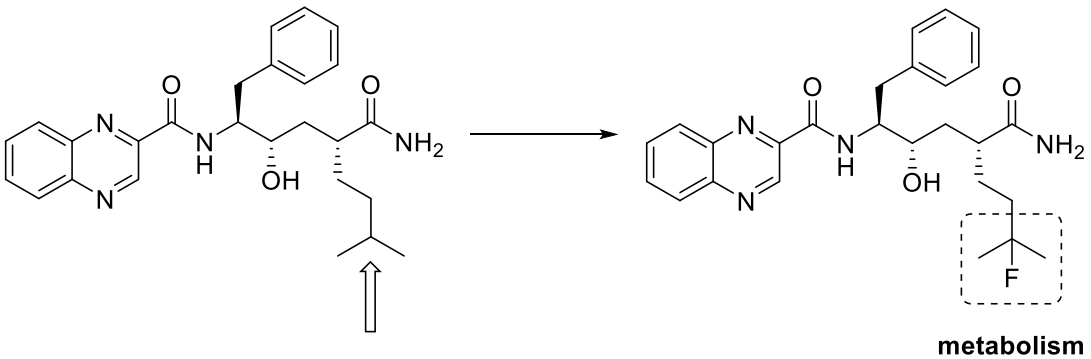

HLM Clint (mL/min/kg) = 202
CCL3 binding IC_{50} = 28 nM

HLM Clint (mL/min/kg) = 8
CCL3 binding IC_{50} = 9 nM

Scheme 1: The potency and stability benefits of fluorine when substituted for hydrogen in a metabolism critical position

The metabolic oxidation of aromatics can also be hindered with the introduction of fluorine in a critical position. The scheme below demonstrates how aromatics can be readily oxidised during metabolism with cytochrome P450, whilst the appropriate fluorine substitution can reduce intermediate carbocation stability *via* a lack of resonance stabilisation and by inductive withdrawal of electron density.[54]

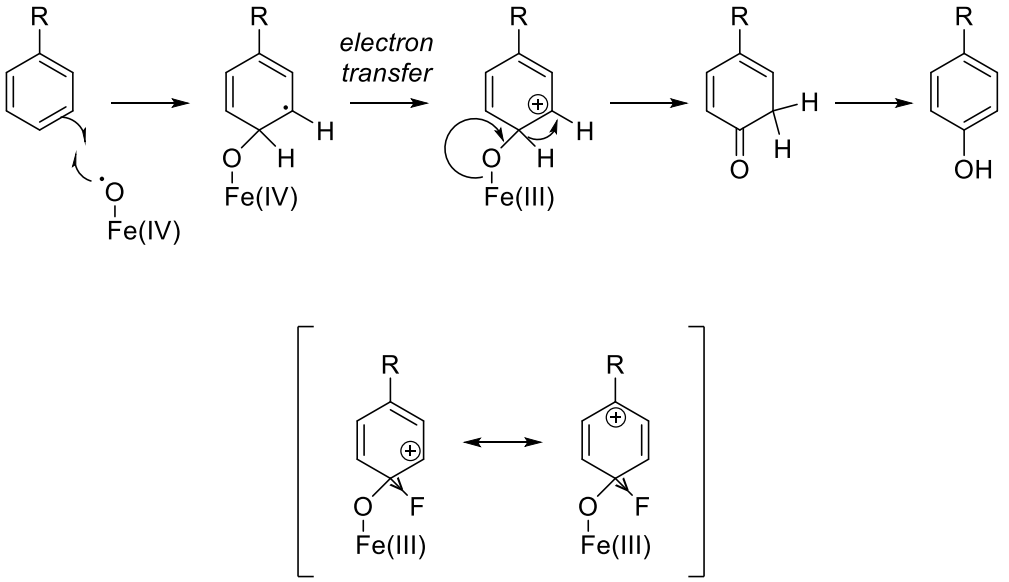

Scheme 2: Reduced carbocation stability during metabolic oxidation as a result of fluorination of an aromatic. Mechanistic pathway for radical oxidation of an aromatic group (top) and the destabilisation effect of fluorine incorporation on an aromatic group as a result of less resonance stability (bottom)

Furthermore, the C-F functionality acts as a mimic or bioisostere for C-H and C-OH, often unrecognised by microorganisms or enzymes, thanks to similarities in Van der Waals radii (1.17 Å and 1.41 Å for H and F respectively) and bond lengths (1.41 Å and 1.43 Å for C-F and C-O respectively), hence making such substitutions well tolerated.[55,56] The addition of even a single fluorine atom onto a drug candidate also substantially enhances the molecule's lipophilicity, determined by the molecule's logD value, although this is somewhat of a generalisation,[57] this feature often gives fluorinated compounds a heightened ability to penetrate cell membranes. Aromatics bearing fluorine noticeably increase the lipophilicity of a molecule as a result of the effective orbital overlap between fluorine 2s / 2p orbitals and the equivalent orbitals on carbon, which makes said C-F bond non-polarisable and thus contributes to the lipophilicity of the molecule.[58] In the event of C-F bond cleavage, the resulting fluoride released is considered relatively non-toxic, particularly at the exceptionally low concentrations administered for PET imaging.

The electronegative nature of fluorine (Pauling scale = 3.98)[59] and its resulting large inductive electron-withdrawing effect can have a considerable effect on the pKa of a drug and thereby effect its physio-chemical properties. This pKa reducing effect of fluorine is particularly noticeable on the addition of multiple fluorine atoms; for example acetic acid, monofluoroacetic acid, difluoroacetic acid and trifluoroacetic acid hold decreasing pKa values of 4.76, 2.59, 1.34 and 0.23 respectively. This increased acidity often produces a knock-on-effect on the bioavailability of a drug as well as its binding affinity for the target receptor, making the addition of fluorine(s) an integral consideration when predicting the desired structure-activity relationship of a drug candidate. The resulting change in pKa, alongside the steric effects of an additional CF_3 group and/or electrostatic effects of an added C-F bond dipole can also substantially influence the bioactivity of a fluorinated drug by affecting its orientation when entering binding sites.[60]

Although generally the inclusion of fluorine increases the lipophilicity of a molecule, the water solubility of a drug can sometimes be subtly tuned by the substitution of fluorine over other halogens, whilst maintaining the very good activity that is associated with halo-derivatives. One example of such a substitution includes Pfizer's development of fluconazole (shown below in Scheme 3), which derived from early anti-fungal azoles including ketoconazole.[61] Here the increased inductively

withdrawing nature of fluorine over chlorine improves the H-donor capability of the neighbouring hydroxyl functionality, hence improving the molecule's water solubility.

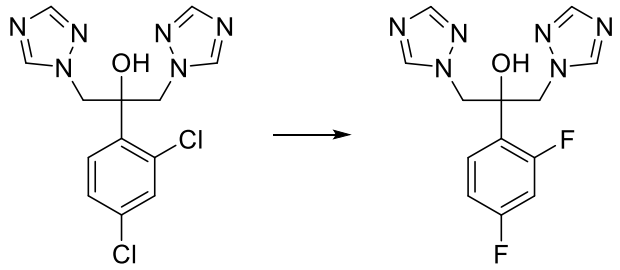

UK-47,265
insoluble in water

Fluconazole
Solubility = 8 mg/mL
in water at room temperature

Scheme 3: UK-47,265 and Fluconazole, two halo-triazole derivatives of ketoconazole with potent activity against systemic fungal infections, but with significantly different water solubility

1.4 PET Imaging with Fluorine-18

With the aforementioned physical and chemical properties that fluorine possess, and the radiochemical characteristics of fluorine-18 described in Section 1.3, the popularity of the radionuclides use in PET is easily conceivable. Whilst the development of novel ^{18}F-labelled imaging agents continues to progress as the imaging modality gains appeal, the vast majority of PET scans today are still conducted with 2-deoxy-2-[^{18}F]fluoro-D-glucose ([^{18}F]FDG).[62] First prepared by Ido and Wolf in 1978,[63] the radiolabelled glucose analogue provides a gold standard method of PET imaging a wide array of cancers,[64,65,66] as well as a host of neurological conditions,[67,68,69] thanks to a common and effective uptake system.

On administration, [^{18}F]FDG is transported throughout the body, particularly to regions of high glucose uptake, before being phosphorylated by the enzyme hexokinase when taken up by cells, a typical pathway for unlabelled glucose. The unlabelled sugar would normally then undergo further metabolism via the glycolytic pathway for energy production. However, [^{18}F]FDG cannot enter the glycolysis reaction cascade and effectively becomes trapped as [^{18}F]FDG-6-phosphate within cells, providing a key benefit to the radiolabel's imaging mode. Many tumours cells express increased numbers of glucose transporters, particularly GLUT-1 and GLUT-

3,[70] as well as higher levels of hexokinase,[71] giving them increased metabolic activity. This correlates to the higher rates of mitosis that are seen with tumours, hence tending to result in higher glucose demand, particularly due to their preference for the less efficient anaerobic route of metabolism.[72]

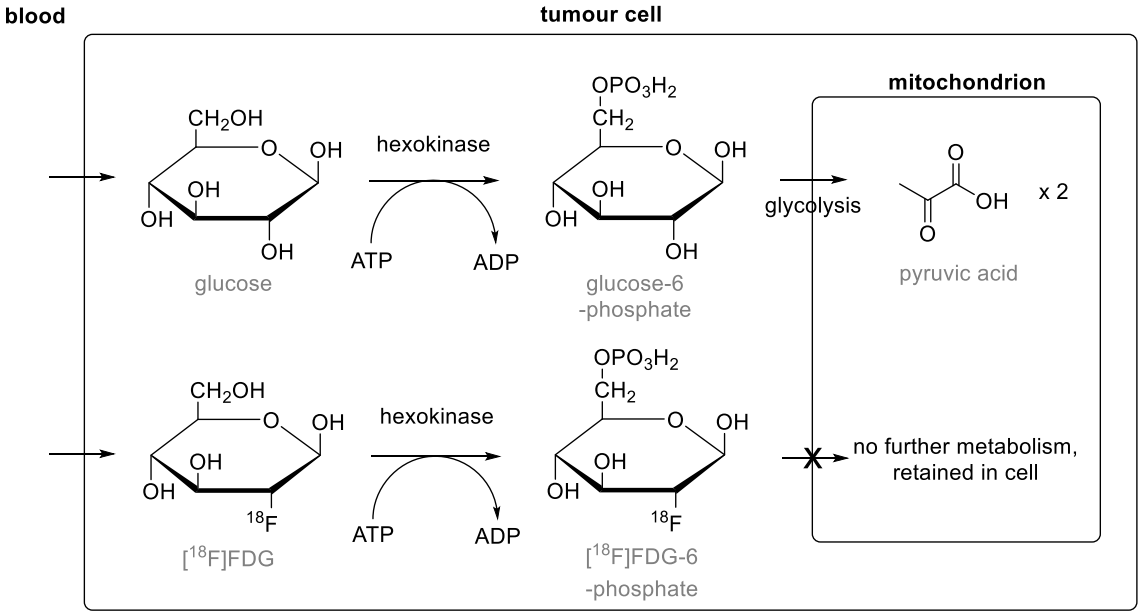

Scheme 4: Initial metabolic pathway of glucose *versus* [^{18}F]FDG

Although [^{18}F]FDG provides a widespread solution to the imaging of many tumour types, offering particularly high sensitivity given the nature of PET imaging with fluorine-18, [^{18}F]FDG is not tumour specific.[73] The radiotracer will accumulate in area of high levels of metabolism and glycolysis, including the heart and brain, as well other areas of muscular and nervous hyperactivity; areas under inflammatory stress such as infections, arthritis and sarcoidosis; and tissue undergoing repair, thus making [^{18}F]FDG unsuitable for imaging studies involving the heart, brain or inflamed tissue.[74]

Prior to the administration [^{18}F]FDG, patients are required to fast for a minimum of 4-6 hours (preferably overnight), allowing blood glucose levels to drop to a desired sub-150 mg/dL level.[75] The dose (usually 10-20 mCi for oncologic imaging) is administered intravenously 60 min before the PET scan, providing sufficient time for intracellular uptake and accumulation, as well as clearance from the blood, without losing excessive activity to decay. In this period the patient is instructed to restrict

movement and rest by lying on a lead-shielded bed until the scan, which can take between 30 and 90 min, where each bed scan can take 5-10 min.[76] This usual procedure for [^{18}F]FDG PET imaging represents the ease and non-invasive characteristics of imaging with ^{18}F-labelled imaging agents. Figure 8 provides an example of how [^{18}F]FDG PET imaging is used to track lymphoma regression (approximately 50% in this case) as a result of chemotherapy.[77]

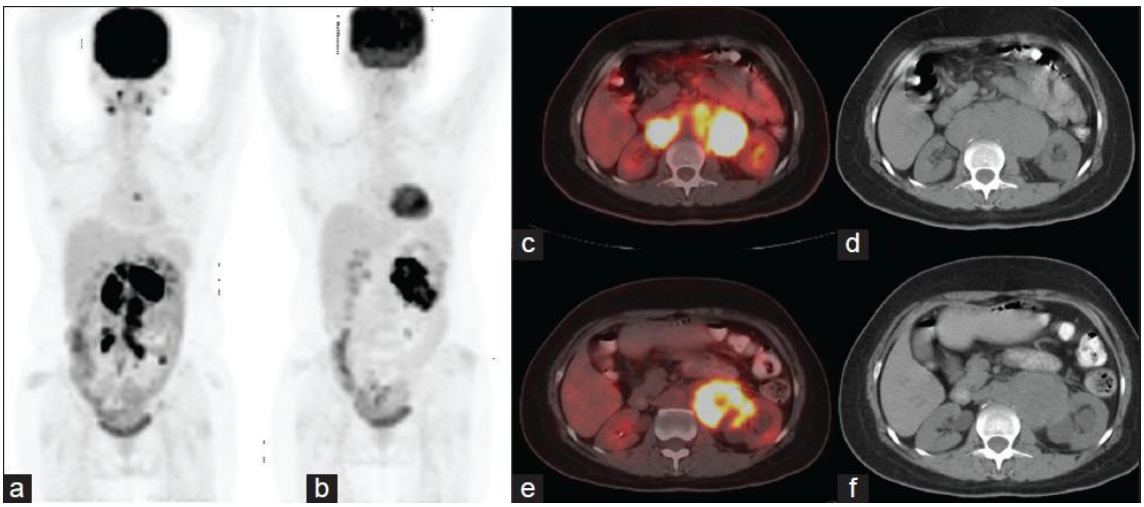

Figure 8: [^{18}F]FDG PET imaging of a patient exhibiting large B cell lymphoma (a) prior to treatment and (b) after six cycles of chemotherapy. Also, transaxial PET/CT and CT pre-treatment images (c and d) and post-treatment PET/CT and CT images (e and f)

1.5 Cyclotron Production of Fluorine-18

As described in Section 1.2, fluorine-18 is routinely prepared *via* bombardment of a target parent nuclide within a particle accelerator known as a cyclotron to produce the daughter nuclide.[78] In essence, cyclotrons utilise a high frequency alternating voltage to accelerate a charged particle beam, applied between two "D"-shaped electrodes within a vacuum chamber to approximately 1/10th of the speed of light. The charged particle beam, usually consisting of protons, deuterons or helium nuclei, is focussed towards the target through a spiral trajectory induced by two electromagnets sat above and below the vacuum chamber. With sufficient speed, the charged particle beams collide with the target nuclide with enough energy to induce change in the subatomic composition of the target nucleus, yielding the

radionuclide.[79] The below schematic provides a simple representation of how a cyclotron functions (Figure 9).[80]

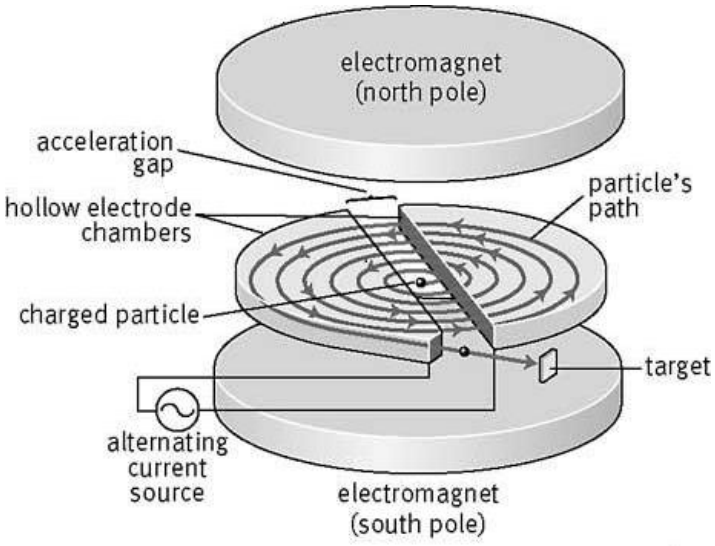

Figure 9: Basic schematic of the workings of a typical cyclotron

First developed by E. O. Lawrence and M. S. Livingston in 1934,[81] winning Lawrence the 1939 Nobel Prize in physics,[82] the cyclotron offered a number of notable advantages over traditional linear particle accelerators, in particular, the reduced cost and space requirements substantially increased their real world application. Unlike their linear counterparts, cyclotrons are capable of producing continuous streams of particles to bombard the target with, which results in a relatively high average beam energy; to achieve similar power a linear accelerator would need to be ludicrously long. The compactness of cyclotrons also reduces the costs associated with radiation shielding, supporting foundations and housing facility requirements.

Since Lawrence's early inventions, efforts in cyclotron advancement has continued to strive towards producing more powerful, higher beam energy accelerators, as well as the development of smaller and cheaper cyclotrons, allowing their incorporation into medical imaging centres more realistic. The development of lower energy, ultra-compact cyclotrons has seen particular interest in the last 15 years, because of the ease of their integration into PET pharmacies. Manufacturing giants such as GE, IBA and Siemens have successfully exploited this demand for cyclotrons with greatly

reduced environmental footprints and running costs, with systems like the GE PETtrace (Figure 10, right).[83]

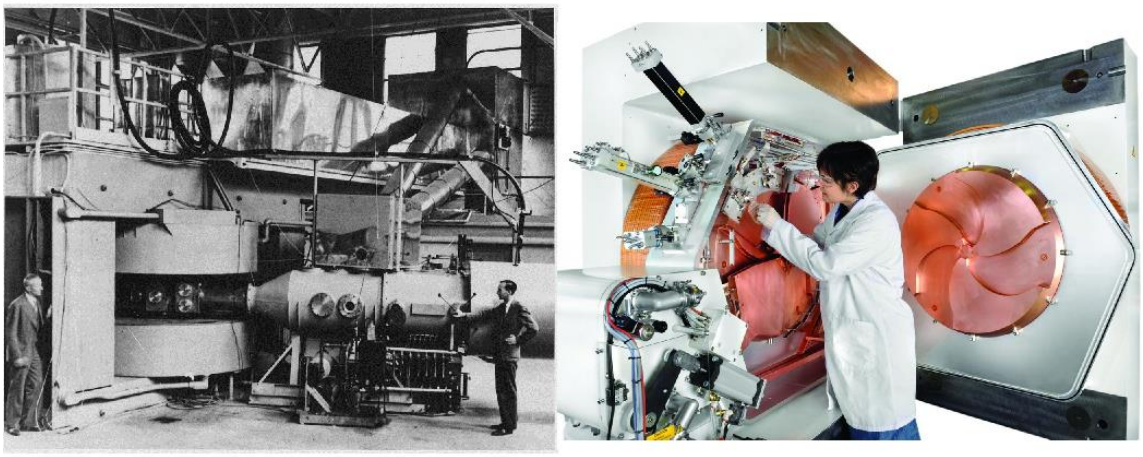

Figure 10: Lawrence's '60 inch' cyclotron, the most powerful cyclotron at the time when pictured in 1938 (left)[82] and the GE PETtrace 800 series cyclotron (right)

These compact cyclotrons are intended to produce isotope of sufficient quantity to provide for multiple patient doses, without occupying a large amount of space, allowing them to be installed as close to an imaging centre as possible. Not only are these systems designed to be easy to use, but their reduced power capability decreases the number of radioactive metal contaminants that are often seen in notable amounts with full-size, high power cyclotrons. A lower beam energy and low activity radioisotope products also reduces the safety concerns associated with particle accelerators; yet another features that has helped increase the accessibility of PET radioisotopes across the world as a result of low-power ultra-compact cyclotrons.[84]

1.5.1 Radiochemical Terminology

The products and processes of radiochemical reactions are characterised in a very different manner to the products of typical organic or inorganic chemical reactions. With only a handful of IUPAC definitions in place for radiochemical characterisation,

it's important to understand which measurements give a true representation of the data under discussion.

Achieving a very high reaction yield in a radiochemical reaction isn't usually of significant importance to a radiochemist. Typically, radiochemists are concerned with the radiochemical yields (RCYs) of their reactions, which are defined as the yield of a radiochemical separation expressed as a fraction of the activity originally present,[85] *i.e.* the activity of the radioactive product *versus* the activity of the radioactive starting material. However, the RCY doesn't take into account the activity lost as a function of time as the radionuclide decays, and without distinct indication of the start time and end time it becomes an inaccurate description of the true yield of a radiochemical reaction. More commonly, radiochemists take into account the decay constant of the radionuclide in question and report yields as decay-corrected radiochemical yields, which in practice is calculated as:

$$\mathrm{RCY(DC)} = \left(\frac{\text{'END'} \times 2^{\mathrm{n}}}{\text{'START'}} \right) \times 100$$

Where 'END' is the activity of the product(s), 'START' is the activity of the starting material and n is the number of half-lives that have occurred in the time frame. However, theoretically the decay corrected RCY is more accurately described as:

$$A_0 = \left(A_t \times e^{\lambda t} \right)$$

Whereby A_0 is the count at time 0 (the decay corrected counts), A_t is the raw, uncorrected count at time t, 'λ' is the decay constant and 't' is the elapsed time. The decay constant is derived from the half-life ($t_{1/2}$) of the radionuclide under analysis and is represented as such:

$$\lambda = \frac{\ln(2)}{t_{1/2}}$$

The decay constant, also known as the disintegration constant, describes the probability of a nuclear decay within a time interval divided by that time interval.

Radioactivity itself has a number of conventionally used units, the becquerel (Bq), being the SI unit, is the modern format for activity; where 1 Bq is defined as one

disintegration per second.[85] However, the curie (Ci) has long been the preferred format for activity for and despite its use being discouraged, it still sees regular use within the literature. Originally defined to correspond to one gram of radium-226,[86] 1 Ci is now more accurately defined as being equivalent to 3.7×10^{10} Bq (37 GBq).

Given the practical considerations of using radiation in medicine, as well as the safety concerns surrounding radioactive material, the dosage of radioactivity a subject experiences is usually a better indication of exposure rather than the actual activity. The gray (Gy) and the sievert (Sv) are both SI units used to quantify the intensity of radioactive exposure; whereas the roentgen equivalent man (rem) is an older, much less frequently used unit of dose (1 rem = 0.01 Sv). IUPAC defines the gray as the energy imparted to an element of matter by ionizing radiation, divided by the mass of that element equal to 1 joule per kilogram, (*i.e.* Gy = Jkg^{-1}) hence the gray is often reserved for doses of radiation that can cause acute physical damage to a subject. The sievert itself is defined as the dose equivalent equal to one joule per kilogram *i.e.* the biological damage caused by the radiation, taking into account the total energy absorbed and also the rate of energy loss per unit distance as the radiation travels through the subject. To put sieverts as a measure of dosage into context, one can expect to receive 400–600 μSv per two-view mammogram,[87] 10–30 mSv for a single full body CT scan,[88] 250 mSv for a 6-month trip to Mars,[89] and an acute dose of 1 Sv provides a 5.5% chance to develop cancer.[90]

Specific activity (SA), the activity of a material per unit mass of a material or per mole of compound, is another major consideration for synthetic radiochemists and is a key requirement for knowledge of the radiochemical purity of a sample. Often, specific activity is lost when unwanted inclusion of stable isotope counterparts of the radionuclide are incorporated into the product, *i.e.* ^{19}F in place of ^{18}F. This becomes of particular concern when the radiolabelled product is intended for use as a radioligand and the ^{19}F-bearing variant acts as a competitor for the radioligand's target active site.

There are also a number of non-IUPAC terms of practical importance, including radiochemical incorporated yield (RCIY), which is the percentage of radioactive starting material that is successfully incorporated into the desired product (sometimes also referred to as the chromatographic radiochemical yield); and

effective specific activity, which takes into account any additional materials that bind to the same target(s) as the radioligand but do not contribute to PET imaging.

1.5.2 Production of Electrophilic Fluorine-18

Although fluorine-18 is largely prepared *via* cyclotron proton bombardment of oxygen-18 to yield nucleophilic [^{18}F]fluoride, the production of electrophilic [^{18}F]fluorine ([^{18}F]F_2) is useful in a number of applications,[91,92] and usually most organic chemists seek to introduce fluoro-groups into molecules by electrophilic means. Produced as a gas, [^{18}F]F_2 can be prepared from neon-20 by deuteron bombardment or by bombardment of oxygen-18 gas with protons in the presence of nickel, as signified by the nuclear conversions in Figure 11.[93]

$$^{20}\mathrm{Ne}(d,\alpha)^{18}\mathrm{F} \longrightarrow [^{18}\mathrm{F}]\mathrm{F}_2$$

$$^{18}\mathrm{O}(p,n)^{18}\mathrm{F} \longrightarrow [^{18}\mathrm{F}]\mathrm{F}_2$$

Figure 11: Two nuclear conversions resulting in electrophilic fluorine-18 production, note the bombardment species (A) and the species lost as a result of bombardment (B) denoted as (A,B)

[^{18}F]Fluorine gas is fairly unattractive as a reagent itself; as well as being a very powerful oxidant and extremely reactive, it tends to react in a very exothermic manner. Further complicating the handling of [^{18}F]F_2, the gas reagent is incompatible with a vast number of solvents, hence, the overly reactive gas is usually rapidly converted into more amenable secondary or tertiary reagents, despite this inclusion of additional steps resulting in detrimental impact on the final RCY.[94]

Hypofluorites ([^{18}F]RCOOF) and N-F reagents ([^{18}F]R^1R^2NF) can provide electrophilic sources of fluorine-18 that are drastically easier to handle,[95,96] have more selective reactivity and are compatible with an increased range of solvents, however, having stemmed from [^{18}F]F_2 means that they carry a very undesirable characteristic, low specific activity. This low specific activity is a consequence of the preparation process, as the [^{18}F]F_2 requires extraction from the target using carrier fluorine-19 gas, resulting in isotopic contamination and a SA of 100–600 MBq/μmol).[97] Being a

carrier added (c.a.) process leads to increased mass of the final radiotracer and hence reduced activity per gram or mole of material;[98] and ultimately a reduction in PET signal from specific binding.[99]

Cause of low specific activity can be attributed to more than use of the carrier added approach to fluorine-18 production alone, in fact, fluorine-19 contamination can present a significant challenge throughout the radiosynthetic pathway. Radiochemical impurities yielded by fluorine-19 incorporation can be acquired from precursors, solvents and tubing (particularly fluoro-polymers such as PTFE) and other reagents; and their presence even at nmol concentrations can result in much reduced SA.[100] With low SA being of particular concern for radiochemists working with electrophilic fluorine-18 there have been a number of efforts made to resolve this; including micro-scaling *i.e.* process miniaturisation which reduces contaminants available from starting materials and leeched from tubing and vessels. Alternative approaches include drastically upscaling the initial amount of radioactivity by increasing the bombardment time and maintaining the same target volume; or utilising process optimisation by eliminating all potential sources of contamination or by improving the target system.[101,102] Another recent attempt to boost the specific activity of $[^{18}F]F_2$ involves work by Bergman and Solin, where a specific activity of 55 GBq/μmol was achieved by preparation of [^{18}F]methyl fluoride using nucleophilic [^{18}F]fluoride, which was then mixed with carrier F_2 in an inert neon matric and then atomized by employing an electric discharge to encourage isotopic exchange.[103]

1.5.3 Production of Nucleophilic Fluorine-18

Given the numerous drawbacks associated with the use and production of $[^{18}F]F_2$, the majority of fluorination strategies are developed with a nucleophilic radiofluorination strategy at their core. Regardless of cyclotron size or power, nucleophilic [^{18}F]fluorine-18 is prepared by proton bombardment of oxygen-18 enriched heavy water ($[^{18}O]H_2O$) to yield an aqueous solution of [^{18}F]fluoride. Unlike $[^{18}F]F_2$, the resulting $[^{18}F]F^-$ is easily extracted from the target, hence the process is no-carrier added (n.c.a.) and therefore offers markedly higher in specific activity.[103,104,105]

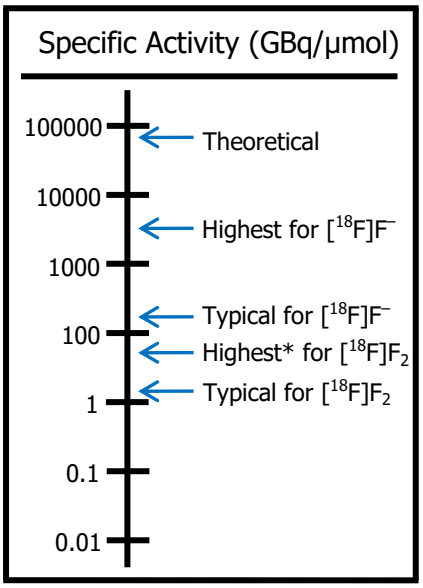

Figure 12: A scale chart comparing the theoretical and actual specific activities offered by $[^{18}F]F^-$ and $[^{18}F]F_2$. *Highest SA for $[^{18}F]F_2$ achieved by the Solin method *via* CH_3F[102,103]

The resulting $[^{18}F]$fluoride requires extraction from the remaining target $[^{18}O]H_2O$, an unsuitable solvent for most radiofluorination chemistry, quickly and effectively to avoid loss of activity to time. The retained $[^{18}O]H_2O$ can be recycled to avoid wasting the expensive stable isotope,[106] which can cost $200 per gram[107] or more depending on current worldwide availability. However, the poor solubility of the fluoride ion in the majority of organic solvents, coupled with its weakly nucleophilic nature makes the application of $[^{18}F]$fluoride in organic solvents less than trivial.

Typically, extraction from the aqueous media is achieved by trapping the anion on an ion exchange column or cartridge, followed by elution with a weak base, often potassium carbonate, as a solution in acetonitrile and water.[99] Any remaining water can then be reduced by multiple cycles of azeotropic distillation and the application of a phase transfer reagent reduces solvation the fluoride anion and thereby substantially improves its nucleophilicity. Without this key step, the high charge density of fluoride would remain strongly hydrated (ΔH_{hydr} = 506 kJ/mol) and hence nucleophilically inactive.

The multidentate ligand, Kryptofix-222® (K_{222}) **1** is commonly used as a phase transfer reagent for radiofluorinations; the cryptand complexes with the potassium

cation of [^{18}F]KF strongly to afford a 'naked' and thereby more nucleophilic fluoride anion.

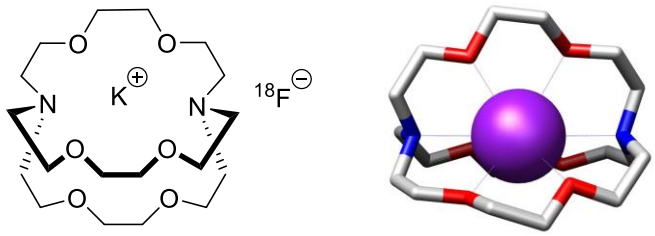

1

Figure 13: Structure of [^{18}F]KF.K_{222} (left) and x-ray crystal structure of [2.2.2]cryptand encapsulating a potassium cation (right)[108]

Tetraalkylammonium compounds such as tetrabutylammonium bicarbonate and tetraethylammonium bicarbonate have also been shown to provide very suitable routes to organic-soluble, nucleophilic fluorination reagents; yielding [^{18}F]tetra-butylammonium fluoride ([^{18}F]TBAF)[109] and [^{18}F]tetraethylammonium fluoride ([^{18}F]TEAF).[110] The convenience of these reagents lies in their ability to both provide a means to solubilise the [^{18}F]F^- and to synchronously act as a source of weak base, allowing elution from the ion exchange resin and complexation to occur in tandem.[111] In addition, recent work by Reed *et al*, has highlight the use of [^{18}F]TEAF as a reagent with comparable radiofluorination capabilities to [^{18}F]KF.K_{222}, that also reduces the occurrence of blockages within microfluidic systems, a common problem for those operating such systems with [^{18}F]KF.K_{222}, and avoids the formation of clathrates when compared to [^{18}F]TBAF, thereby providing a more anhydrous source of [^{18}F]fluoride.[110,112]

1.5.4 Radiopharmaceutical Production

The production of radiopharmaceuticals places demand on fast, robust and automated systems that allow for the rapid conversion of cyclotron produced

[^{18}F]fluoride into a patient-ready formulation, ensuring that there is sufficient activity on delivery, as well as high chemical and radiochemical purity.

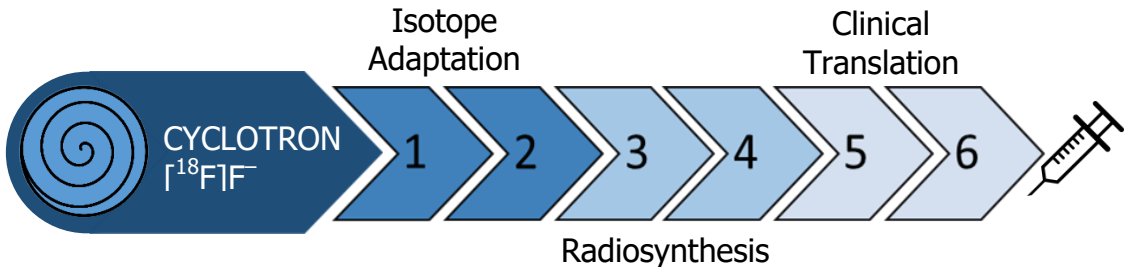

Figure 14: Typical radiopharmaceutical production sequence. 1) [^{18}F]fluoride collection and transfer; 2) Trapping and drying of [^{18}F]fluoride; 3) Radiofluorination (and additional chemical steps e.g. removal of protecting groups); 4) Isolation and purification of radiolabelled product e.g. radio-HPLC; 5) Formulation to clinical requirements and 6) QC and transport to PET imaging centre.

As the efficiency and output of cyclotrons has developed, and PET scanners have seen more frequent installation into imaging centres, the development of automated, micro-scaled radiolabelling platforms has also continued to grow to meet the need for safe and automated radiosynthesis.[113,114] Efforts here focus on production speed, reduced contamination through use of closed, controlled systems, reduced manual handling through automation and thereby improved safety.[115]

Whether the radiolabelled targets are intended for direct use in the clinical setting, drug discovery R&D, radiochemical methodology purposes or a combination there of, the installation of a PET pharmacy requires careful planning. Like many other emerging PET chemistry facilities across the globe, the assignment of Newcastle University's radiopharmaceutical production facility, opened as 'The Sir Bobby Robson Foundation PET Tracer Production Unit' in 2012 by Lady Elsie Robson (Figure 15) was required to be multi-functional, ultra-compact and designed for streamlined radiosynthesis.

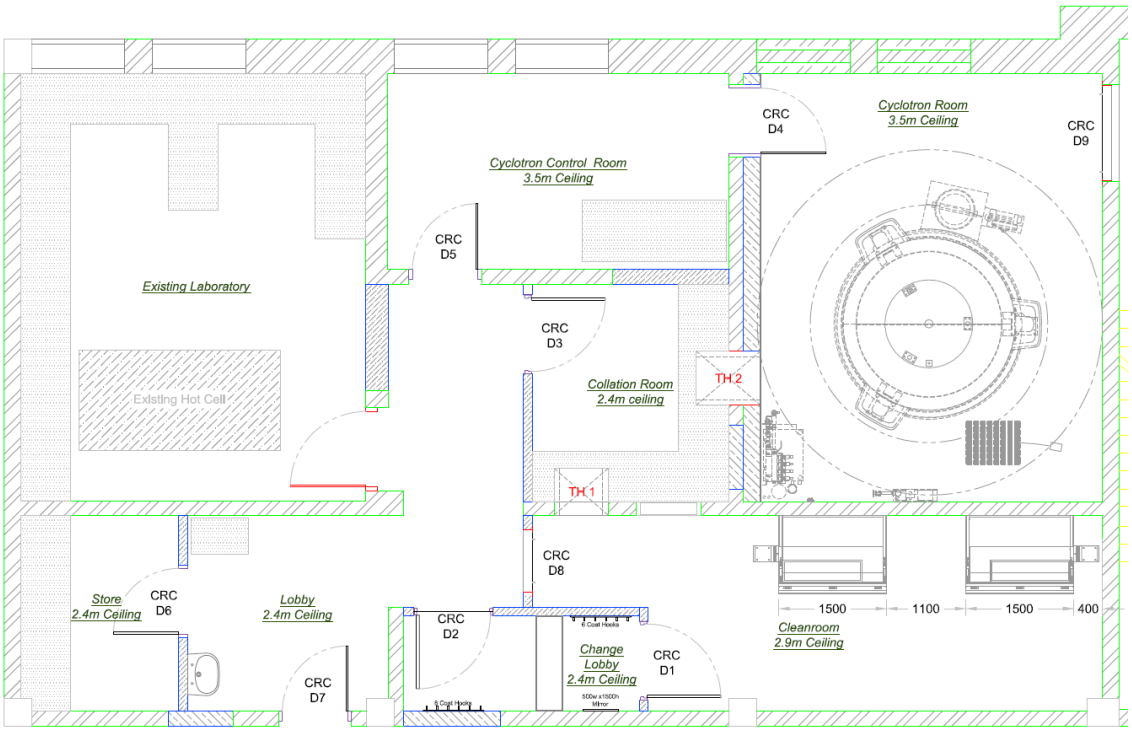

Figure 15: Facility layout schematic of The Sir Bobby Robson Foundation PET Tracer Production Unit at Newcastle University, School of Chemistry

As discussed in Section 1.5 Cyclotron Production of Fluorine-18, the traditional approach to fluorine-18 PET chemistry involves the need for a large, concrete bunker shielded cyclotron, capable of producing $[^{18}F]F^-$ in very high activity (>50 GBq), allowing for transportation of the radionuclide to remote scanning sites, dose splitting or even tolerating low RCYs. However, the convenience, reduced cost and improved safety offered by compact cyclotrons greatly outweighs the use of larger cyclotrons in condensed facilities like the Newcastle PET radiopharmacy, hence the acquisition of the ABT Biomarker Generator (Figure 16).[116]

Figure 16: The Advanced Biomarker Technology (ABT) biomarker generator 'mini-cyclotron', with concrete shielding in the raised position (left) and the cyclotron without shielding (right)

The 7.5 MeV positive ion 'dose-on-demand' cyclotron, allows for the production of 2 GBq of [^{18}F]fluoride (maximum) per 1 h run, at a rate of 1.0 mCi/min. The miniature particle accelerator employs a 1.16 T magnet and provides a beam current of 2–5 μA, making it highly suitable for the production of low-levels of [^{18}F]fluoride for immediate, single dose production. Work within the group has also validated that the ABT system is capable of yielding [^{18}F]fluoride with lower levels of radioactive metal contaminants *versus* other systems,[117] and also extremely low tritium contamination,[118] never exceeding 2.4 Bq per μL compared to the typical 140–180 Bq per μL.[119]

The hazardous nature of working with sources of ionising radiation presents a number of risks, procedures and requirements that highlight the major differences between practical radiochemistry and standard laboratory bench chemistry. Most distinctly, the use of shielding throughout preparation is needed and the systems employed for radiolabelling and radiochemical analysis are ideally placed in shielded fume hoods, known as 'hot cells' (Figure 17).

Figure 17: Gravatom 'hot cells' housing radiolabelling equipment, at The Sir Bobby Robson PET Tracer Production Unit, Newcastle University.

When handling radioisotopes or radiolabeled compounds outside of 'hot cells', the use of lead bricks, leaded glass windows and lead transport containers provide ample protection against the gamma radiation produced by positron-emitters, similarly lead safes allow for safe storage of radioactive standards used for equipment calibration. Stringent radiation safety training is also undertaken by radiochemists, which teaches users to maintain a minimum safe working distance between the operative and the open source by using tongs and other forms of remote manipulation where possible. The effective dose to the radiation worker (in sieverts) is strictly monitored by the use of electronic personal dosimeters (EPDs) for live readings, as well as other cumulative dosimeters for long-term monitoring; and area activity counters to safeguard other workers in the laboratory throughout radiation work.

1.6 Approaches to [^{18}F]Fluorine Radiolabelling

Formerly, methods of incorporating fluorine-18 into organic molecules were rather limited, however, ever expanding research into the area has afforded new, more

diverse applications for radiofluorination chemistry. For a full spectrum of fluorine-18 radiolabelling strategies, the reader is directed to a number of a detailed reviews,[97,120,121,122] however, the remainder of this chapter will highlight a number of key approaches. The numerous labelling strategies can be divided into direct labelling *i.e.* incorporation of fluorine-18 onto a target drug; or alternatively indirect labelling, whereby a smaller prosthetic group is tagged with fluorine-18, which can then be used to label biomolecules such as peptides. This two-step tagging approach allows radiolabelling of molecules with sensitive functionalities and/or larger biomolecules that would usually be intolerant of standard radiofluorination conditions. Similarly, the use of either electrophilic [^{18}F]fluorine or nucleophilic [^{18}F]fluoride present two contrasting strategies for fluorine-18 integration.

1.6.1 Electrophilic [^{18}F]Fluorinations

As described in Section 1.5.2, the use of overly reactive [^{18}F]F_2 is generally avoided by converting the radiolabelled gas into a easier to handle, more selective reagents, such as those depicted below (Figure 18). Although these reagents offer definite practical improvements over the direct use of [^{18}F]F_2, complete regioselective control when radiolabelling electron-rich arenes and alkenes remains a challenge.[123]

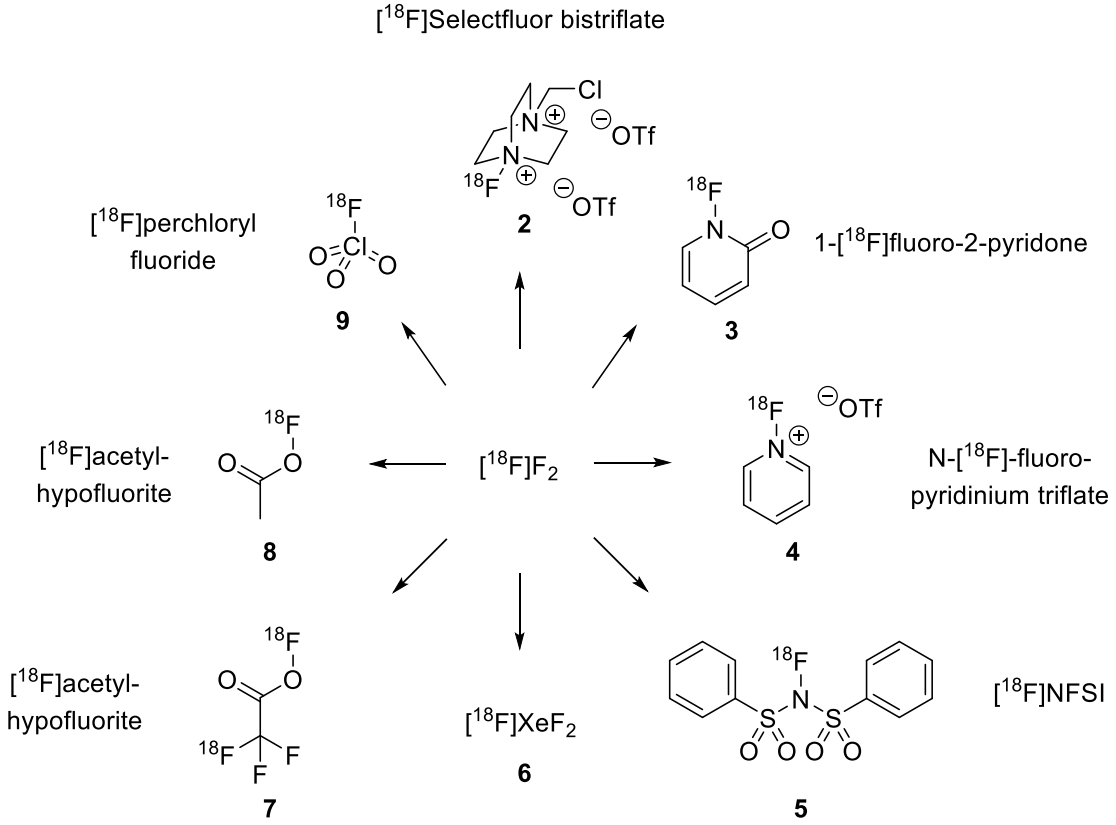

Figure 18: Several reported electrophilic [^{18}F]fluorinating agents.[124,125]

However, some strategies involve *in situ* formation of these intermediate fluorination reagents, hence omitting the need for an additional isolation step which would likely result in a lower RCY; an example of which is preparation of 5-[^{18}F]fluorouracil **11**, first reported by Visser *et al* (Scheme 5).[126] Direct administration of [^{18}F]F_2 to a solution of **10** in acetic anhydride and a trace amount of acetic acid at room temperature afforded [^{18}F]**11**, with selectivity ensured by the simultaneous formation of [^{18}F]acetyl hypofluorite **8**.

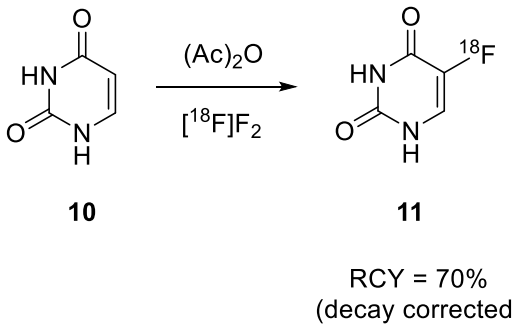

Scheme 5: Preparation of 5-[^{18}F]fluorouracil *via in situ* formation of [^{18}F]acetyl hypofluorite.

Another historically important example of [^{18}F]acetyl hypofluorite **8** application is in the early preparations of [^{18}F]FDG **13** from precursor **12** (Scheme 6). Although modern preparations of [^{18}F]FDG utilise higher SA nucleophilic [^{18}F]fluoride, early radiosyntheses with [^{18}F]acetyl hypofluorite allowed for rapid preparation of radiolabelled sugar in relatively good RCYs, suitable for successful PET imaging.[127]

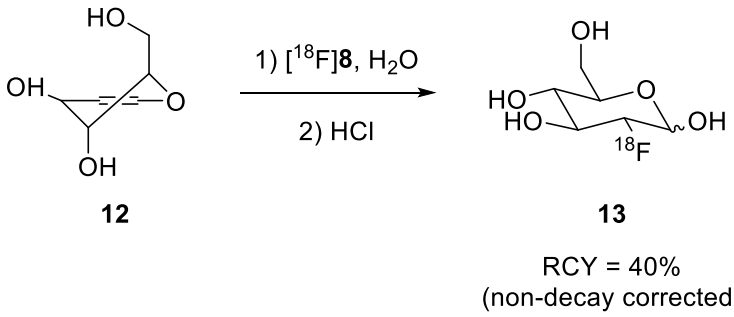

12 **13**

RCY = 40%
(non-decay corrected)

Scheme 6: Preparation of [^{18}F]FDG *via* electrophilic [^{18}F]acetyl hypofluorite

This method provided a large improvement over previous methods, where direct electrophilic fluorination with [^{18}F]F_2 yielded a 3:1 ratio of the [^{18}F]fluoro-glucose and [^{18}F]fluoro-mannose isomers, which required subsequent separation by preparative gas chromatography before hydrolysis, affording [^{18}F]FDG with a poor RCY of 8%.[128]

Other major approaches for improving electrophilic radiofluorinations by enhancing regioselectivity largely involve demetallation of organometallic precursors; for example, early work by Coenen *et al* allowed for improved radiofluorination regioselectivity of aromatics bearing both electron-rich substituents and some electron-deficient substituents *via* fluorodestannylation with [^{18}F]F_2 or [^{18}F]acetyl hypofluorite (Scheme 7).[129] This work highlighted the scope for highly regiospecific radiofluorinations provided by arylstannane precursors, however specific RCYs were not provided.

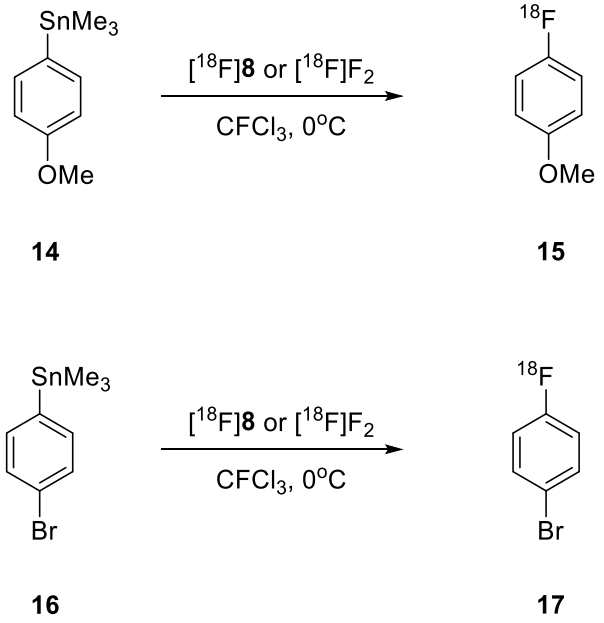

Scheme 7: Electrophilic [^{18}F]fluoro-destannylation of electron-rich and electron-deficient aromatics (RCYs not given)

Although precursors based on alternative metals for fluoro-demetallation radiochemistry have been explored, namely silicon,[130] germanium,[129] and mercury,[131] organotin precursors remain the prevalent reagent for this approach, despite the obvious toxicity concerns.

N-F fluorinating reagents have also demonstrated utility in selective electrophilic fluorination strategies, one of definite worth is *N*-[^{18}F]fluorobenzenesulfonamide **5** ([^{18}F]NFSi), which displays highly stable yet reactive character and allows for selective ^{18}F-labelling of silyl enol esters and allylsilanes to yield α-fluorinated ketones and [^{18}F]allylic fluorides, respectively. The preparation for which was first realised by Teare *et al* who bubbled [^{18}F]F_2 through a solution of sulfonamide **18** in acetonitrile:water to yield a stock solution of [^{18}F]NFSi (Scheme 8) as well as [^{18}F]NaF as a by-product.[132]

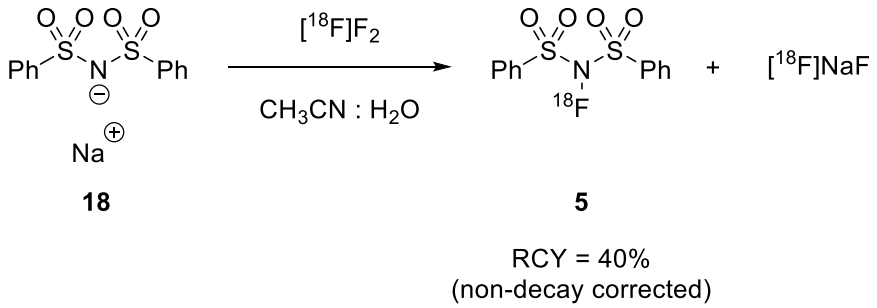

Scheme 8: Preparation of [^{18}F]NFSi

Teare *et al* demonstrated the highly selective nature of [^{18}F]NFSi in the radiolabelling of allylsilane **19** to afford drug-like structure **20** (the 1α–fluoro-substituted fragment of an important fluorinated analogue of vitamin D_3) and the *syn*-diastereomer **21** as a minor product (Scheme 9), with a total chemical conversion of 87% (for **20** and **21**), however, RCYs were not provided.[132]

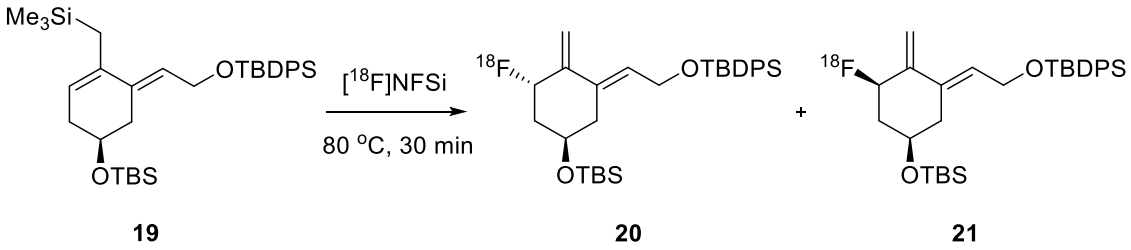

Scheme 9: Electrophilic fluorination of an allylsilane with [^{18}F]NFSi

More recently, the preparation of a N-F reagent based on Selectfluor™, [^{18}F]Selectfluor bis(triflate) affords another highly selective, non-toxic, electrophilic fluorination reagent suitable for [^{18}F]fluorination of organotin reagents, mediated by silver triflate, under very mild conditions.[124] The reagent bares favour over [^{18}F]NFSi due to increased reactivity with a wide array of substrates and the already much accepted use of the ^{19}F counterpart.

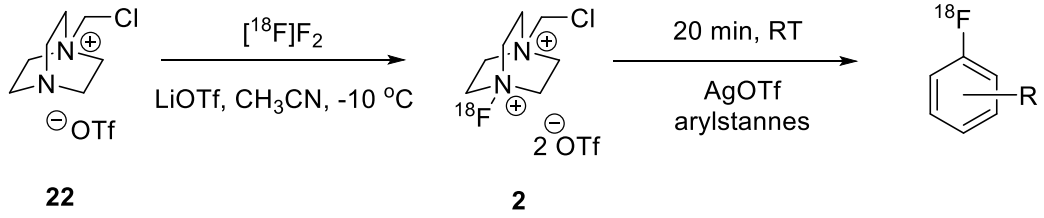

22 **2**

Scheme 10: Preparation and reactivity of [^{18}F]Selectfluor™ for fluoro-destannylation of aromatics under mild conditions

1.6.2 Nucleophilic [^{18}F]Fluorinations

The attractiveness of nucleophilic [^{18}F]fluorination strategies largely owe themselves to the higher SA offered by the carrier-free method of preparing [^{18}F]fluoride, despite the relatively poor nucleophilicity of the reagent. As a result, there are host of very varied chemistries already available, with newer strategies focussed on the benefits acquired by a late-stage radiofluorination to attain high RCYs which will be summarised in a latter sub-section, for further information the reader is directed to a number of excellent reviews. [98,120,133]

As with electrophilic ^{18}F-labelling strategies, nucleophilic approaches to fluorine-18 incorporation can also be divided into a number of sub-genres, most simply they can be split into aliphatic radiolabelling and aromatic radiolabelling, both of which can be direct labelling to yield a complete imaging agent or can involve indirect 'tagging' of biomolecules using prosthetic groups (Section 1.7).

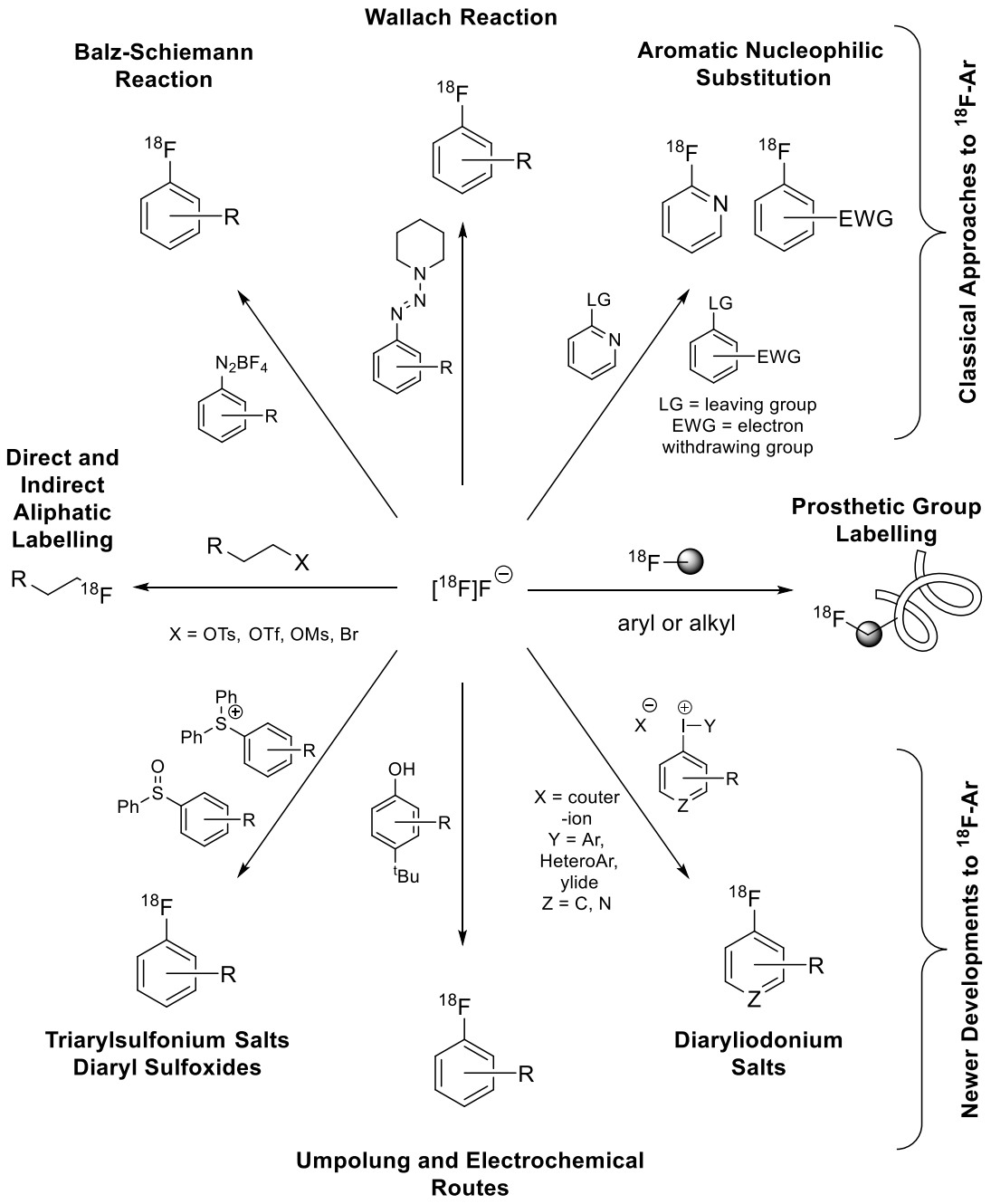

Figure 19: Summary of nucleophilic [^{18}F]fluoride radiolabelling strategies

1.6.2.1 Nucleophilic Aliphatic Substitutions with [^{18}F]Fluoride

Due to the simplicity of precursor design, radiofluorination strategies that operate *via* nucleophilic aliphatic substitution remain the most prominent of routes to a number of clinically important ^{18}F-labelled radiopharmaceuticals, including [^{18}F]FDG, [^{18}F]fluoroethylcholine (FEC) **23**, 3'-deoxy-3'-[^{18}F] fluoro-L-thymidine (FLT) **24** and *O*-2-[^{18}F]fluoroethyl-L-tyrosine (FET) **25** (Figure 20).[134,135]

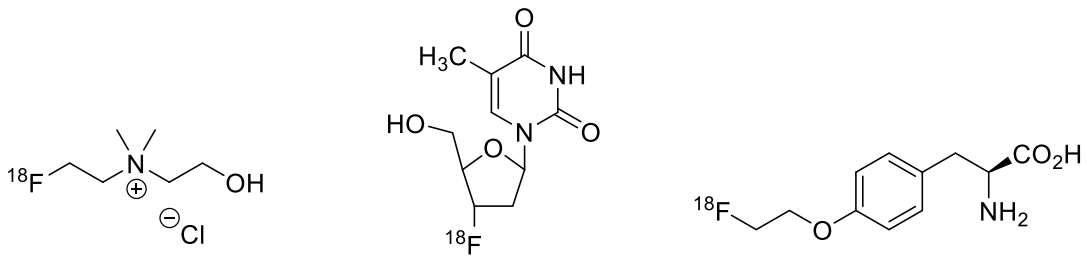

23 **24** **25**

Figure 20: Important ^{18}F-labelled radiotracers routinely prepared by nucleophilic aliphatic substitution for clinical use

As with most S_N2 type reactions, the successful radiosynthetic design of a precursor relies heavily on the choice of leaving group, where expected reactivity follows the order of leaving group ability; Cl < Br < I < tosylate < mesylate < nosylate < triflate.[102] Similarly, precursors bearing a primary benzylic or a primary alkyl substituted carbon adjacent to the leaving group fare better, as do precursors that allow solubility in polar aprotic solvents. Leaving group selection requires further consideration, given the usual requirement for a basic radiofluorination environment to promote successful labelling and the competing elimination reaction that occurs under basic conditions, which is enhanced for better leaving groups.[98]

It may worth noting at this stage, that the use of acids as catalysts or reagents in tandem with [^{18}F]fluoride presents a major concern in the potential formation of [^{18}F]HF, which even at low concentrations holds significant destructive capabilities and is hence avoided.[136] This highly favourable protonation (E_B = 565 kJ/mol) also renders the [^{18}F]fluoride unavailable for further chemistry.

Although imaging agents **23** and **25** can be prepared by direct tosylate displacement with [^{18}F]fluoride, they are more commonly prepared by [^{18}F]fluoroalkylation with [^{18}F]fluoroethyltosylate **26**. Similarly, both strategies of direct and indirect [^{18}F]fluoride radiolabelling have been successfully implemented to yield human benzodiazepine receptor imaging agents **28** ([^{18}F]fluoroethylflumazenil) and closely related flumazenil derivative **30**; from either precursor **27** to afford **28** (Scheme 11)[98] or from desmethyl-flumazenil precursor **29** (Scheme 12) *via* *N*-[^{18}F]fluoroalkylation in a one-pot protocol utilising tosylate **26** to yield **30**.[137,138]

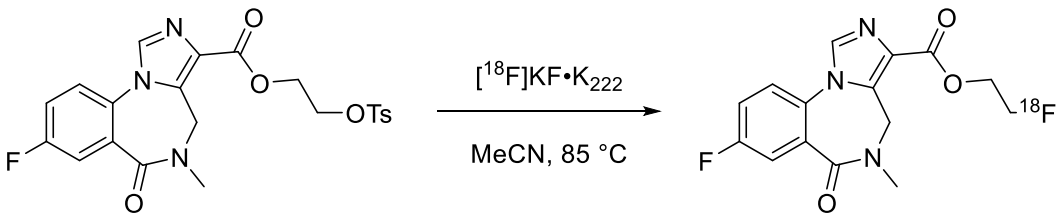

27 **28**

RCY = 68%
(decay corrected)

Scheme 11: One step preparation of [^{18}F]fluoroethylflumazenil *via* direct nucleophilic aliphatic substitution

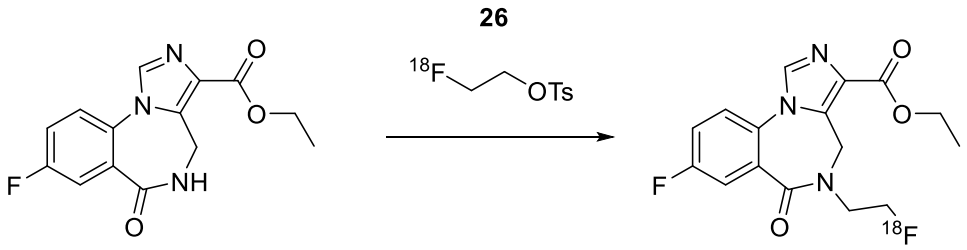

29 **30**

Scheme 12: One-pot preparation of [^{18}F]30 *via N*-[^{18}F]alkylation of precursor 29 (RCY not provided)

Other interesting approaches to nucleophilic aliphatic substitution include [^{18}F]fluoride ring-opening reactions, such as that in the preparation of cancer proliferation marker **24** from cyclic pyrimidine analogue **31** (Scheme 13).[139]

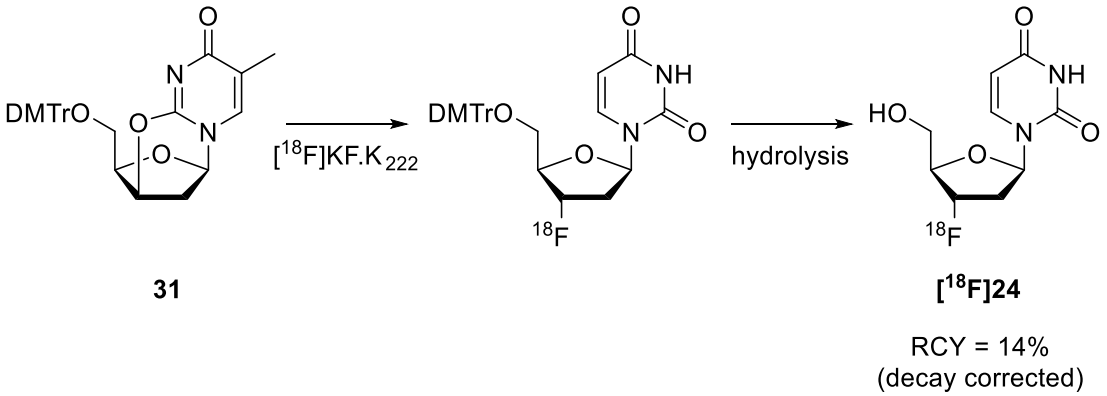

31 **[^{18}F]24**

RCY = 14%
(decay corrected)

Scheme 13: Preparation of [^{18}F]FLT *via* ring opening of cyclic precursor 31 with [^{18}F]F^{-}

Once a nucleophilic aliphatic substitution fluorine-18 labelling approach is fully optimised, (in terms of leaving group choice, counter-ion selection, *etc*.), high RCYs under moderate temperatures (< 100 °C) can often be achieved, usually with beneficially short reaction times (< 15 min),[140] and can be easily automated. However, the use of aliphatic substitution as a radiolabelling strategy in this manner is accompanied by a number of drawbacks; firstly the metabolic stability of [^{18}F]fluoroalkyl groups is relatively poor, particularly *versus* [^{18}F]fluoroaryl radiolabelling strategies; and secondly the range of tolerated functionalities and substitution positions can be limited target receptor morphology.[74,99]

1.6.2.3 Nucleophilic Aromatic Substitutions with [^{18}F]Fluoride

As previously mentioned, the possession of an aryl-^{18}F label within an fluorine-18 imaging agent provides a very attractive means to drive towards successful PET imaging, hence strategies towards robust aromatic [^{18}F]fluorinations are well developed.[98] Considered as the simplest approach to this challenge, nucleophilic aromatic substitution (S_NAr) chemistry allows for direct [^{18}F]fluoride radiolabelling of aromatics bearing strongly electron-withdrawing groups in *ortho*- or *para*- positions, with an appropriate leaving group (Scheme 14).[141,142,143]

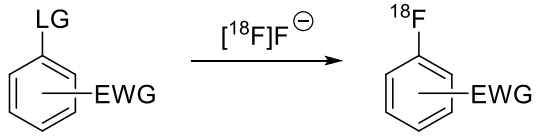

EWG = NO_2, CN, CHO, RCO, COOR, Cl, Br, I
LG = Cl, NO_2, $NR_3^+X^-$ (X =TfO^-, TsO^-, ClO_4^-, I^-)

Scheme 14: Preparation of [^{18}F]fluoroarenes from arenes bearing electron-withdrawing substituents

However, there are a number of prerequisites that dictate the success of these reactions; firstly the use of a phase transfer reagent, such as K_2CO_3/Kryptofix-222® or tetraethylammonium bicarbonate to activate the fluoride towards nucleophilicity, is crucial, secondly the reaction only proceeds through relatively harsh conditions, requiring temperatures exceeding 100 °C with DMSO typically as the solvent.[98] The use of a base is also often necessary, however, with precursors possessing base labile hydrogen atoms, the use of a Kryptofix-222® bicarbonate / oxalate buffer system can be employed.[144] The reactivity of arenes with different leaving groups and electron-withdrawing groups in *ortho*- and *para*- positions has been studied by multiple groups in depth.[141,142,144,145] Provided below is a summary of the effect of leaving groups on the RCY for *para*- substituted nitro-arenes and cyano-arenes subjected to nucleophilic aromatic substitution with [^{18}F]F^- (Table 2).[144]

EWG	**LG**					
	I	**Br**	**Cl**	**F**	**NO_2**	**NR_3^+**
NO_2	10%	35%	70%	47%	87%	-
CN	-	33%	24%	70%	73%	68%

Table 2: The effect of leaving group on RCY with *para*-nitro and *para*-cyano substituted arenes when reacted with [^{18}F]KF.K_{222} at 150 °C in DMSO. NR_3^+ as the triflate salt

Note that the above table also describes a commonly utilised route for direct displacement of a [^{19}F]fluoro- leaving group by [^{18}F]fluoride, known as isotopic

exchange, which is somewhat effective for strongly activated arenes, as seen above. However, as with other strategies where fluorine-19 contamination is unavoidable, the detrimental effect on the final specific activity of the product may nullify the use of this approach for radiotracers in imaging applications that are limited by low binding capacities.[146] The trialkylammonium leaving group provides excellent nucleofugic properties, particularly when employed with weakly electron-withdrawing *para*-substituents such as halides. (Table 3).[147,148] Although a range of counter-ions are available, trialkylammonium triflates typically provide superior results, particularly when used in conjunction with dimethylacetamide as the solvent, as illustrated in Table 3.[98]

LG	**EWG**							
	Cl	**Br**	**I**	**$COCH_3$**	**CHO**	**CN**	**CF_3**	**NO_2**
NO_2	<0.1%	<0.1%	-	67%	77%	81%	67%	88%
NMe_3^+	-	12.5%	15%	79%	71%	87%	-	88%

Table 3: The effect of various *para*-substituted electron-withdrawing groups on the S_NAr [^{18}F]radiofluorination of nitro-arenes and trimethylammonium-arenes as RCYs where *p*-nitro-arene fluorinations are conducted at 150 °C in DMSO and *p*-trimethylammonium-arene fluorinations are conducted at 140 °C in dimethylacetamide

The radiosynthesis of [^{18}F]labelled cyclooxygenase inhibitor **33** ([^{18}F]SC58125) by McCarthy *et al* provides an excellent example of nucleophilic aromatic substitution achieved through use of a trialkylammonium triflate leaving group, permitting late-stage radiofluorination of a weakly activated aromatic (Scheme 15).[149]

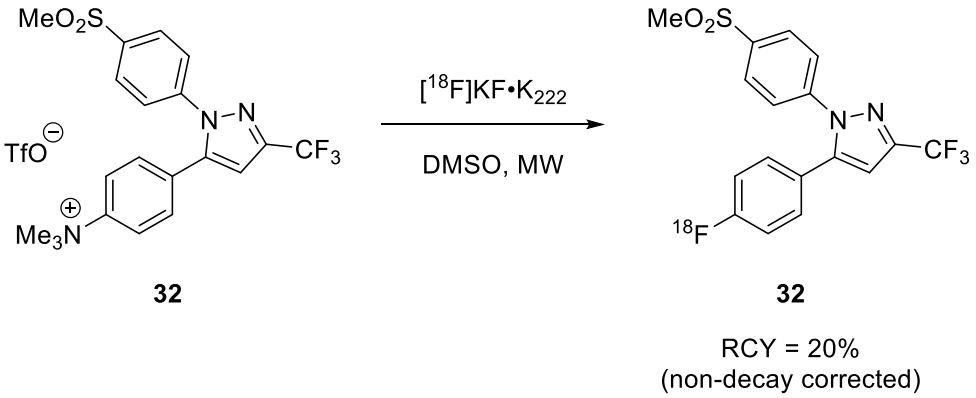

Scheme 15: Preparation of [^{18}F]SC58125 (33) *via* direct S_NAr utilising a trimethylammonium triflate leaving group

However, the use of trialkylammonium leaving groups does present a notable disadvantage *versus* some methods; the functional group is susceptible to direct nucleophilic aliphatic substitution and hence [^{18}F]S_NAr is contested by formation of [^{18}F]fluoromethane. This competing reaction is amplified with haloarenes, an observation which correlates to the low σ Hammett constants observed for haloarenes subject to *para*- substitution (Figure 21),[150] which mirrors the limited RCYs of 1-[^{18}F]fluoro-4-haloarenes described in Table 3. Whereas *para*-substituted arenes with higher σ Hammett constants correlate to a preference for [^{18}F]fluoroarene formation over the competing [^{18}F]fluoromethane side product (Figure 21).

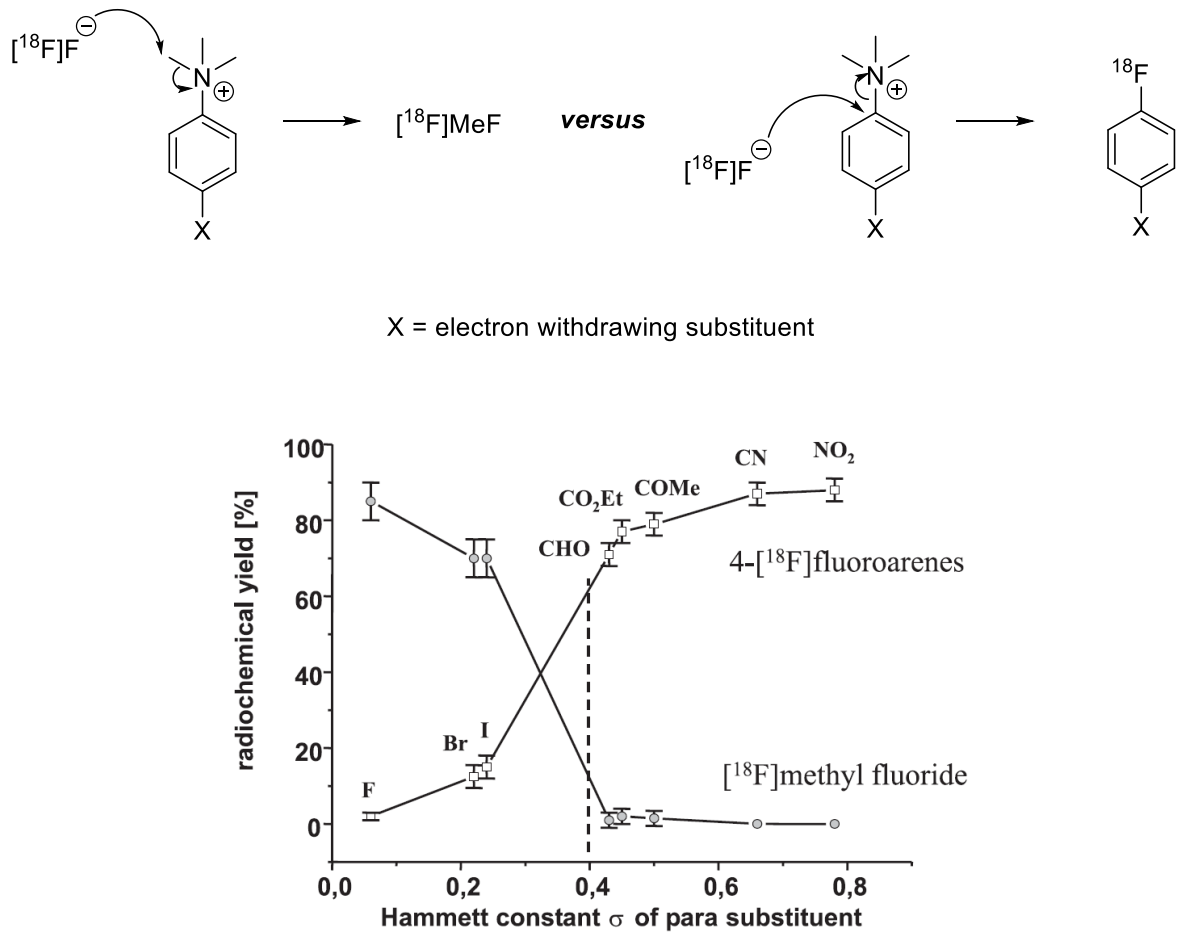

Figure 21: Competing nucleophilic aromatic substitution and nucleophilic aliphatic substitution of trimethylammonium triflates with [^{18}F]fluoride (top) and corresponding Hammett plot (bottom)[98]

The benefits of using phase transfer reagents to enhance the nucleophilicity of [^{18}F]fluoride in direct nucleophilic radiolabelling are clear, however, in doing so the potential for nucleophilic attack on other labile functionalities (as seen above) increases and results in the necessity for the application protecting groups for precursors bearing alcohols, primary amines and/or carboxylic acids. However, the subsequent deprotection, being an additional post-radiofluorination step, can only result in a reduction in product RCY.

An alternative strategy to [^{18}F]fluorination of aromatics is the preparation of [^{18}F]heteroaromatics, which when they are of sufficient electron deficiency can facilitate [^{18}F]fluorination of simple precursors *via* direct nucleophilic [^{18}F]fluorination.[151] Nucleophilic attack on mono-substituted pyridine, for example, benefits from a markedly lower LUMO energy *versus* the benzene analogue; a common feature of heteroarenes that together with the recently improved availability

of heteroaromatic pharmaceuticals, has aided popularisation of this approach to [^{18}F]fluoroheteroarenes.

Unlike standard aromatics, 2- and 4- [^{18}F]fluoropyridines are afforded without the need for a *para*- electron-withdrawing group, utilising similar leaving groups and reaction conditions (>100 °C, inclusion of a base and DMSO/DMF as solvents) as the hetero-atom-free counterparts to achieve rapid [^{18}F]S_NAr (Scheme 16). However, [^{18}F]fluorination of pyridine derivatives in the 3- position demands the use of a strongly electron-withdrawing group *para*- to the leaving group in order to progress the reaction.[152]

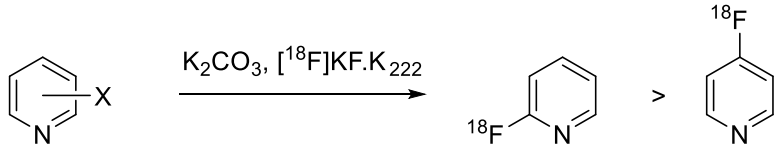

$X_{2,4} = Me_3N^+ >> NO_2 > I > Br > Cl$

Scheme 16: [^{18}F]fluorination of pyridine without the need for an electron-withdrawing substituent

The radiosynthesis of high-affinity metabolic glutamate receptor subtype 5 ($mGluR_5$) ligand **35** from 2-chloro-thiazole **34** (Scheme 17)[153] provides an example of where direct nucleophilic aromatic substitution of heteroarenes can be useful tool. [154] Here, the installation of fluorine-18 directly onto the 1,3-thiazole moiety reduces the risk of radiodefluorination that is seen with human PET studies of related compound **36**;[155] and is a considerably easier approach than preparing analogue **37** ([^{18}F]MTEB) (Figure 22),[156] both of which have also been used for preclinical imaging $mGluR_5$ receptor expression.[153]

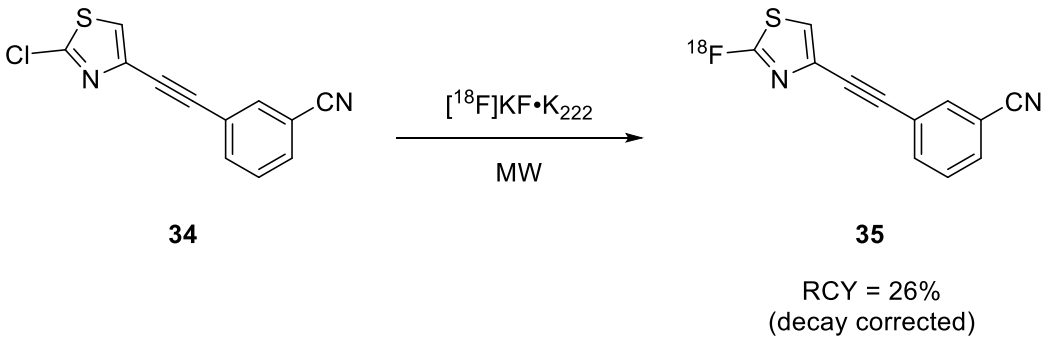

34 **35**

RCY = 26%
(decay corrected)

Scheme 17: Preparation of 2-[^{18}F]fluorothiazole 35 *via* nucleophilic aromatic substitution for use as a mGluR$_5$ ligand

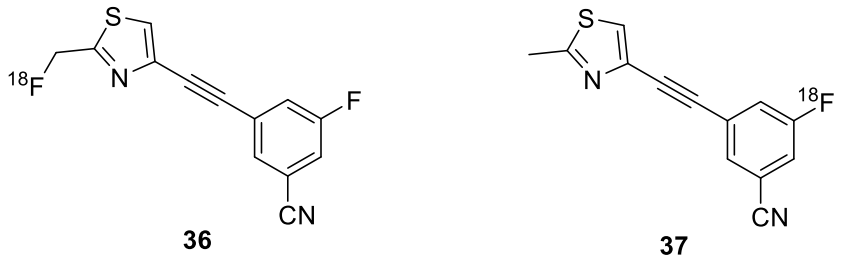

36 **37**

Figure 22: Structures of 36 ([^{18}F]SP203) and 37 ([^{18}F]MTEB), both PET ligands for mGluR$_5$ receptors with distinct limitations

This nucleophilic heteroaromatic substitution approach to **35** triumphs over the two pre-existing radioligands presented above (Figure 22) by providing a robust route to a mGluR$_5$ ligand with sub-nanomolar target affinity, over 10,000 fold selectivity for mGluR$_5$ over other metabotropic receptor subtypes and doesn't suffer from *in vivo* radiodefluorination.[153]

1.6.2.3 The Balz-Schiemann and Wallach Reactions

The preceding section describes how the use of S$_N$Ar chemistry to install fluorine-18 onto aromatic rings provides a sound strategy for the preparation of some [^{18}F]fluoroarenes, however, this approach is limited to arenes and heteroarenes with regiospecific electron-withdrawing functionality, thus negating the preparation of a huge number [^{18}F]fluoroaromatics. Two classical transformations that provide access to other regioisomers of [^{18}F]fluoroaromatics *via* dediazoniation with [^{18}F]fluoride and without the

need for S_NAr activating groups are the Wallach and Balz-Schiemann reactions.[157,158] Initial work by Wallach in 1886 highlighted an opportunity for radiochemists to achieve regiospecific incorporation of a [^{18}F]fluoride onto electron-rich arenes by exploiting the thermal decomposition of aryltriazenes in the presence of an acid catalyst (Scheme 18).[157]

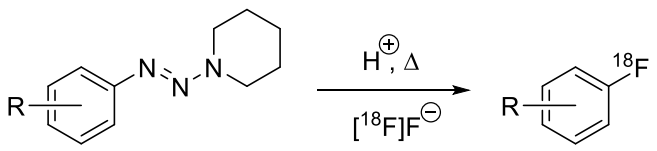

Scheme 18: The Wallach labelling reaction, most effective where R is an electron donating substituent

The RCYs of Wallach transformations are, however, often quite poor as a result of mechanistic limitation; the reaction proceeds *via* a S_N1 type route, resulting in the formation of a reactive aryl cation species which is susceptible to attack from any nucleophile in the system. This ultimately results in the production of multiple side product and as a result a reduced RCY. The radiosynthesis of [^{18}F]haloperidol **39**, a dopamine receptor ligand that allows regional mapping of brain metabolism hemodynamics, does demonstrate how this labelling method can be advantageous when a controlled reaction system is employed (Scheme 19).[159]

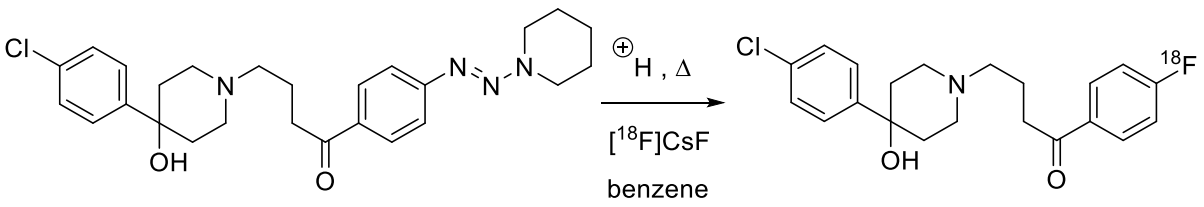

38 **39**

Scheme 19: Preparation of [^{18}F]haloperidol 39 *via* the Wallach reaction (RCY not provided)

Similarly, the application of the Balz-Shiemann reaction is accompanied by a considerable drawback in the formation of a cationic arene intermediate, which is again highly vulnerable to nucleophilic attack.[158] The reaction utilises pyrolysis of aryl

diazonium tetrafluoroborate salts in the presence of [^{18}F]fluoride to yield the product [^{18}F]fluoroarene, however, use of the BF_4^- counter-ion, in theory, limits the RCY to 25% at best, as a result of ^{19}F/^{18}F isotopic exchange, which will also greatly reduce the SA of the radiolabelled product.[98]

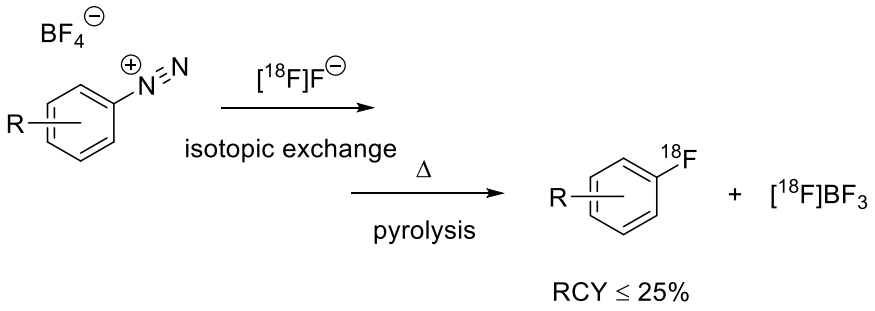

Scheme 20: Formation of [^{18}F]fluoroarenes *via* the Balz-Shiemann reaction

1.6.2.4 Newer Strategies for Fluorine-18 Incorporation

The expansion of PET into common clinical imaging practise has largely been limited by the development of robust and high-performance [^{18}F]radiolabelled pharmaceuticals beyond [^{18}F]FDG, rather than PET scanner quality or lack on demand.[160] Amongst the many challenges radiochemists face, developing new radiolabelling chemistry that coincides with the demands of radiosynthetic practise and yields highly selective target labelling, whilst maintaining high RCYs and high SA is the most demanding. However, in the last 10–15 years, the integration of other more specialised areas of chemistry into PET chemistry has allowed for the growth of new routes to radiolabelled compounds, and with better understanding of target receptors and proteins, new and improved target molecules have been elucidated. Although there has been a host of new and unconventional strategies produced, such as supramolecular PET nanoparticles,[161] multimodal PET/MRI/fluorescence imaging agents,[162] and miniaturised digital microfluidic PET chips,[163] to mention just a few, this sub-section will focus on new routes to [^{18}F]fluoroarenes relevant to the project.

Activated sulfur systems, such as triarylsulfonium salts have recently been employed to provide a strategy for S_NAr [^{18}F]fluorinations that encompasses a broad range of

substrates, without the need for activating groups.[164] This approach has been proven to provide high RCYs of substrates with numerous sensitive functionalities, such as the preparation of tetra-peptide **41** from triarylsulfonium salt **40** (Scheme 21), without the formation of the expected by-product [^{18}F]fluorobenzene, and achieved under standard [^{18}F]S_NAr conditions (*i.e.* with a base at 110 °C).[164]

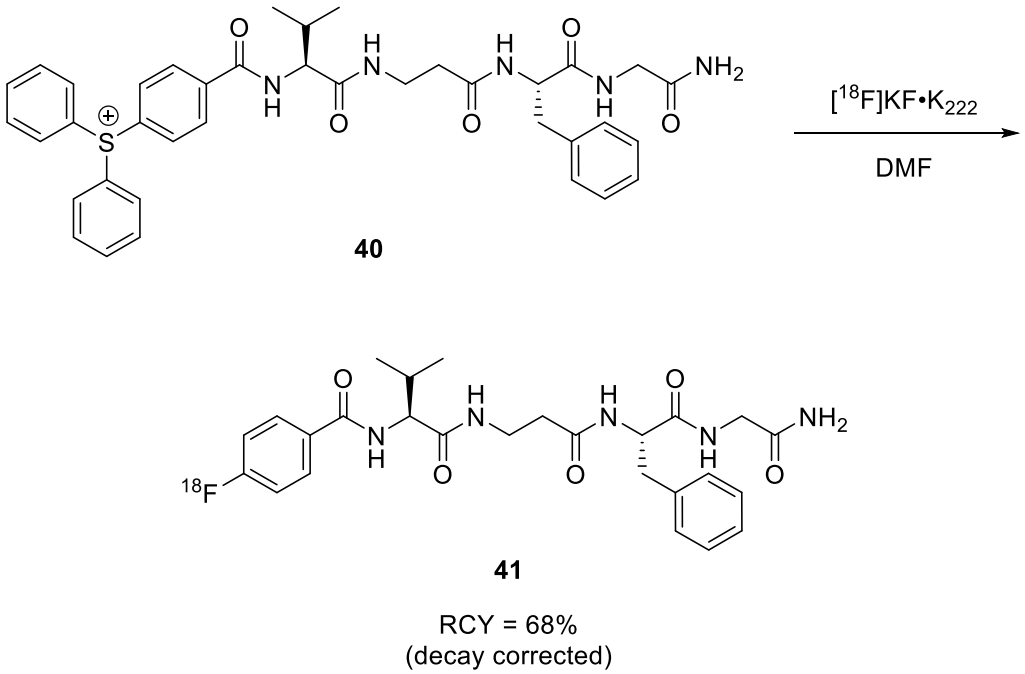

Scheme 21: Preparation of [^{18}F]labelled tetra-peptide 41 from triarylsulfonium salt 40

Through a similar approach, Chun *et al* have explored the use of diaryl sulfoxides as precursors to [^{18}F]fluoroaromatics bearing *para*-substituted electron-withdrawing groups, [^{18}F]fluorinated under relatively mild conditions.[165] Although the route is limited to substrates with electron-withdrawing functionality, the reaction proceeds within minutes and affords excellent RCYs, demonstrated by the [^{18}F]fluorination of sulfoxide **42** to selectively yield [^{18}F]fluoroarene **43** (Scheme 22).[165]

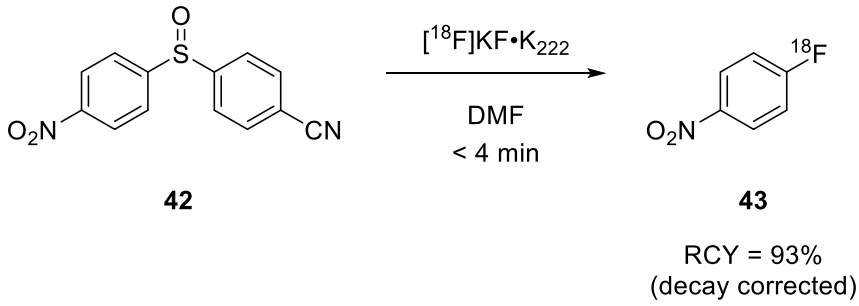

Scheme 22: High yielding [^{18}F]fluorination of a diaryl sulfoxide

Electrochemical approaches to [^{18}F]fluoroaromatics *via* potentiostatic anodic oxidation have also been exposed as potentially very useful transformations,[120] however, further work in the area is required to raise RCYs to a standard that is radiosynthetically useful.[166] This approach entails the use of an electrolytic solution of [^{19}F]$Et_3N.3HF/Et_3N.HCl$ in acetonitrile (therefore making it a carrier added process) and platinum electrodes which produces an aryl cation species, regaining aromaticity as it fluorinated with [^{18}F]fluoride.[167] [^{18}F]fluorophenylalanine derivative 45, an imaging agent suitable for imaging central motor disorders in the brain that correlate to Parkinsonian symptoms,[168] has been successfully prepared by Kienzle *et al* from protected precursor 44 *via* this electrochemical method as a mixture of regioisomers (*ortho*- 50%, *meta*- 11%, *para*- 39%) (Scheme 23).[166]

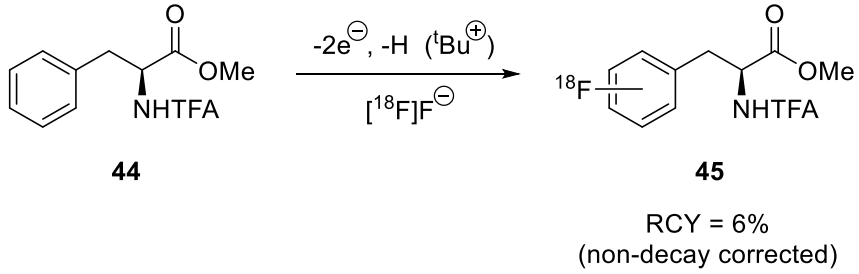

Scheme 23: Preparation of [^{18}F]fluorophenylalanine derivatives *via* electrochemical radiofluorination

More recently and so far more successfully, an umpolung approach to [^{18}F]fluorinations has accomplished some excellent progress in the field of high SA, high RCY [^{18}F]fluoroarene preparation.[120] Much of this work has been centred around the uptake of [^{18}F]fluoride into palladium based aryl complexes, which essentially affords a reactive, no carrier added source of electrophilic fluorine-18.[169] Typically, direct oxidation of fluoride into electrophilic 'F^+' is infamously challenging (for 2 F^- –>

F_2 + $2e^-$ E^0 = -2.87 volts), [170] however, Brandt *et al* conceptionalised a radiosynthetic strategy that allows for integration of the oxidant and the [^{18}F]fluoride within a high oxidation state Pd complex, where direct oxidation of the [^{18}F]fluoride is avoided.[171]

Although there are a number of plausible mechanisms discussed regarding this approach (S_N2 at fluoride, SET/fluorine atom transfer and SET/fluoride transfer/SET),[176] generally pre-synthesis of an aryl precursor-Pd complex **48** from boronic acid **47** and complex **46** under mild conditions is required, before rapid [^{18}F]fluoride capture by the palladium complex **49** yielding the electrophilic [^{18}F]F-Pd complex **50** (Scheme 24). The subsequent oxidation reaction facilities rapid fluorination of the aromatic precursor, reductively eliminating the [^{18}F]fluoroarene product, often with good RCYs, as outlined in the below scheme.[170]

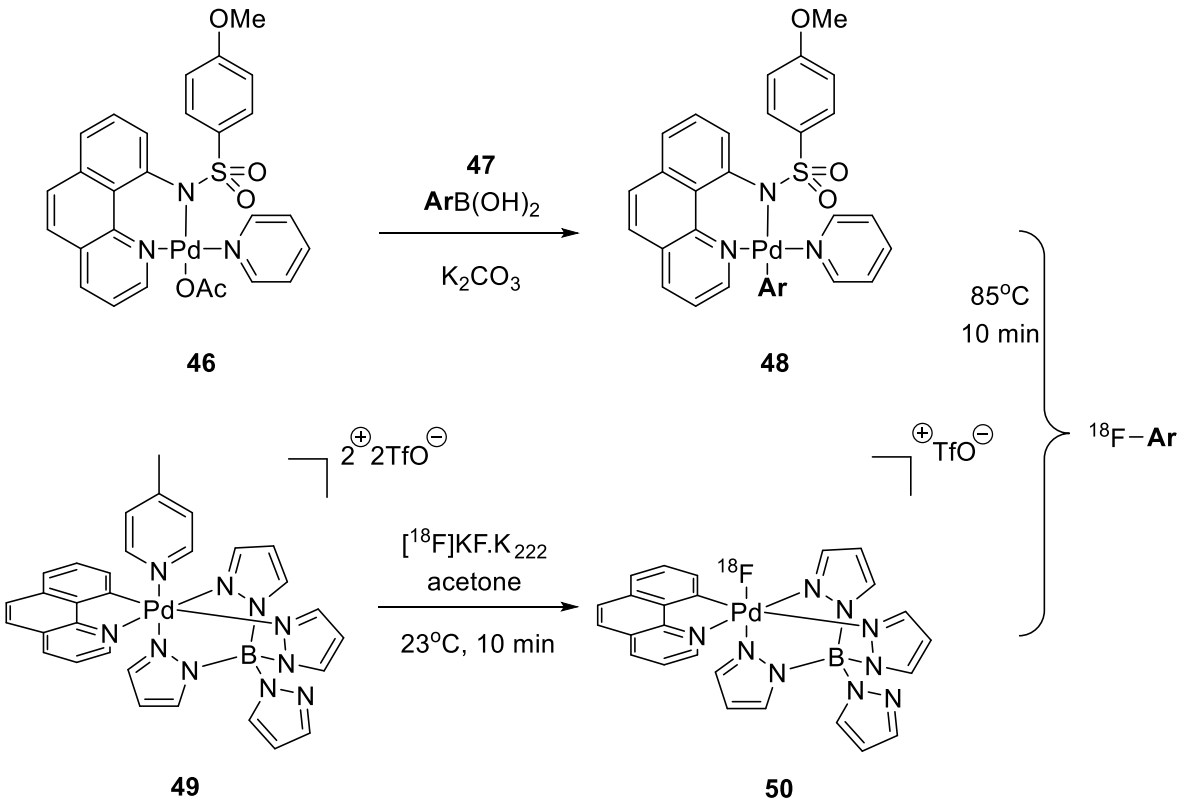

Scheme 24: Preparation of [^{18}F]fluoroarenes *via* umpolung fluoride trapping with paladium (IV) complexes and subsequent oxidative fluorination

Further work by the Ritter group utilised this innovative palladium-mediated approach to aromatic radiofluorination, which allows for highly desirable late-stage

fluorination, to afford [^{18}F]labelled deoxyestrone **52** from precursor **51** (Scheme 25),[172] a potentially useful imaging agent for estrogen receptor breast carcinomas.[173]

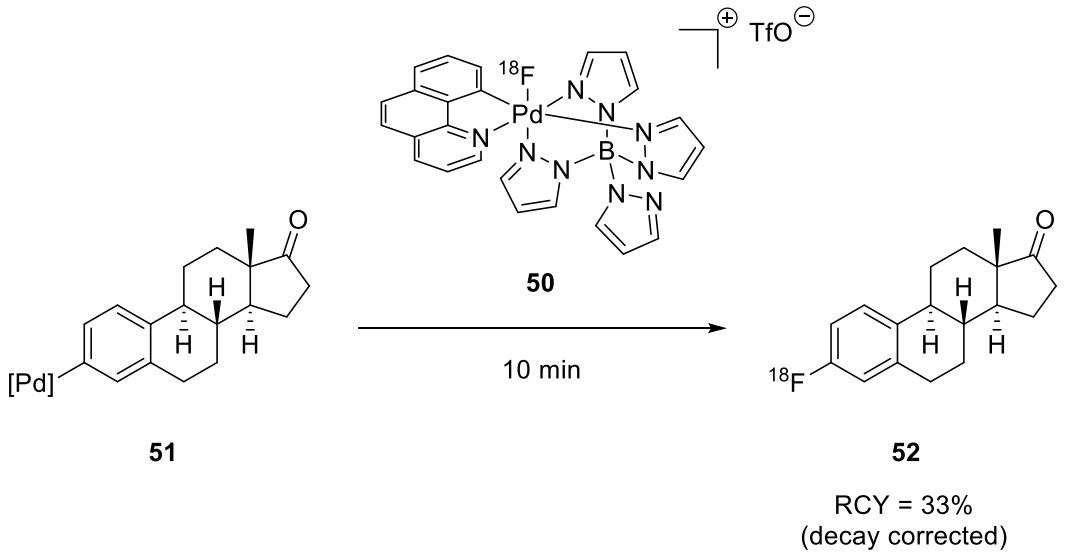

Scheme 25: Preparation of [^{18}F]deoxyestrone 52 *via* palladium mediated [^{18}F]fluorination

An alternative radiosynthetic umpolung strategy has also been developed, a route that promotes oxidative radiofluorination of electron-rich arenes,[174] a highly sought after target class given the lack of available routes to n.c.a. [^{18}F]fluoroaromatics with electron-rich character. Here, Gouverneur *et al* have provided a method of producing arene umpolungs (contrary to the [^{18}F]fluoride strategy described above) *via* oxidation, followed by direct nucleophilic [^{18}F]fluorination to afford a series of [^{18}F]fluorophenols in a one-pot protocol (Scheme 26), without the need for prior phenol protection, which thereby removes the necessity for an additional post-radiofluorination deprotection step.[174]

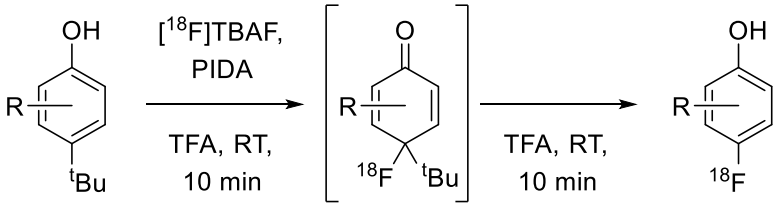

Scheme 26: Preparation of [^{18}F]fluorophenols *via* a one-pot oxidative [^{18}F]fluorination

This new route makes use of iodine (III) compound phenyliodonium diacetate (PIDA), also known as bis(acetoxy)iodobenzene, as an effective, metal-free oxidant that allows the transformation to occur rapidly under mild conditions described above (Scheme 26). The group expanded the scope of this work by including a range of functionalities in the *ortho*- and *meta*- positions, demonstrating the reactions tolerance for other reactive moieties as well as the potential for further chemical coupling and prosthetic group chemistry.[175]

Another recently developed approach to the challenge of late-stage aromatic [^{18}F]fluorination that employs the use of an oxidative transition metal process as well as another hypervalent iodine oxidant is that work by Lee *et al*.[176] This preparation involves the use of aryl-nickel complex precursors, such as **53**, that allow for nucleophilic [^{18}F]fluorination with tetrabutyl ammonium difluorotriphenylsilicate ([^{18}F]TBAT) **54** with iodine(III) reagent **55** to afford ultra-fast radiolabelling (Scheme 27). This method benefits from a reduced number of radiosynthetic steps *versus* the aforementioned two-step approach with palladium complexes,[172] as well as omitting the need for time-consuming azeotropic [^{18}F]fluoride drying, as here aqueous [^{18}F]fluoride can be used.[176]

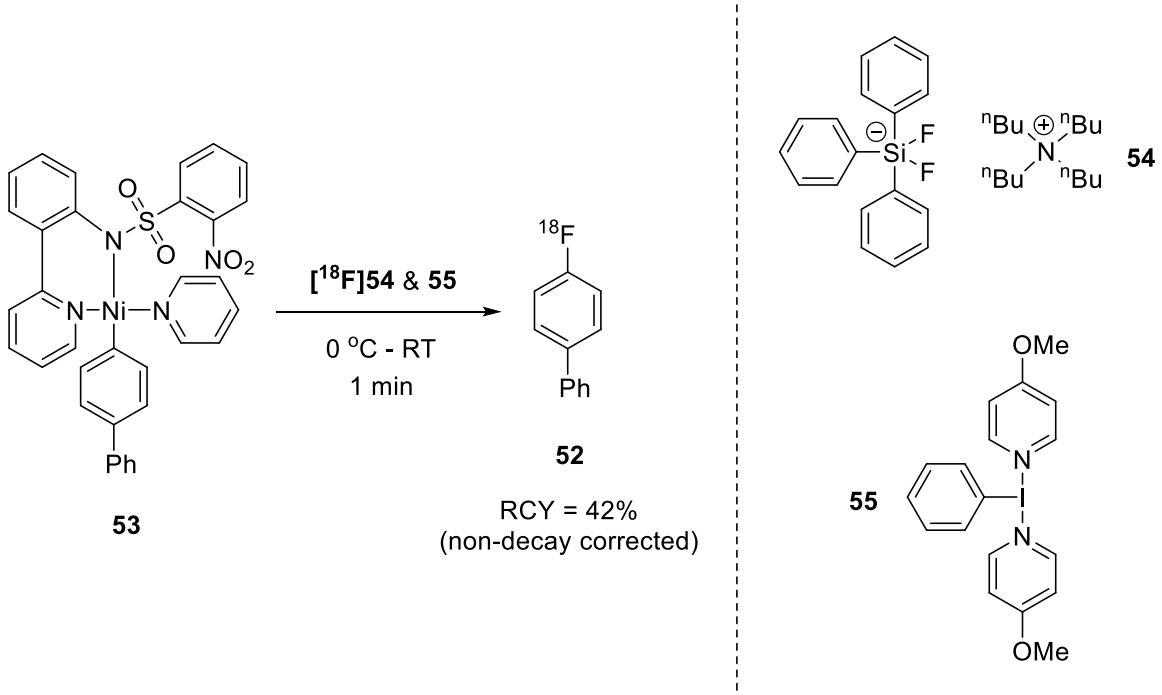

Scheme 27: Direct oxidative [^{18}F]fluorination of Ni(II)-aryl complex precursors under mild, aqueous conditions

The very fast reaction times and reduced number of post fluorine-18 incorporative steps provide a real benefit towards the radiosynthesis of [^{18}F]fluoroarenes, those features coupled with reproducibly good RCYs, such as the radiofluorination of **57** to yield [^{18}F]estrone derivative **52** (Scheme 28), make this route an excellent strategy towards [^{18}F]fluoroarene production.[176]

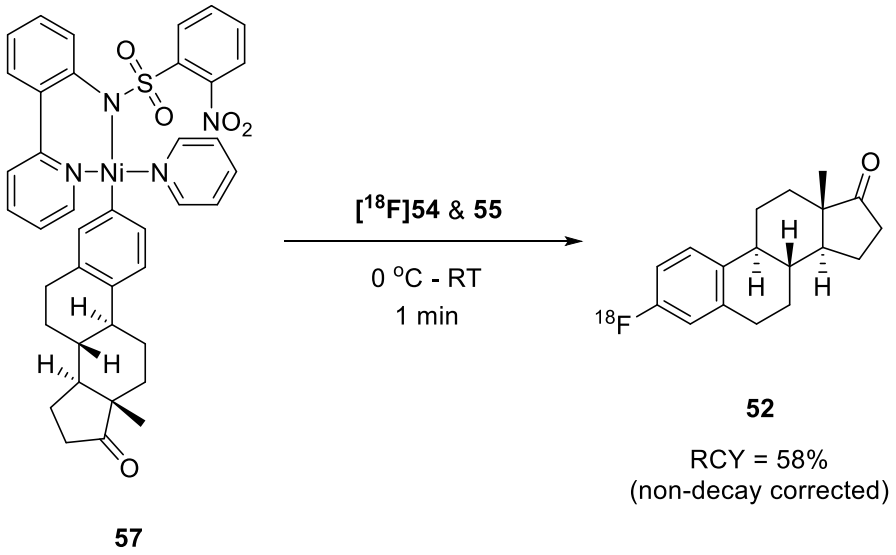

Scheme 28: Preparation of [^{18}F]deoxyestrone 52 *via* nickel mediated [^{18}F]fluorination

Many of the approaches described above are limited to aromatics with activating moieties and specific electronic character; require extensive and complex precursor synthesis; are restrained by substrate functionality; or result in poor RCYs and/or low SA. Although methods utilising transition metals present an attractive means to achieve late stage radiofluorination of complex precursors, in the practice the metal-carbon bond is highly prone to protolysis and application of these organometallic precursors in radiofluorination can result in the production protio- by-products. And given that the protio- and [^{18}F]fluoro- products will be bioisosteres of one another and thereby difficult to separate, they will competitively target the same receptor and ultimately result in a lower virtual specific activity (as opposed to typical specific activity as an artefact of [^{18}F]/[^{19}F] competition).

The application of diaryliodonium salts presents an opportunity to achieve n.c.a. [^{18}F]fluoride incorporation on aromatic systems, without the need for prior activation and without regiospecific constraints *via* a one-step radiofluorination that typically

affords high RCYs and high SA.[98] The first published use of diaryliodonium salts for this purpose was provided by Pike *et al* in 1995,[177] where the group prepared a range of simple symmetric and asymmetric diaryliodonium salts (Scheme 29), with a range of counter-ions and investigated the outcome of radiofluorination with [^{18}F]fluoride.

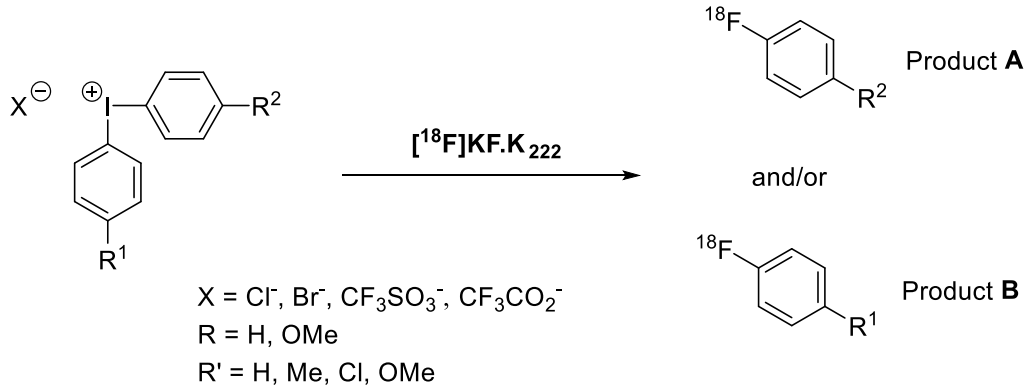

Scheme 29: Nucleophilic [^{18}F]fluorination of diaryliodonium salts

The study highlighted the value of diaryliodonium salts as a versatile, late-stage n.c.a. radiofluorination strategy and provided preliminary information on the effect of counter-ions and substituents on the resulting [^{18}F]fluoroarenes, which some of the key outcomes summarised below (Table 4).[177]

Precursor Diaryliodonium					**Distribution of Product [^{18}F]Fluoroarenes**	
R	**R'**	**X⁻**	**Conditions**	**RCY**	**% A**	**% B**
H	H	Cl^-	110 °C, 35 min	78%	100	
H	H	$CF_3SO_3^-$	110 °C, 35 min	15%	100	
H	Me	$CF_3SO_3^-$	85 °C, 40 min	68%	60	40
H	Cl^-	$CF_3SO_3^-$	110 °C, 35 min	14%	40	60
H	OMe	Br^-	110 °C, 35 min	35%	100	0
H	OMe	Br^-	85 °C, 40 min	88%	100	0

Table 4: Summary of n.c.a. [^{18}F]fluorinations of diaryliodonium salts by Pike *et al*, demonstrating RCY and product distribution dependence on reaction conditions, the choice of counter-ion and the electronic nature of aromatic substituents[177]

This initial investigation into diaryliodonium precursors paved the way for much more work in the area, including numerous mechanistic studies into the reaction of diaryliodonium salts with nucleophiles; development of many diaryliodonium salt precursors to existing and new [^{18}F]fluoroaromatics bearing imaging agents; and augmentations of the fluorination reaction such as those using iodonium ylide precursors and transition-metal catalysed fluorinations.[178,179,180]

The preparation of benzodiazepine receptor marker [^{18}F]DAA1106 **59** from diaryliodonium salt **58** provides an excellent example as to how the iodonium approach to nucleophilic [^{18}F]fluorination can allow for direct regiospecific n.c.a. radiofluorination, with a precursor bearing sensitive functionality and afford both selectivity for the target ring systems and a high RCY (Scheme 30).[181] Here the resulting ratio of the two possible [^{18}F]fluoroarenes exhibits a major preference for the target ring; 71:29 **[^{18}F]59**: 4-[^{18}F]fluoroanisole. Substitution of the 4-methoxybenzene moiety in precursor **58** for unsubstituted benzene resulted in a substantial reduction in the RCY of **59** (RCY = 3%), highlighting the necessity for an electron-rich aromatic in this site, given the electron-rich nature of the target.[181]

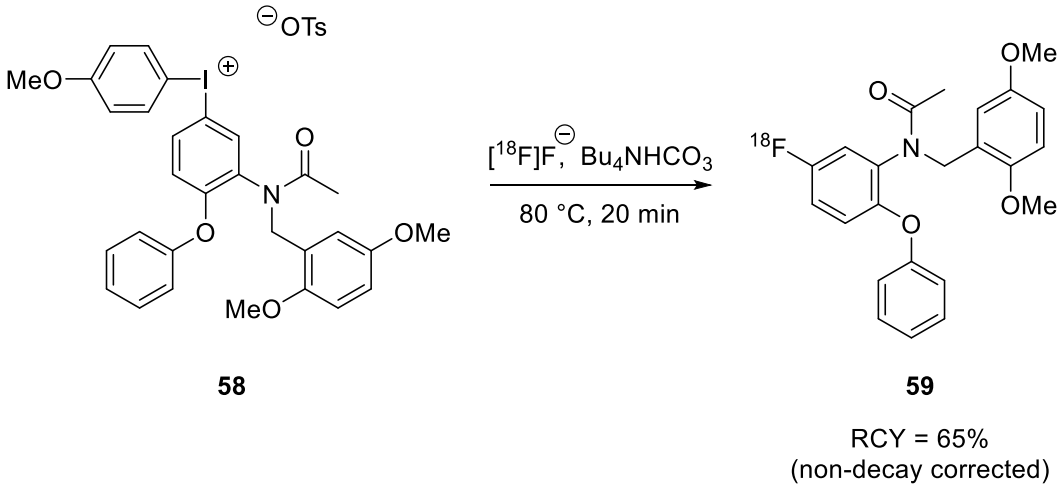

58 **59**

RCY = 65%
(non-decay corrected)

Scheme 30: Preparation of [^{18}F]DAA1106 59 *via* nucleophilic [^{18}F]fluorination of diaryliodonium salt precursor 58

Given the relevance of diaryliodonium salt precursors to the main study of this thesis, further discussion on the synthesis of hypervalent iodine reagents; the chemistry

surrounding these compounds and their application in the preparation of electron-rich [^{18}F]fluoroarenes can be found in Chapter 2.

Recent developments in the area of diaryliodonium salts towards the production of electron-rich [^{18}F]fluoroarenes includes work on the aforementioned iodonium ylides,[180] which when prepared as dicarbonyl or (PhIC(COR)$_2$)[182] or sulfonyl (PhIC(SO$_2$R)$_2$)[183] derivatives are sufficiently stable to permit applications in various applications, including carbine synthesis.[184] Although unsubstituted dicarbonyl(phenyl)iodonium ylids are inherently unstable and poorly soluble in most solvents, introduction of electron-donating substituents on the systems aryl ring, particularly in the *ortho* position, improves stability of the precursor and allows for practical application in common solvents.[180] Iodonium ylides exhibit very similar hypernucleofugic reactivity to diaryliodonium salts when presented with an appropriate nucleophile and x-ray crystal structures have shown that they also afford a close to 90° C-I-C bond angle between the aryl and stabilised carbanion components, confirming their equivalence to diaryliodonium salts and agreement with the hypervalent iodine(III) model.[185]

Here the use of Meldrum's acid as the preferred malonate ester has seen regular use a substrate for iodonium ylid preparation, which are can be coupled with (diacetoxy)iodoarenes or utilised in one-pot procedures with an appropriate oxidant and the substrate iodoarene to afford the target ylid. The latter method has been applied to the preparation of iodonium ylid **61** from protected iodoarene **60** (Scheme 31), which was subsequently fluorinated to afford neuroendocrine tumour (NET) and serotonin transporter (SERT) imaging agent 3-[^{18}F]FPPMP **62**.[186]

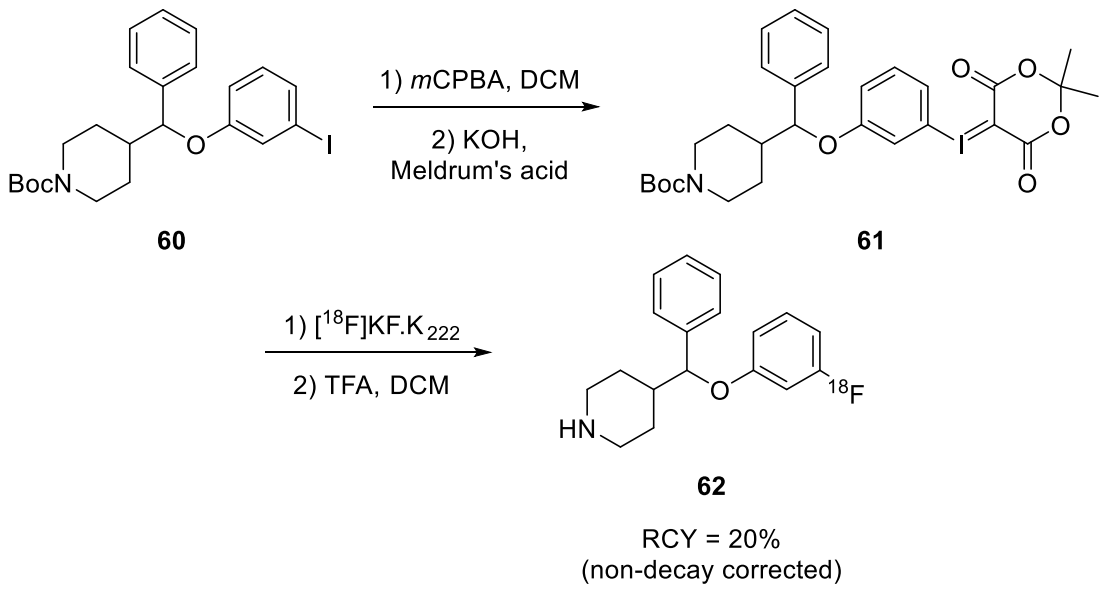

Scheme 31: Preparation of [^{18}F]FPPMF 62 *via* nucleophilic [^{18}F]fluorination of iodonium ylid 61, which was prepared by a one-pot procedure from 60

The widespread adoption of iodonium ylides as precursors to electron-rich [^{18}F]fluoroarenes has been relatively slow however, potentially as a feature of the poorly reproducible one-pot preparation utilised or the challenge of preparing the (diacetoxy)arenes involving sensitive or complex functionality when preparing iodonium ylides *via* the step–wise approach.[180] Some groups have also reported difficulty in the numerous by-products produced in the iodonium ylid reaction from the [^{18}F]fluorinated product, hence posing a threat to the SA of the resulting imaging agent.[186]

1.7 Fluorine-18 Labelling with Prosthetic Groups

For the fluorine-18 radiolabelling of small molecules direct incorporation of nucleophilic [^{18}F]fluoride is generally preferred, however, larger molecules and/or those bearing multiple sensitive functionalities are often unsuitable for direct fluorination. Here, the application of radio-labelled 'tagging' molecules, termed prosthetic groups, is more appropriate for [^{18}F]fluorination of macromolecules such as aptamers and oligonucleotides, as well as for labelling small molecules incompatible with direct fluorination conditions.[133] A prosthetic group is defined as a

pre-[^{18}F]radiolabelled small molecule bearing a reactive functionality that allows the molecule to be rapidly incorporated into another structure, usually under mild conditions.

The use of [^{18}F]radiolabelled bioactive macromolecules are rapidly gaining popularity over small molecule imaging agents for a number of reasons, firstly the application of non-labelled oligomers within therapeutics is already well known and very effective, often providing very high target specificity and nanomolar potency.[187] This highly specific nature of therapeutic macromolecules also reduces the likelihood of interacting with other biological processes and therefore diminishes the risk of side effects; and their functionality is a direct feature of their complex structure, something that small molecules struggle to convincingly mimic. The body is also drastically more familiar with biomolecules, than it is to alien small molecules with unnatural pharmacophores and hence is less likely to produce an aggressive immune system response to a bioactive macromolecular drug.[187] Thereby PET imaging with [^{18}F]fluorinated biomolecules presents an attractive alternative to traditional small molecule approaches.

In terms of commercialisation, macromolecular therapeutics generally benefit from faster FDA/EMA approval than small molecules; possessing unique structural qualities and exclusive functionality makes the patenting of specific proteins for a specific applications a very attractive prospect.[188] As is commonly seen with the development of therapeutic trends, the continued development of peptide-based treatments is catalysed by the continued growth of the market, which coupled with their ever increasing success rate (now over 35%, which is better than that of small molecules),[189] makes the sustained growth of peptide based drugs; and by extension [^{18}F]fluorinated biomolecules, a very likely scene.[190]

Although there are a handful of examples that describe successful direct [^{18}F]radiolabelling of biomolecules,[191,192,193] biomolecules largely undergo hydrolysis/decomposition when subject to direct radiofluorination conditions; hence [^{18}F]fluorination *via* modular synthesis provides a more feasible route to [^{18}F]labelled biomolecules. With much of the focus of prosthetic group development directed towards the radiolabelling of biomolecules, a wide number of strategies have been developed that allow for tagging macromolecules bearing commonly occurring

moieties, such as amines, thiols, and suitably reactive carbonyl groups, making each prosthetic group strategy instantly widely applicable.[97]

Figure 23 provides a handful of commonly utilised prosthetic group strategies used to radiolabel biomolecules, however, the literature can offer a vast number of alternative approaches,[97,122,133] many of which are beyond the scope of this work, but some key examples will be highlighted in coming sub-sections.

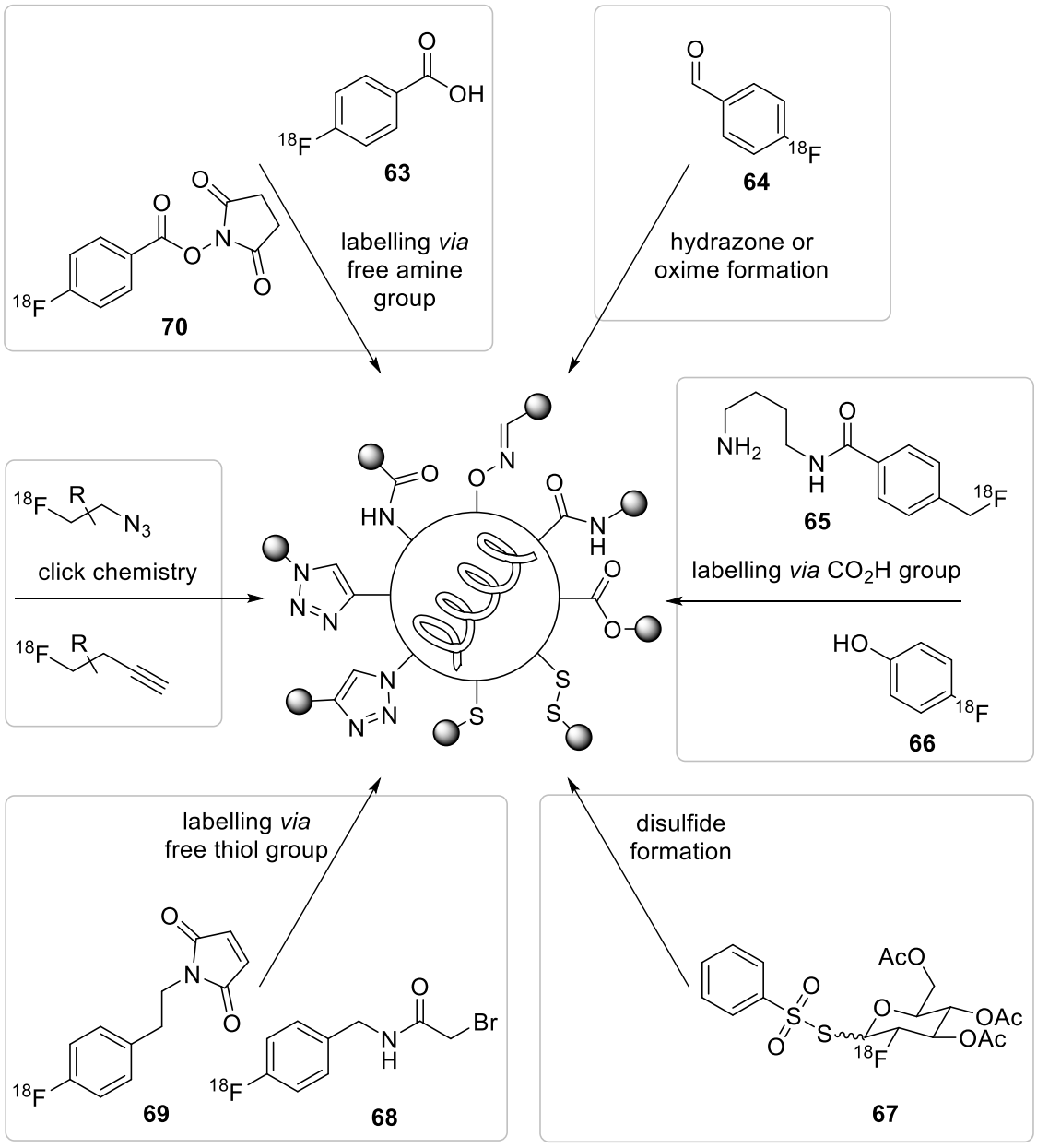

Figure 23: An overview of various prosthetic groups for [^{18}F]labelling of bioactive macromolecules, many of which are also applicable to modular build up small molecule targets. (R = alkyl or aryl linker)[133]

One commonly employed prosthetic group based radiolabelling strategy not illustrated above (Figure 23) is [^{18}F]fluoroalkylation, which has been described in an earlier section (Section 1.6.2.1) in the application of 2-[^{18}F]fluoroethyltosylate **26** for indirect small molecule labelling, in which it has a wide number of applications.[194] Similarly, 2-[^{18}F]fluoroethyltosylate has been utilised in simple peptide labelling, such as prostate specific membrane antigen (PSMA) ligand **72** ([^{18}F]FEt-Tyr-urea-Glu) from precursor **71** (Scheme 32).[195] The simplicity of this modular labelling strategy allows for rapid incorporation and a high RCY, demonstrating the capability of biomolecule [^{18}F]fluoroethylation, which is often less controlled with larger peptides bearing multiple reactive functionalities.[196]

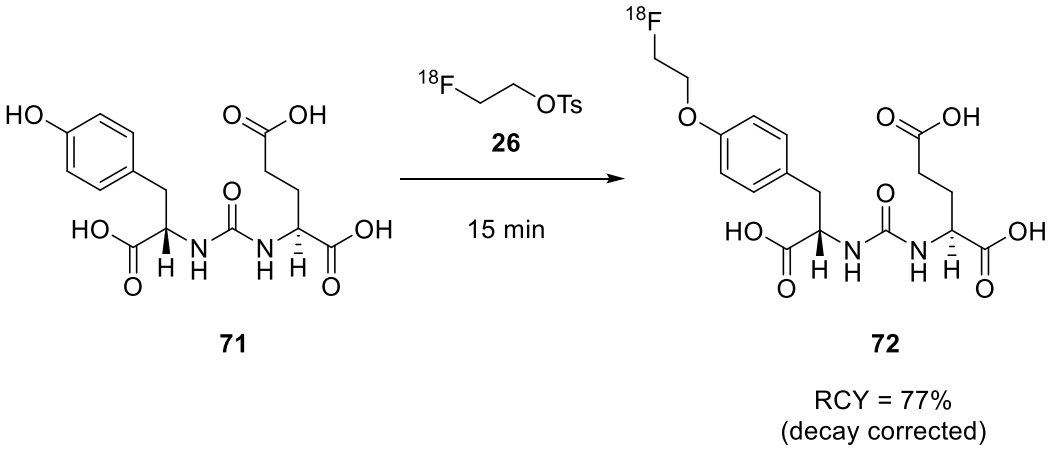

Scheme 32: Preparation of [^{18}F]FEt-Tyr-urea-Glu ([^{18}F]FEtTUG) *via* [^{18}F]fluoroethylation of precursor 71

[^{18}F]Fluoroalkylation chemistry can also be extended to the use of [^{18}F]trifluoroalkyl prosthetic groups, which have recently come into precedence for providing effective *N*-, *S*- and *O*-[^{18}F]fluoroethylations (as well as [^{18}F]fluoromethylations and [^{18}F]fluoropropylations). This resourceful approach allows for the direct [^{18}F]fluorination of difluorovinylsulfonate to yield [^{18}F]fluoro-2,2-difluoroethyltosylate, which was then subsequently used to radiolabel a number of nucelophile bearing precursors.[197]

1.7.1 Amine Reactive Prosthetic Groups

Numerous research groups have exploited the work of peptide chemists in utilising amide bond formation to couple free amine groups within peptides and amine-terminated oligonucleotides with various [^{18}F]labelled prosthetic groups, often manipulating coupling agents and global protection strategies to achieve rapid [^{18}F]radiolabelling under very mild conditions.[198,122]

N-Succinimidyl 4-[^{18}F]fluorobenzoate ([^{18}F]SFB) **67** is one amine reactive prosthetic group that has proven to be a very popular approach to peptide,[199,200] however, preparation of the prosthetic group is far from trivial and most preparations require a multi-step synthesis including post-[^{18}F]fluorination conversions (Scheme 33).[201]

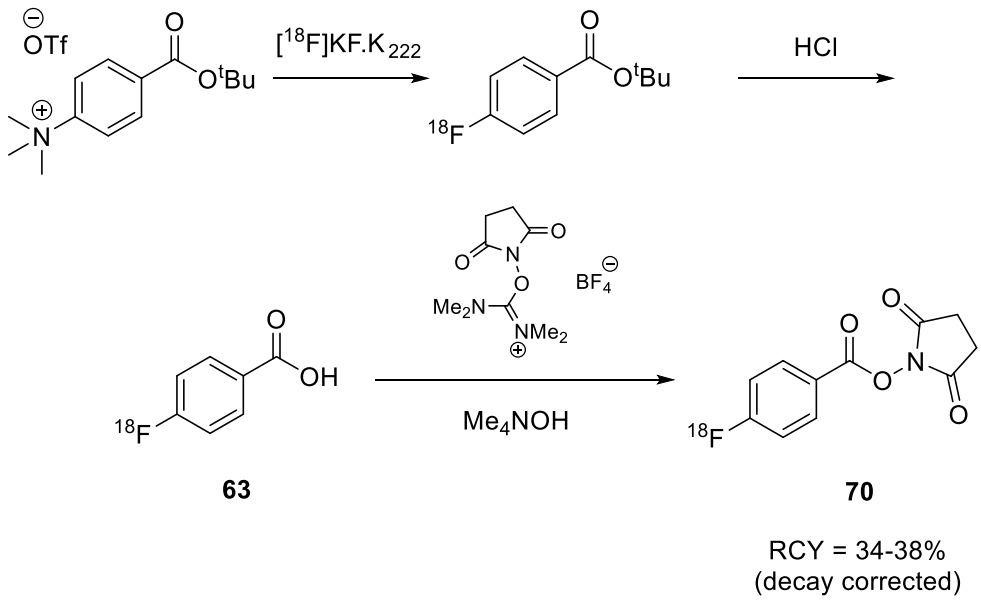

Scheme 33: Modular preparation of [^{18}F]SFB *via* nucleophilic aromatic substitution of a trimethylammonium aryl precursor followed by additional steps.

Many other amine reactive prosthetic groups utilise the [^{18}F]fluorobenzoyl moiety in a similar fashion, including 4-[^{18}F]fluorobenzoic acid **63**, 4-[^{18}F]fluorobenzaldehyde and *N*-succinimidyl-4-([^{18}F]fluoromethyl)benzoate,[202,203] to produce a highly stable [^{18}F]radiolabelled amide-macromolecule link, further benefitting from the increased metabolic stability of the [^{18}F]fluoroarene label. The dimeric cyclic RGD (arginylglycylaspartic acid) peptide E[c(RGDyK)]$_2$ **73** (Figure 24) has been effectively

radiolabelled in this manner in a RCY of 20–30% (from [^{18}F]SFB, n=3) and allows for glioblastoma imaging thanks to high tumour uptake and prolonged cellular retention.[204]

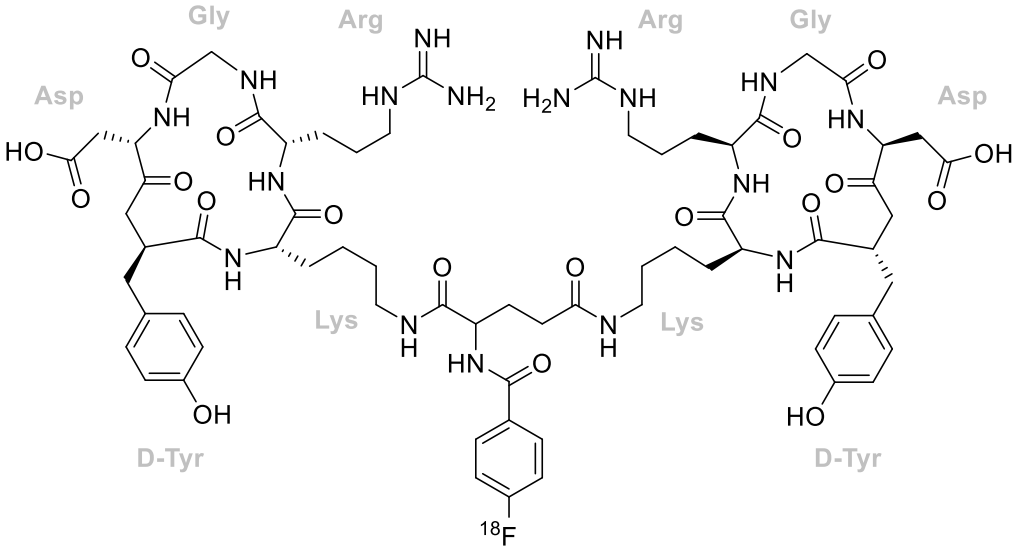

73

Figure 24: [^{18}F]FB-E[c(RGDyK)]$_2$; a demonstration of macromolecule radiolabelling *via* acylation of the peptide amino group with [^{18}F]SFB

In a very similar approach, the use of 4-[^{18}F]fluorobenzaldehyde ([^{18}F]FBA) **64** as a prosthetic group for biomolecules terminated with aminooxy functionality, to form oxime linkers has been well explored,[205,206] as has the application of [^{18}F]FBA for producing hydrazone linkers when reacted with hydrazinyl-terminated macromolecules.[207] The preparation of oncology target [^{18}F]FBOA-minigastrin **74** (Scheme 34, left) *via* the former method yields the radiolabelled peptide in an excellent RCY of 90% within 15 min (from [^{18}F]FBA);[205] whereas the later hydrazone linker strategy has been applied to the formation of blood-pool imaging agent [^{18}F]fluoro hydrazinonicotinicacid-human serum albumin conjugate ([^{18}F]HYNIC-HSA) **75** (Scheme 34, right), with RCYs reported to be in a very similar range.[207]

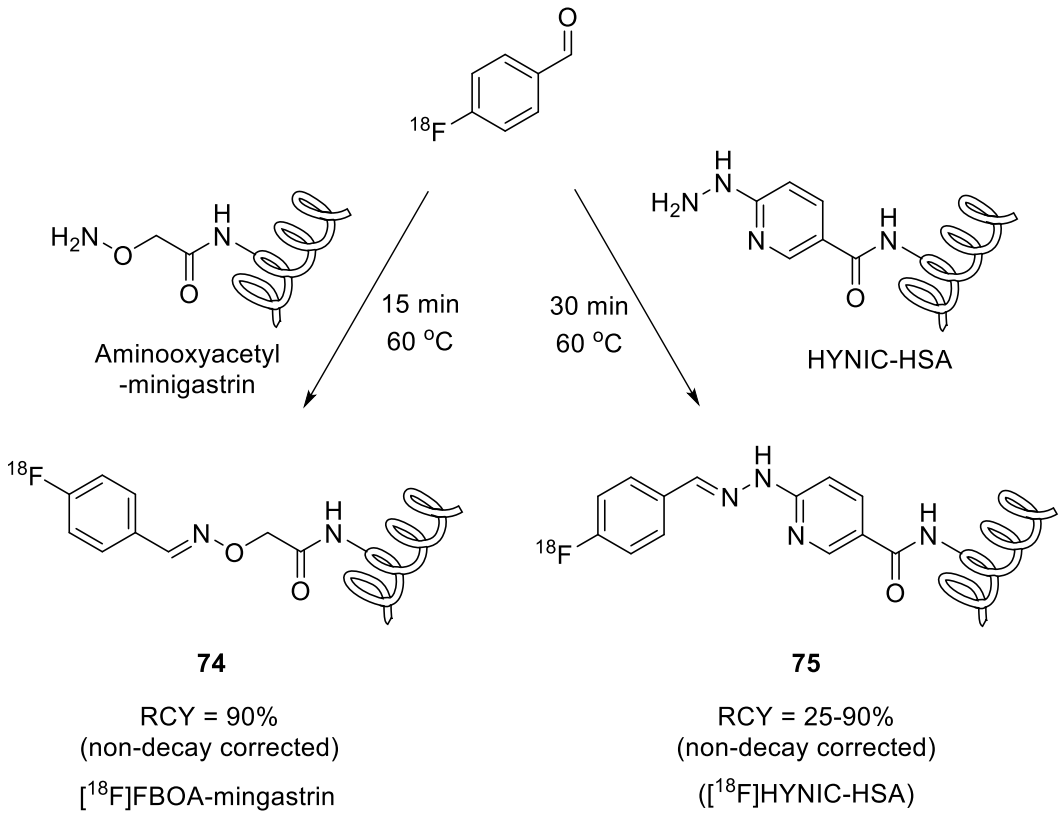

Scheme 34: Two examples of rapid and effective peptide radiolabelling with the prosthetic group [^{18}F]FBA *via* oxime formation (74) and hydrazone formation (75)

1.7.2 Thiol Reactive Prosthetic Groups

Thiol-bearing cysteine residues are commonly seen within peptides and proteins, their presence provides a distinct handle for prosthetic group radiochemistry. The inclusion of multiple cysteine units within a macromolecule also often sees the formation of disulfide bridges, another functionality that radiochemists can exploit to incorporate [^{18}F]fluoroaromatic tagging groups.[122] A wide number of thiol reactive prosthetic groups have been developed, including [^{18}F]fluorophenacyl bromide ([^{18}F]FPB), *N*-(4-[^{18}F]fluorobenzyl)-2-bromoacetimide ([^{18}F]FBnBrA **68**, 4-([^{18}F]fluorophenyl)maleimide ([^{18}F]FPM) and ([^{18}F]fluorobenzamido)ethyl maleimide ([^{18}F]FBEM) **69**, many of which make use of the maleimide moiety to achieve thiol specificity.[208,209,210]

One of the more popular examples, [^{18}F]FBEM **69**, is prepared *via* coupling of *N*-(2-aminoethyl)maleimide with [^{18}F]SFB **70** (Scheme 35), despite the inclusion of this additional post-^{18}F-incorporation step the prosthetic group has been used to label

sulfhydryl-RGD peptides to yield analogues of [^{18}F]FB-E[c(RGDyK)]$_2$ **73** in similarly high RCYs (RCY = 85%) in just 20 min.[209]

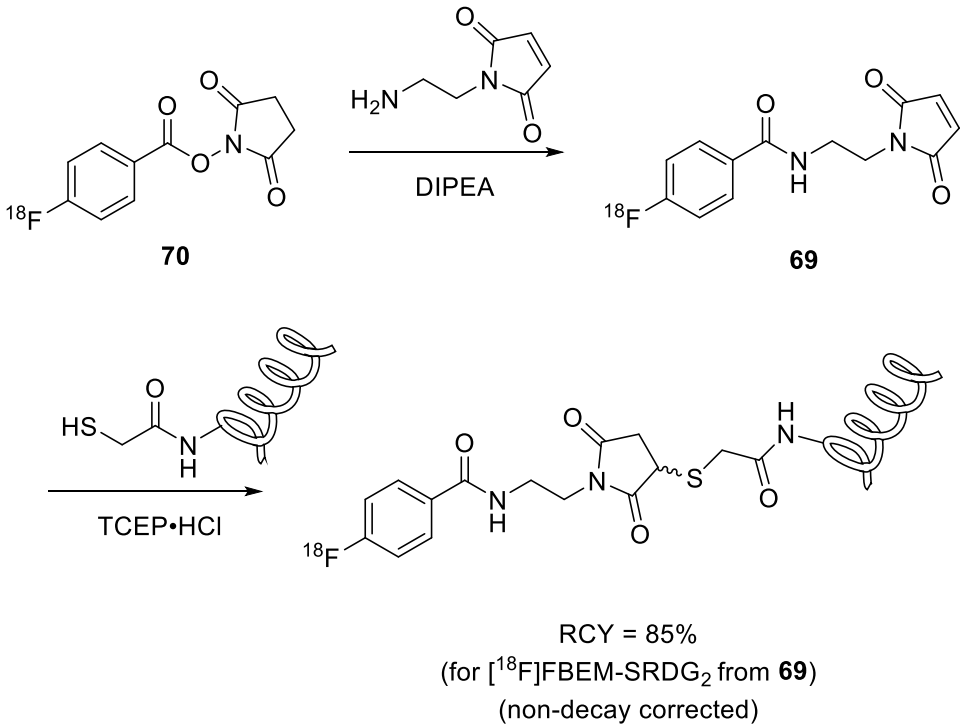

70 69

Scheme 35: Preparation of [^{18}F]FBEM 66 from [^{18}F]SFB 67 and subsequent coupling with sulfhydryl-RGD peptides

Phosphorothioate monoester functional groups which are often commercially available end groups of oligonucleotides can be selectively alkylated with the haloacetimide prosthetic group [^{18}F]FBnBrA **68**, thus omitting the need for biomolecule functionalisation prior to radiolabelling and reducing the need for additional purification steps, which is often a challenge with macromolecules. This approach has seen successful application in the mild and rapid radiolabelling of 18*mer* oligonucleotide **76** to afford ^{18}F-tagged oligonucleotide **77** by Kühnast *et al* (Scheme 36).[211]

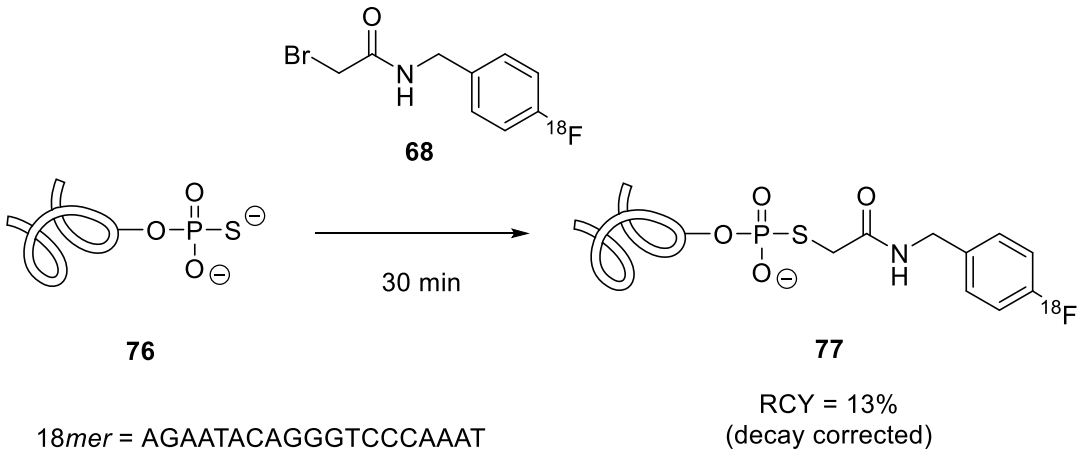

Scheme 36: Prosthetic group tagging of an oligonucleotide phosphorothioate monoester group using [^{18}F]FBnBr 68

[^{18}F]Fluorinated glycosyl phenylthiosulfonates, such as prosthetic group **67** have been introduced as appropriate glycosyl donors for the glycoconjugation of thiol containing peptides and proteins.[212] Prante *et al* have demonstrated the efficiency of this peptide labelling strategy in the radiosynthesis of [^{18}F]CAKAY ([^{18}F]C(S,S'-Ac_3-FGlc)AKAY) **79** (Scheme 37), a model pentapeptide to demonstrate substrate potential, achieving a RCY of 95% in a mere 15 min.[213]

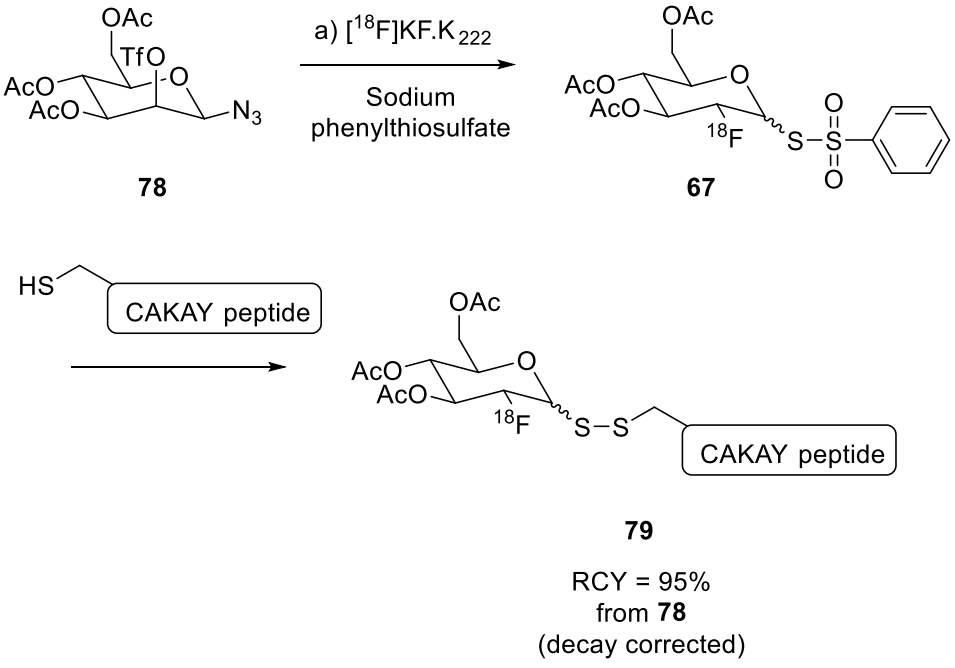

Scheme 37: Preparation of pentapeptide [^{18}F]CAKAY 77 *via* [^{18}F]glycosylation using fluorine-18 labelled glycosyl phenylthiosulfonate 67

1.7.3 Click-Chemistry Approaches to Fluorine-18 Labelling

Bioorthogonal approaches to modular build up, such as some click chemistry strategies have also proven to be highly successful methods of prosthetic labelling, particularly because such systems are intended to be rapid, highly selective and are typically conducted in mild, biological environments.[97] These efficient copper-catalysed click reactions allow for the formation of very stable 1,4-disubstitued 1,2,3-triazoles at ambient temperatures and provide a highly robust means for the incorporation of [^{18}F]fluoroalkyl/aryl azides and alkynes into appropriate biomolecules.[214] Despite the inherently reactive nature of azides and alkynes, they are usually inert to biological species and hence this orthogonality removes the need for protecting groups, making their application very convenient.[215]

An excellent example of this copper-catalysed azide alkyne cycloaddition (CuAAC) method of radiofluorination is provided in the preparation of [^{18}F]labelled folic acid derivative **82**, utilising 6-[^{18}F]fluorohexyne **81** (Scheme 38) by Ross *et al*.[216] Achieving RCYs as high as 35% and radiochemical purity of >99% for the complete radiosynthesis of **82** allowed the group to apply the radiolabelled biomolecule to mice bearing folate receptor(FR)-expressing KB tumours.[216]

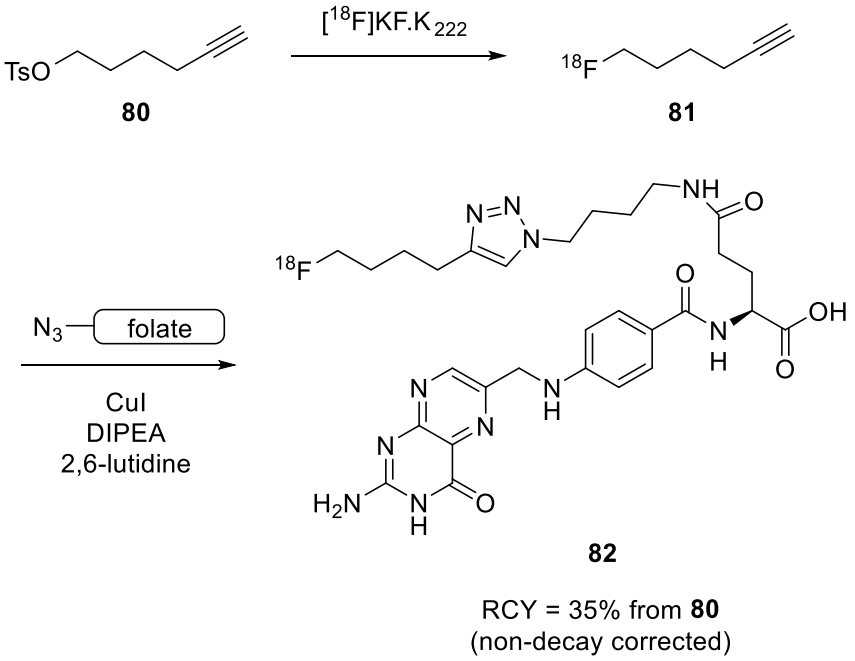

Scheme 38: Preparation of [^{18}F]-labelled folic acid derivative *via* copper-catalysed click chemistry using a 6-[^{18}F]fluorohexyne prosthetic group

The inverse approach, the employment of an azide bearing prosthetic group for coupling with a propargyl-terminated biomolecule has also been explored extensively, such as in common use of [^{18}F]FDG azide derivative **84** for targets such as [^{18}F]FRGD type peptides or [^{18}F]labelled neurotensin derivatives (Scheme 39). The application of this [^{18}F]fluorodeoxyglcosylation prosthetic group strategy has shown to benefit from good blood clearance and stability in $\alpha_v\beta_3$-integrin expressing tumours, thus prolonging the PET imaging window.[217]

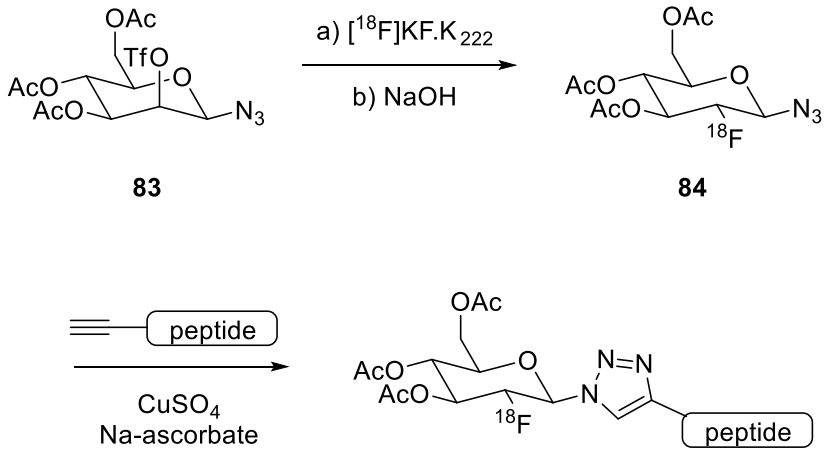

Scheme 39: [^{18}F]glycosylation *via* a click chemistry approach using [^{18}F]fluoro-mannopyranosyl azide 84

Although a large number of innovative click-based routes to fluorine-18 prosthetic group radiolabelling have been developed, only one target, [^{18}F]FRGD-K5 has made it as far as clinical trials.[214] This likely to be an artefact of the potentially cytotoxic nature of copper catalysts utilised in the 1,3-dipolar Huisgen cycloadditions described above and hence a demand for metal-free click reactions for use in PET chemistry is desired. Other related approaches to click-based incorporations of prosthetic groups include strain-promoted alkyne-azide cycloaddition, where this need for a metal catalyst is removed by introducing strain on the alkynyl systems increasing their reactivity towards terminal azides;[218] and Staudinger Ligation, a method of utilising *in situ* formation of an aza-ylide *via* hydrolysis of an iminophosphorane species produced by the reaction of an azide and a phosphine group. The nucleophilic aza-ylide can then be captured by an ester moiety (or other electrophilic trap) to form a covalent adduct, capable of forming a stable amide bond upon rearrangement.[219,220]

1.7.4 Transition-metal Catalysed Cross-coupling Prosthetic Groups

Another important class of indirect [^{18}F]fluorination reactions includes the use of transition-metal mediated coupling reactions, many approaches of which are likely to be a consequence of the palladium-catalysed cross-coupling reactions bloom initiated by the 2010 Nobel Prize in Chemistry awarded to Heck, Negishi and Suzuki.[122] Although the use of cytotoxic metals in pharmaceutical production is generally avoided, the scope for rapid formation of C-C bonds is too attractive a concept to be ignored and many groups have developed strategies that utilise this strategy very effectively.

Here, the application of diaryliodonium salt chemistry has proven to be useful direct method of preparing 4-[^{18}F]fluoro-1-iodobenzene,[221] an exceptionally useful prosthetic group for palladium-catalysed Sonogashira,[222] Suzukhi[223] and Stille coupling reactions (Scheme 40).[224]

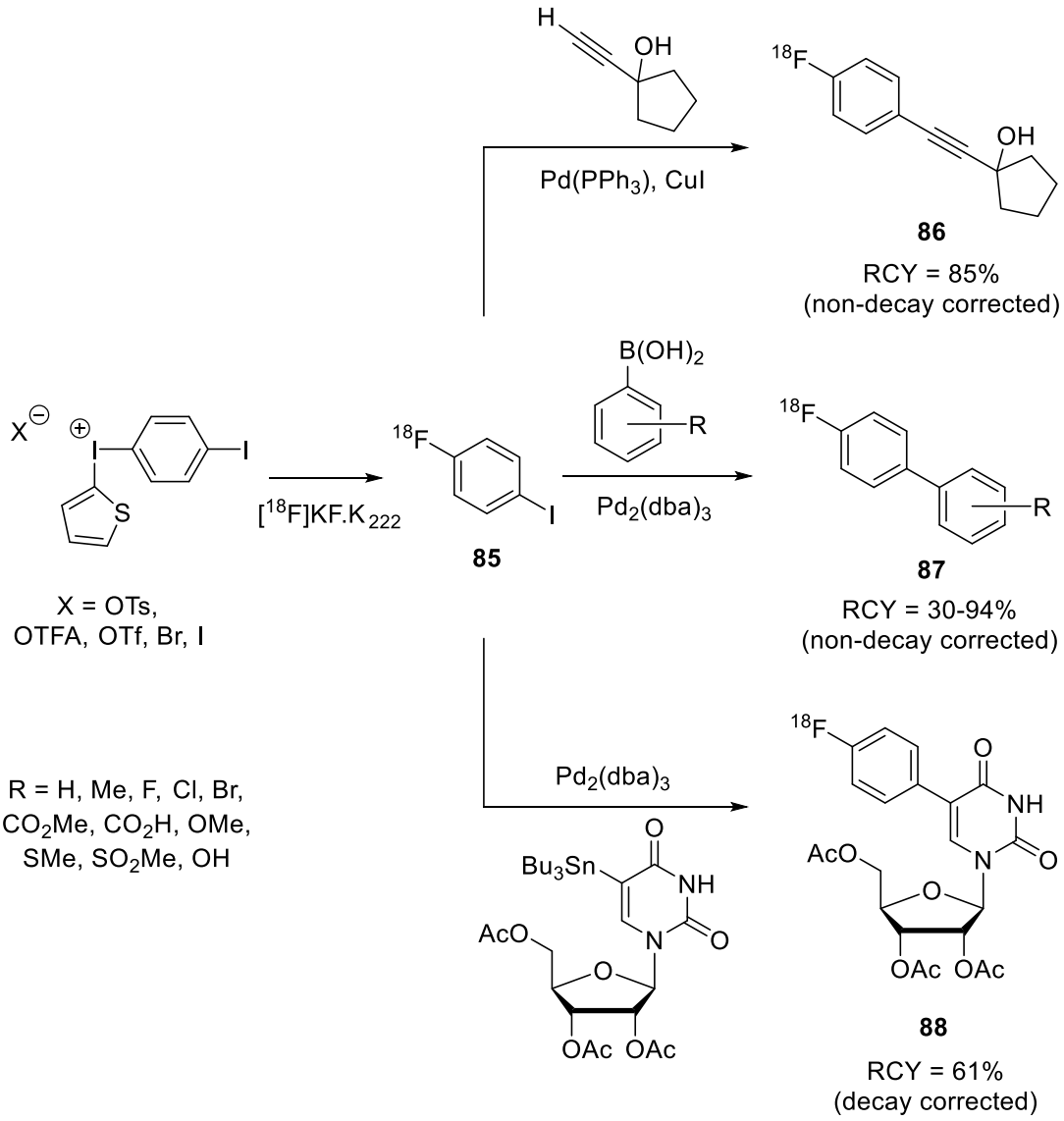

Scheme 40: Various palladium-mediated cross-coupling reactions using 4-[^{18}F]fluoro-1-iodobenzene

A vast number of variations on this chemistry exist, such as the preparations involving inversely reactive [^{18}F]fluoroboronic acids and [^{18}F]fluorophenyltrialkyltin reagents; as well as Grignard intermediates such as [^{18}F]fluorophenyl lithium, however, their discussion is beyond the scope of this chapter, for further information the reader is directed to a number of review articles.[98,122]

1.7.5 Carbonyl Reactive Prosthetic groups

The literature presents just a handful of prosthetic groups bearing amine- and alcohol- moieties intended on targeting carboxylic acid and activated ester functionalities, despite these approaches leading to relatively stable [^{18}F]labelled products. The reason behind this is likely to be selectivity concern, as substrates with amine or alcohol functionalities are likely to form inter- or intramolecular crosslinks. However, for simpler substrates that don't possess such nucleophilic character, a -OH or NH_2-bearing prosthetic group provides an excellent means to achieve rapid coupling under mild conditions; or alternatively, protecting group chemistry can be applied to safeguard these sensitive functionalities.

Successful [^{18}F]radiolabelling of the hormone peptide insulin **92**, as model for general peptide radiolabelling has been achieved *via* these means as early as 1989, utilising carboxyl-reactive prosthetic group 1-(4-[^{18}F]Fluoromethylbenzoyl)-aminobutane-4-amine ([^{18}F]FMBAA) **65** (Scheme 41).[225] This approach, whilst fairly lengthy, demonstrates the ability to selectively radiolabel a strategic portion of the peptide, by utilising simple protecting group chemistry to defend reactive functionalities within the macromolecule and activation of the desired amine through an alkyl-linked *N*-succinimidyl ester using disuccinimidyl suberate (DSS).

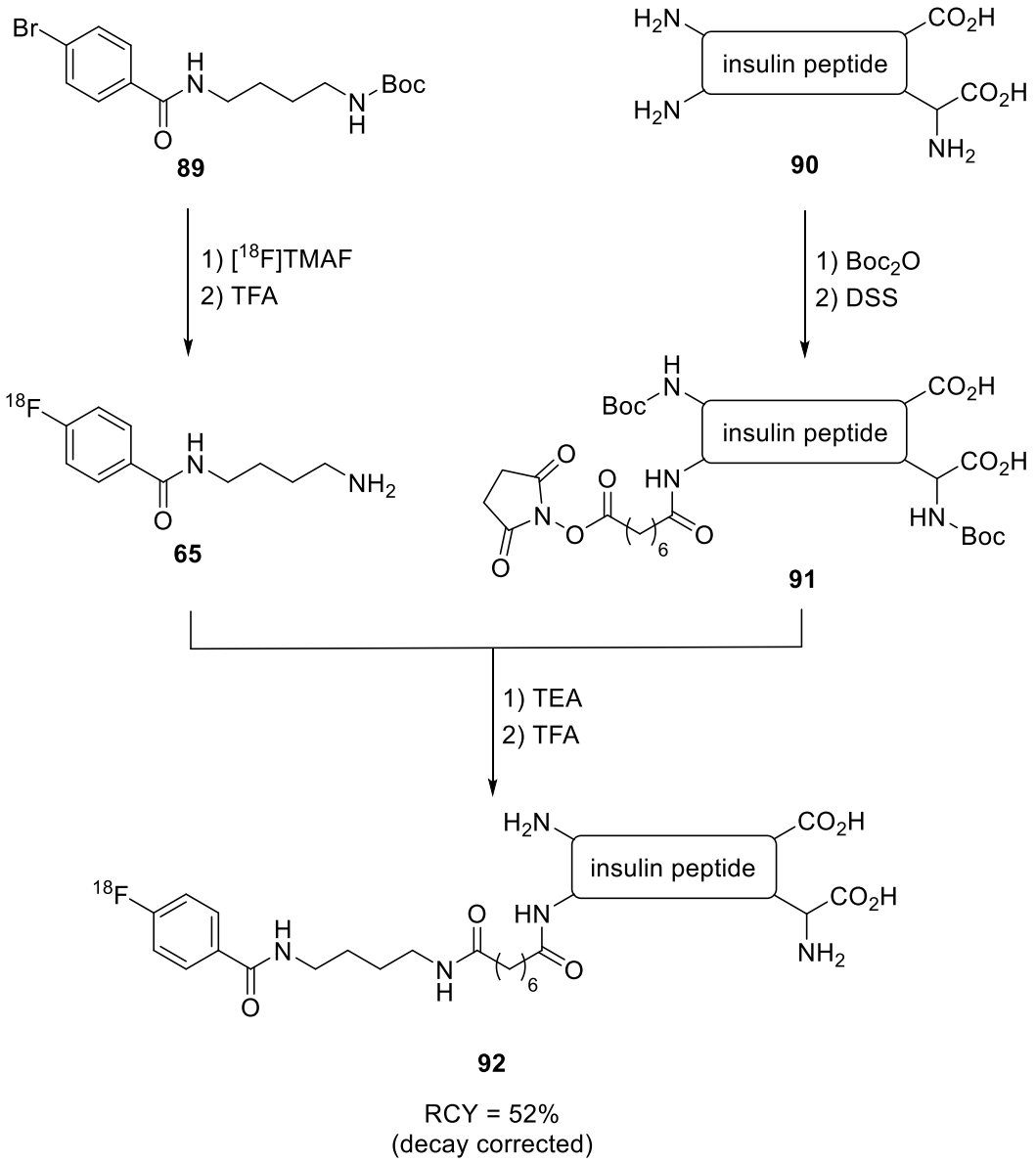

Scheme 41: Preparation of [^{18}F]labelled porcine insulin (closely related analogue of human insulin) using carboxyl-reactive prosthetic group ([^{18}F]FMBAA 65

1.8 [^{18}F]Fluorophenols as Prosthetic Groups

Section 1.7 provides an overview of the various approaches radiochemists have taken to achieve modular synthesis of fluorine-18 labelled bioactive macromolecules, as well as small molecule targets that benefit from a convergent radiosynthesis strategy. As was indicated in the closing sub-section of the literature review, strategies involving [^{18}F]fluorophenols and [^{18}F]fluoroarylamine prosthetic groups are relatively underdeveloped, and present an opportunity for further study. The 4-

[^{18}F]fluorophenoxy- moiety is a radio-synthon of particular interest for segmental radiosynthesis given its frequency in a wide number of pharmaceuticals and bioactive molecules.[120] Traditional preparations of [^{18}F]fluorophenols typically utilised Wallach or Balz-Shiemann chemistry (Section 1.6.2.3), which are restricted to low RCYs and long reaction times (maximum achieved = 33% in 60 min) and require multiple steps post fluorine-18 incorporation or preparation of anhydrous tetrachloroborate, [226] making them far from ideal.

Baeyer-Villiger oxidations on [^{18}F]fluorobenzaldehydes and [^{18}F]fluorobenzo /acetophenones provided an advancement on the preparation of [^{18}F]fluorophenols, where RCYs as high as 60% have been achieved, but require strongly electron-withdrawing substituents on the [^{18}F]fluorobenzophenone system to reach these RCYs.[227] Again, this approach suffers from the necessity for multiple post-radiofluorination steps and a lengthy reaction time, which ultimately limits the maximum RCY complicates radiosynthesis, as seen in the synthesis of 4-[^{18}F]fluorophenol **97** by oxidation of [^{18}F]fluorobenzophenone **90** using hydrogen peroxide (Scheme 42).

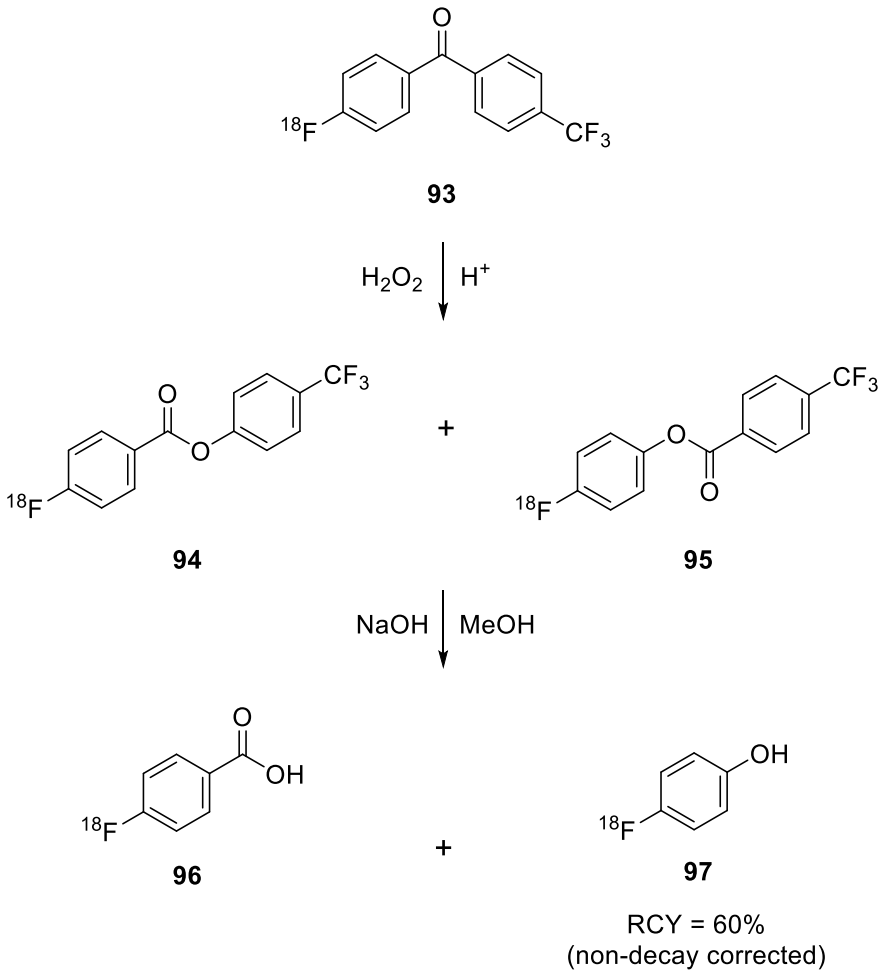

Scheme 42: Preparation of 4-[^{18}F]fluorophenol 97 *via* Baeyer-Villiger oxidation of 4-[^{18}F]fluoro-4'-trifluoromethylbenzophenone 93

More recently, oxidative [^{18}F]fluorinations of tert-butylphenols *via* the aryl umpolung as discussed in Section 1.6.2.4 (Scheme 26), present an innovative route to [^{18}F]fluorophenols, which benefit from not requiring a phenol protection strategy, but are again limited by the substituents required on the aromatic to allow for successful radiofluorination, thus limiting their application.[174]

Diaryliodonium salts as precursors provide a drastically more versatile route to [^{18}F]fluorophenols, being relatively unrestricted by substituents on the ring system enhancing the range of potential applications greatly. Work on aryl(thienyl)iodonium salt precursors to yield 4-[^{18}F]fluorophenol *via* batch-type radiosyntheses by Ross *et al* highlights the greatly improved reaction times (as fast as 20 min) offered by these hypervalent iodine precursors;[228] which outweighs the need for protecting group chemistry providing a strategy that allows for rapid deprotection is selected. This approach to the highly versatile 4-[^{18}F]fluorophenol prosthetic group, and commonly

occurring [^{18}F]fluorophenoxy- moiety has formed the basis of work in later chapters, with a focus on optimising the conditions towards high RCYs and increasing the speed of radiosynthesis.

One previously developed method of incorporating 4-[^{18}F]fluorophenol into small molecule imaging agents includes more work from the Coenen group, whereby Ullman ether coupling was used to produce 2-(4-[^{18}F]fluorophenoxy)-*N,N*-dimethylbenzylamine **99** and 2-(4-[^{18}F]fluorophenoxy)-*N,N*-methylbenzylamine **98**, (Scheme 43) developed as analogues of serotonin reuptake transporter site (SERT) imaging agent [^{123}I]ODAM **100**.[229]

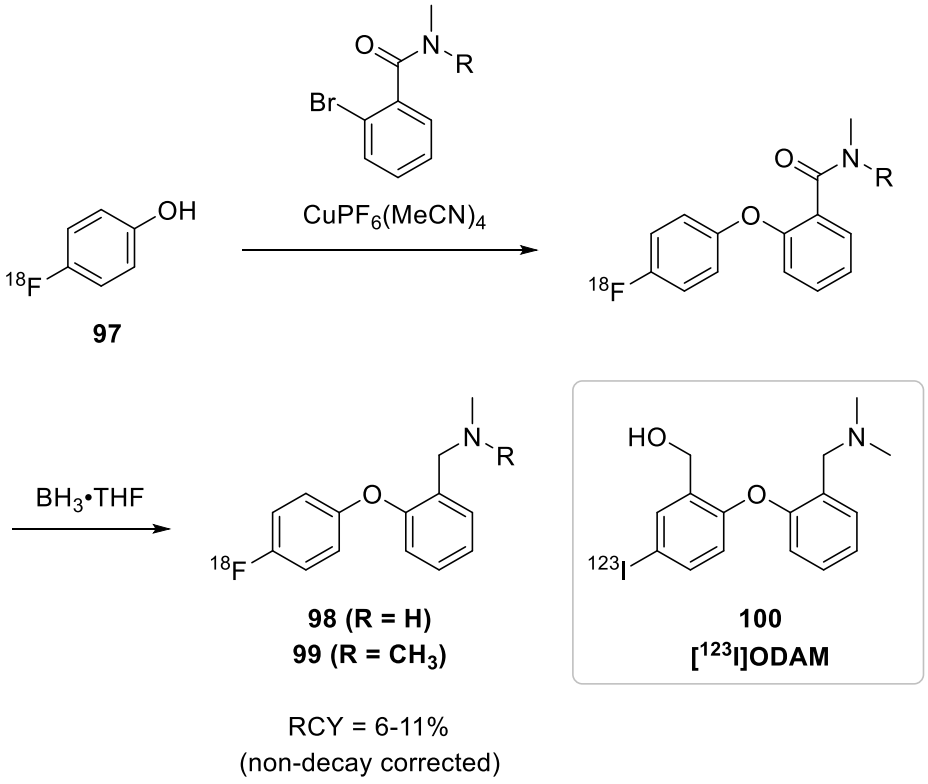

Scheme 43: Application of Ullman ether coupling for 4-[^{18}F]fluorophenol incorporation

Here the catalytic application of tetrakis(acetonitrile)copper(I) hexafluorophosphate permitted short reaction times for the coupling stage (20 min) and ultimately resulted in RCYs as high as 65% (from 4-[^{18}F]fluorophenol) despite multiple post-radiofluorination synthetic steps.

Another successful introduction of the [^{18}F]fluorophenoxy- moiety into a small molecule target includes work by Mühlhausen *et al*, here the group utilised 1-(3-

bromopropoxy)-4-[^{18}F]fluorobenzene **101** prepared from 4-[^{18}F]fluorophenol **97** as a amine-reactive prosthetic group in the radiosynthesis of [^{18}F]R91150 **102** (Scheme 44), a selective and high-affinity ligand for serotonin 5-HT_{2A} receptors.[230] This strategy allowed for relatively late-stage incorporation of the [^{18}F]radiolabel, affording a RCY of 4% over six steps and a SA of 335 GBq/µmol.

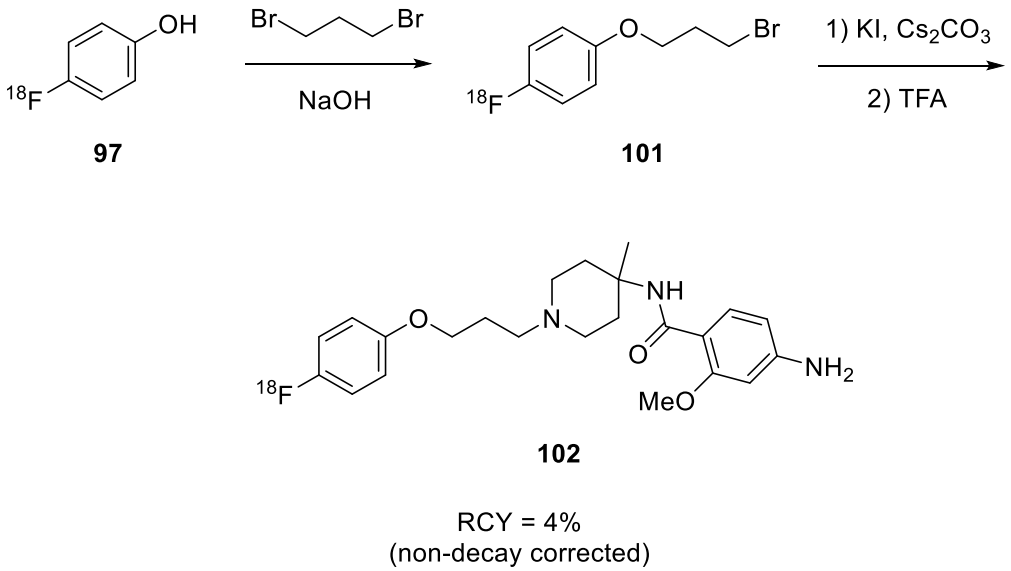

Scheme 44: Preparation of [^{18}F]R91150 102 demonstrating the application of 4-[^{18}F]fluorophenol *via* amine-reactive prosthetic group 101

This prosthetic group, 1-(3-bromopropoxy)-4-[^{18}F]fluorobenzene **101** was used in the same context to prepare the highly selective dopamine D_4 receptor ligand (3-4-[^{18}F]fluorophenoxy)propyl)-2-(4-tolylphenoxy)ethyl)amine ([^{18}F]TEFPA) with a respectable RCY of 50% from 4-[^{18}F]fluorophenol **97**, where again the approach benefits from a convergent strategy.[231]

Despite these successful applications of [^{18}F]fluorophenol towards modular radiosynthesis of small targets, very few strategies have extended this application towards the radiolabelling of bioactive macromolecules, most likely because the poor compatibility of [^{18}F]fluoride with these substrates and the relatively poor nucleophilicity of alcohols, particularly aryl alcohols, however, the chemistry described in Section 1.7.5 demonstrates that there is scope for this work. Nonetheless, the frequency of the fluorophenoxy- moiety in drug-like molecules and bioactive compounds makes the availability of [^{18}F]fluorophenols a very attractive

concept, demonstrating the demand for a robust route to n.c.a. [^{18}F]fluorophenol, in particular the *para*- substituted regioisomer.

2 Diaryliodonium Salts for Radiolabelling Electron-rich Aromatics

Chapter 1 discusses a broad range of methods for incorporating [^{18}F]fluorine into organic compounds, focussing on approaches yielding [^{18}F]fluoroaromatics within PET imaging agents using nucleophilic n.c.a. [^{18}F]fluoride. This chapter goes on to describe the use of diaryliodonium salts as precursors that allow for late-stage radiofluorination of electron-rich aromatics, centering on the first radiosynthetic target, 4-[^{18}F]fluorophenol, a valuable prosthetic group for convergent radiosynthesis and a model for other electron-rich systems. Here the aim of this work was to develop an easy to follow route to electron-rich diaryliodonium salt preparation, allowing for the preparation of multiple, stable diaryliodonium salt precursors bearing a series of phenolic protection strategies; followed by validation of their potential as precursors to [^{18}F]fluorophenol by conducting model [^{19}F]fluorinations.

2.1 Introduction to Hypervalent Iodine Chemistry

First reported in 1886 by Willgerodt,[232] hypervalent iodine reagents have received notable attention for their use as clean, metal-free oxidants and versatile cross-coupling reagents for C-C and C-N bond formation. Willgerodt's first hypervalent iodane, (dichloroiodo)benzene, prepared by passing chlorine gas through a solution of iodobenzene in cold chloroform,[233] demonstrated the potential for iodine oxidation states beyond (I); with iodine (III), (VI) and (VII) compounds now well understood and with characterised hypervalency.[234]

IUPAC nomenclature gives these (and other) hypervalent iodine species the λ-notation to signify their atypical bonding arrangement, since any element within groups 15-18 can have the potential to exhibit hypervalency, when it possesses more than 8 electrons than the octet in their valence shell.[235] Iodine (III) reagents with 3 ligands possess 10 electrons in their valence shell, giving them the classification [10-I-3] *versus* mono-valent iodine compounds which would typically be classified as [8-

I-1], a system that can be extended to all hypervalent iodine compounds (Figure 25).[234]

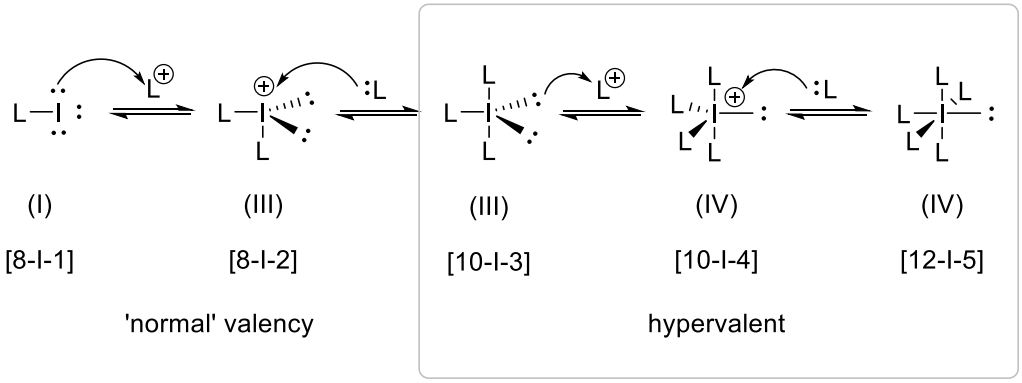

Figure 25: Oxidation of iodides and resulting classifications of hypervalent iodine compounds

Although the term "iodonium salt" is commonly used and accepted as a descriptor for a hypervalent iodine compound bearing three ligands, the compounds in this class are more accurately defined as λ^3-iodanes. In actual fact, the term "salt" in iodonium salts is a poor descriptor for these compounds, as x-ray crystallography has revealed they commonly adopt a pseudotrigonal bipyramidal structure (Figure 26).

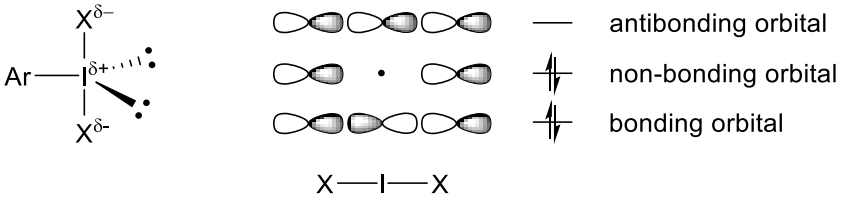

Figure 26: General structure of aryl-λ^3-iodanes (left) and a 3-centre–4-electron bond molecular orbital diagram (right). One heteroatom ligand X is exchanged for an aryl group in the case of diaryliodonium salts

Occupancy of the apical positions of the λ^3-iodane by electronegative ligands is preferred, as this contributes to stabilisation of the electron density provided by the surplus pair of electrons on iodine, giving those ligands a partial negative charge.[236] This affords a three centre–four electron bond (3c–4e) including the two apical ligands and iodine (Figure 26), an iconic feature of λ^3-iodanes that gives the

compound class its distinct reactivity properties. The resulting filled non-bonding orbital, which features a node on the iodine atom promotes a positive charge build up on iodine giving the iodane its characteristic electrophilic behaviour. The build-up of positive charge on iodine is partially alleviated by electron-deficient ligands, typically aryl, alkynyl or alkenyl groups, inhabiting the equatorial position, hence supporting stabilisation of the hypervalent species. It is worth noting here, that in the case diaryliodonium salts bearing electron-rich aromatics, only one electronegative ligand is able to provide reasonable stabilisation of the hypervalent 3c-4e bond, making these compounds less stable than the $ArIX_2$ counterparts.[235]

The discovery and application of λ^5-iodanes Dess-Martin Periodinane (DMP) **103**[237] and iodoxybenzoic acid (IBX) **104**[238] (Figure 27) as highly effective and selective oxidising agents,[239] drastically improved the reception of hypervalent compounds, opening up their development to more applications. Many of the advantages these reagents provide over chromium and Swern based approaches, such as milder reaction conditions, shorter reaction times, reduced toxicity, higher yields, *etc.*), can be accredited to their hypervalent nature and the two orthoganol 3c-4e bonds that they each possess.

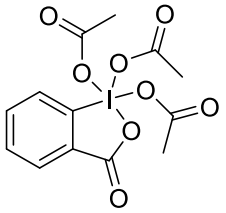

103

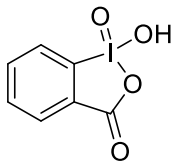

104

Figure 27: Examples of λ^5-iodanes used as oxidants, Dess-Martin Periodinane (DMP) 103 and iodoxybenzoic acid (IBX) 104

Oxidations with λ^3-iodanes are also often applied in organic chemistry, with phenyliodo bis(acetate) **105**, (also commonly referred to as diacetoxyiodobenzene, or phenyliodo diacetate) and iodosobenzene (also known as iodosylbenzene) **106** providing two commonly utilised examples (Figure 28).[240]

105 106

Figure 28: Examples of λ³-iodanes used as oxidants, phenyliodobisacetate 103 and iodosobenzene (iodosylbenzene) 106

Other RIL_2-type λ^3-iodanes have similar oxidative properties, but are also commonly employed as precursors to R_2IL reagents like diaryliodonium salts, classical examples include Koser's reagent **107**,[241] Stang's reagent **108**[242] and Zefirov's reagent **109**[243] (Figure 29); all of which have seen further development into augmented derivatives with improved reactivity or selectivity.[178] R_3I-type λ^3-iodanes, *i.e.* iodonium species bearing three carbon-based ligands, are thermally unstable and usually not synthetically useful, although the literature does describe a handful of examples that presented sufficient stability to allow characterisation.[244,245]

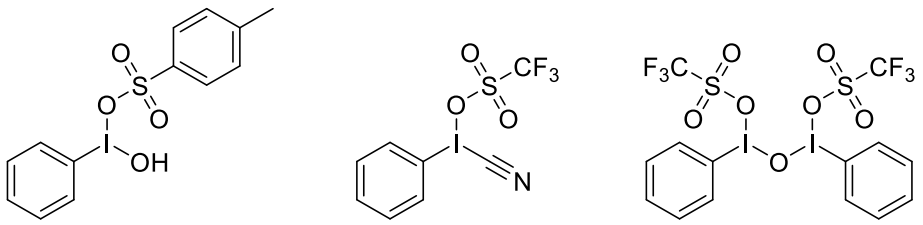

107 108 109

Figure 29: Structures of Koser's reagent 107, Stang's reagent 108 and Zefirov's reagent 109

However, the focus of this work on diaryliodonium salts explores the use of Ar_2IL type λ^3-iodanes, which exhibit somewhat different chemical properties and reactivities. Although the solid state structure of diaryliodonium salts is known to be pseudotrigonal bipyramidal, little is known about the structural conformation of these compounds in solution, as it is likely the counter-ion, solvent use and temperature will affect the structural characteristics of these λ^3-iodanes. Similarly, asymmetric diaryliodonium salts can adopt either of two structures, depending on which aromatic

ring has higher preference for the equatorial position. The T-shaped structural format is widely accepted as the most accurate representation of these compounds, however, diaryliodonium salts are conventionally drawn in their "salt form" (Figure 30). Note that radiochemists that utilise these compounds as precursors to [^{18}F]fluoroaromatics often refer to the aromatic to be fluorinated as the target ring and the other aryl group as the non-participating ring (n.p.r.), although use of this terminology is mainly used in context with the electronic and steric characteristics that dictate the outcome of radiofluorination.[253]

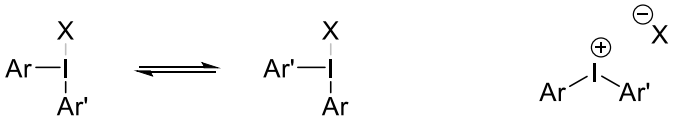

Figure 30: Equatorial/apical exchanging of aryl groups of diaryliodonium salts in solution (left) and the conventional representation of diaryliodonium salts in the "salt form" (right). X = Cl, Br, I, OTf, OTs, TFA, BF_4, PF_6, *etc.*

The choice of counter-ion plays an important role in diaryliodonium salt design because of the resulting effects it can have on the salt's stability and reactivity. The nucleophilic nature of halides make them poor counter-ions, as do anions that strongly coordinate to the I^+ centre, hence poorly nucleophilic, weakly coordinating counter-ions such as trifluoroacetate, triflate, tosylate and tetrafluoroborates (and other non-exchangeable fluoride bearing counter-ions) are usually preferred.

2.2 Reactivity of Diaryliodonium Salts

Generally, initial nucleophilic attack on the electrophilic iodonium salts species initiates with a ligand exchange, with displacement of a heteroatomic ligand by the nucleophile. There is much debate surrounding the mechanism of this reaction and a number of mechanisms have been suggested,[246] mechanistically, it is plausible for both the ligand to dissociate from the iodonium salt prior to nucleophilic attack or for ligand loss to occur after coordination of the nucleophile; providing two conceivable reaction pathways (Scheme 45).[246]

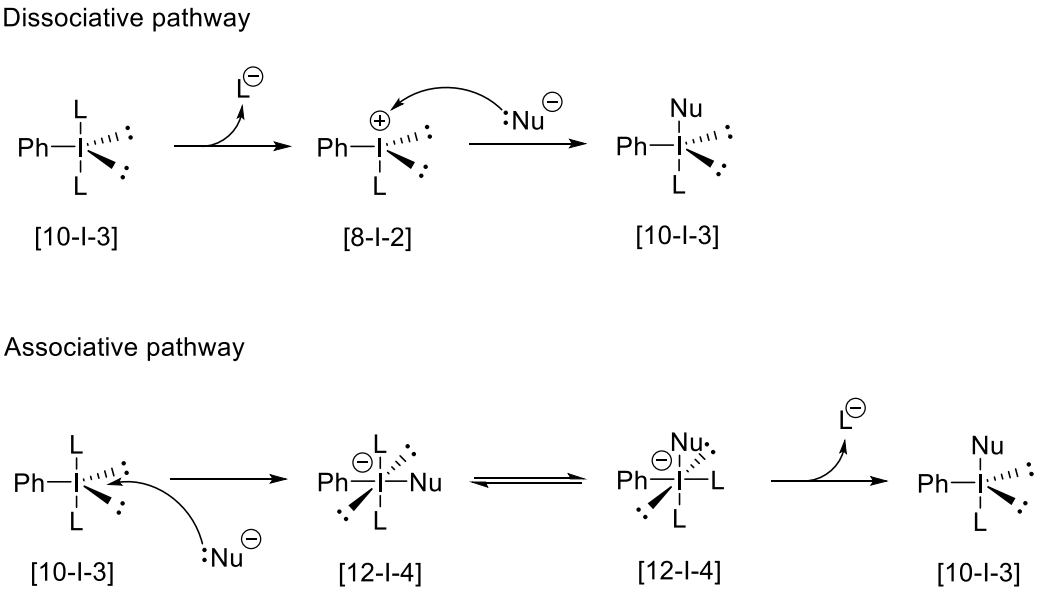

Scheme 45: Dissociative and associative pathways for formation of "T-shaped" PhLINu complexes as a result of nucleophilic attack on λ^3-iodanes

The existence of the cationic [8-I-2] species above (Scheme 45) has been validated for many λ^3-iodanes by mass spectrometry thus enforcing the dissociative mechanism, however, studies have also shown that on dissociation of the counter-ion/ligand, the vacant position is rapidly reoccupied by a solvent molecule.[247] X-ray diffraction studies on iodosylbenzene whilst subjected to aqueous conditions indicated that the species was ligated by a water molecule as $[PhI(H_2O)OH]^+$, where the water molecule occupied one of the apical sites as part of the hypervalent 3c-4e bond, displaying a bond angle of nearly 180° which satisfies λ^3-iodane "T-shape" geometrical requirements.[248] There is also research to suggest that the associative pathway, which involves the formation of the intermediary square planar [12-I-4] *cis* and *trans* complexes (Scheme 45), is also valid; as x-ray analyses of similar, stable square planar tetra-ligand iodanes, *i.e.* $[IL_2L'_2]^-[SCl_3]^+$ have been observed.[249]

In the case of nucleophilic attack of diaryliodonium salts it is widely accepted that the nucleophile displaces the ligand to yield a "T-shaped" intermediate by one of the above two mechanisms, before undergoing simultaneous reductive elimination of the iodoarene leaving group and ligand coupling between the nucleophile and the equatorial aryl group. With this process being critical to radiochemists that conduct radiofluorinations of diaryliodonium salts, the mechanism and resulting regioselectivity between [^{18}F]fluorination of the two aromatic ligands has been

studied in detail and the below "turnstile" mechanism has been proposed (Scheme 46).[152]

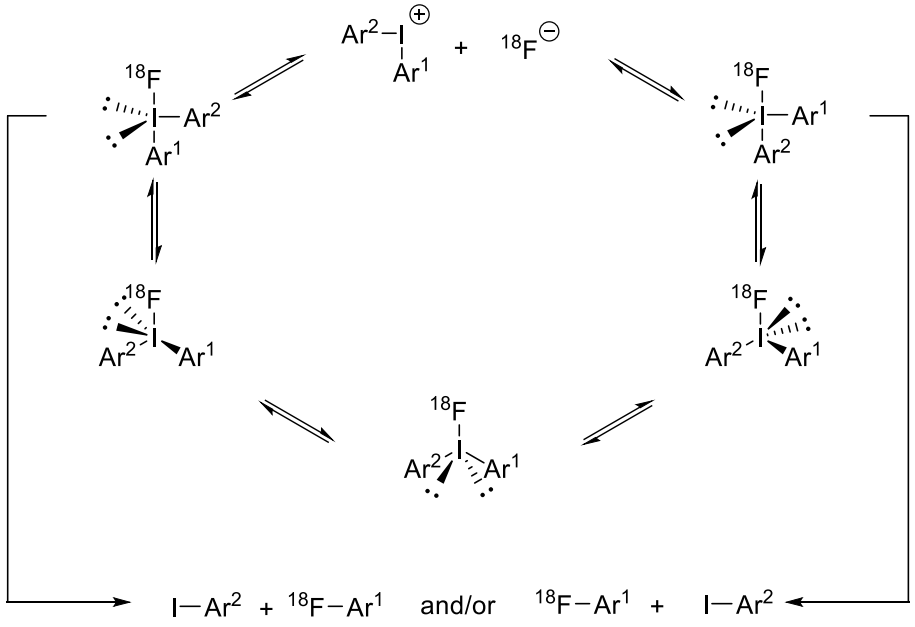

Scheme 46: [^{18}F]Fluorination of a diaryliodonium salt *via* the proposed "turnstile" mechanism[152]

The final irreversible step sees the collapse of the tricovalent intermediate to yield the [^{18}F]fluoroaromatic and iodoarene products, potentially as a mixture of both regiochemical outcomes. The stable iodoarene leaving group, bearing no formal charge on elimination, is an outstanding leaving group, which is 10^6 times better leaving group than the "super leaving group" triflate anion.[250] This extraordinary leaving group ability of the iodoarene earns it the term hypernucleofuge and provides the reaction with a major driving force towards elimination of this species.[235]

2.2.1 Chemoselectivity of Diaryliodonium Salt Fluorination

As mentioned above, nucleophilic attack on an asymmetric diaryliodonium salt can provide a number of products that are a direct result of the substituents featured on the precursor. In the absence of a transition-metal catalyst and with substrates

without functionality in the *ortho*- positions, the more electron-deficient aryl ring will be fluorinated in preference.[251]

Here, the aryl group that predominantly occupies the equatorial position is the species that is transferred to the nucleophile during ligand coupling, which in the ground state is the more electron-poor aryl group (Scheme 47), given its ability to help alleviate the build-up of negative charge in the transition state (**113**).[252]

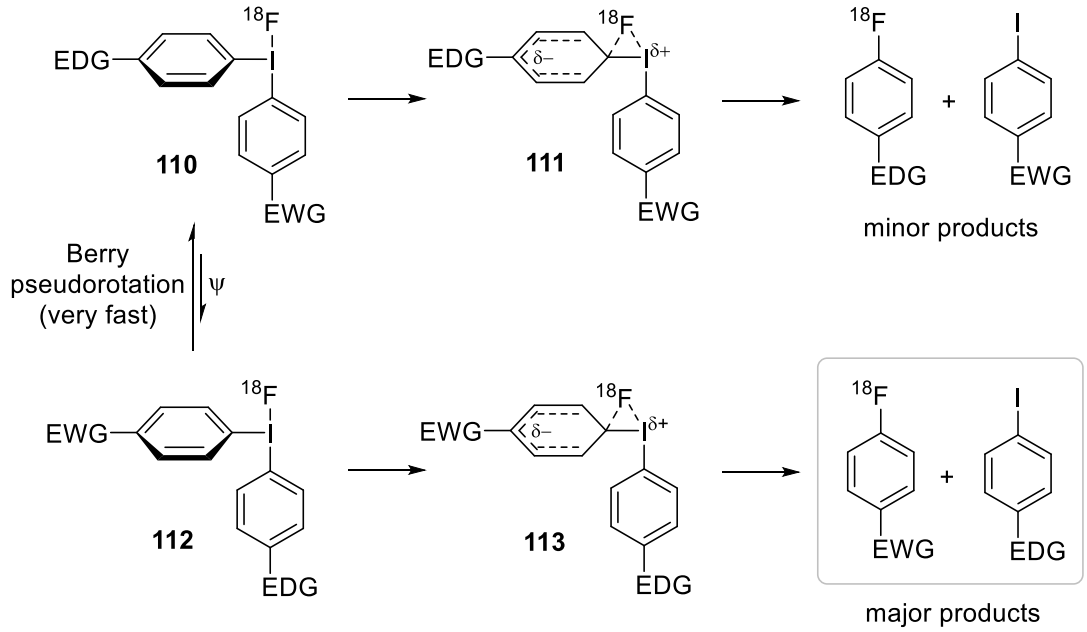

Scheme 47: Berry pseudorotation of diaryliodonium salt during [^{18}F]fluorination and the preference for electron-poor aromatic occupation in the equatorial position.

Similarly, the transition state exhibits a build-up of positive charge on iodine, which can be stabilised by the presence of an electron donating aryl group situated in the apical position and lower the energy of the transition state associated with this pathway, hence providing a major preference for the products highlighted above (Scheme 47). However, favouring of this reaction pathway is in spite of complex **110** displaying higher stability than complex **111**, since an electronegative species in the apical position is preferred to stabilise the hypervalent 3c-4e bond, but transitioning between the two "T-shaped" complexes is afforded by rapid Berry pseudorotation (ψ), allowing for a fluxional equilibrium between the species; however, there is also evidence to suggest that this pathway may be of too high energy to be realistic.[253,254]

As well as electronic influences, steric factors also provide a major contribution to the regiochemistry of diaryliodonium salt fluorination, whereby aryl groups bearing steric bulk in the *ortho*- position see that group take preference for the equatorial position over the apical one.[255] This observation is an artefact of the equatorial position being less hindered than the apical counterpart and often provides an overriding effect that facilitates fluorination of the electron-rich aryl ring when both arenes are of equal electron-density; an extremely useful tool for radiochemists looking to produce electron-rich [^{18}F]fluoroaromatics, commonly referred to as the *ortho*-effect (Scheme 48).[256]

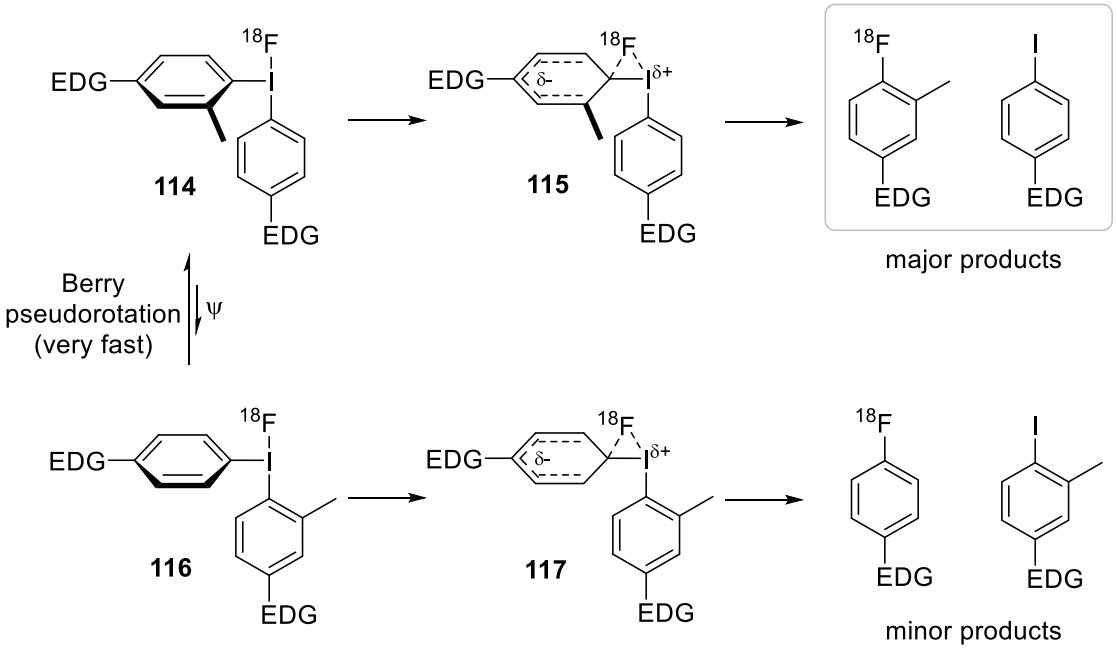

Scheme 48: Demonstration of the *ortho*-effect on [^{18}F]fluorination of a diaryliodonium salt bearing *ortho*-bulk

A fully comprehensive study of nucleophilic reactions of diaryliodonium salts with regards to electronic factors *versus* steric factors has yet to be published, although our group has described some interesting observations in this area previously.[257] Largely the *ortho*-effect appears to have a substantial effect over product selectivity when the arenes on iodine are of similar electronic character,[255,256] however, there are examples of aryl groups bearing *ortho*- bulk that were not transferred to the nucleophile where carbon nucleophiles were employed,[258] as such as the work by

Ochiai and co-workers in their use of chiral diaryliodonium salts in the asymmetric transfer of aryl groups (Scheme 49).[259]

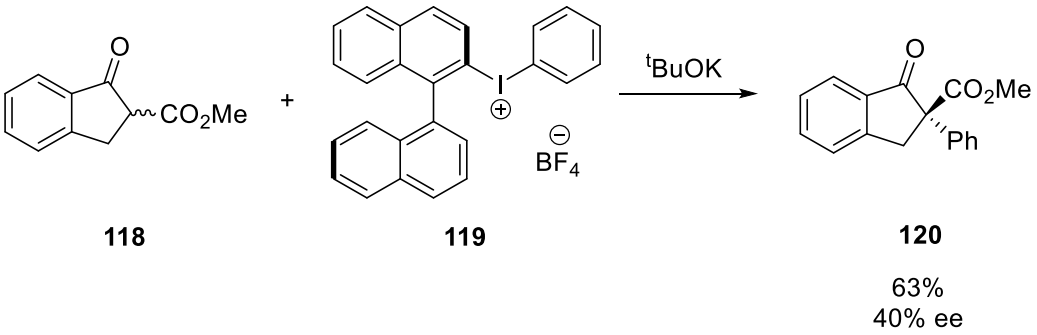

Scheme 49: Asymmetric α-phenylation of β-keto ester enolates using chiral diaryliodonium salts

Aside from the substituents on the aromatic rings of diaryliodonium salts, the choice of counter-ion has also been shown to have a remarkable effect on the outcome of radiofluorinations on such λ^3-iodanes. Work by Ross *et al* developed an understanding on the influence of different counter-ions on [^{18}F]fluorinations using 2-methoxyphenyl(2-thienyl)iodonium salts **121** as model compounds (Scheme 50), finding that the application of a bromide counter-ion afforded superior RCYs (Figure 31).[221] Although the low nucleophilicity of organic counter-ions would be expected to benefit the [^{18}F]fluorination of diaryliodonium salts, they also exhibit a more pronounced covalent interaction with the iodonium centre *versus* their inorganic counterparts, which can result in steric and electronic hindrance; whilst the application of the bromide counter-ion can promote formation of arylbromide by-products, which may be difficult to separate from the arylfluoride product.

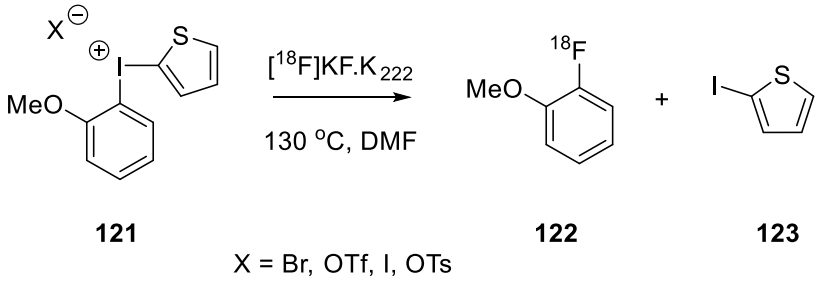

Scheme 50: [^{18}F]Fluorination of 2-methoxyphenyl(2-thienyl)iodonium salts with different counter-ions

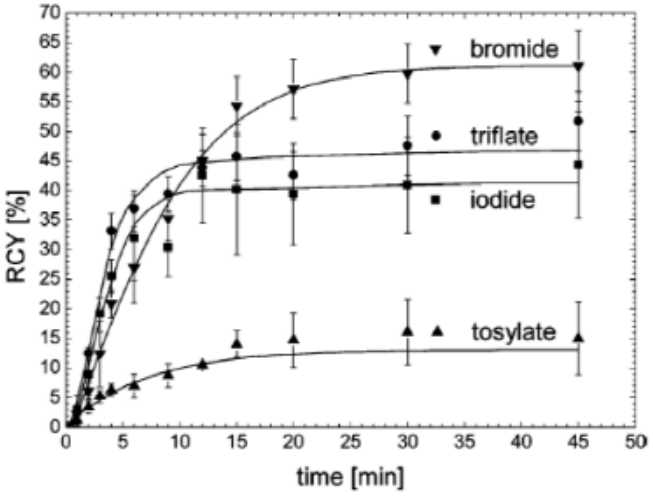

Figure 31: The influence of counter-ion selection on the [^{18}F]fluorination RCYs of various 2-methoxyphenyl(2-thienyl)iodonium salts[221]

Hence a balance is struck between counter-ions that provide better stabilisation of the hypervalent 3c-4e bond but display increased nucleophilicity which supplements the competing substitution reaction; and counter-ions that are less strongly bound to iodine and thereby dissociated, allowing for increased [^{18}F]fluoride interaction with the electrophilic centre.[221] Despite the relatively high nucleophilicity of the trifluoroacetate anion, the counter-ion sees frequent use in this application because of the convenience of preparing diaryliodonium trifluoroacetates.[260,261]

The performance of diaryliodonium salt fluorination reactions is also highly dependent on a number of other factors - as expected reaction times, substrate concentration and temperatures play major roles, but the choice of solvent also greatly effects the RCY of [^{18}F]fluoroaromatics produced. S_NAr chemistry employed for [^{18}F]fluorinations typically rely on aprotic, polar solvents for success, where DMSO sees regular application. However, the $S^{\delta+}$–$O^{\delta-}$ dipole demonstrated by the solvent often negates its effectiveness for chemistry with diaryliodonium salts, possibly as result of cation solvation.[262]

The use of acetonitrile (CH_3CN) and dimethylacetamide (DMAA) have also shown to achieve very limited RCYs,[221] whereas the use of dimethylformamide (DMF) has displayed drastically better results for diaryliodonium salt [$^{18/19}$F]fluorinations across multiple studies, [263] which has been demonstrated by Wüst *et al* in the fluorination of symmetric 4,4'-diiododiphenyliodonium salts (Table 5).[222]

Counter-ion	Rxn Conditions	Solvent	Yield of 4-[^{18}F]fluoroiodobezene
Cl$^-$	80 °C	CH_3CN	0.5–1.0%
Cl$^-$	120 °C	CH_3CN	1.3–2.8%
Cl$^-$	100 °C	DMF	3–12%
Cl$^-$	160 °C	DMF	15–52%
TsO$^-$	100 °C	CH_3CN	0.5–2.5%
TsO$^-$	140 °C	DMF	21–46%
TfO$^-$	100 °C	CH_3CN	2.5–5%
TfO$^-$	140 °C	DMF	11–22%
TfO$^-$	140 °C	DMSO	0.5–1.0%
Cl$^-$	MW	DMF	15–70%

Table 5: Reaction conditions for the preparation of 4-[^{18}F]fluoroiodobenzene from 4,4'-diiodophenyliodonium salts with various counter-ions and conducted in a range of solvents

The above summary table not only describes the benefits of using DMF over other solvents in these reactions, as well as the improvement seen by utilising triflate or tosylate counter-ions, but also the scope for the higher reaction temperature afforded by DMF, which appear to be greatly beneficial for high RCYs from diaryliodonium salt [^{18}F]fluorination;[264] however, error ranges remain consistently large. This trend of increasing RCYs could be extended through higher temperatures, however, are limited by the physical properties of DMF, which is known to decompose to dimethylamine and carbon monoxide at temperatures exceeding 160 °C,[265] a clear limitation of conducting these reactions in non-closed systems.

Microwave-assisted heating has seen fairly frequent use in [^{18}F]fluorination chemistry,[169] including some diaryliodonium salts,[180,266,267] but has yet to be applied to a wide range of diaryl-λ^3-iodane systems. In the above table, the application of

microwave heating offers greatly reduced reaction times, a very welcome benefit for radiochemists, and does see an improvement in the maximum achievable RCY, however, the range of RCYs is also markedly wider, which raises a reproducibility concern (Table 5).[222]

Similarly, the use of chloride counter-ion *versus* other anions also displays a large amount of deviation in the RCY output, an issue that commonly observed in the [^{18}F]fluorination of diaryliodonium salts, until a strategy was developed by Carroll and co-workers that greatly improved the robustness of the chemistry.[261] Here the group attributed this inconsistency to the unprompted and random formation of aromatic radical species, produced by homolytic cleavage of the aryl-iodine bond when subjected to heating. They found that the application of various radical scavengers (Table 6), such as butylated hydroxytoluene (BHT), galvinoxyl and 2,2,6,6-tetramethylpiperidine-1-oxyl (TEMPO) **124** (Scheme 51) could halt further propagation by the radical species and thereby reduce the inconsistency seen over multiple [^{18}F]fluorination runs (Table 6) and reduce the formation of side products formed by this competing radical mechanism.[261]

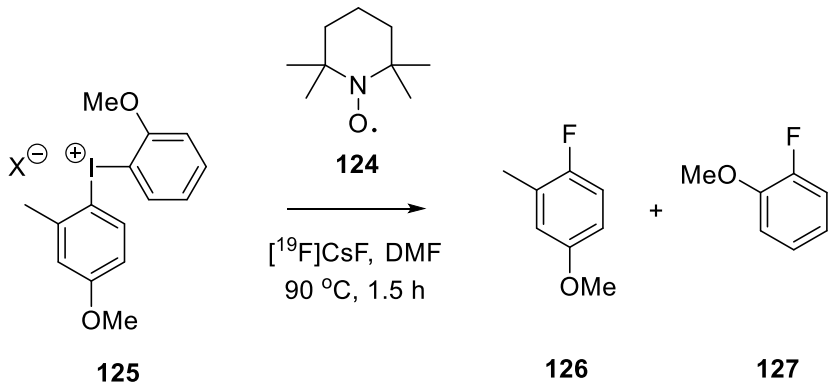

Scheme 51: Application of radical scavenger TEMPO to improve reproducibility of diaryliodonium salt fluorinations

Radical Scavenger	Yield	Average yield	**123:124**
none	<5%	<5%	1.1:1
BHT	14-28%	21%	1.3:1
Galvinoxyl	22-29%	26%	1.3:1
TEMPO	24-26%	25%	1.3:1

Table 6: [^{19}F]Fluorination of diaryliodonium salt 122 with and without various radical scavengers (10 mol%), whereby TEMPO provided the most reproducible results[261]

2.2.2 Applications of Diaryliodonium Salts

Aside from their applications as hypernucleofuge centred precursors to [^{18}F]fluoroarenes, aryl-λ^3-iodanes also have a number of other chemistries at their disposal, allowing employment into a number of very varied applications.[178] The aforementioned exchange of heteroatomic ligands is common and although the substrate scope is exceptionally wide, the general transformation is the same. In contrast, the numerous reactions encompassed under the umbrella of 'reductive eliminations' can be categorised into a number of sub-types, consisting of: reductive α-elimination, reductive β-elimination, hypernucleofuge reductive elimination, reductive elimination with fragmentation, reductive elimination with substitution, reductive elimination with rearrangement, homolytic cleavage and ligand.[235]

With regards to diaryl-λ^3-iodanes, these reagents have seen substantial success in a variety of organic transformations, including use as arylation reagents for a wide range of substrates,[268,269,270,271] including heteroatomic nucleophiles;[272,273] as metal-catalysed and metal-free cross-coupling reagents;[274,275,] as efficient Lewis acid catalysts (e.g. for three component Mannich reactions),[276] precursors to biaryl and benzyne systems;[277278] strategies to macromolecule syntheses;[279] and applications in photochemistry and polymerisation.[178,280,281] Scheme 52 provides a pictorial summary of some of the applications of diaryl-λ^3-iodanes outside of [^{18}F]fluoroaromatic preparations.

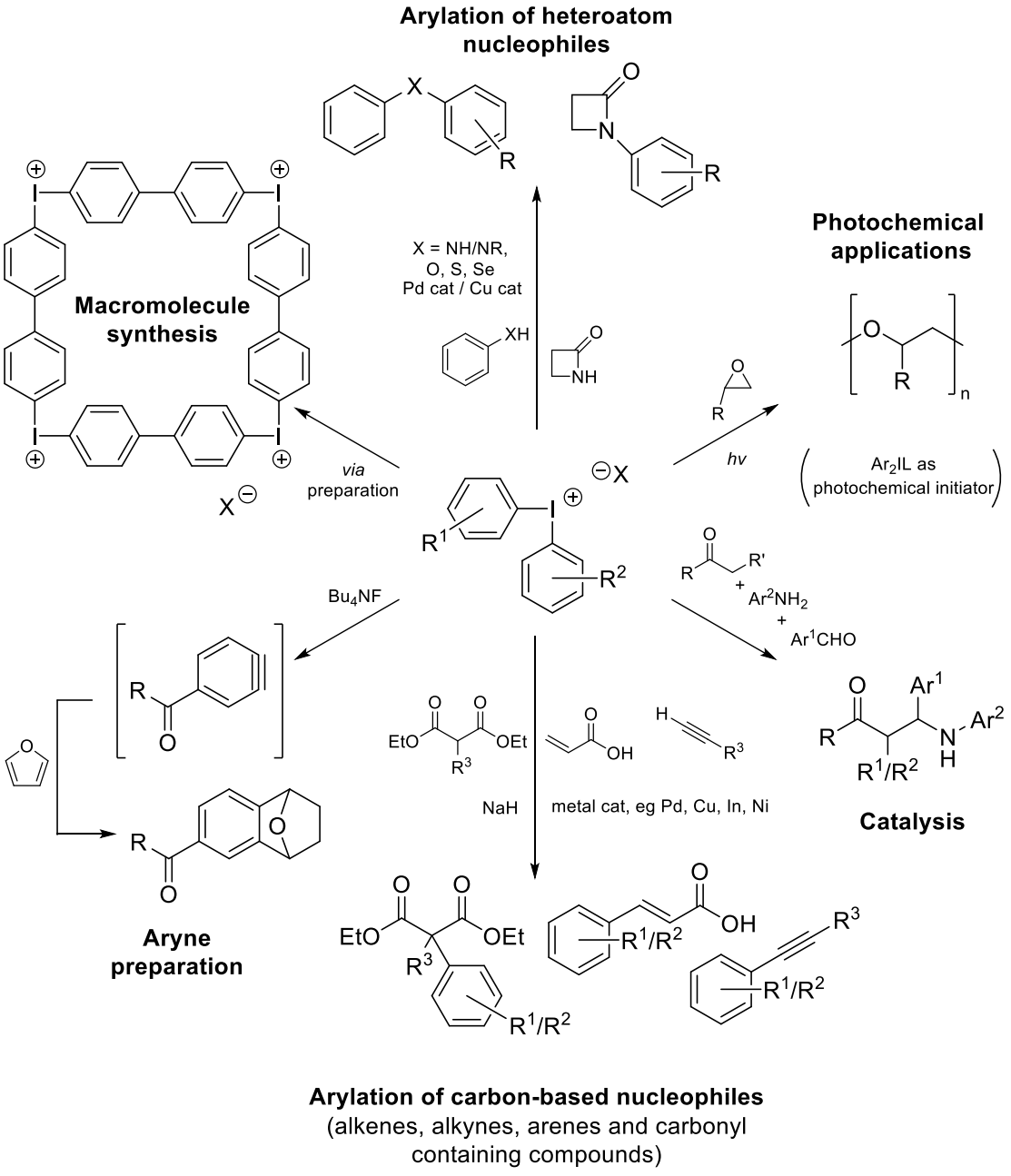

Scheme 52: A summary of some of the transformations possible with diaryl-λ^3-iodanes outside of [^{18}F]radiofluorinations

2.3 Synthesis of Diaryliodonium Salts

The literature presents a number of strategies for the preparation of diaryliodonium and aryl(heteroaryl)iodonium salts from commercially available starting material, many of which involve the oxidation of an iodoarene to an intermediary $ArIL_2$ λ^3-iodane compound, which undergoes ligand exchange with a nucleophilic aryl compound to achieve the target diaryliodonium salt compound;[282] and if desired, a

counter-ion exchange reaction can be undertaken to yield a diaryliodonium salt with an anion more suited to its purpose.[283] This very versatile and convenient method provides a clean, two-step route to diaryliodonium salts and is tolerant of a wide range of functionalities (Scheme 53). Here some commonly utilised oxidants include hydrogen peroxide,[284] sodium periodate,[285] mCPBA[286] and sodium perborate,[287] all of which allow for preparation of functionalised λ^3-iodanes under mild conditions.[288]

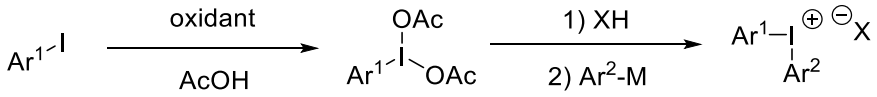

Scheme 53: Preparation of diaryliodonium salts *via* aryliodobis(acetate)s

The subsequent transformation is, again, very adaptable, with most procedures utilising organic acids such as triflic acid, tosylic acid or trifluoroacetic acid to activate the λ^3-iodane towards nucleophilic attack; where arylstannane reagents, arylboronic acids and arylsilanes are commonly employed to afford the diaryl-λ^3-iodane under mild, substrate tolerant conditions, whilst providing regiochemical control.[178] This method came as a much needed improvement over the dated application of iodosylarenes (ArI=O) and iodoxyarenes ($ArIO_2$), which typically afford poor yields, required lengthy preparations and are inherently explosive.[289]

Koser's reagent **107** (Figure 29) and its derivatives have seen regular use as a mild and convenient routes to diaryl-λ^3-iodanes since their deployment, but were largely limited by modest yields. However, Kita *et al* demonstrated the use of 2,2,2-trifluoroethanol (TFE) as a superior solvent for coupling the $ArIL_2$ reagent with electron-rich arenes (Scheme 54), providing high yielding route to diaryliodonium salts that easily adapted for a variety of substrates.[290] Koser's reagent and related compounds also allow for the incorporation of electron-deficient arenes, again by utilising boronic acid, silyl- and stannyl- based precursors.[291,292,293]

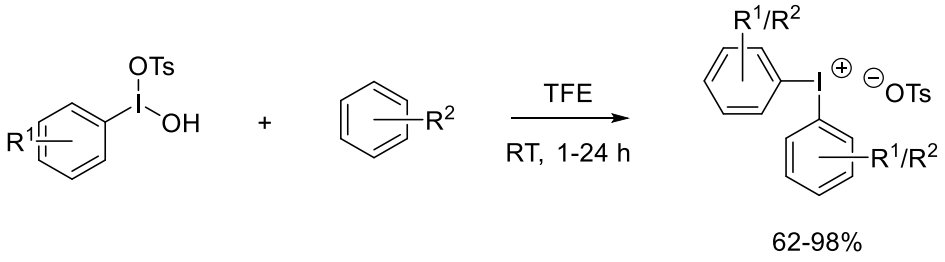

Scheme 54: High yielding preparation of diaryl-λ³-iodanes using Koser's reagent and its derivatives

Alkenyl-λ³-iodanes, despite their instability, have also seen multiple applications as precursors to both symmetrical and unsymmetrical diaryl-λ³-iodanes, often providing good yields. However, their highly reactive nature comes at the cost of the need for delicate reagent pre-synthesis using strong bases and low temperatures.[178] Traditional uses of unstable iodanes in this application demanded highly acidic conditions, which not only limits substrate scope but also deactivates functionality susceptible to protonation such as heteroarenes, however Beringer and Nathan defined a method for using the reagent class that allowed diaryliodonium salts formation under basic conditions.[294,295] Here the group prepared *trans*-chlorovinyliodoso dichloride **129** from ethyne **128**, then immediately treated the reagent with a variety of lithiated arenes to afford diaryliodonium chlorides in modest to excellent yields (Scheme 55).[294]

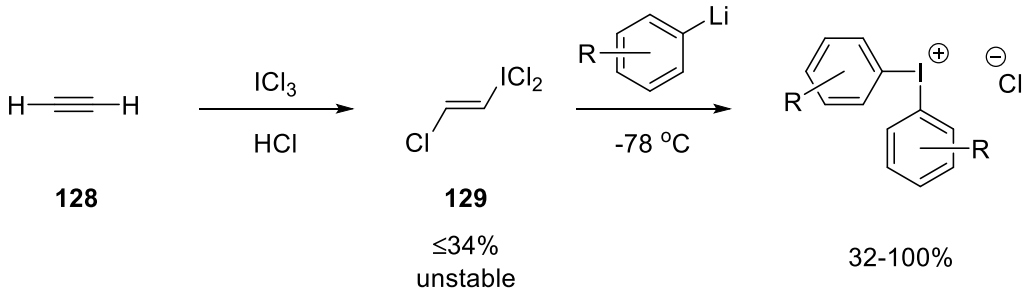

Scheme 55: Preparation of diaryl-λ³-iodane chlorides *via* a highly reactive alkenyl-λ³-iodane reagent

A number of other research groups have also looked to exploit the high reactivity of unstable λ³-iodanes to achieve a rapid route to diaryliodonium salts, for which inorganic hypervalent iodine(III) reagents, (*i.e.* a λ³-iodane bearing no ligands that are bound to iodine *via* a carbon atom) are often very applicable. Iodosyl sulfate,[296]

Iodosyl triflate[297] and tris(trifluoroacetoxy)-λ^3-iodane **130** (Scheme 56)[298,299] have all been investigated as suitable inorganic iodine(III) precursors that yield symmetrical diaryliodonium salts from electron-rich (hetero)aromatics and electron-deficient arenes activated with stannyl-, silyl- or boronic acid functionality. However, as with alkenyl-λ^3-iodanes, their frequent application is limited by the difficulty of their syntheses and their potentially explosive character.

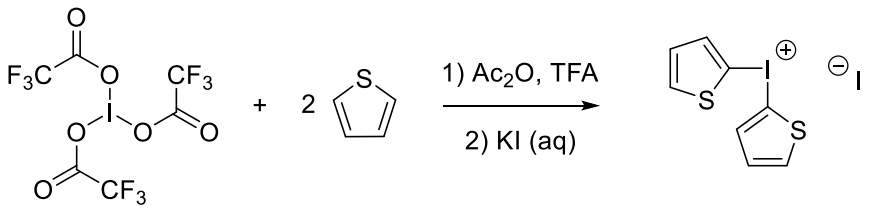

130 **131**
67%

Scheme 56: Preparation of symmetrical electron-rich diaryliodonium salts using iodine(III) trifluoroacetate

Recently some more direct, one–pot strategies for diaryliodonium salts preparation from arenes and iodoarenes have also been developed (Scheme 57),[178] however, although these approaches offer very high yields at small scale, larger scale production *via* these routes proved to be problematic and substantially lower yielding in practice, many also have rather specific substrate requirements.

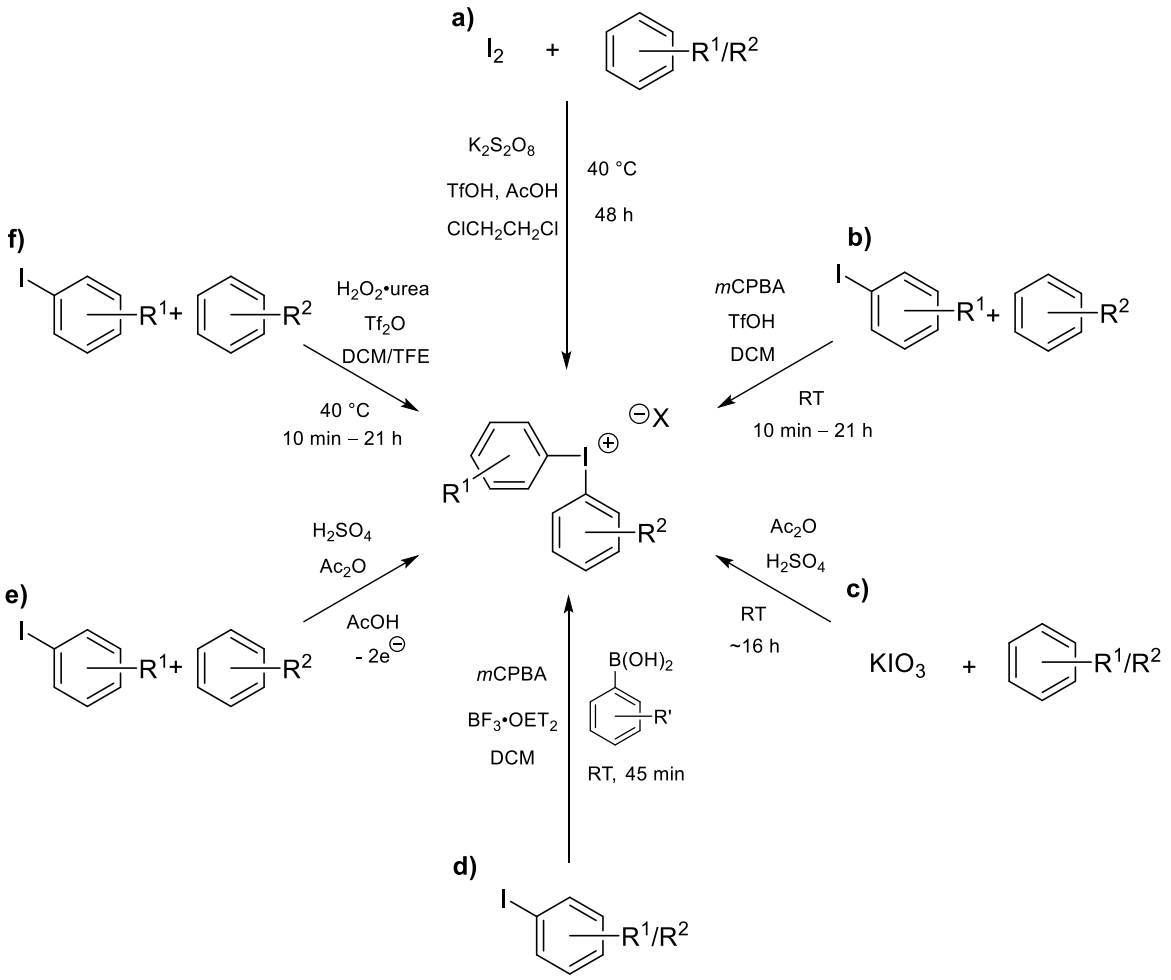

Scheme 57: Multiple one-pot approaches to diaryl-λ³-iodane synthesis, a),[300] b),[301] c),[302] d),[303] e)[304] and f)[305]

2.4 A Strategy for 4-[^{18}F]Fluorophenol Production

Of the numerous strategies discussed in Section 2.3, aryliodobis(acetate)s were employed as robust and adaptable precursors to a range of diaryliodonium trifluoroacetates (Scheme 53) that deliver a n.c.a. route to 4-[^{18}F]fluorophenol. This strategy for diaryliodonium trifluoroacetate preparation has been well developed within the group,[260,261] and has seen successful application to a number of diaryliodonium salts, including precursors for 4-[^{18}F]fluorobenzaldehyde], *N*-(4-[^{18}F]fluorophenylmaleimide, 2-, 3-, and 4- regioisomers of ethyl [^{18}F]-fluorobenzoate, [^{18}F]DAA1106, [^{18}F]SFB and [^{18}F]3-fluoro-5-[(2-methy-1,3-thiozol-4-yl)ethynyl] benzonitrile ([^{18}F]MTEB). Here the general approach begins with preparation (and protection if necessary) of the target aryl halide, whilst preparation of the "non-

participating ring" (n.p.r.) aryliodobis(acetate)s from a simple, usually electron-rich iodoarene is conducted in tandem. After stannylation of the target aryl halide, convergent coupling of the activated aryliodobis(acetate)s with the aryl stannane affords the target diaryliodonium trifluoroacetate; hence providing a versatile strategy to the preparation of diaryliodonium salts that yield 4-[^{18}F]fluorophenol on radiofluorination and deprotection (Scheme 58).

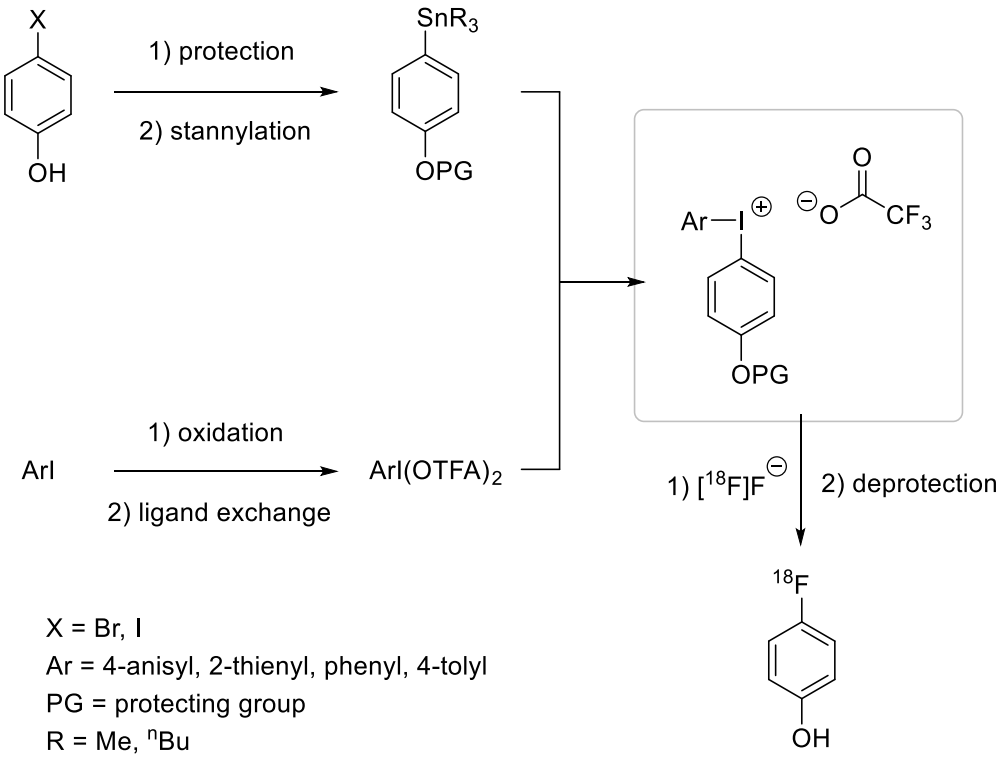

Scheme 58: General route for the preparation of diaryl-λ^3-iodane precursors that yield 4-[^{18}F]fluorophenol on treatment with [^{18}F]fluoride

Although the use of organotin chemistry presents a serious toxicity concern, careful purification of the product diaryl-λ^3-iodane from the reaction mixture, either by column chromatography or multiple recrystallisations eliminate any detectable amounts organotin precursor of by-products.

2.5 Preparation of Aryliodobis(acetate)s

Numerous research groups have published a range of strategies that permit oxidation of iodoarenes to aryliodobis(acetate)s under mild conditions in modest to good yields,[284,285,286] Here the procedure developed by McKillop *et al* [287,306] was utilised because the method allows for broad substrate scope, a simple work up procedure and utilises sodium perborate tetrahydrate ($NaBO_3 \cdot 4H_2O$) as a cheap oxidant, allowing for the production of aryliodobis(acetate)s **132**-**137** (Scheme 59).

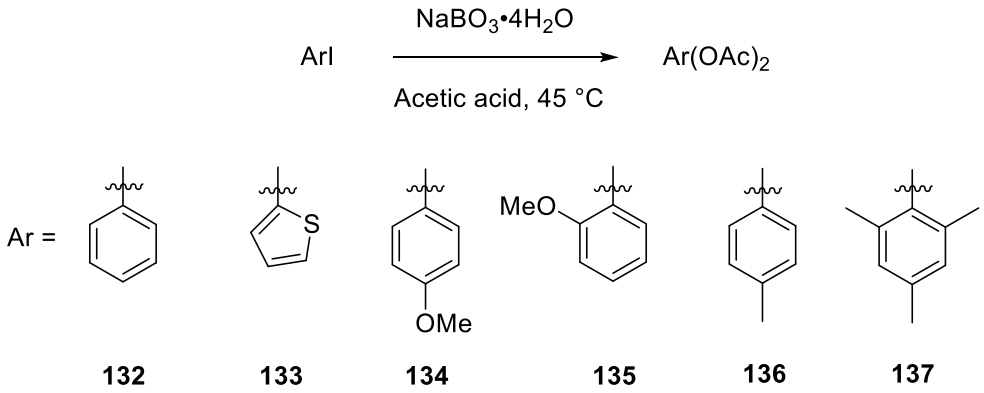

Scheme 59: Preparation of aryliodobis(acetate)s *via* oxidation of iodoarenes with $NaBO_3 \cdot 4H_2O$

McKillop and Sanderson have proposed that the active species in this reaction is an oxidative peracetoxyborane species, formed *in situ* by the mixing of sodium perborate tetrahydrate, known to be the disodium salt of 1,4-borate dianion **138**,[307] with acetic acid (Scheme 60).[306]

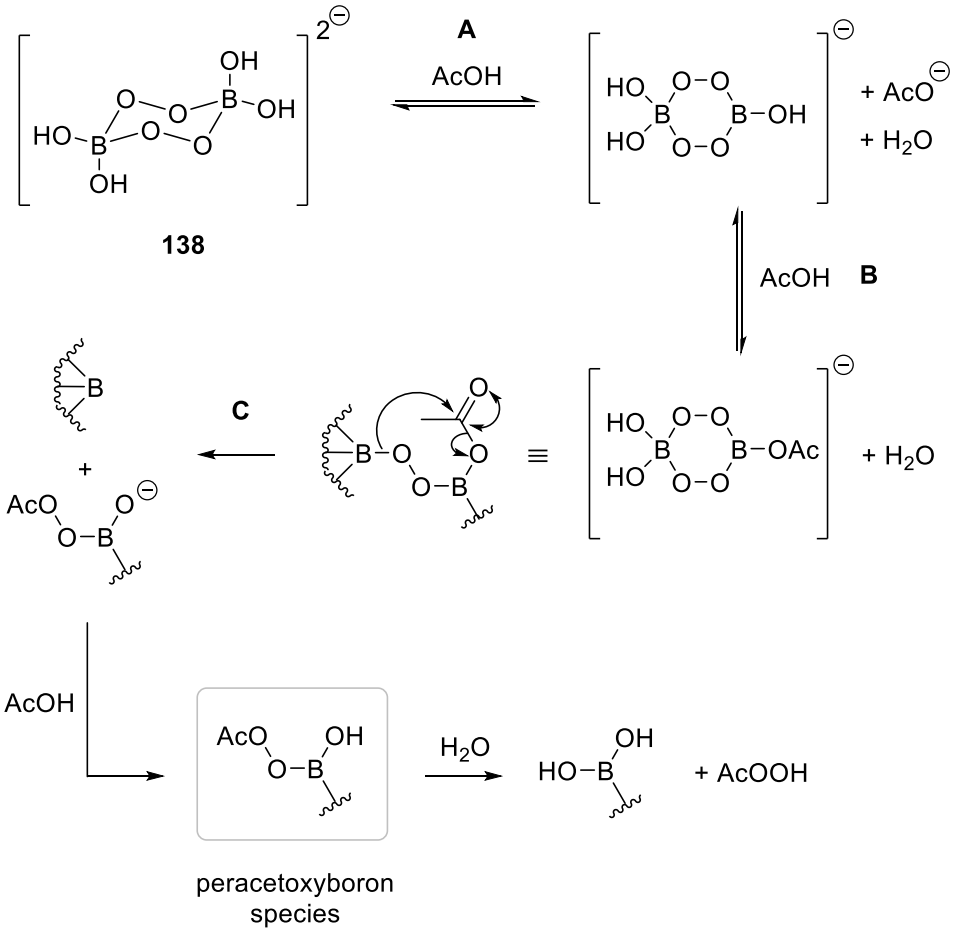

Scheme 60: Formation of a reactive peracetoxyboron species expected to be the active oxidant in the preparation of aryliodobis(acetate)s *via* oxidation of iodoarenes using sodium perborate tetrahydrate

In the above scheme, it is speculated that the species reacting in step C may be the same as that in step B, or that an intermediary solvolysis of the first BOOB linkage may have occurred. It was also considered that the numerous species bearing BOOAc units could also potentially act as oxidants on organic substrates, in tandem with or in place of the peracetoxyboron species afforded by the final acid-catalysed hydrolysis.[306]

In practice, monitoring the progress of the reaction proved to be a challenge, as analysis *via* chromatographic methods (TLC) could not be utilised and the literature provides few examples of accurate reaction times, which can vary substantially depending on the electronic character of the substrate. Here the most practical method of judging the reaction progress of a aryliodobis(acetate) preparation was by visual observation of the reaction mixture, the homogenous starting mixture gradually yields an off-white precipitate, where a higher opacity typically correlated

to a higher yield. With extended reactions times (> 5 h) the reaction mixture was seen to revert to homogeneity and in these instances a drastically lower yield was afforded, and hence for lack of a better method, reaction progress was monitored by the proportion of precipitate in the reaction mixture, with optimal reaction times ranging between 4 and 5.5 hours. Given that aryliodobis(acetate)s are useful precursors to diaryliodonium salts, multiple batch-based productions of aryliodobis(acetate)s not only provided information on the achievable yields of the oxidation reaction (Figure 32), but also allowed for stock-piling of the synthetic precursor providing the λ^3-iodane was correctly stored.

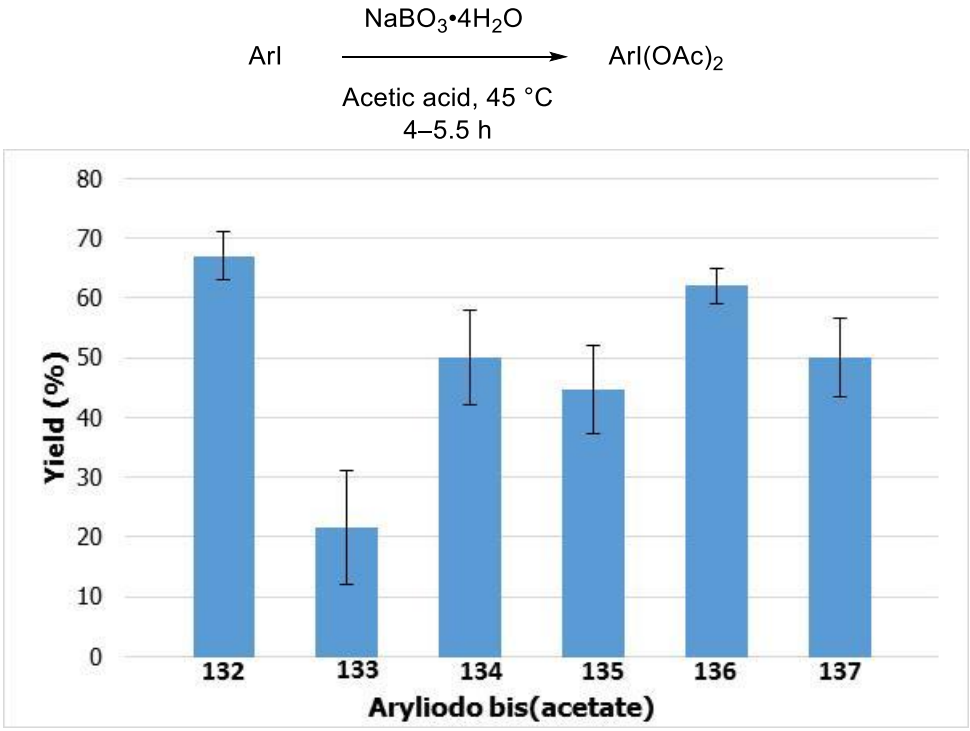

Figure 32: Yields of aryliodobis(acetate)s preparations *via* oxidation of iodoarenes with sodium perborate tetrahydrate. Ar = phenyl (132), 2-thienyl (133), 4-anisyl (134), 2-anisyl (135), 4-tolyl (136) and mesityl (137); n = 3 minimum

It was found that the most electron-deficient phenyl system **132** in the series exhibited the highest yield and the oxidation of 4-iodotoluene to **136** afforded a similarly high yield, both with relatively good reproducibility. However, with increasingly electron-rich iodoarenes, yields were seen to lower accordingly and become less consistent. In particular, the 2-thienyliodobis(acetate) **133**, afforded

yields that were not only very inconsistent, but also even at best, were markedly lower than the other (diaceoxy)iodoarenes in the series.

In an effort to optimise the preparations of the most commonly utilised aryliodobis(acetate)s and to study the effect of substrate electronics on the reaction time, the reaction progress for the formation of **132**, **133**, **134** and **135** was monitored by ^{1}H NMR in 30 min increments for 7 h. Here an expected downfield shift of protons *ortho*- to the iodine centre from 7.3 – 7.5 ppm for aryliodide starting materials to 7.7 – 8.0 ppm for $ArI(OAc)_2$ species could be observed and was utilised to determine the conversion progress of the reaction.[261] This experiment highlighted the dependence reaction time has on electronic character of the substrate, note that complete consumption of the starting material is rarely seen and even with optimised reaction times, substantial starting material remained, attributing to the relatively poor conversions seen above (Figure 32).

Aryliodobis(acetate)	Ar	Time	Product: SM ratio
132	phenyl	5.5 h	6:1
133	2-thienyl	4.0 h	3:1
134	4-anisyl	4.5 h	4:1
135	2-anisyl	4.5 h	4:1

Table 7: Optimal reaction times for production of aryliodobis(acetate)s 132-135

In general, it was found that substrates endowed with electron-donating groups in *ortho*- or *para*- positions provided higher yields with shorter reactions times, as did the electron-rich heteroarene **133**, which is in line with initial findings by McKillop and co-workers, who found that arenes bearing electron-withdrawing *meta*-substituents also exhibited accelerated oxidation, whereas systems with *ortho*- or *para*- electron-withdrawing groups required longer reaction times.[287]

The decomposition of the aryliodobis(acetate)s when exposed to atmospheric conditions, when stored in solution over distinct periods of time and when heated has been studied in detail using electrospray ionisation mass spectrometry (ESI-MS)

by Silva *et al*,[308] a feature of this compound class that was also noted in this work. Here ESI-MS was performed on a freshly prepared sample of phenyliodobis(acetate) **132** (Figure 33, A) dissolved in acetonitrile, a sample of **132** stored in acetonitrile at room temperature for 24 h (Figure 33, B) and a freshly prepared sample of **132** heated to 80 °C in acetonitrile prior to analysis (Figure 33, C).

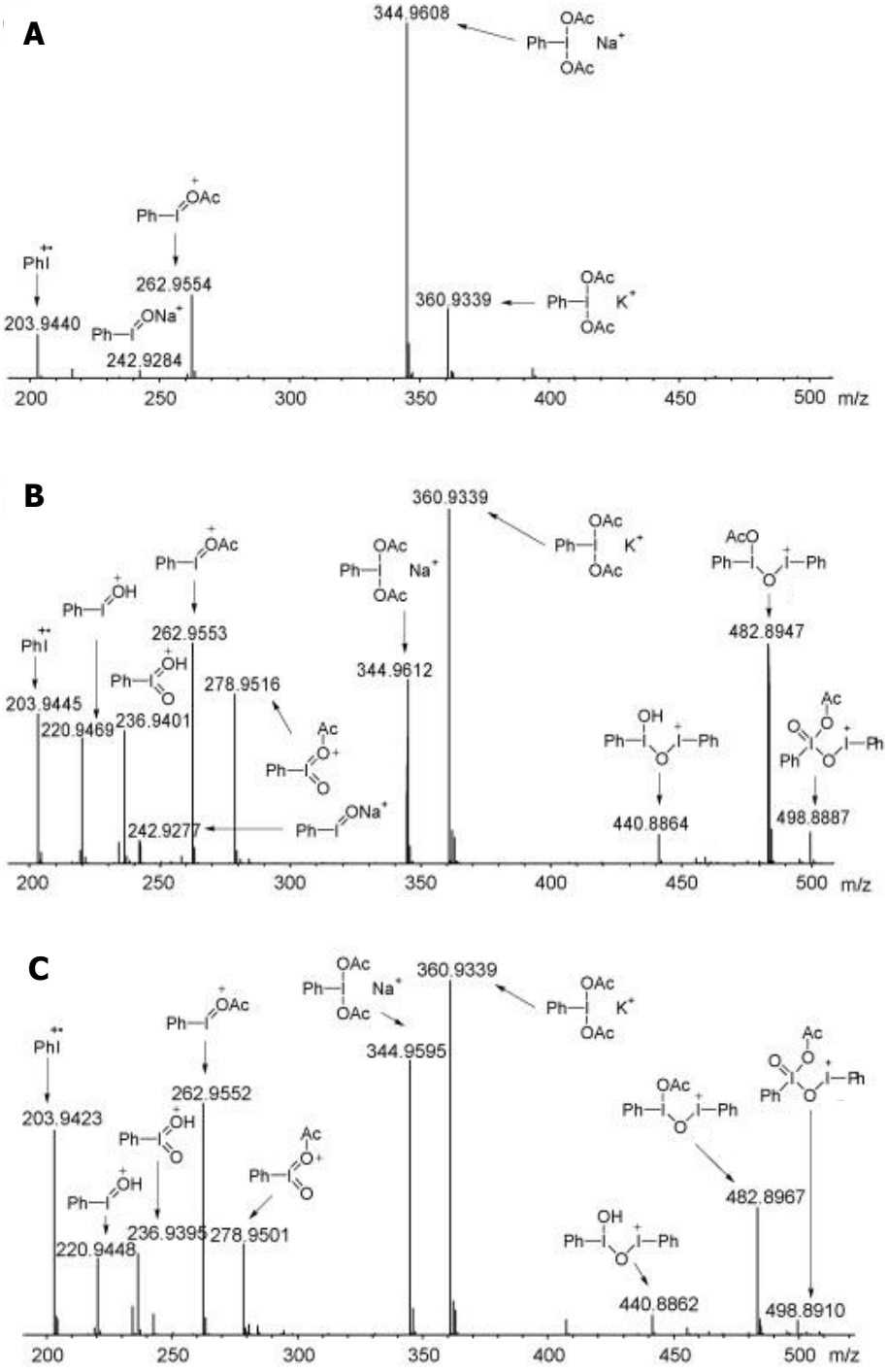

Figure 33: Decomposition products of (diacetoxy)iodobenzene 132 when subject to B: extended period in solvent (MeCN, 24 h at RT) and C: when heated (MeCN, 80°C) *versus* A: a freshly prepared solution of 132 (MeCN, RT) as observed by ESI-MS

The ESI-MS study emphasised the potential that aryliodobis(acetate)s have for rapid decomposition when stored in solution for relatively short periods of time and when heated in solution, to afford the numerous dimeric and iodosyl species highlighted above. It is expected that a degree of decomposition to these species also occurs during the reaction conditions, which competes with the formation of the desired oxidation product and hence further limits the resulting yields of aryliodobis(acetate) production. Despite the unreliability and relatively poor yields afforded by McKillop and co-workers' general method for aryliodobis(acetate) production,[287] the procedure does provide a simple route for batch preparation of the valuable λ^3-iodanes when performed in relatively large scale (60 mmol), whilst utilising cheap, commercially available starting materials and an oxidant that allows for mild reaction conditions and affords non-toxic by-products.

A further improvement was made on the yield for the most commonly employed aryliodobis(acetate), **134**, by utilising an Asynt ReactoMate CLR jacketed reactor system (Figure 34), which provided more efficient heat distribution through the use of an overhead stirrer coupled with Julabo temperature control circulator.[309] The simple reaction set up allows for easy extraction of the product aryliodobis(acetate) through a filter port at the bottom of the vessel, a practically useful feature for when the preparation is conducted at large scale. Not only was a noteworthy increase in the average yield of this reaction observed (>15% increase), but the consistency of yields also saw drastic improvement (± 3% with the jacketed reactor system *versus* ± 18% with a standard round bottomed flask and magnetic stirrer).

Figure 34: Asynt ReactoMate CLR Jacketed system (pictured left) and the scheme for improved production of aryliodobis(acetate) 134 (right)

Here the optimisation of the aryliodobis(acetate) preparation protocols for the λ^3-iodanes described in this section (**132**–**137**) provided a relatively reliable and quick to synthesise source of the diaryliodonium salt precursors largely bearing the desired electron-rich character. Once prepared, these reagents were stored in a freezer, in the dark for a limited period (maximum of 2 weeks) before being utilised in the subsequent coupling reaction, once the corresponding arylstannane had been produced. The oxidising nature of aryliodobis(acetate) synthesis denies the incorporation of sensitive functionalities and hence our general approach entails the preparation of the arylstannane component as the more functionalised 'target' aromatic ring, rather than the reverse.

2.6 Preparation of Arylstannanes

The use of arylstannane reagents in this application (and as in many other applications) provide a means for nucleophilic coupling of the stannylated aryl group on an electrophilic centre, being the aryliodobis(acetate) hypervalent iodine centre in this case. Other commonly utilised applications of the reagent class include carbonylation reactions,[310] and Stille coupling reactions,[311] but these methods often involve a different substrate scope to those discussed in this work. The benefits of using arylstannane reagents here over the alternative boronic acids or silane based reagents not only includes improved reactivity towards electrophilic species, but in addition their preparation is generally very tolerant to the inclusion of multiple sensitive functionalities, hence being beneficial to our general approach to diaryliodonium salt formation.

A forgoing requirement to stannylation of the phenol halides is protection of phenolic functionality, for which two simple approaches, benzylation (Scheme 61) and acetylation (Scheme 62) provided robust means to protect the alcohol functionality whilst allowing for simple and quick deprotection of the target fluoroarene.

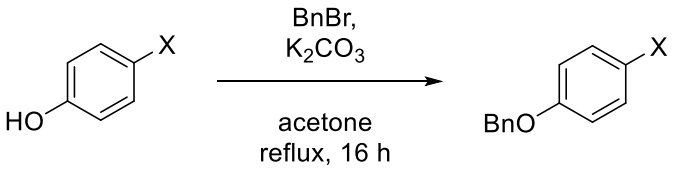

138, X = I
139, X = Br

140, X = I, 91%
141, X = Br, 94%

Scheme 61: Simple benzylation protection of 4-iodophenol and 4-bromophenol

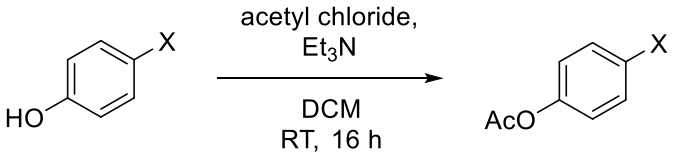

138, X = I
139, X = Br

142, X = I, 92%
143, X = Br, 79%

Scheme 62: Simple acetylation protection of 4-iodophenol and 4-bromophenol

These easily scalable protocols provided access to substantial amounts of the required protected aryl halide starting materials, that were not only simple to purify but also sufficiently stable for long term storage. Here both bromo- and iodo-derivatives of the fluorination target were prepared to determine which provided the superior substrate for stannylation and whether or not use of 4-iodophenol over 4-bromophenol outweighed the substantial difference in starting material cost (£41.27 for 25 g[312] *versus* £28.50 for 100 g[313] respectively).

In development of this protection strategy, it is important to consider the subsequent deprotection required after the prospective [^{18}F]fluorination of the diaryliodonium salts; here this cleavage step must be fast to avoid loss of RCY, must be high yielding to avoid loss of protected-4-[^{18}F]fluorophenol of which concentrations might be low, and must yield easily separable by-products. For the two protection methods described above (Scheme 61 and Scheme 62), methods of achieving rapid and high (chemical) yielding deprotection have previously been described (Scheme 63 and Scheme 64).[314,315]

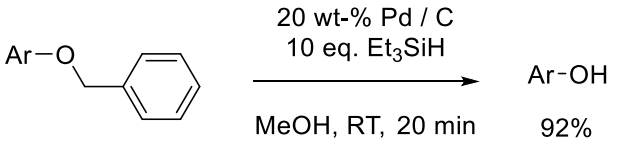

Scheme 63: Rapid cleavage of benzyl protecting group *via* the *in situ* generation of molecular hydrogen through the addition of triethylsilane to palladium on charcoal[314]

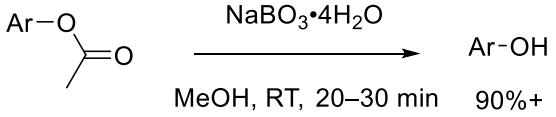

Scheme 64: Rapid cleavage of the acetyl protecting group using sodium perborate, providing a clean and highly selective procedure[315]

A number of routes to arylstannanes from arylhalides are available and here more traditional approaches including palladium mediated stannylation (Scheme 65)[316] and stannylation *via* halogen-lithium exchange (Scheme 66)[317] were initially considered.

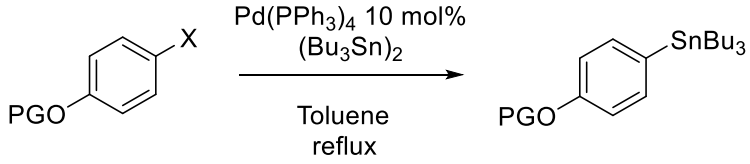

X = I, Br; PG = Bn, Ac

Scheme 65: Preparation of arylstannanes *via* palladium catalysed stannylation

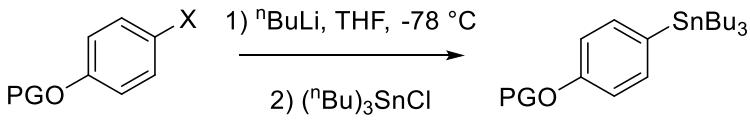

X = I, Br; PG = Bn

Scheme 66: Preparation of arylstannanes *via* halogen-lithium exchange

However, these methods of arylstannane synthesis proved to have a number of associated limitations. Although the tetrakis(triphenylphosphine)palladium (0) catalysed process produces good yields and is tolerant of a wide range of reactive

functionalities, use of the costly transition metal at the significantly high catalyst loading described above; coupled with the requirement for two equivalents of the considerably toxic hexa-*n*-butylditin reagents; and the high potential for biaryl formation through homo-coupling makes this approach relatively unattractive.[316] Similarly, stannylation achieved *via* halogen-lithium exchange can provide a fast, simple and low-cost route to arylstannanes, however, the use of *n*-butyllithium considerably limits the substrate scope, making this approach an inadequate method for preparation of arylstannane precursors with acidic protons and/or remotely electrophilic functionality.[317]

An alternative method for trialkylstannanyl arene production that evades some of the constraints of the two approaches described above, includes the work of Gosmini and co-workers,[318] which has demonstrated broad substrate scope, without the need for an expensive catalyst and without calling for two equivalents of a ditin reagent; all whilst affording good stannylation yields under mild conditions.[319,320] This innovative conversion of arylhalide to arylstannanes proceeds with acidic activation of zinc dust to facilitate the reduction of cobalt (II) bromide, which then leads into the catalytic cycle depicted below (Scheme 67). The catalytic process continues *via* oxidative insertion of the resulting cobalt (I) bromide species into the substrate aryl bromide C-Br bond (or aryl iodide C-I bond), affording a trivalent arylcobalt dibromide complex. The subsequent transmetallation (provided by excess zinc in the system) accounts for the formation of the reactive organozinc species and simultaneous regeneration of cobalt (II) bromide (Scheme 67).[320]

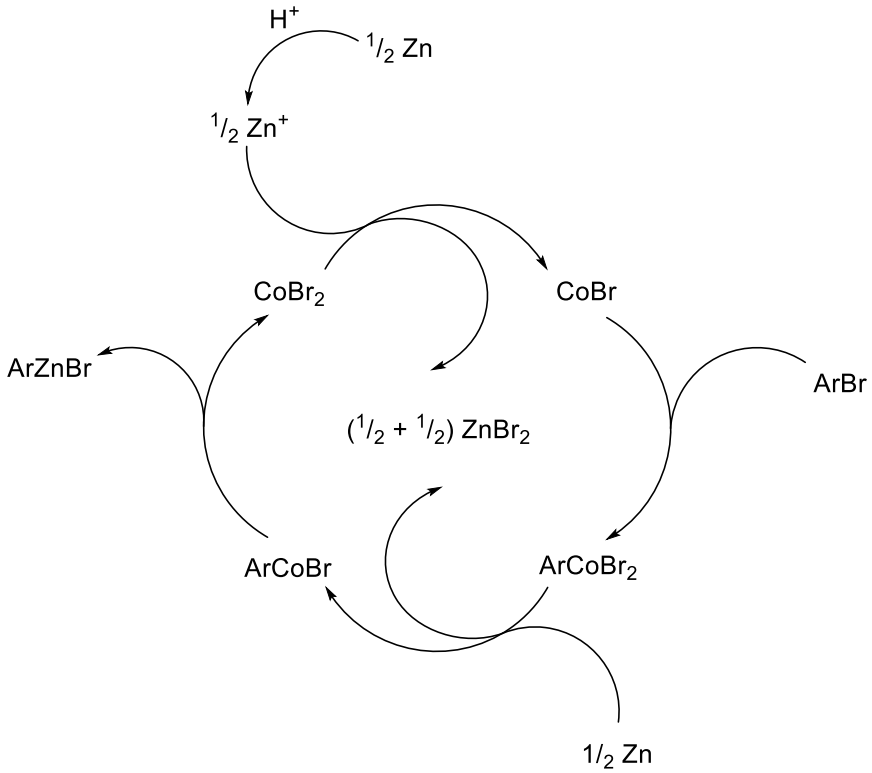

Scheme 67: Cobalt (II) bromide catalysed formation of arylzinc species in Gosmini and co-workers' preparation of arylstannanes

Administration of the substrate arylhalide in tandem with the stannylating reagent, tributylstannyl chloride, allowed for *in situ* formation and reaction of the key organozinc reagent, affording one-step preparation of the desired tributylstannylarene products in 3-16 h with gentle heating (50 °C).

Small modifications to the stoichiometry of the original procedure provided an optimised, simple-to-follow, one-step route to tributylstannylarenes from simple arylhalide substrates bearing various protected phenol functionality, affording yields of 53-91% (Scheme 68).

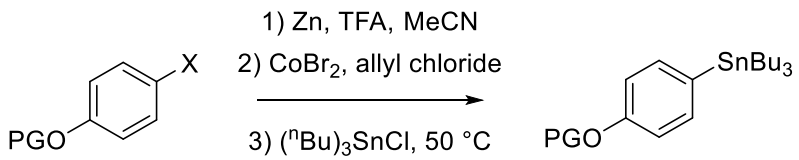

140, X = I; PG = Bn
141, X = Br; PG = Bn
142, X = I; PG = Ac
143, X = Br; PG = Ac
144, X = I; PG = Me
145, X = Br; PG = Me

146a, PG = Bn, 68% (from **140**)
146b, PG = Bn, 86% (from **141**)
147a, PG = Ac, 53% (from **142**)
147b, PG = Ac, 61% (from **143**)
148a, PG = Me, 70% (from **144**)
148b, PG = Me, 91% (from **145**)

Scheme 68: One-step preparation of tributylstannylarenes from protected 4-halophenols *via* cobalt catalysed *in situ* arylzinc preparation

Despite the increased reactivity offered by aryliodides *versus* the bromide counterparts, they suffer from notably lower yields across the series, which is mostly likely an artefact of competing by-product formation *via* homo-coupling,[319] however, compared to methods described earlier (Scheme 65 and Scheme 66) this route provides comparable yields without the need for costly catalysts or more forcing reaction conditions.

Initial preparations of arylstannanes by this adapted method highlighted potential difficulty in the separation of the stannylated product and other tributylstannyl by-products, believed to be oxidised organostannanes such as Bu_3SnO and $Bu_3Sn\text{-}O\text{-}SnBu_3$. Although purification by column chromatography on SiO_2 did, on occasion, afford the desired purified arylstannanes on one attempt, often multiple purifications were required and similarly, the potential for destannylation of the product on the acidic sorbent afforded reduced yields. This challenge was overcome by utilising reverse phase chromatography with neat acetonitrile as the eluent, a purification method that would otherwise prove to be grossly expensive on moderate/large scale, however, in this case flash chromatography allowed for rapid purification with reduced volumes of solvent. Likewise, the risk of destannylation was mitigated by employing flash reverse phase chromatography and provided the good yields described above (Scheme 68).

This work demonstrates the scope of cobalt catalysed/organozinc mediated tributylstannyl arene preparation as an excellent alternative to conventional

approaches, *via* an easy to replicate, one-pot process, further supported by an ultra-simple purification protocol.

2.7 Preparation of Diaryliodonium Salts for 4-[^{18}F]Fluorophenol Production

As outlined in Section 2.3 the literature presents a number of diverse routes to diaryliodonium salts with various advantages and limitations. A general approach that could facilitate the production of electron-rich diaryliodonium systems; utilised the preferred trifluoroacetate counter-ion; and was tolerant of potentially sensitive protecting groups and/or other functionality was desired. In this work, a general procedure developed by Pike and co-workers[321] was modified to meet this demand and was found to permit coupling of arylstannanes and aryliodobis(acetate)s activated with trifluoroacetate to yield the product diaryliodonium trifluoroacetate under very mild conditions (Scheme 69).

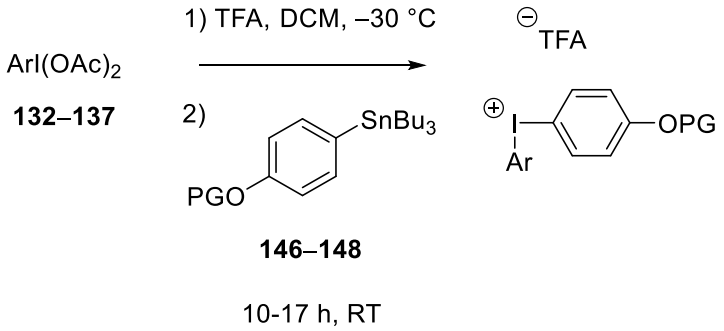

Scheme 69: General method for the preparation of diaryliodonium trifluoroacetates from aryliodobis(acetate)s and arylstannanes

Although the method is uncomplicated, there are a number of crucial finer points that must be followed stringently to achieve successful diaryliodonium salt formation, firstly preparation under anhydrous conditions using dried solvent and reagents is strongly recommended. Dropwise addition of trifluoroacetic acid (2 eq.) to the cold (–30 °C) solution of aryliodobis(acetate) (as prepared in Section 2.5) is also vital for the *in situ* formation of a reactive aryliodo bis(trifluoroacetate) species, which when

subjected to an appropriate arylstannane (as prepared in Section 2.6, also administered at –30 °C affords the objective diaryliodonium trifluoroacetate after a period of stirring (10-17 h) in the dark, at room temperature.[321] Unlike alternative approaches, this method avoids the necessity for heating the reaction, which can to some extent result in a reduced yield given the heat sensitive nature of hypervalent iodine compounds.[300,305]

The nucleophilic character of the arylstannane C-Sn bond facilitates its attack on the electrophilic aryl-λ^3-iodane (Scheme 70), a feature greatly enhanced by incorporation of the trifluoroacetates ligands. There is more evidence to suggest that this attack on the hypervalent species proceeds by an associative mechanism,[322] rather than a dissociative mechanism (introduced in Section 2.2), however both mechanisms require elimination of a ligand in the equatorial position, which can only occur *via* the conformational interchange of a dimeric species provided by Berry pseudorotation (ψ) in the example below (Scheme 70).[254] Note that up until this point, only monomeric models have been considered, however, as more is discussed it will become apparent many postulations rely on the existence of dimeric and polymeric species for them to occur.

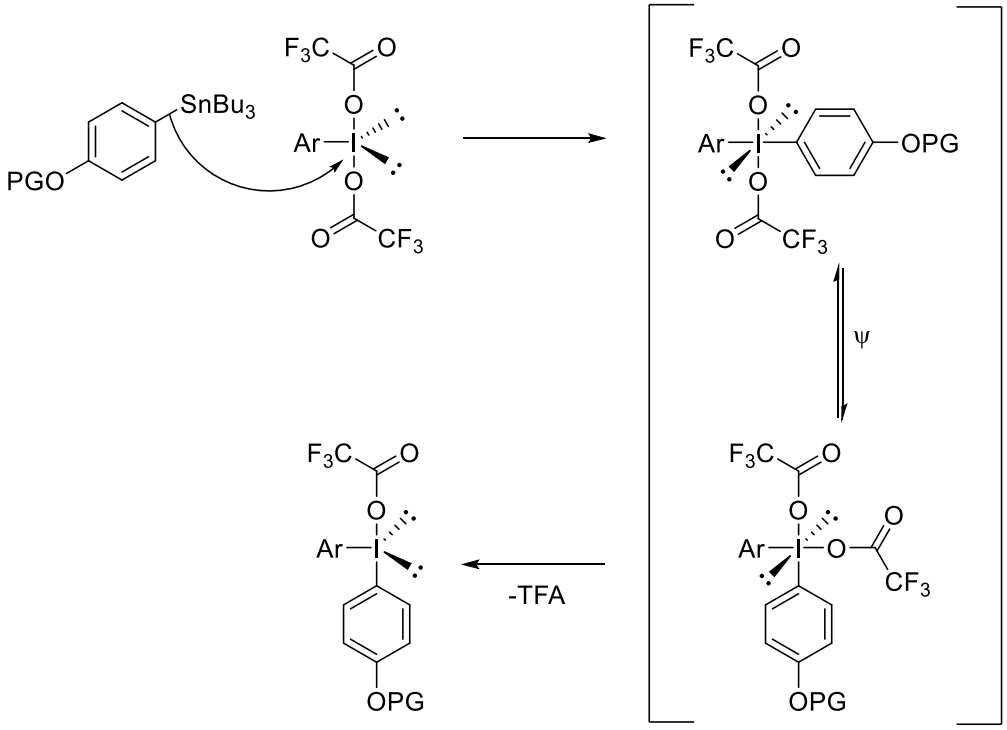

Scheme 70: A proposed mechanism for the formation of diaryliodonium trifluoroacetates, including consideration of an associative pathway in the mechanism

Practically, the formation of the diaryliodonium salt product could be monitored by TLC, as could the consumption of the arylstannane and aryliodobis(acetate) starting materials; and the subsequent product extraction procedure involved removal of ~75% of the solvent e.g. DCM and addition of a lower polarity solvent e.g. petrol 40-60 to afford crystallisation of the product.

To promote crystallisation of the product diaryliodonium salt over remaining aryliodobis(acetate), preparations utilising a slight excess of arylstannane reagent were trialled. ^{1}H NMR of the crude reaction mixture typically highlighted the success of the conversion as well as the proportion of arylstannane reagent remaining, however, when this impurity was present in substantial amounts, crystallisation of the product often proved challenging. In these circumstances column chromatography effectively removed these contaminants to yield purified diaryliodonium trifluoroacetates, however, this extended period of exposure to moisture, light, silica and potential nucleophiles understandably reduced the yields obtained, as did the inherent instability of the compound class, given the electron-rich nature of the diaryliodonium salts' arene substituents, *versus* diaryliodonium salts bearing electron-poor aromatics.

Hence the above procedure (Scheme 69), was used to prepare diaryliodonium salts **149-153** (Figure 35), with special care taken to ensure molar equivalency of the arylstannane and aryliodobis(acetate) reagents employed.

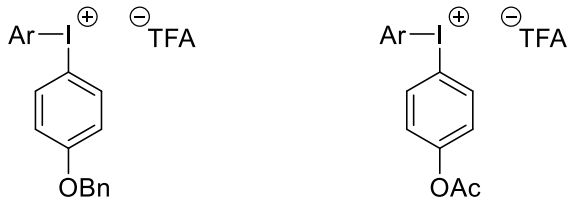

149, Ar = 4-anisyl
150, Ar = 2-thienyl
151, Ar = phenyl

152, Ar = 4-anisyl
153, Ar = 2-thienyl

Figure 35: Diaryliodonium trifluoroacetates prepared from arylstannanes and aryliodobis(acetate)s

The challenges in product isolation (as well as product instability) resulted in inconsistent yields for all diaryliodonium salts prepared (n ≥ 3), but particularly for

products bearing the 2-thienyl functionality. In an attempt to improve the yields of some diaryliodonium salts through the application of an alternative solvent (of which options are limited), acetonitrile, was trialled in place of DCM and was also found to have a notable effect on the resulting yields (Table 8).

Bu_3SnAr (Ar =)	$ArI(OAc)_2$ (Ar =)	Solvent	Product	Yield
146 (4-(BnO)C_6H_4)	**134** (4-anisyl)	DCM	**149**	39-71%
146 (4-(BnO)C_6H_4)	**134** (4-anisyl)	MeCN	**149**	52-67%
146 (4-(BnO)C_6H_4)	**133** (2-thienyl)	DCM	**150**	29-55%
146 (4-(BnO)C_6H_4)	**133** (2-thienyl)	MeCN	**150**	44-56%
146 (4-(BnO)C_6H_4)	**132** (phenyl)	DCM	**151**	70-78%
147 (4-(AcO)C_6H_4)	**134** (4-anisyl)	DCM	**152**	32-47%
147 (4-(AcO)C_6H_4)	**133** (2-thienyl)	DCM	**153**	14-33%

Table 8: A series of unsymmetrical protected phenoxy-iodonium trifluoroacetates prepared from coupling arylstannane and aryliodobis(acetate) reagents

These findings highlight the enhanced instability afforded when the 2-thienyl moiety is incorporated into diaryliodonium salts, regardless of the protecting group on the other aromatic or the solvent used; likely to be a consequence of the arene's increased electron density *versus* the other two non-participating ring (n.p.r.) systems. By the same rational, it was found that the integration of a phenyl n.p.r. into diaryliodonium salts such as **151** over the electron-rich arenes afforded higher yields, an expected observation given the preference for electronegative ligands in apical positions of diaryliodonium salts when compared to the other diaryliodonium systems, which bearing two electron-rich arenes are unable to provide stabilisation to the hypervalent 3c-4e bond.[235]

Diaryliodonium salt **151,** albeit more stable, is not a useful substrate for the production [^{18}F]fluorinated protected phenol derivatives, as [^{18}F]fluorobenzene is likely to be the major product given that is more electron-deficient than the other

arene, however, this diaryliodonium will be retained in the series as it provides support to the methodology of diaryliodonium salt fluorination.

Another clear observation provided by the results in Table 8 includes the notable benefit to yields achieved with benzylated arylstannanes over acetylated arylstannane substrates, most likely owing to the improved resistance to nucleophilic species within the reaction mixture, given that acetate groups are prone to *in situ* hydrolysis. Provisionally, this work suggest that substituting DCM for acetonitrile provided more consistent yields, such as diaryliodonium salts **149** and **150**, however, further work on the conversion would be required to fully validate that claim.

^{1}H- and ^{13}C-NMR spectra of diaryliodonium salts **149**–**153** were generally as expected and comparable to previously published derivatives,[260,261] displaying a downfield shift of protons *ortho*- to the iodane between 8.0 – 8.3 ppm, relative to the protons in the same position on aryliodobis(acetate) starting materials, which typically exhibited a shift between 7.7 – 8.0 ppm. ^{1}H-NOESY NMR also provided a means to discriminate proton environments experiencing very similar electronic influences, by collecting resonances from nuclei that are spatially close, as exemplified below for diaryliodonium salt **149**.

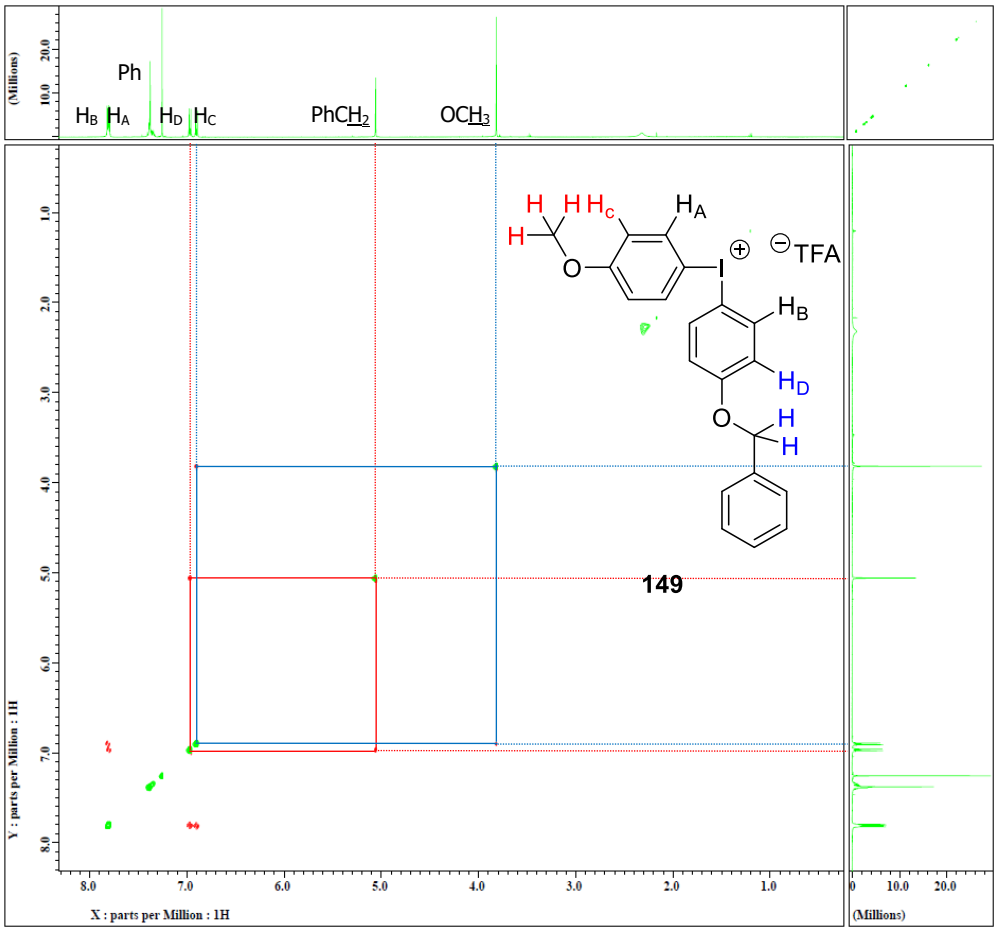

Figure 36: ^{1}H-NOESY NMR of diaryliodonium salt 149

The general method for the preparation of electron-rich diaryliodonium salts described above (Scheme 69) proved to yield the desired target compounds **149**–**153** of sufficient purity for radiofluorination (as deemed by ^{1}H NMR, ^{13}C NMR, HR-MS and elemental analysis), where amounts of contamination considered to be insignificant can lead to reduced RCYs and poor SAs. Further structural information of the electron-rich diaryliodonium salts was desired and hence a simple procedure for obtaining crystalline product suitable for crystallographic analysis was required. Multiple recrystallisation methods and various solvent combinations were examined, of these, recrystallisation *via* slow vapour diffusion using acetonitrile as the sample solvent and 50:50 diethyl ether:petrol as nucleation inducing solvent system, with two week freezer storage afforded crystals of sufficient quality for x-ray crystallography (Figure 37).

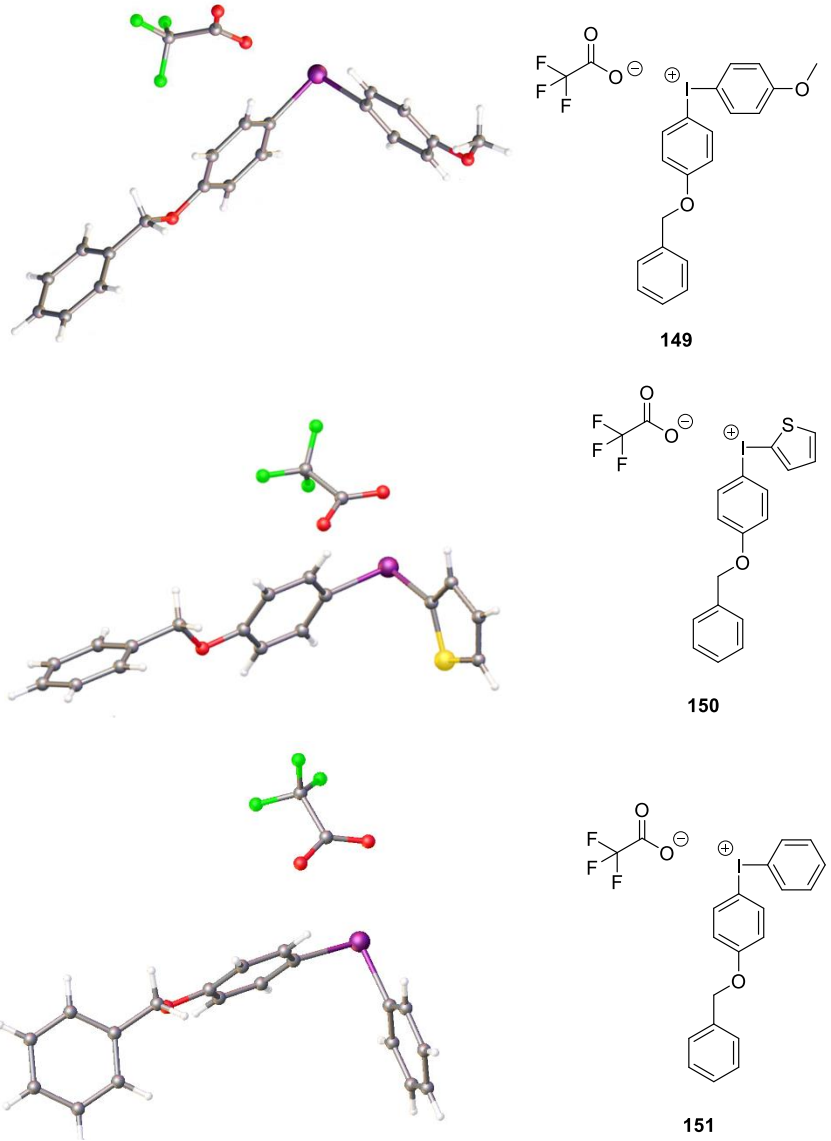

Figure 37: X-ray crystal structures of diaryliodonium salts 149-151, prepared *via* slow vapour diffusion recrystallisation from acetonitrile and 50:50 diethyl ether:petrol

As briefly discussed in Section 2.5, aryl and diaryliodonium salts are known to form numerous polymorphs; with dimers, trimers and polymeric structures frequently observed. Dimerism and polymeric interactions were also seen for diaryliodonium salts prepared within the **149**-**153** series (Figure 38).

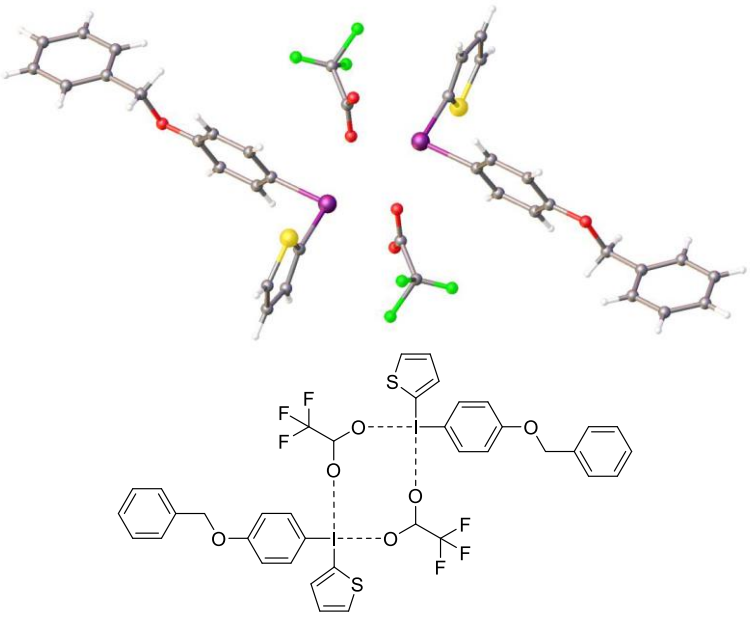

150

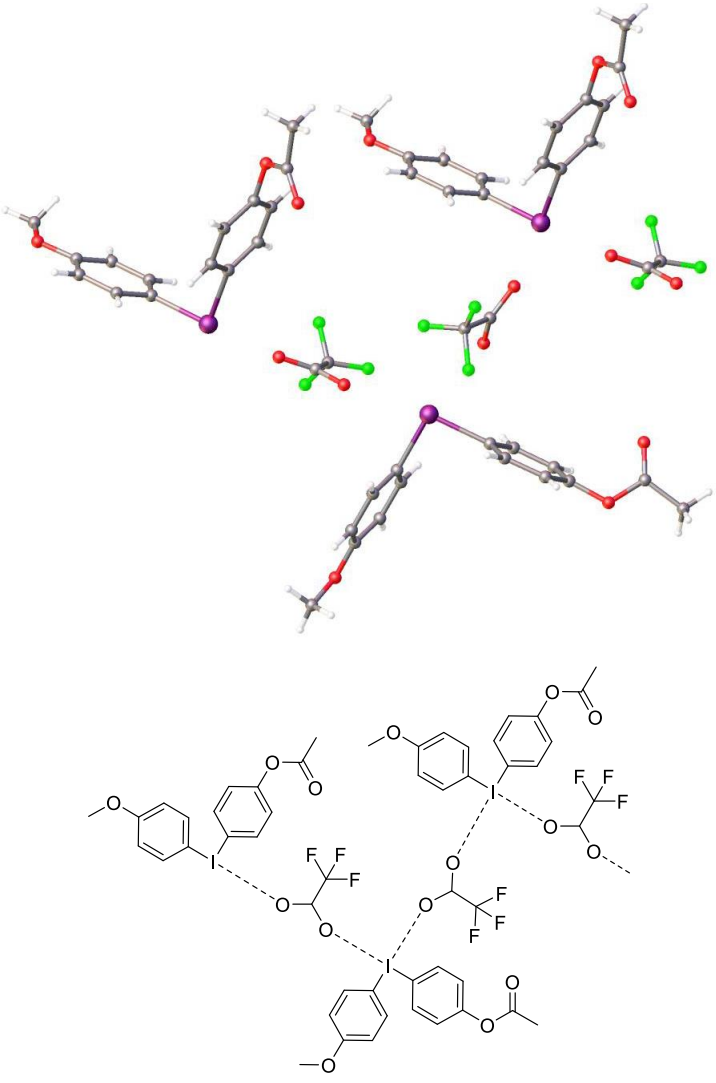

152

Figure 38: X-ray crystal structures of dimeric polymorph of diaryliodonium salt 150 and polymeric polymorph of diaryl iodonium salt 153

At this stage, it is worth noting that very few published monomeric crystal structures of diaryliodonium salts are true representations of the ground-state structure of the species, as they are often extracted from dimeric or polymeric structures like those shown in Figure 39. For example, the orientation of the ring systems within the dimeric crystal structure of **150** (Figure 38) could be interpreted in two different ways (Figure 39), where arenes exchange between pseudo-equatorial and pseudo-apical positons is facilitated by the dimeric nature of species.

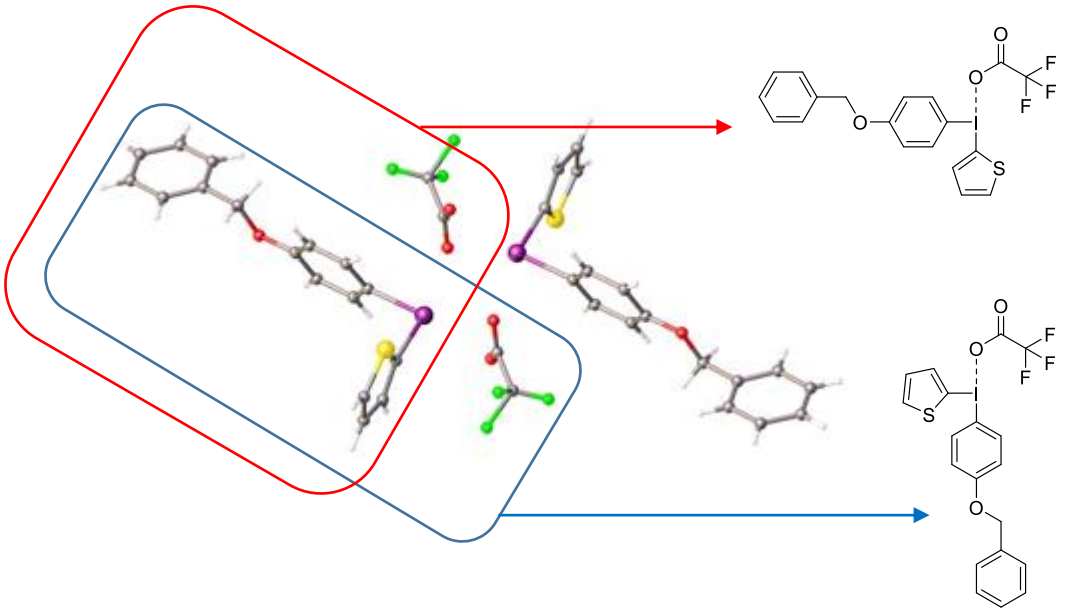

Figure 39: Ground-state conformation can be elucidated differently depending on which portion of the unit cell is selected

The optimised procedures for the production of diaryliodonium salts (*via* Scheme 69) and the parent aryliodobis(acetate)s (Section 2.5) and arylstannanes (Section 2.6) allowed for the routine production of diaryliodonium salts suitable for the [$^{18/19}$F]fluorinations described in the upcoming sections. However, an alternative route to some of these diaryliodonium salts, which negates the need for arylstannanes or other aromatic activated to nucleophilic attack, was also found to be useful. Investigations by Pike *et al*,[321] highlighted the application of this route for preparing a variety of substituted electron-rich diaryliodonium triflates and trifluoroacetates, from simple electron-rich arenes (Scheme 71).

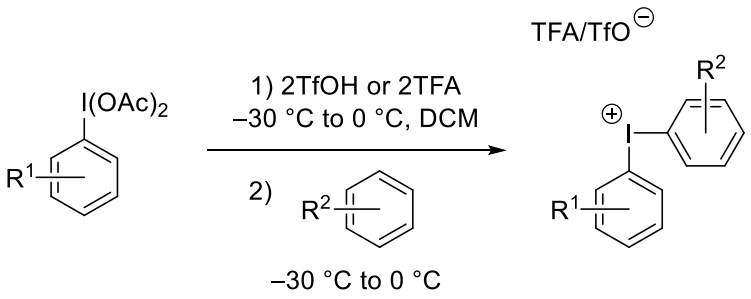

Scheme 71: Preparation of electron-rich diaryliodonium salts from aryliodobis(acetate)s and simple electron-rich arenes[321]

This route does appear to be markedly simpler than our method involving arylstannanes, and omits the need for the toxic reagent and the associated stringent diaryliodonium salt purification required to ensure removal of organostannanes residues. For the production of diaryliodonium triflates incorporating simple (4-anisyl, 4-tolyl, 2,4,6-trimethylphenyl) electron-rich arenes, this method afford good to excellent yields (60–85).[321] However, for the production of more desirable diaryliodonium trifluoroacetates, yields reported *via* this route are limited to 30–60% for simple systems; and replication of this procedure for the synthesis of marginally more complex diaryliodonium trifluoroacetates such as **149** and **152** produced unsatisfactory results (Scheme 72).

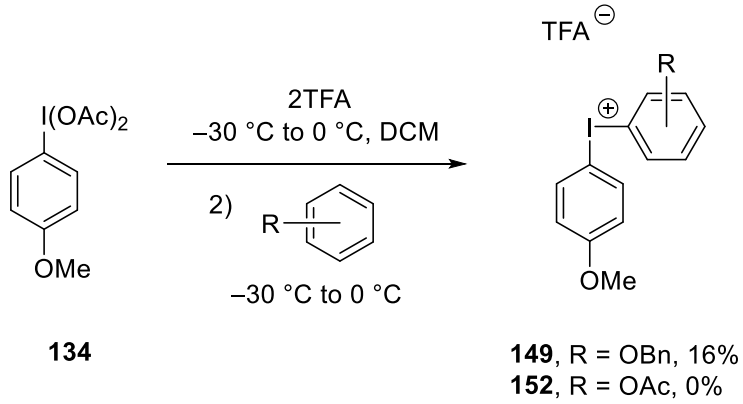

Scheme 72: Production of diaryliodonium trifluoroacetates *via* direct coupling of aryliodobis(acetate)s and protected phenols

This more direct route to simple, electron-rich diaryliodonium trifluoroacetates, albeit convenient, suffers from very poor yields and hence the use of arylstannane reagents

outweighs its application, particularly when preparing more intricate diaryliodonium salts. In addition, use of the arylstannane route allows for the preparation of a variety of regioisomers, unlike the simple route which affords on certain regioisomers as dictated by electronics.

2.8 [^{19}F]Fluorination of Diaryliodonium Salts

Prior to conducting [^{18}F]fluorinations of the diaryliodonium salts prepared in Section 2.7, it was deemed wise to conduct provisional [^{19}F]fluorination experiments of the precursors, with an aim to quickly validate the relative magnitude of fluorination of the target ring *versus* the non-participating ring. As previously mentioned, the more electron-deficient arene of a diaryliodonium salt sees preferential fluorination over electron-rich counterparts.[323] Hence for diaryliodonium salts **149**–**153**, where the electron density of the two arenes on all examples is near equivalent, a 50:50 selectivity profile between the target ring and the n.p.r. can be considered an encouraging outcome, and will aid selection of the most suitable diaryliodonium salts for the subsequent radiofluorination work.

A simple protocol for [^{19}F]fluorination of diaryliodonium salts was adapted from Shah and co-workers' method;[324] here the reactions were conducted on a small scale with deuterated DMF as the solvent of choice, since most radiofluorinations of this manner exploit DMF for its reagent compatibility and extended temperature range (up to 130 °C). Furthermore, application of the isotopologue allows for observation of the reaction progress in real time *via* ^{1}H and ^{19}F NMR.

Caesium fluoride was selected as the model [^{19}F]fluorination reagent, despite the actual species used for radiofluorination being different, however, work by Nairne *et al* has elucidated that caesium fluoride provides superior yields and the most suitability for these model [^{19}F]fluorination experiments (Table 9).[261]

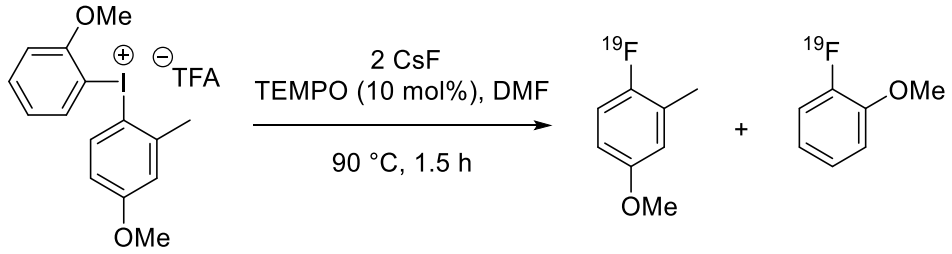

154 **155** **156**

Fluoride source ("$F^{\ominus}$")	Yield	Ratio 155:156
CsF	25%	1.3:1
TBAF	< 5%	n/a
KF	< 5%	n/a
KF/K_{222}	9%	1.3:1
KF/18-crown-6	13%	1.3:1

Table 9: Assessment of [^{19}F]fluorination reagents using model diaryliodonium 154 to observe the selectivity profile between products 155 and 156[261]

In this work, dynamic ^{1}H- and ^{19}F-NMR [^{19}F]fluorination studies were completed on diaryliodonium salts **149**–**153,** using one equivalent of the parent diaryliodonium salt and two equivalent of caesium fluoride in deuterated DMF within a NMR tube. The reactions mixtures were heated up to 140 °C from room temperature in 20 degree increments over 2 h, whilst being monitored by ^{1}H- and ^{19}F-NMR, providing insight on the fluorination selectivity profiles of each diaryliodonium salt (Scheme 73).

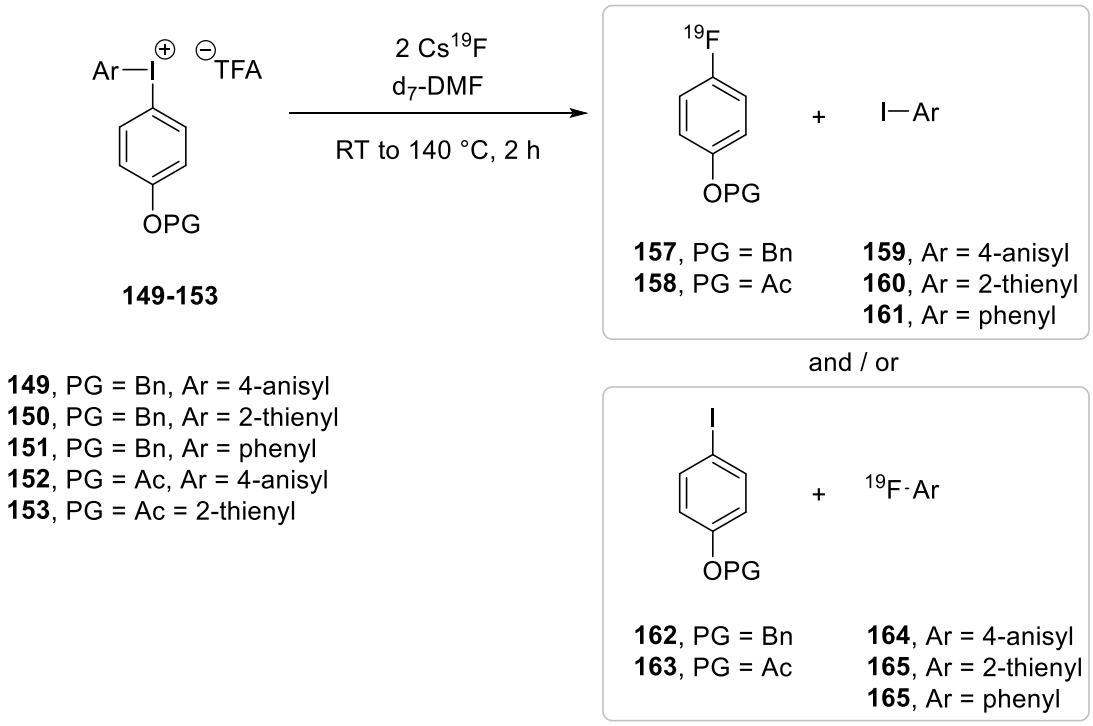

Scheme 73: Dynamic ^{1}H- and ^{19}F-NMR [^{19}F]fluorination study with diaryliodonium salts 149-153, highlighting the potential fluoro- and iodoarene products

After each reaction had been maintained at 140 °C for a minimum of 10 min, each was administered with a small amount of the desired fluoroaromatic product reference standard, analysed by ^{1}H- and ^{19}F-NMR, and then also co-injected with authentic standards of the other expected fluoroaromatic product before being analysed by ^{1}H- and ^{19}F-NMR once more, as shown for precursor **149** below (Figure 40 and Figure 41). [^{19}F]Fluorination of diaryliodonium salts **149**–**153** *via* this method provided a simple means to rapidly assess the effectiveness of each precursor candidate without expending excessive amounts of material.

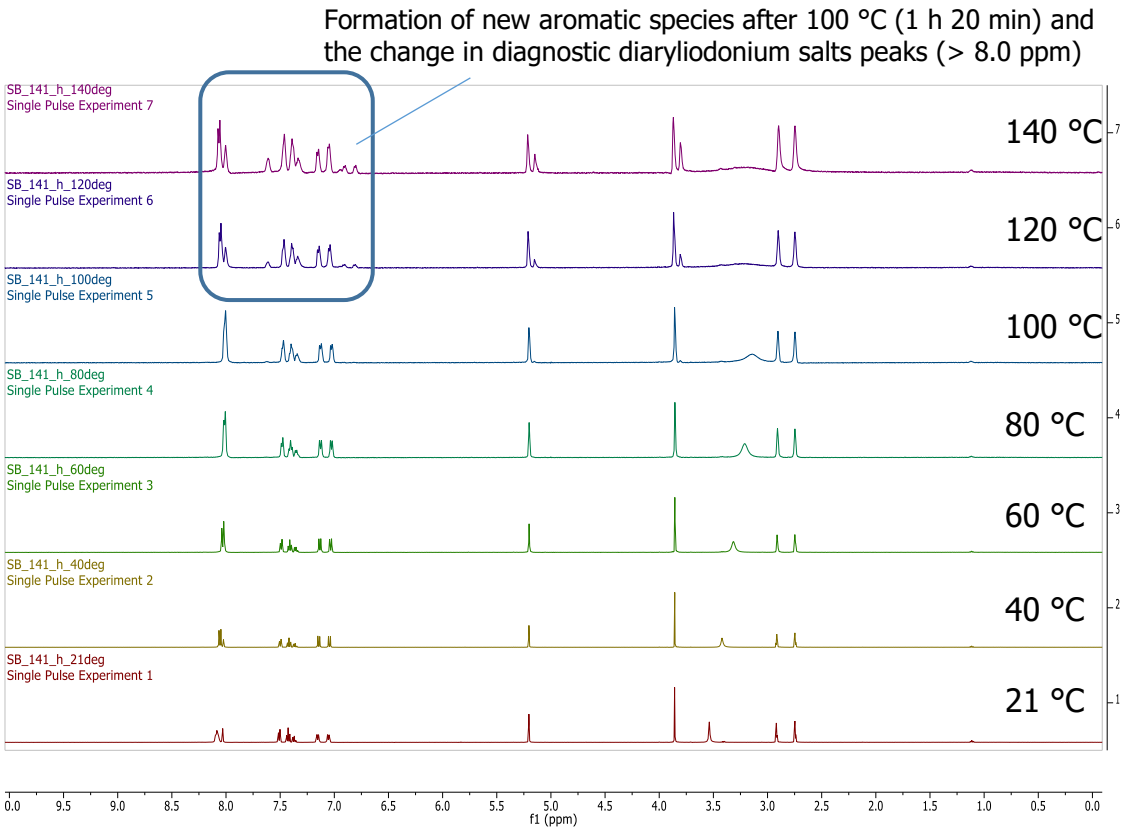

Figure 40: Dynamic ^{1}H-NMR experiment following the fluorination of (4-benzyloxy)phenyl)(4-methoxyphenyl)iodonium trifluoroacetate (149)

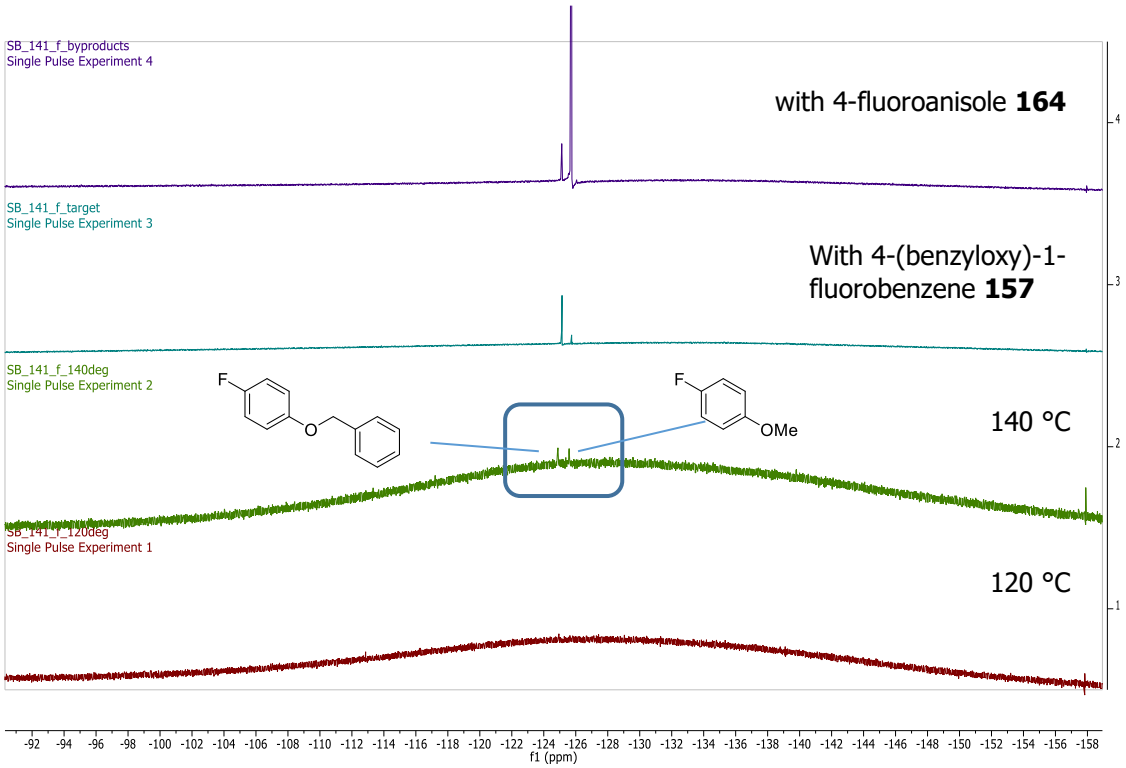

Figure 41: Dynamic ^{19}F-NMR experiment following the fluorination of (4-benzyloxy)phenyl)(4-methoxyphenyl)iodonium trifluoroacetate (149), spiked with 4-fluoroanisole (164) and 4-benzyloxy)-1-fluorobenzene (157)

[^{19}F]Fluorination of diaryliodonium salts **149**–**153** were conducted as depicted above and can be summarised by the following observations (Table 10). In all cases a decrease in the amount of diaryliodonium salt as the reaction proceeds above 100 °C could be observed; and the formation of new aromatic multiplets for substrates **149** and **151** was also recorded, corresponding to the expected formation of fluoro- and iodoarenes as per the anticipated fluorination outcome (Scheme 73).

Diaryliodonium salt	Fluoroarenes observed (^{19}F-NMR shift)	Ratio
149	**157** (-124.9 ppm); **164** (-125.6 ppm)	1:1
150	**157** (-124.9 ppm)	-
151	**165** (-114.4 ppm)	-
152	none observed	-
153	**158** (-118.92 ppm)	-

Table 10: Summary of dynamic ^{1}H- and ^{19}F-NMR study following the [^{19}F]fluorination of diaryliodonium salts 149–153

Diaryliodonium salt **149** provided the expected 50:50 selectivity profile corresponding to fluoroarenes **157** and **164**, unsurprising given the electronic similarity between the target ring and n.p.r. Whereas precursor **150**, anticipated to be relatively unstable due to the incorporation of the 2-thienyl n.p.r., saw loss of the characteristic diaryliodonium salt proton shift of 8.2 ppm for the protons *ortho*- to the iodine centre after reaching 80 °C (1 h), suggesting that much of the material decomposed prematurely. However, a very small amount of the target fluoroarene **157** was detected, yet the corresponding fluorinated product, 2-fluorothiophene **165** was not observed. Although it is conceivable that **157** was produced in preference over **165**, it is also likely that relatively low boiling 2-fluorothiophene (bp = 82 °C)[325] was produced to some extent but not detected, given that the reaction was not performed within a closed system, thus a selectivity profile ratio could not be assigned. This highlights a clear limitation in this method of diaryliodonium salt fluorination selectivity analysis for precursors bearing the 2-thienyl n.p.r., in that

many small fluoro- and iodoarenes will not be retained in the reaction mixture and thereby cannot be observed by $^{1}H/^{19}F$-NMR. Another limitation of this method includes the loss of resolution seen for NMR spectra obtained at higher temperatures, where line broadening occurs as a result of poor NMR probe shimming at elevated temperatures.

The control diaryliodonium salt, **151**, bearing the markedly less electron-rich phenyl n.p.r. behaved as predicted, yielding fluorobenzene **165** as the sole fluorinated aromatic and appeared to avoid decomposition of the parent diaryliodonium salt, a hallmark of its improved stability over the more electron-rich diaryliodonium salts in the series. Note that fluorobenzene also has a similarly low boiling point (84 °C) to 2-fluorothiophene, however 2-fluorothiophene exhibits a remarkably higher vapour pressure than that of fluorobenzene and hence detection of the fluorobenzene was possible.

Acetyl-protected diaryliodonium salts **152** and **153** provided less conclusive outcomes in this study, possibly as an artefact of increased susceptibility to nucleophiles afforded by this protection strategy; here no peaks corresponding to fluoroaromatics were seen in the ^{19}F-NMR spectra for the [^{19}F]fluorination of precursor **152**, however, ^{1}H-NMR revealed the formation of new para-substituted aromatic species. Despite bearing the instability inducing 2-thienyl n.p.r, [^{19}F]fluorination of diaryliodonium salt **153**, did yield evidence of new aromatic compounds in the ^{1}H-NMR as well as ^{19}F-NMR peak corresponding to 4-(acetoxy)-1-fluorobenzene **158**, albeit these peaks were miniscule in proportion *versus* the fluoroaromatic products seen for the rest of the series.

Table 10 captures many of the key outcomes from this dynamic [^{19}F]fluorination study, most importantly, diaryliodonium salt stability at elevated reaction temperatures is directly affected by electronics of the aryl substituents attached to iodine and as a consequence, *in situ* decomposition of the parent diaryliodonium salt ultimately results in a loss of product fluoroarene(s). Similarly, application of the acetyl protection strategy (**152** and **153**) also suffers from stability concerns and provides a lower proportion of fluoroarene products *versus* diaryliodonium salts baring the benzyl protection strategy **149**–**151**, possible as a result of oxidisable phenol generation as an artefact of acetyl group hydrolysis. Table 10 also describes the expected selectivity profiles for diaryliodonium salts **149** and **151**, whereby more

electron-deficient arenes are preferably fluorinated over electron-rich arenes, and in the absence of any substantial difference in electron density the resulting fluorinated target ring and fluorinated n.p.r. ratio is approximately 1:1.

In summary, although dynamic ^{1}H- and ^{19}F-NMR observation of diaryliodonium salts **149**–**153** has provided valuable insight into the stability and [^{19}F]fluorination selectivity profiles of the precursors, it is apparent that prolonged, gradual heating of the sensitive reagents is far from an ideal reaction environment. Conducting such fluorinations at higher temperatures (180 °C+) under a drastically shorter timeframe, within a closed system vessel would likely afford superior results, and also allow for analysis of low boiling aromatics such as 2-fluorothiophene *via* an in-line chromatography system and UV detector.

2.9 Improving Selectivity

As mentioned, diaryliodonium salts bearing two electron-rich arene components are limited to a maximum yield of 50% (with respect to the target fluoroarene product) when subject to [$^{18/19}$F]fluorination conditions. This section describes efforts to combat the limitation associated with diaryliodonium salts as precursors to electron-rich fluoroaromatics, where two new strategies for the preparation of 4-(benzyloxy)-1-fluorobenzene were envisaged, since benzyl protection of the phenol functionality has already proven to generate diaryliodonium salt precursors stable under the reaction conditions. Firstly, it was proposed that production of a symmetrical diaryliodonium salt would negate the concern of n.p.r. fluorination which was prepared as below (Scheme 74); and secondly a precursor diaryliodonium with additional electron density upon the n.p.r., with the intention of driving fluorination to the less electron-rich target ring, was also designed and synthesised (Scheme 75). Both of the strategies depicted below involved preparation of protected phenoxy aryliodobis(acetate) **166**, an inversion of our usual method of diaryliodonium salt production. For the preparation of the below arylstannane compounds (**141** and **169**), the corresponding bromoarenes were utilised over the iodoarene counterparts because they were dramatically cheaper as starting materials.

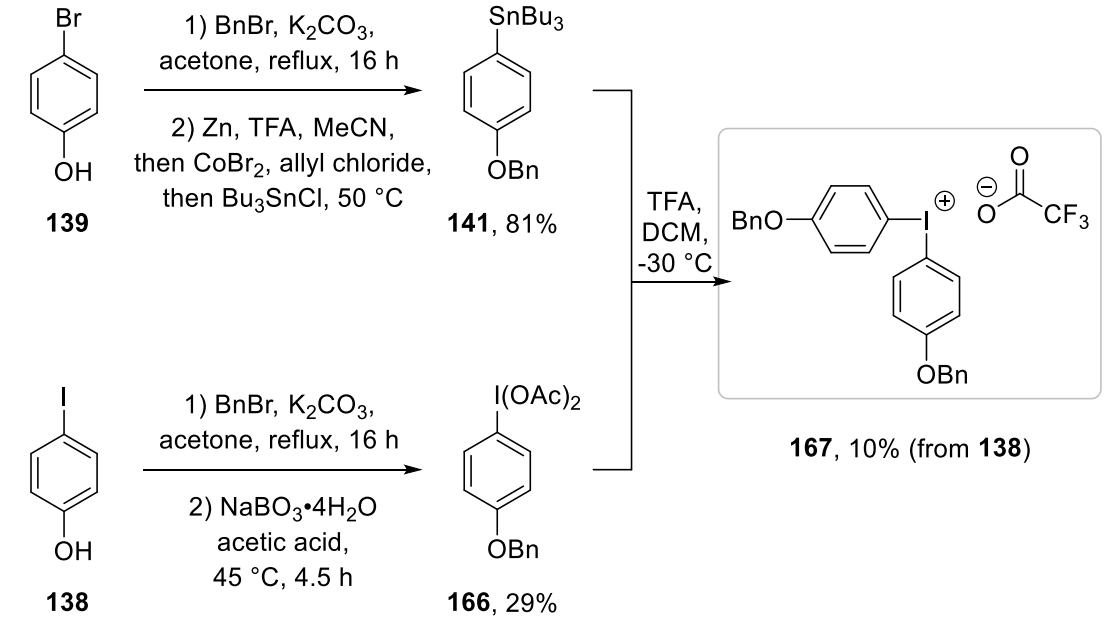

Scheme 74: Synthesis of symmetrical diaryliodonium salt 167

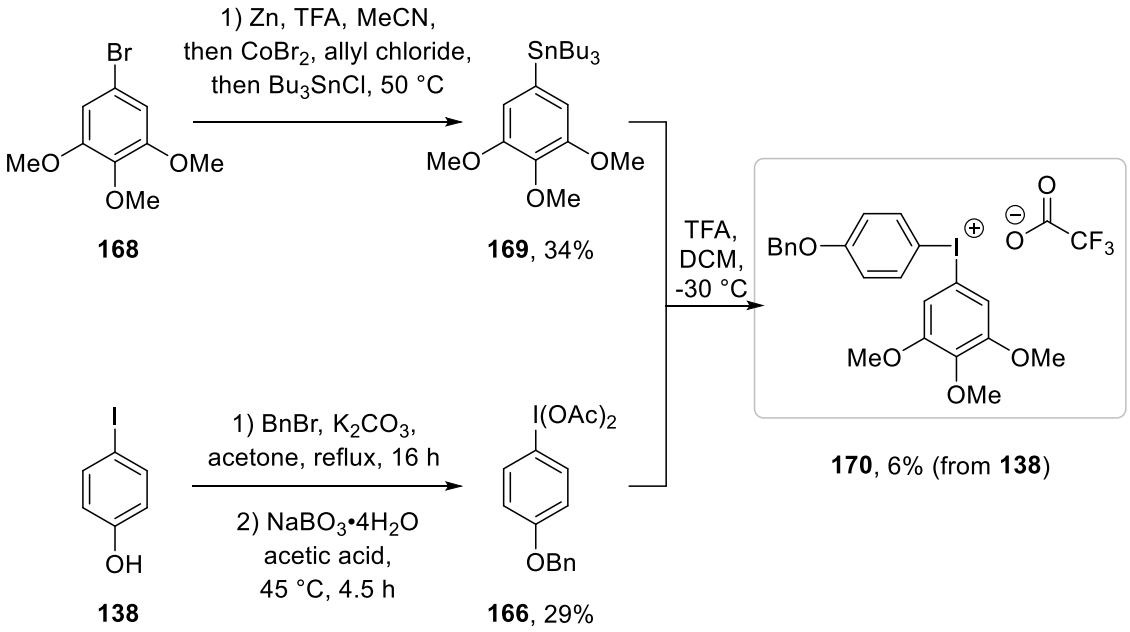

Scheme 75: Synthesis of diaryliodonium salt 170, bearing trimethoxyphenyl n.p.r.

The overall synthetic yields for **167** and **170** were very poor, largely due to the limited yield associated with the oxidation of 4-(benzyloxy)-1-iodobenzene to aryliodobis(acetate) **166**. Similarly, purification of arylstannane **169** proved challenging, requiring multiple purification steps and typically saw destannylation of over 50% of the crude material during column chromatography (as compared to the estimated crude product yield assessed by ^{1}H-NMR of the crude material). Despite

these poor yields, preparation of these unique diaryliodonium salts demonstrated the versatility of the general route to electron-rich diaryliodonium salts described in Section 2.7 and provided sufficient material for [^{19}F]fluorination testing.

As before, dynamic ^{1}H- and ^{19}F-NMR [^{19}F]fluorination studies were conducted on both diaryliodonium salts **167** and **170** as a means to rapidly obtain an understanding of their stability under the reaction conditions, as well as the selectivity outcome of fluorination. Here it was anticipated that symmetrical diaryliodonium salt **167** would afford a single fluoroarene (^{19}F-NMR peak corresponding to 4-(benzyloxy)-1-fluorobenzene **157**). Diaryliodonium salt **170** was also expected to largely yield the same fluoroarene (**157)** over the unlikely formation of 3,4,5-trimethoxy-1-fluorobenzene, although it was also considered that the distinctly electron-rich diaryliodonium salt may be poorly stable to the reaction conditions.

Analysis of the [^{19}F]fluorination reaction of **167** by ^{1}H-NMR displayed the formation of para-substituted aromatics species from 100 °C (1 h 20 min) as per the previous diaryliodonium salts **149**–**151** (Figure 42). However, observation of the reaction by ^{19}F-NMR also highlighted the formation of an unexpected fluorinated product **X** (-79.36 ppm, suggesting a CF_3 group), as well as a prominent peak for corresponding to the formation of 4-(benzyloxy)-1-fluorobenzene **157** (-125.13 ppm).

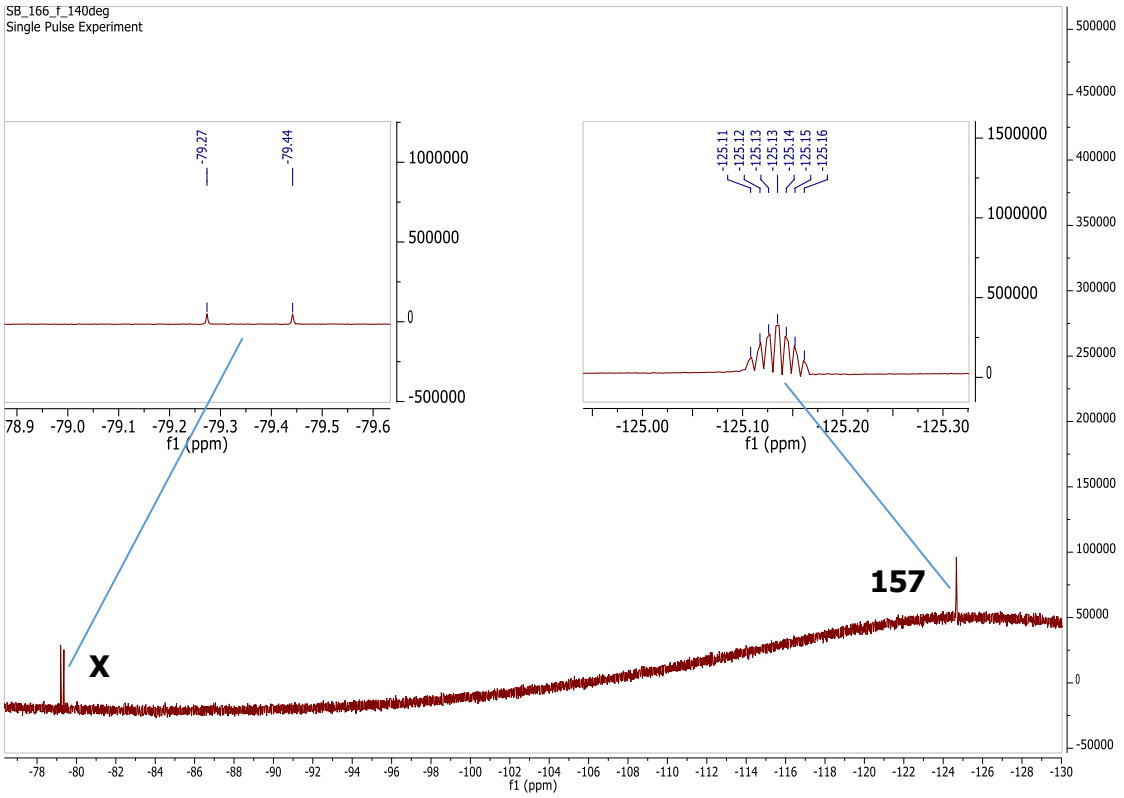

Figure 42: [^{19}F]Fluorination products of symmetrical diaryliodonium salt 167

It was initially considered that **X** represented the formation of the counter-ion addition product **171** (Scheme 76), an outcome that should be avoided given the non-nucleophilic nature of the trifluoroacetate counter-ion; however this suggests that the fluorination reaction proceeds slowly for electron-rich diaryliodonium salts (versus diaryliodonium salts bearing one or more electron-deficient arene), whilst decomposition of electron-rich diaryliodonium occurs at a faster rate.

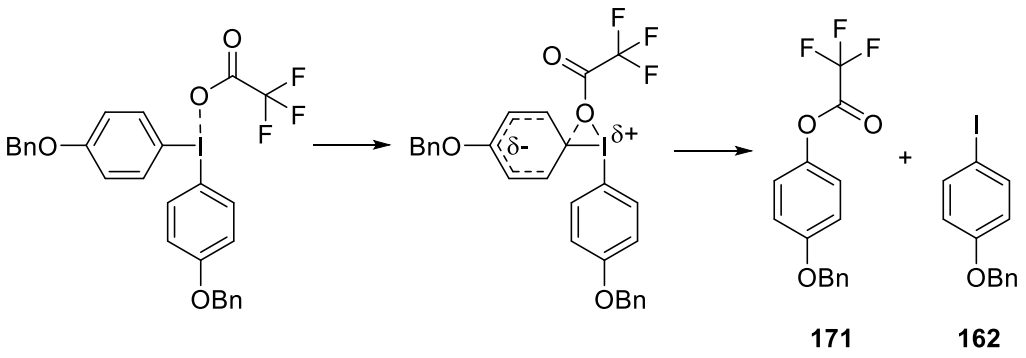

Scheme 76: Conceivable formation of counter-ion addition product 171 through the decomposition of symmetrical diaryliodonium salt 167

However, on preparation and ^{19}F-NMR of counter-ion addition product **171**, the compound was found to have a notably different shift (-75.1 ppm) to **X**, furthermore the literature provided no insight into any potentially generated fluorinated compounds that provided a ^{19}F-NMR shift around -79 ppm and hence the identity of species **X** remains unknown.

Tailored diaryliodonium salt **170** also provided disconcerting results when subjected to our [^{19}F]fluorination procedure, as ^{19}F-NMR shifts for the desired fluoroarene 4-(benzyloxy)-1-fluorobenzene **157** (recorded as -125.13 ppm) and for formation of the less favoured 3,4,5-trimethoxy-1-fluorobenzene species (expected around -113.6 ppm)[416] were both absent. This is despite dynamic ^{1}H-NMR observation of the fluorination reaction suggesting that the formation of a *para*-substituted aromatic entity had been achieved. Given the ambiguity surrounding the [^{19}F]fluorinations of diaryliodonium salts **167** and **170** at this stage, they were considered as secondary substrates for [^{18}F]fluorination, behind the more successful precursor candidates of the foremost series **149**–**153**.

2.10 Chapter 2 Summary

This chapter describes the successful development of a simple and highly versatile method for the preparation of electron-rich diaryliodonium salts, afforded by optimised aryliodobis(acetate) preparation coupled with a modified method for arylstannane synthesis and purification. With a robust protocol in place, this process was utilised to produce a series of diaryliodonium trifluoroacetates, including novel examples, that are capable of affording [^{18}F]fluorophenol when subject to [^{18}F]fluorination and subsequent deprotection. Further information on the structural details, relative stabilities and [^{19}F]fluorination outcomes for these diaryliodonium salt precursors were obtained though x-ray crystallography and dynamic ^{1}H- and ^{19}F-NMR [^{19}F]fluorination of the compounds. This work has provided a number of lead candidates deemed suitable for the radiofluorination studies described in the subsequent section.

3 Microfluidic Radiofluorination of Diaryliodonium Salts

Chapter 2 describes preparation of electron-rich diaryliodonium salt precursors, intended on providing a route to the valuable prosthetic group 4-[^{18}F]fluorophenol after radiolabelling with nucleophilic [^{18}F]fluoride. The chapter also specifies the limitations in performing [^{19}F]fluorination of diaryliodonium salts in open vessels at elevated temperatures, imposed by the solvent, DMF, which begins to decompose at 137 °C[326] and boils at 152 °C and hence prevents performing the reactions at higher temperatures. It is thereby speculated that conducting fluorinations of diaryliodonium salts within closed systems at higher temperatures (190 °C) should allow better conversion of the precursors into the daughter fluoroarene(s). The use of sealed microfluidic systems, capable of operating at remarkably high pressures (over 20 bar) permits the use of solvents well above their boiling points (Table 11) and also provide some distinct benefits over traditional glassware based approaches when applied to radiochemical transformations, as is discussed in this chapter.

	Boiling point (°C) at		
Solvent	1 bar	6.9 bar	17.0 bar
Dichloromethane	41	109	153
Methanol	65	138	185
Tetrahydrofuran	66	140	186
Isopropanol	82	159	207
Acetonitrile	82	159	207
Water	100	181	231
1,4-Dioxane	101	182	234
Dimethylformamide	**153**	**244**	**301**
Dimethylacetamide	165	259	318

Table 11: Variation of common solvent boiling points with pressure calculated according to Trouton's rule[327]

3.1 Automated Radiochemistry

The last twenty years have seen the use of automated synthesis platforms and microfluidic reactor systems rapidly develop, with applications spanning robust chemical syntheses to niche academic projects yielding novel reaction conditions. For detailed information on these developments the reader is directed to some well written reviews,[328,329,330] whilst key points are summarised below.

The most obvious benefit provided by using automated apparatus for radiochemical transformations includes the reduced handling (and hence radiation dose to the operator) required for radioisotope manipulation. Typically, once the radioisotope has been transferred from the cyclotron to the synthesis platform, shielding (*i.e.* by housing the equipment inside a 'hot' cell) can negate any further radiation exposure to the radiochemist, allowing the user to remotely operate the apparatus safely. A host of markedly different types of radiosynthesis platforms are now commercially available, as well as many reaction–specific bespoke systems; encompassing batch systems, lab-on-a-chip devices, and microfluidic platforms.

Batch-based radiosynthesis systems are the most commonly seen in PET centres and are often designed for easy-operation, routine production of multi-dose, high-demand PET imaging agents, however, these are typically limited to performing chemistry similar to that particular radiotracer/ligand. More adaptable modular systems, like the Eckert and Ziegler Modular-Lab (Figure 43)[331] allow for incorporation of microwave systems, multiple reaction vessels, in-line SPE purification, *etc*. facilitating their application in R&D as well as the clinical setting;[332] Others are often even self-shielded,[333] owing themselves to cartridge-based radiosynthesis in clean-room facilities, with aims of integrating radiolabelling, purification, formulation and QC, providing a complete radioisotope to patient-ready imaging agent workflow, reducing radiosynthesis time and maximising RCY.

Figure 43: Eckert and Ziegler Modular-Lab Standard, a customisable radiosynthesis platform for batch production of PET imaging agents

Micro-scaled lab-on-a-chip (LOC) devices provide a contrasting view on radiopharmaceutical production, where efforts are based on minimising the apparatus with a view of minimising potential fluorine-19 contamination from tubing, glassware and the atmosphere in a bid to maximise SA; as well as potentially reducing the considerable costs that accompany radiosynthesis platforms; and provide to a more streamlined approach to radiolabelling through automations, hence removing the need for extensively trained radiochemists in clinical settings. In addition, cheaply manufactured LOC devices can be used as disposable, single-use items, reducing the sometimes lengthy post-radiosynthesis cleaning and validation protocols

Although these approaches currently remain in the early stages of their development, they have already seen some success in affording miniaturised multi-step radiosyntheses, such as the work by Quake and co-workers on the routine micro-production of [^{18}F]FDG (Figure 44),[334] *via* a five step protocol, integrating [^{18}F]fluoride concentration, water evaporation, radiofluorination, solvent exchange and hydrolytic deprotection, all within a single, digitally–controlled device.

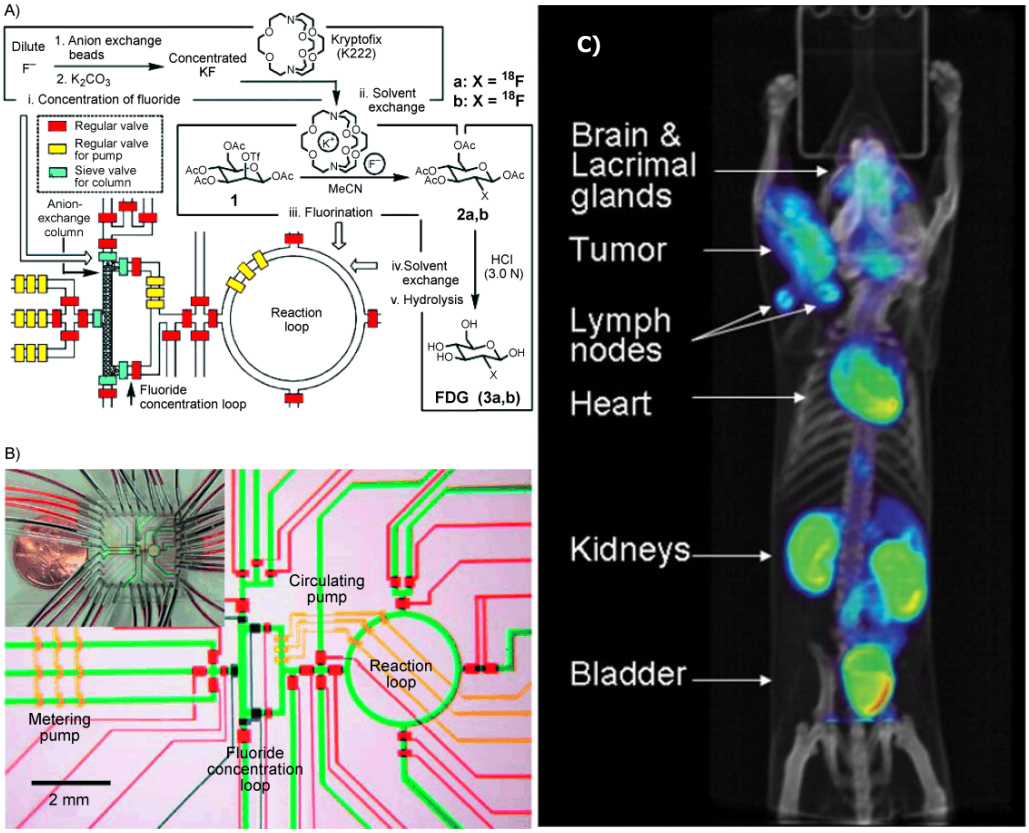

Figure 44: A schematic representation of micro-scaled production of [^{18}F]FDG (top, A); an optical micrograph of the central area of the circuit (bottom, B); with an image of the device next to a penny (inset, B); and the resulting microPET/CT image of a tumour-bearing mouse using a 375 µCi dose of [^{18}F]FDG produced *via* this method.[334,335]

Micro-structured devices for LOC radiosynthesis provide an exciting new avenue of research for radiochemists and could potentially deliver an ultra-low cost, efficient means for single–dose radiopharmaceutical production, imaginably achievable by the patient's side since they employ drastically reduced amounts of shielding when compared to more cumbersome batch-scale radiosynthesis platforms.[336] The current major limitation inhibiting further development of chip based devices involves the polydimethylsiloxane (PDMS) from which they are fabricated. The versatile viscoelastic material allows for high precision injection moulding of micro-channels and simple, high-strength bonding protocols, however, PDMS is poorly resistant to most organic solvents, seriously limiting its application in a variety of radiochemical applications.[337]

Microfluidic capillary systems, such as the Advion NanoTek (Figure 45), provide a convenient intermediate between adaptable modular systems and robust batch-

based synthesis platforms, whilst maintaining the benefits of microfluidic chemistry utilised by LOC devices.

Figure 45: Advion NanoTek microfluidic radiosynthesis system[338]

Exploiting microfluidics to conduct chemical transformations not only provides faster and more reproducible reaction protocols, as well as the elevated solvent temperatures described earlier, but also allows for more controlled solvent mixing through uniform, fluid dynamics. Narrowing the channels of a microfluidic reactor, results in a monumental increase in the surface area:volume ratio of the reaction vessel (Table 12), assisting the heat loss from the channel and conversely, allowing for ultra-fast heating (as well as cooling) of the system and more accurate thermostatic control.[339]

Reactor type	Surface area:volume ratio (cm^2/cm^3)
1 m^3 reactor	0.06
100 ml rb flask	1
1.0 mm ID channel	40
100 µm ID microchannel	400

Table 12: Relative surface area:volume ratio of different reactor vessels with the same internal volume

Microfluidic systems are often expected to operate under laminar flow (Figure 46), which induces atypical reaction environments often affording improved yields and reduced by-product formation,[340] a major advantage in radiochemistry where extended chromatographic purification can significantly limit the RCY.

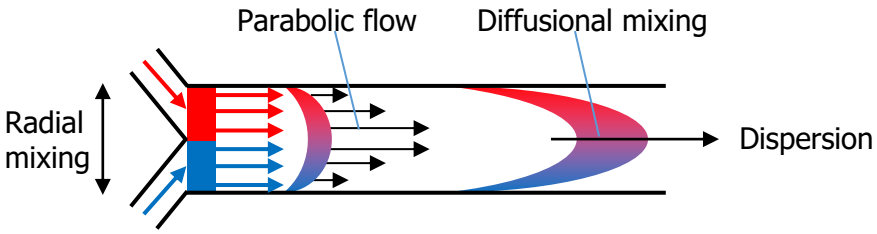

Figure 46: Diagrammatic representation of laminar flow, whereby mixing occurs by radial diffusion rather than turbulent flow

Laminar flow (an alternative to turbulent flow which occurs within a standard round bottom flask) affords mixing of the two reagent streams through radial diffusion as the fluidic bolus rapidly disperses through the microchannel, a form of mixing that is not only highly reproducible but also very fast when applied to channels with very small dimensions (hence encouraging rapid and reproducible mixing). Again, as an artefact of channel based fluidics, the reaction mixture bolus adopts a parabola-like shape as the fluid closest to the inner wall of the channel experiences friction.[328] The properties of a flow system can be characterised by calculating the system's Reynolds number (R_e), a dimensionless quantity that describes the interactions between fluid speed, the diameter of the channel and the internal viscosity of the fluid, as defined by the equation:

$$R_e = \frac{inertial\ forces}{viscous\ forces} = \frac{mean\ fluidic\ velocity\ x\ diameter}{kinetic\ viscosity} = \frac{\upsilon_s L}{v}$$

It is expected that a fluidic system that provides a Reynolds number below 2500 is operating under laminar flow and hence behaves as described above. However, some microfluidic systems intentionally incorporate elements of turbulent mixing

through static mixer geometries,[341] providing a hybrid laminar–turbulent flow system.[342]

Microfluidic reactor systems also provide a number of benefits relevant to radiochemistry, including the ability to conduct a series of reactions utilising just milligram quantities of precursor material, avoiding the waste of material associated with batch-based radiosynthesis, imperative when working with precursors that require lengthy syntheses, are expensive, or only available in trace amounts, such as bespoke peptides. Similarly, a single provision of [^{18}F]fluoride can provide enough radioisotope to complete a series of radiofluorinations, again thanks to the micro-scaling of vessels and tubing, and the nature of flow processes. The nature of microfluidic synthesis lends itself to rapid optimisation studies given that many platforms allow for specific control of multiple reaction parameters, such as temperature, reaction time, system pressure, reagent stoichiometry; providing a means to rapidly screen parameters of a process still under development.

3.2 Radiosynthesis with the Advion NanoTek Microfluidic System

The previous section highlights a number of key advantages offered by remotely controlled microfluidic radiosynthesis platforms, owing to the selection of the Advion Nanotek as the primary tool for [^{18}F]fluorination of diaryliodonium salts in this chapter of work. The modular synthesis system boasts microscale radiolabelling capability, versatile operation software, as well as temperature and pressure monitoring, making the platform an excellent choice for R&D-type [^{18}F]fluorination optimisation as well as potential upscaling for PET imaging studies.[343]

Other researchers have demonstrated the capability of Advion's radiosynthetic hardware through microfluidic production of multiple fluorine-18 labelled PET imaging agents, including tau radioligand [^{18}F]T807 for Alzheimer's disease,[344] metabotropic glutamate receptor subtype type 5 (mGluR5) imaging agent,[345] and [^{18}F]fallypride which has seen application in a US clinical trial, imaging dopamine D_2 and D_3 receptors for the treatment of psychosis in Alzheimer's disease.[346]

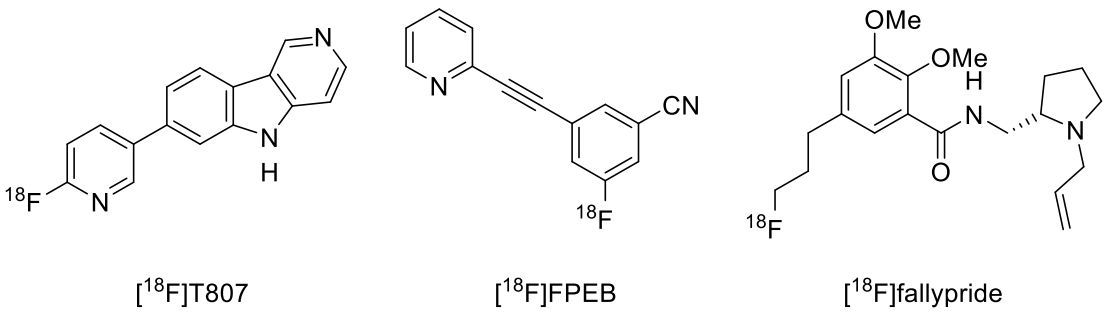

[18F]T807 [18F]FPEB [18F]fallypride

Figure 47: Examples of desirable PET imaging agents prepared by microfluidic [18F]fluorination

In order to conduct radiofluorination of the diaryliodonium salts prepared in Section 2 with a commercially available Advion NanoTek a number of augmentations were required (Figure 48), including the coupling of an auto-injector for transferral of reaction mixtures to a radio-HPLC for in-line purification and characterisation, as well as numerous radioactivity counters, SPE cartridges and the development of bespoke operation macros.

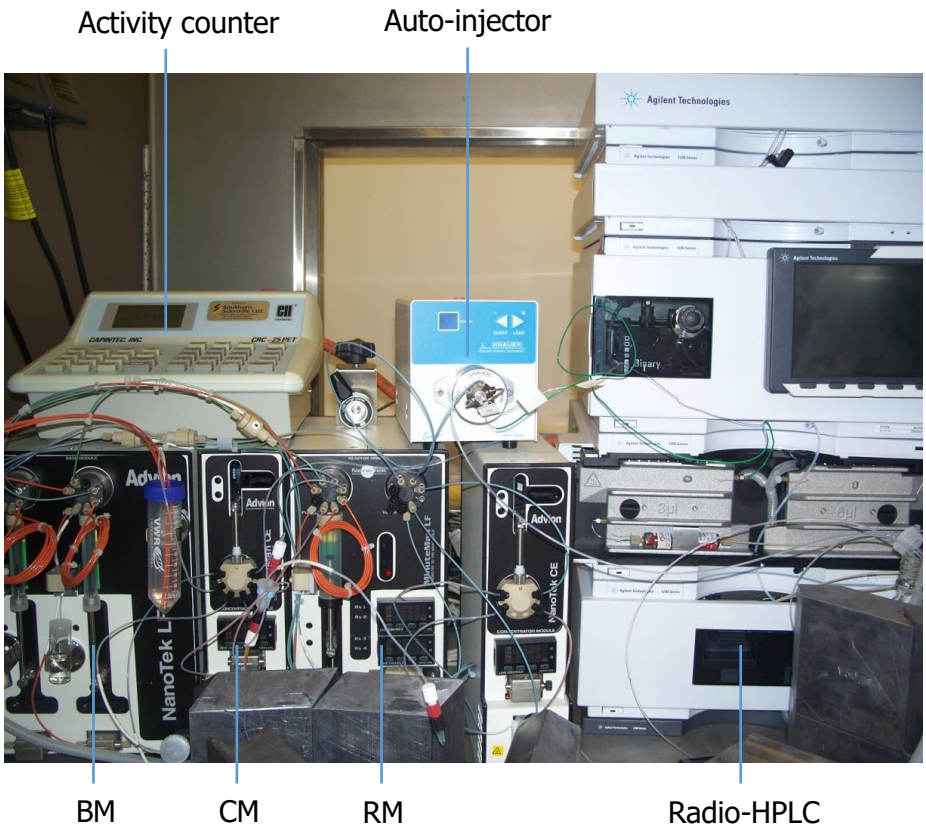

Figure 48: Advion NanoTek base module (BM), concentrator module (CM) and reactor module (RM) coupled with an auto-injector (Knauer Smartline Valve Drive), radio-HPLC (Agilent Technologies 1200 series with a LabLogic Flow Count) and activity counter (Capintec CRC ® -25PET Dose Calibrator); all allowing for in-line radiolabelling, purification and activity characterisation

As depicted by the image above, the Advion Nanotek system comes with a number of core components, including a base module (BM) which provides reagent solutions to the reactor from reagent loops *via* two syringe pumps (P1 and P2); a concentrator module (CM) which provides removal of the [^{18}O]H_2O from the [^{18}F]fluoride solution *via* azeotropic distillation; and reactor module (RM) which houses up to four microreactors (Figure 49) within an aluminium heating block.

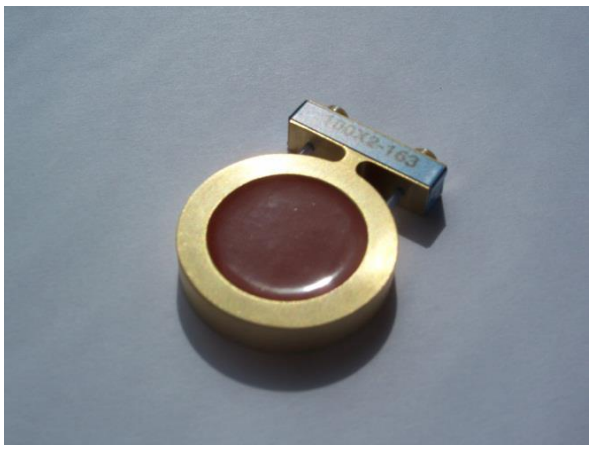

Figure 49: Advion NanoTek microreactor coil, normally housed within the reactor module of the system within an aluminium heating block

For this work, silica glass capillary microreactors as 4 metre coils, with an internal diameter of 0.1 µm, coated in a red thermoresist polymer and a brass shell for protection as seen above (Figure 49) were selected because of their resilience to the reaction medium, their convenient temperature range (up to 200 °C) and for their scope as closed system vessels which allows for detection of volatile products which would otherwise remain undetected.[347]

[^{18}F]Fluorination of diaryliodonium salts typically commenced with loading the Advion NanoTek with all non-decaying reagents, SPE cartridges and anhydrous solvents required for radiolabelling, prior to loading the [^{18}F]fluoride onto the system. This highlights the necessity for a judicious and well-orchestrated system preparation procedure, as well as a timely delivery of the radioisotope, produced in-house using the ABT cyclotron. Here production of n.c.a. [^{18}F]fluoride in [^{18}O]H_2O, *via* bombardment of the target [^{18}O]H_2O for 1 hour, with a proton beam current of 4 µA,

set at a target angle of 5° typically yielded between 1 and 2 GBq of [^{18}F]fluoride in 250 µL of [^{18}O]H_2O per run.

After transferral of the 'wet' isotope to the Advion NanoTek CM and careful application of a syringe line to the [^{18}F]fluoride vessel to ensure full isotope uptake the 'hot cell' access ports can closed, completely safeguarding the user from the radiation. Our bespoke macro-dictated drying procedure then utilised the CM's low pressure, six-way valve to transfer and trap the [^{18}F]fluoride onto a quaternary ammonium resin (QMA) cartridge whilst eluting the [^{18}O]H_2O into a receiving vial for recycling. A solution of tetraethylammonium bicarbonate is then utilised as a phase transfer agent (PTA) to liberate the [^{18}F]fluoride from the QMA cartridge into a vial housed in the CM heating block. Three iterations of azeotropic distillation with acetonitrile completes the drying process, affording a dry [^{18}F]fluoride/TEA•HCO_3 complex, which is then extracted from the CM using anhydrous DMF (Figure 50).

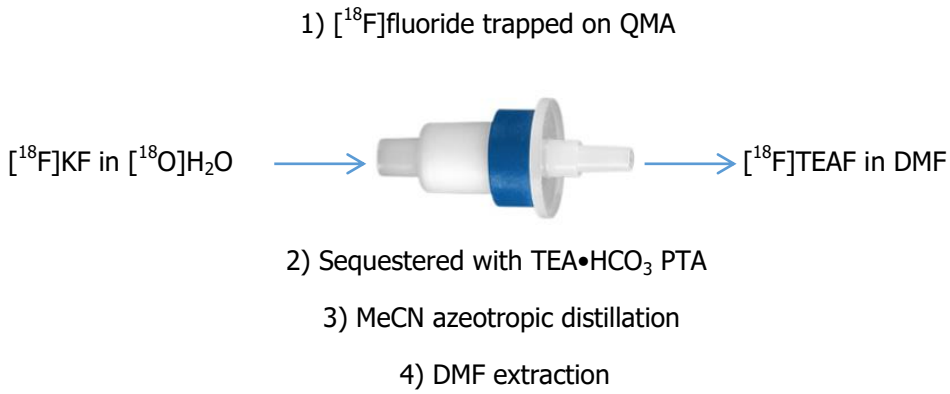

Figure 50: Preparation of radiofluorination-ready 'naked' [^{18}F]fluoride *via* a trap and release mechanism on a QMA cartridge, facilitated by a phase transfer agent and followed by azeotropic drying. QMA image from the manufacturer's website[348]

As mentioned in Section 1.5.3, the use tetraethylammonium bicarbonate provides a means of yielding an organic solvent soluble [^{18}F]fluoride complex, whilst simultaneously providing sufficient basicity to release the [^{18}F]fluoride from the QMA resin, a highly convenient method developed within the research group.[110] Use of this PTA over traditional cryptands and longer chain tetraalkylammonium reagents greatly reduced the risk of microreactor blocking, a problem often seen when working with microreactor channels of 0.1 µm internal diameter or less.[110]

The resulting [^{18}F]TEAF/DMF mixture is transferred to the RM where pump 3 (P3) facilitates loading of the radioisotope solution into loop 3, ready for administration into the microreactor (Figure 51). From here the microreactor can be simultaneously charged with precursor diaryliodonium salt from loop 1 and [^{18}F]TEAF from loop 3, with flow rates, temperature, reaction time and stoichiometry pre-set by the user.

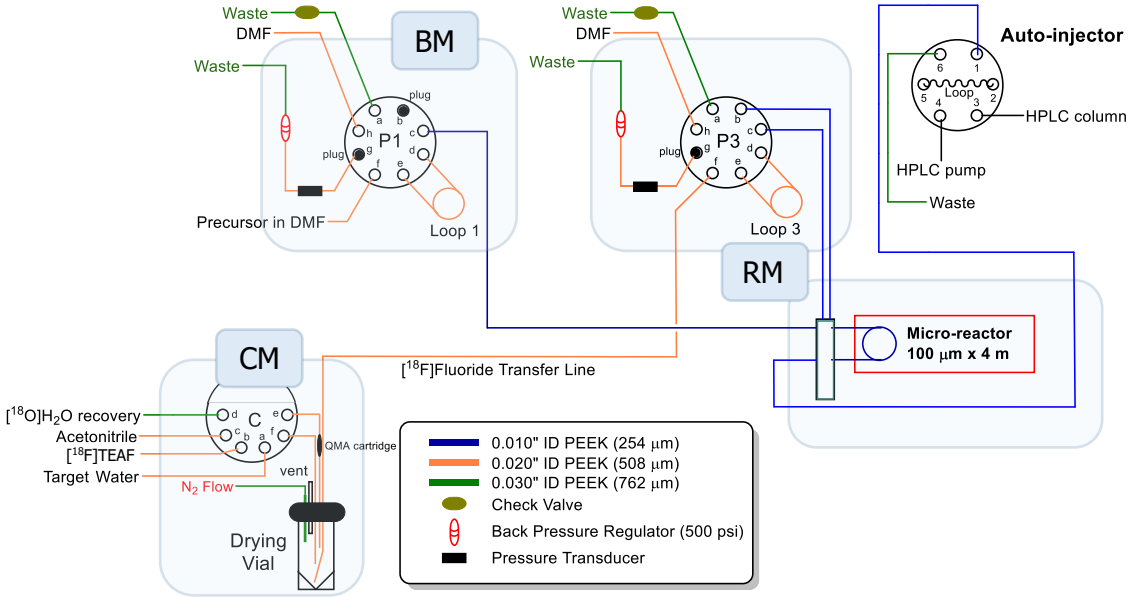

Figure 51: Schematic of bespoke [^{18}F]fluorination set-up using the Advion NanoTek coupled with an auto-injector and in-line radio-HPLC. Image adapted from publication by Reed *et al*[110]

After the desired reaction time, anhydrous DMF is used to sweep the crude reaction mixture towards the Knauer Smartline Valve Drive auto-injector, which harbours a large loop to store the reaction mixture whilst the 4 m microreactor is emptied. The auto-injector is then directed to transfer the reaction mixture onto the pre-equilibrated HPLC column (C-18 Phenomenex or C-Phenyl Phenomenex) for analysis of the products.

3.3 Radiosynthesis of Protected-4-[^{18}F]fluorophenol

The [^{19}F]fluorination studies of diaryliodonium salts **149**—**153**, **167** and **170** prepared in Chapter 2 were used to select the more stable and more fruitful precursors for [^{18}F]fluorination. Here diaryliodonium salts **149**, **150**, **151** and **152**

were selected as primary substrates for this work, where it was expected that **149**, **150** and **152** would afford higher radiochemical yields (RCYs) of protected-4-[^{18}F]fluorophenol over the other diaryliodonium salts in the series and it was deemed that precursor **151** would provide an excellent control substrate which should see formation of mainly [^{18}F]fluorobenzene **[^{18}F]165** on treatment with [^{18}F]TEAF (Scheme 77).

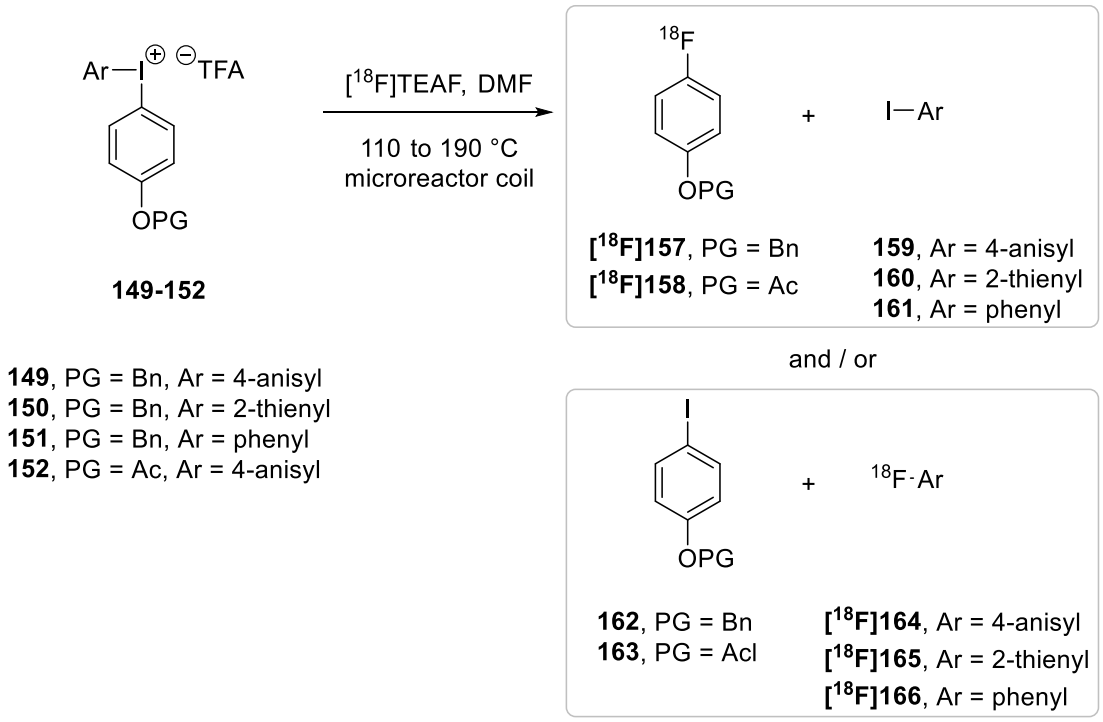

Scheme 77: Radiofluorination of diaryliodonium salts 149-152 using [^{18}F]TEAF in a microreactor

Prior to radiofluorination of the selected diaryliodonium salt series **149—152**, each precursor required development of a detailed HPLC method, which allowed for identification (based on the relative retention times) of each potential component of the reaction mixture in real-time. Consider diaryliodonium salt **149**, which when treated with [^{18}F]TEAF can potentially yield the desired **[^{18}F]157** protected-4-fluorophenol species, as well as **159**, **162**, **[^{18}F]164** and the parent diaryliodonium salt itself. Hence a development method for the HPLC analysis of **[^{19}F]157**, **159**, **162**, **[^{19}F]164** and **149** was sought, most of which were commercially available, or were synthesised when unavailable. Ideally, separation of the fluoro- and iodoarene products and the starting material should be achieved within a timely manner, given

time sensitivity of decaying species, and should afford baseline separation between all components, as can be seen for the HPLC spectrum of diaryliodonium salt **149** and its potential products (Figure 52).

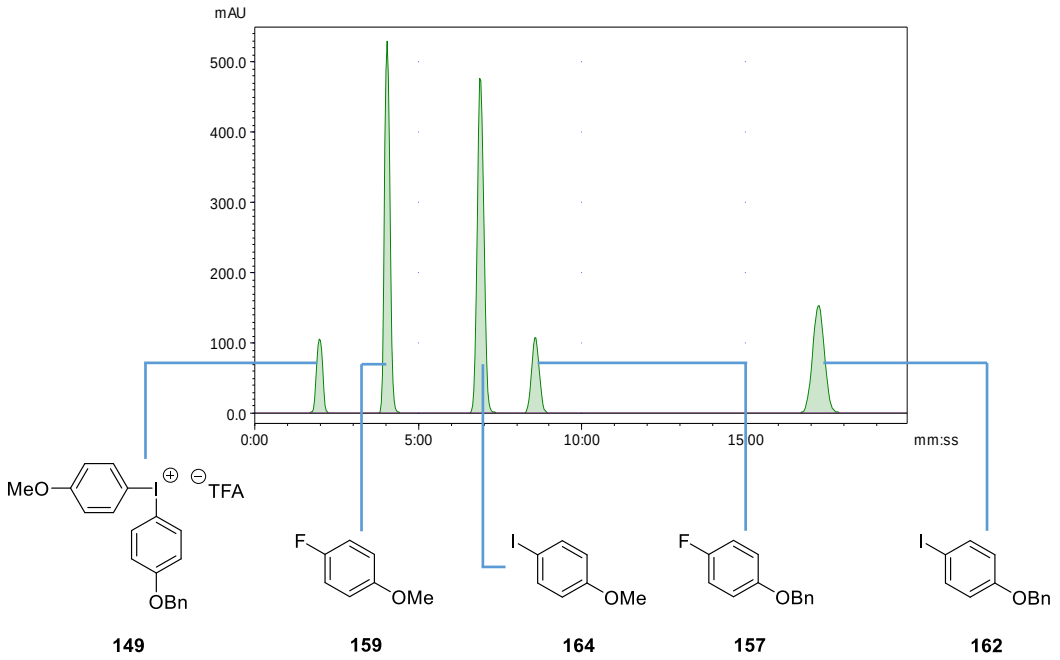

Figure 52: HPLC chromatogram of diaryliodonium salt 149 and potential fluoro- and iodoarene products yielded when fluorinated, HPLC method achieved using a C-phenyl reverse phase silica HPLC column (Phenomenex, Kinetex) 60:40 MeCN:H_2O eluent system at 1.1 ml/min, Agilent 1200 Series

Establishing the retention times of fluoroarenes and iodoarenes greatly assisted in the identification of the products for the [^{18}F]fluorination reactions of diaryliodonium salts **149**—**152**, however, on occasion, other non-radioactive by-products were observed, which were shown to be protio-derivative decomposition products when compared to commercially available reference standards.

Preliminary [^{18}F]fluorination reactions on diaryliodonium salts **149**—**152** together with the [^{19}F]fluorination work discussed in Chapter 2, as well as prior work on the [^{18}F]fluorination of diaryliodonium salts within the research group[349] has determined that temperature has the greatest effect on the yield of these reactions, hence other parameters were kept constant for the entirety of this work (Table 13). Here a temperature range between 110 °C and 190 °C was deemed appropriate, taking into

account that fluoroarene formation was inadequate and poorly measurable below 110 °C and that the integrity of the microreactor is limited to 200 °C.

Parameter	Optimal conditions
microreactor dimensions	coil ID 0.1 μm, 31.41 μL volume
diaryliodonium salt concentration	10 mg/mL
[^{18}F]TEAF volume	10 μL
P1:P3 injection volume ratio	1:1
reagent loading flow rate	10 μL/min
Reaction time	5 min 23 sec
Reaction bolus transfer rate	60 μL/min

Table 13: Parameters to be held constant as temperature is varied for [^{18}F]fluorination reactions of diaryliodonium salts 149-152. In addition, P1 loop volume, load line volume and collection line volumes were maintained at 386, 39 and 88 μL respectively; P2 loop volume, load line volume and collection line volumes were maintained at 220, 21, 71 μL respectively; the microreactor to auto-injector line volume was maintained at 32 μL; and the auto-injector to radio-HPLC line volume was maintained at 30 μL

[^{18}F]Fluorination of each diaryliodonium salt in the series at each temperature increment was completed in triplicate (at least) and the upper and lower RCYs achieved for each is displayed by error bars in the forthcoming graphs (Figure 54, Figure 55, Figure 56 and Figure 57). Note, that the focus of this chapter's work was to screen reaction conditions and study the outcome of [^{18}F]fluorination for diaryliodonium salt precursors **149**—**152**, whilst reviewing the effect of protecting groups and n.p.r. selection of [^{18}F]fluorination selectivity, hence isolation of individual [^{18}F]fluoroarenes was not conducted. Instead RCYs were reported as the amount of radioactivity of the product [^{18}F]fluoroarenes as a percentage of the total radioactivity in the reaction mixture, as detected by radio-HPLC, validated by frequent calibration against known samples. An example of a typical radio-HPLC trace of a [^{18}F]fluorination reaction is shown below (Figure 53), the spectrum is superimposed with the corresponding UV HPLC chromatogram for the

radiofluorination of diaryliodonium salt **149**. It is important to note, that all RCYs reported in this Chapter are delivered as non-decay corrected, analytical RCYs.

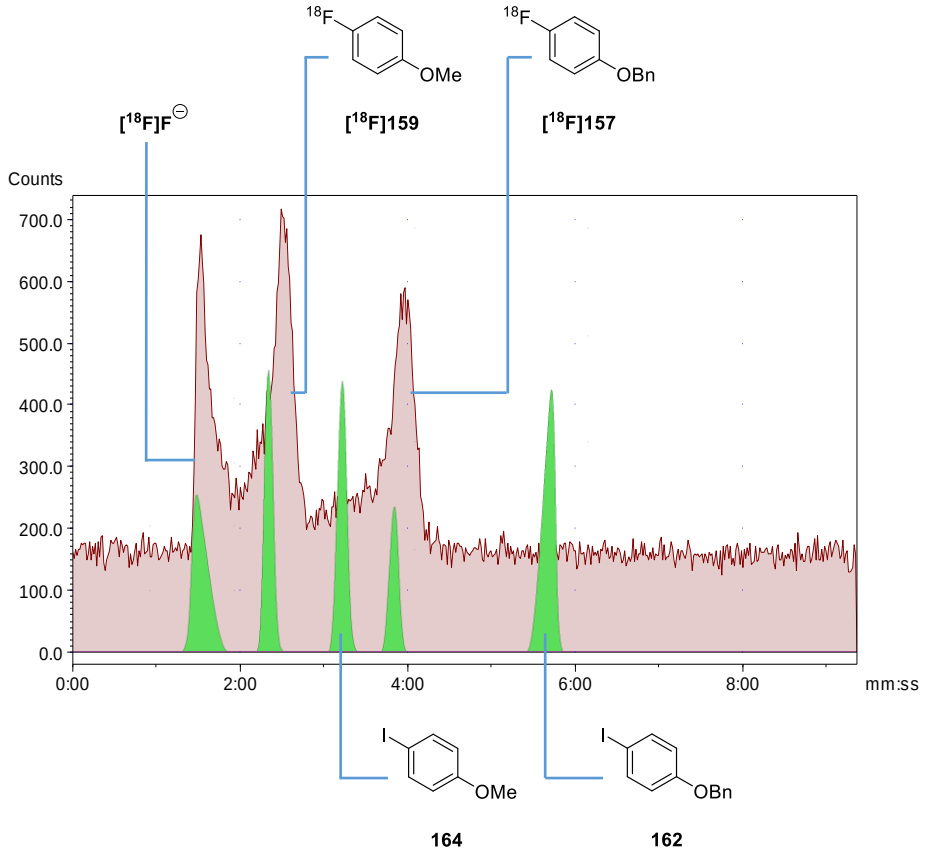

Figure 53: HPLC spectrum of product mixture yielded by the reaction of diaryliodonium salt 149 with [^{18}F]TEAF, bearing the radio-HPLC trace overlain with UV HPLC trace, validating the identity of the [^{18}F]fluoroarene products. HPLC conditions: C-18 reverse phase silica column (Phenomenex), 60:40 MeCN:H_2O, 0.1% formic acid, flow rate = 1.1 mL/min. [^{18}F]fluorination reaction conducted at 190 °C

Optimised HPLC conditions were achieved through the application of an alternative column type (C-18 rather than C-Phenyl), as well as the introduction of 0.1% formic acid additive, which allowed for elution of the desired [^{18}F]fluoroarene **[^{18}F]157** within 5 min. This reduction of retention times, whilst maintaining clean separation of products can be highlighted as a highly beneficial outcome given the necessity for fast product purification, especially important when further post-radiofluorination steps are required, such as deprotection to yield the target 4-[^{18}F]fluorophenol as in this case. Note also, the rapid elution of unreacted [^{18}F]fluoride, which was observed across radiofluorination reactions of all diaryliodonium salts within the series **149**—

152. As the lead candidate from the [^{19}F]fluorination study, the [^{18}F]fluorination of diaryliodonium salt **149** {(4-(Benzyloxy)phenyl)(4-methoxyphenyl)iodonium trifluoroacetate} was the first to be studied in detail (Figure 54).

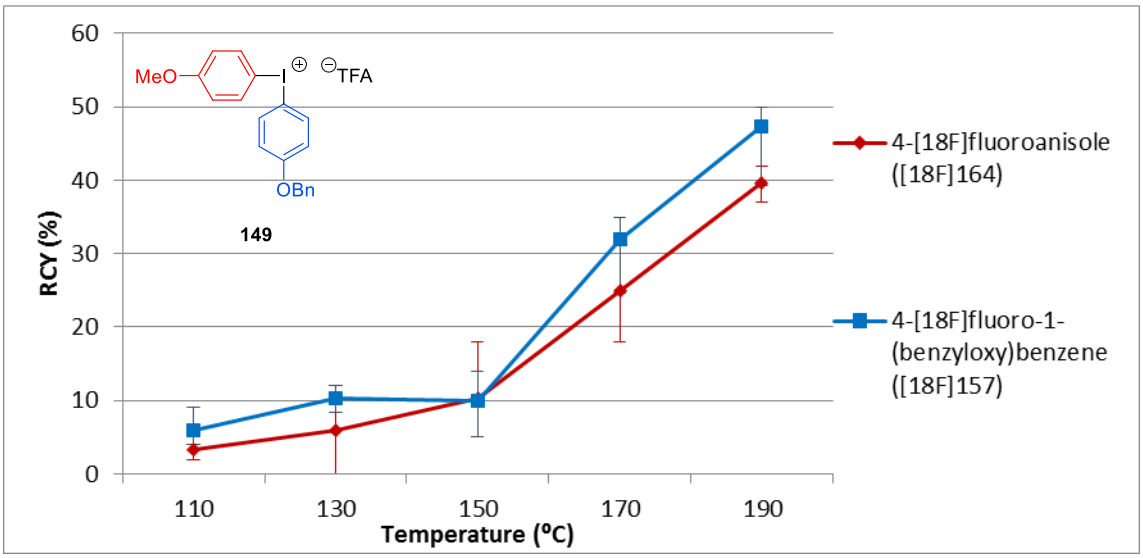

Figure 54: [^{18}F]Fluorination of diaryliodonium salt 149, with the structure of the precursor highlighting the two arenes fluorinated and corresponding RCYs of each resulting [^{18}F]fluoroarene

As seen with the [^{19}F]fluorination experiments (Chapter 2), the [^{18}F]fluorination of diaryliodonium salts bearing two electron-rich arenes, such as **149**, displayed near 1:1 selectivity between the target ring system and the n.p.r. The dramatic increase in RCY afforded at the elevated temperatures (>170 °C) demonstrates the need to formation radiolabelling within closed system reaction systems, since batch based systems would limit the maximum temperature to 130 °C with this solvent and hence limit the maximum RCY achievable. The relatively high RCY (47%, n = 3, s = 4.93) achieved for the target [^{18}F]fluoroarene, 4-[^{18}F]fluoro-1-(benxyloxy)benzene **157**, justifies the utility of diaryliodonium salt precursor **149** for the production of [^{18}F]fluorophenol, as does the short retention time required to elute **157** (t_r = 4 min 22 s), allowing the subsequent deprotection reaction to be conducted promptly, hence reducing the detriment to RCY that would be caused by lengthy HPLC purification (although deprotection could also be conducted prior to purification to remove the need for a second purification stage).

Diaryliodonium salt **150** also performed as anticipated, given that the 2-thienyl n.p.r. bears more electron density than the target ring system, [^{18}F]fluorination was directed to the *ipso*-carbon of the benzyoxyphenyl moiety, affording **[^{18}F]157** in preference over **[^{18}F]165** (Figure 55). However, as noted before (Chapter 2), application of the electron-rich 2-thienyl n.p.r, when the other arene is also electron-rich does appear to result in destabilisation of the diaryliodonium salt, and hence the RCYs reported here are notably lower than those observed for precursor **149** (Figure 54).

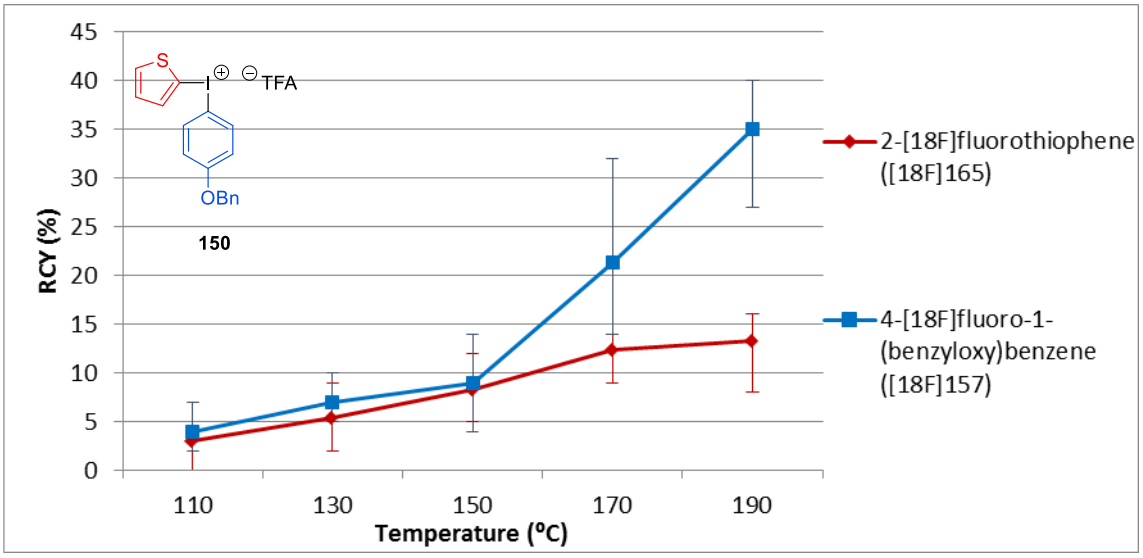

Figure 55: [^{18}F]Fluorination of diaryliodonium salt 150, with the structure of the precursor highlighting the two arenes fluorinated and corresponding RCYs of each resulting [^{18}F]fluoroarene

Again, the elevated temperatures, only achievable through employment of a closed-system reactor like the Advion Nanotek, provided drastic improvement on the incorporation of [^{18}F]fluoride into precursor **150**, a feature also seen with control diaryliodonium salt **151** (Figure 56). Here the incorporation of comparably electron-deficient phenyl moiety in place of an electron-rich n.p.r. saw direction of [^{18}F]fluorination towards this ring system, rather than the target arene. And as seen previously, the majority product observed on [^{18}F]fluorination of **151** proved to be [^{18}F]fluorobenzene **[^{18}F]166**. Note that with an electron-deficient arene in place, [^{18}F] fluorination of diaryliodonium salt **151** afford a markedly higher combined RCY (near 90%) than the other precursor in the series.

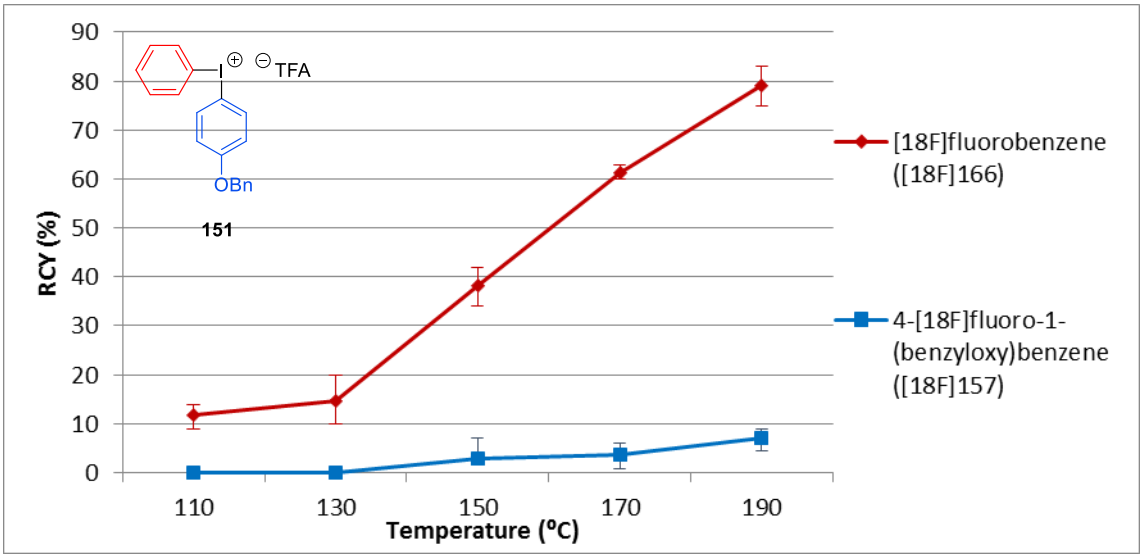

Figure 56: [^{18}F]Fluorination of diaryliodonium salt 151, with the structure of the precursor highlighting the two arenes fluorinated and corresponding RCYs of each resulting [^{18}F]fluoroarene

[^{18}F]Fluorination of precursor **151** not only provided a clear control substrate, but the majority formation of **[^{18}F]166** supported findings similar to those reported formerly,[260,324] and to some extent this observation was also noted in the [^{18}F]fluorination of **152** (Figure 57), since the acetyl protection strategy in place here will reduce some electron density applied by the phenoxy- moiety through resonance withdrawal. Although [^{18}F]fluorination of **152** does see some preference for the formation of **[^{18}F]158** over **[^{18}F]164**, the precursor exhibits questionable stability, as RCYs a markedly lower than those for diaryliodonium salt **149**, as was observed for the [^{19}F]fluorination of this precursor. However, [^{18}F]fluorination of diaryliodonium salt **152** did provide markedly superior results than [^{19}F]fluorination of the precursor, probably owed to the ability to reach higher temperature much more quickly.

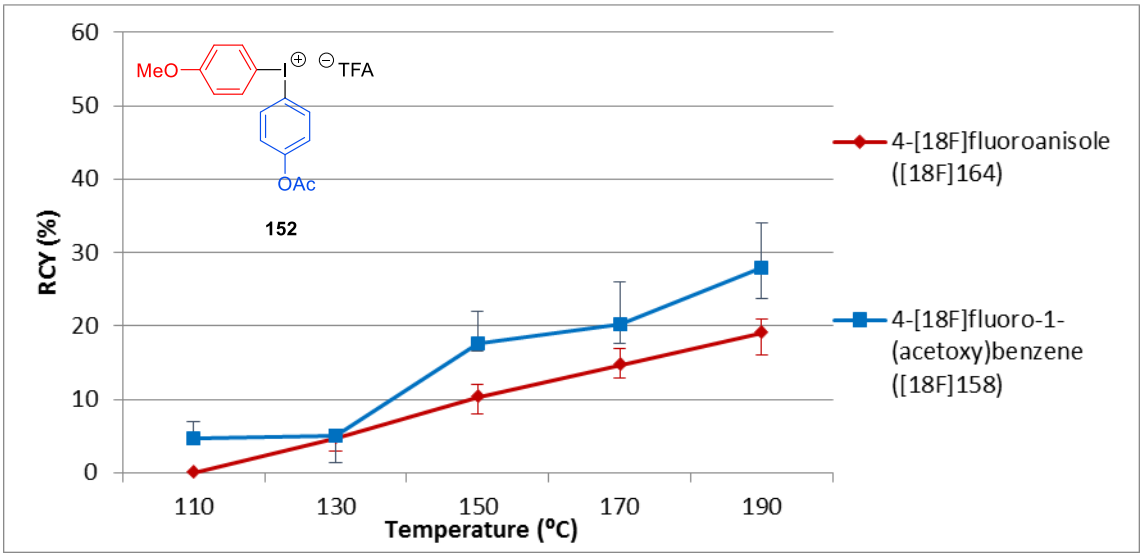

Figure 57: [^{18}F]Fluorination of diaryliodonium salt 152, with the structure of the precursor highlighting the two arenes fluorinated and corresponding RCYs of each resulting [^{18}F]fluoroarene

At this stage, it is worth noting that although achieving a high RCY is always of high importance, the resulting radioactivity of a radiolabelled product is heavily reliant on the starting radioactivity of the cyclotron-produced [^{18}F]fluoride used. Classically, radiosynthesis of PET imaging agents utilises large, powerful cyclotrons, capable of producing 20—50 GBq of activity per [^{18}F]fluoride production run; and hence even with relatively poor RCYs (~5%) the resulting radiopharmaceutical formulation will afford sufficient activity for clinical PET imaging, even if transport to a remote PET centre is required. However, with smaller cyclotrons, such as the ABT system in place here, [^{18}F]fluoride production is limited to a maximum of 2 GBq, which after radiolabelling, purification and formulation is likely to yield a radiopharmaceutical in lower levels of radioactivity (100—200 MBq), barely sufficient for and of limited use for preclinical clinical imaging with a rodent model because of the large volume of product generated. However, as with this work, the smaller, more conveniently placed cyclotrons are seeing substantial application in methodology development and with further optimisation and streamlining of radiosynthetic procedures, radiolabelled products with sufficient activity for on/near-site PET imaging could conceivably be produced utilising ultra-compact cyclotrons like the ABT biomarker generator. Hence, production of 4-[^{18}F]fluoro-1-(benzyloxy)benzene **[^{18}F]157** from precursor diaryliodonium salt **149** and [^{18}F]TEAF within 10 min (5 min 24 sec for radiolabelling and 4 min 22 sec for purification) presents a notable achievement.

3.4 Chapter 3 Summary

Chapter 1 highlighted a need for electron-rich [^{18}F]fluoroarenes both as complete radiopharmaceutical or as simple prosthetic groups, 4-[^{18}F]fluorophenol being a target of particular value for the latter; the subsequent chapter described a robust route to electron-rich diaryliodonium salts that could be used to prepare such [^{18}F]fluoroarenes, unhindered by the limitations of S_NAr chemistry. In this third chapter, rapid production and purification of [^{18}F]fluoroarenes has been demonstrated though the unique benefits provided by microfluidic radiolabelling diaryliodonium salts and an optimised in-line HPLC method, in particular 4-[^{18}F]fluoro-1-(benzyloxy)benzene was prepared in an average RCY of 47% (s = 4.93%, non-decay corrected) within 10 min. The [^{18}F]fluorination of other electron-rich diaryliodonium salts was also explored *via* these means, with results strongly supporting prior research in the area, as well as the benefits of employing microfluidics in the radiolabelling of these precursors.

Although further development of this work, through deprotection of 4-[^{18}F]fluoro-1-(benzyloxy)benzene to afford 4-[^{18}F]fluorophenol and ultimately application of the prosthetic group to radiolabel macromolecules is desired, limitations in the R&D grade cyclotron limited the availability of [^{18}F]fluoride and hence work discussed in the later chapters of this thesis discuss findings on further explorations with diaryliodonium salts and more complex precursors to electron-rich [^{18}F]fluoroarenes.

4 Diaryliodonium Routes to 6-[^{18}F]Fluoro-*m*-tyramine

Since the introduction of PET into the clinical setting, there has been considerable interest into the development of fluorine-18 labelled imaging agents capable of imaging the human dopaminergic projections, which are neural pathways that transmit the neurotransmitter dopamine from one area of the brain to another.[350] 6-[^{18}F]Fluoro-3,4-dihydroxyphenyl-L-alanine ([^{18}F]FDOPA) has seen a huge amount of attention for the imaging of dopamine metabolism and has seen successful PET imaging for a wide number of applications, including Parkinson's disease, neuroendocrine tumours and cerebral gliomas,[351] which will be discussed further in Chapter 5.

However, the development of analogues, derivatives and metabolites of [^{18}F]FDOPA, such as 6-[^{18}F]-L-*meta*-tyrosine,[352,353] 4-[^{18}F]fluoro-3-hydroxyphenylacetic acid,[350] 6-[^{18}F]fluorodopamine,[354] and regioisomers of 6-[^{18}F]fluoro-*meta*-tyramine[354] have also seen substantial attention as PET imaging agent targets. Of these 6-[^{18}F]fluoro-*meta*-tyramine (6-[^{18}F]fluoro-*m*-tyramine) provides a target, that to the author's knowledge, has yet to be investigated fully with regards to preparation using n.c.a. nucleophilic [^{18}F]fluoride, although some provisional methodology work has been conducted within the group[355] and hence in this chapter we look to utilise the diaryliodonium salt precursor methodology developed in chapter 2 to provide a robust, n.c.a. route to high SA 6-[^{18}F]fluoro-*m*-tyramine. Not only does this work provide a new route to a desirable fluorine-18 labelled tracer, but successful application of the diaryliodonium salt strategy for this precursor also demonstrates its potential for more complex electron-rich [^{18}F]fluoroarene imaging agents, such as [^{18}F]FDOPA.

Current routes to 6-[^{18}F]fluoro-*m*-tyramine employ an electrophilic approach either using carrier added [^{18}F]F_2 or use reagents derived from [^{18}F]F_2 and hence are restricted to low SAs, making realistic application of 6-[^{18}F]fluoro-m-tyramine *via* these routes unlikely.

One approach, developed by Garnett and co-workers,[350] utilises anhydrous HF as reaction medium for direct [^{18}F]fluorination carrier of the precursor *m*-tyramine using cyclotron produced [^{18}F]F_2 (Scheme 78). Here they found that use of strong acid,

rather than more commonly seen solvents such as TFA or CH_3CN/BF_3 provided a cleaner, more selective conversion than previous approaches, however, after separation of product regioisomers the resulting RCY of the 6-regioisomer was relatively poor.[350]

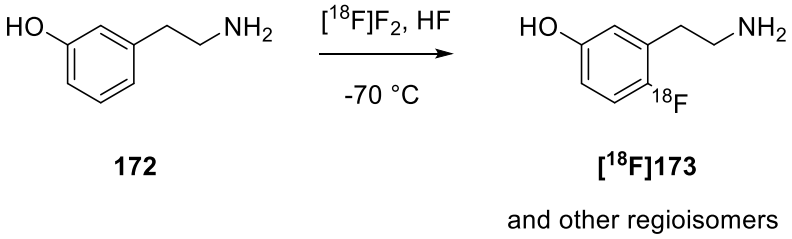

Scheme 78: Preparation of 6-[^{18}F]fluoro-*m*-tyramine [^{18}F]173 *via* direct electrophilic [^{18}F]fluorination of 172 with [^{18}F]F_2

However, as with many routes involving direct electrophilic [^{18}F]fluorination, the use of [^{18}F]F_2 proved to be too unselective, and the extensive separation time required to separate mono-fluorinated and multi-fluorinated regioisomers failed to outweigh the benefits of such simple, one-step conversions.

A more regioselective preparation 6-[^{18}F]fluoro-*m*-tyramine was afforded by [^{18}F]fluorodestannylation of a protected arylstannane precursor (Scheme 79), providing a drastically more useful procedure with improved RCYs.[354,356] Although this route does exploit the toxic trimethylstannyl moiety to ensure regioselectivity, the research group found that tin concentrations within the radiolabelled product could be as low as <15 ppb through standard HPLC purification alone. However, this method is again, still restricted by the limitations associated with electrophilic [^{18}F]F_2 fluorination, such as low SA.

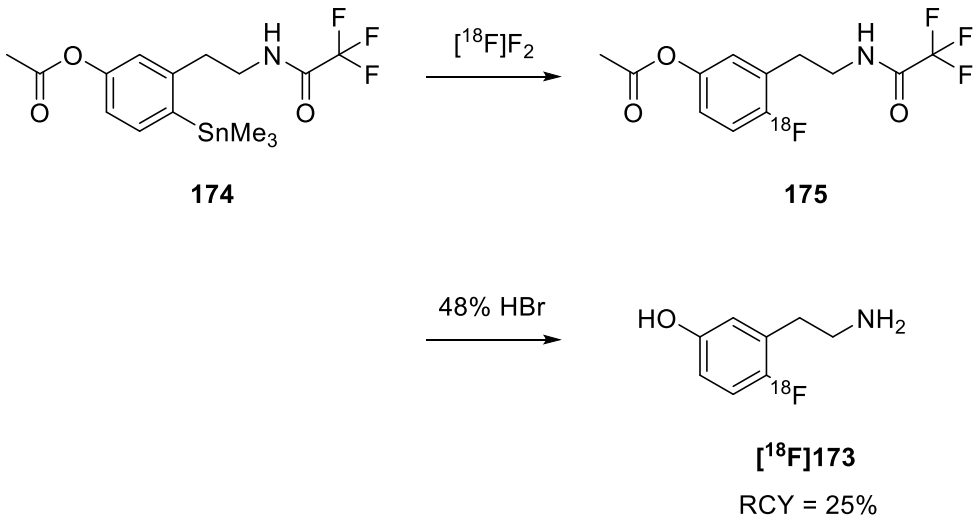

174 **175**

[18F]173

RCY = 25%

Scheme 79: Preparation of 6-[18F]fluoro-*m*-tyramine *via* [18F]fluorodestannylation of 174, followed by a subsequent acid hydrolysis deprotection

Note that precursor **174** also exploits the acetyl group for phenol protection, as with some of the diaryliodonium salts developed in Chapter 2, hence demonstrating that this strategy does occasionally see application in the radiolabelling of electron-rich [18F]fluoroarenes.

4.1 Diaryliodonium Salt Precursors to 6-[18F]Fluoro-*m*-tyramine

It was envisioned that preparation of a diaryliodonium salt precursor for the production of 6-[18F]fluoro-*m*-tyramine would overcome the problems described in prior section, particularly by employing a strategy suited to late-stage radiofluorination with n.c.a. nucleophilic [18F]fluoride to ascertain high RCYs and high SA, although it was appreciated that post-radiofluorination deprotection step would be essential (Scheme 80).

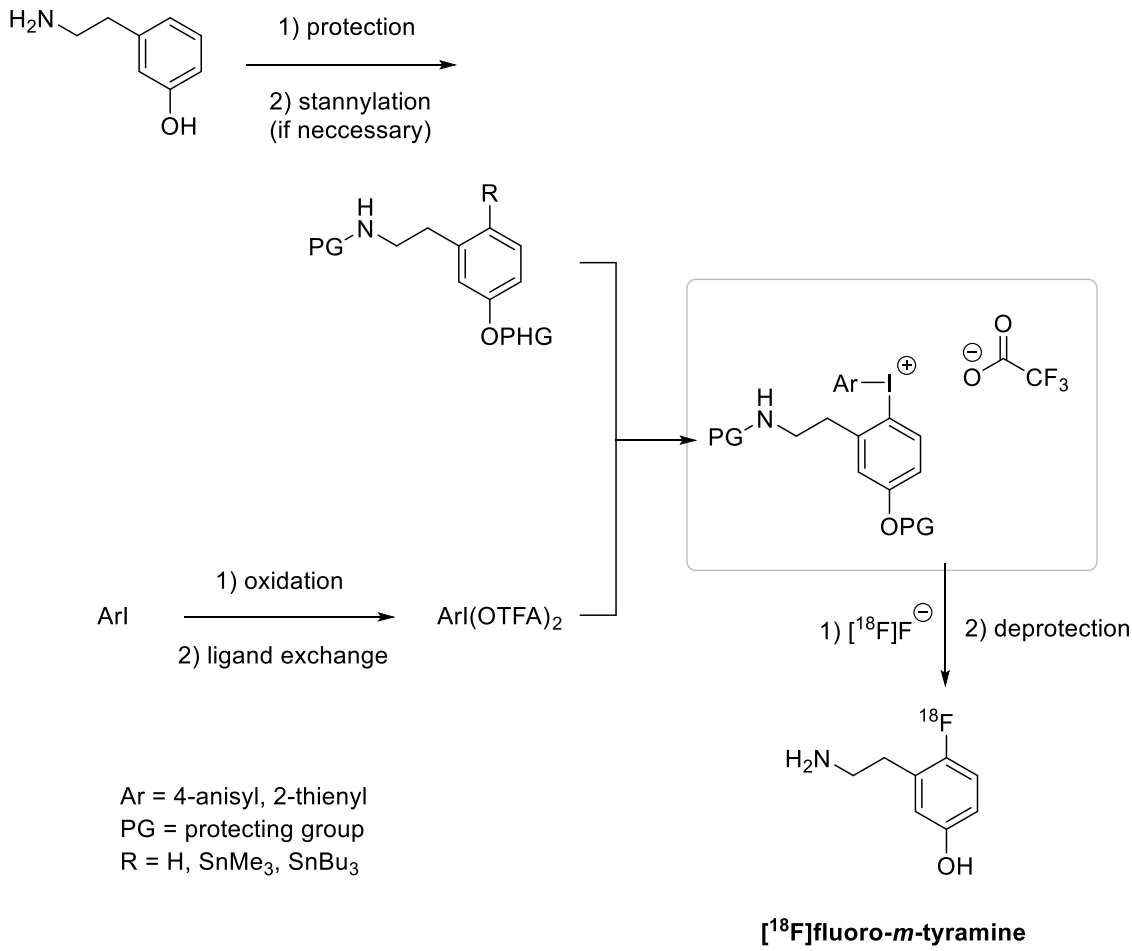

Scheme 80: Planned synthesis route for the production of 6-[^{18}F]fluoro-*m*-tyramine *via* the standard protocol developed in Chapter 2

Here, a simple synthesis strategy involving tandem installation of robust protecting group chemistry was adapted from previous work on the preparation of deuterium labelled phenethylamine derivatives by Xu and Chen,[357] which allowed preparation of the protected *m*-tyramine substrate three steps (Scheme 81). Augmentations were made to this general route to allow for straightforward installation of the diaryliodonium salt hypernucleofuge, built on knowledge obtained through the work discussed in Chapter 2 in that, although very low yielding, diaryliodonium salts can be prepared be reacting aryliodobis(acetate)s directly with appropriately substituted electron-rich arenes, without the need to prepare an arylstannane species. Failing this, it was deemed that iodination of electron-rich arene **179** could allow access to the iodoarene required for the subsequent stannylation, should that be necessary.

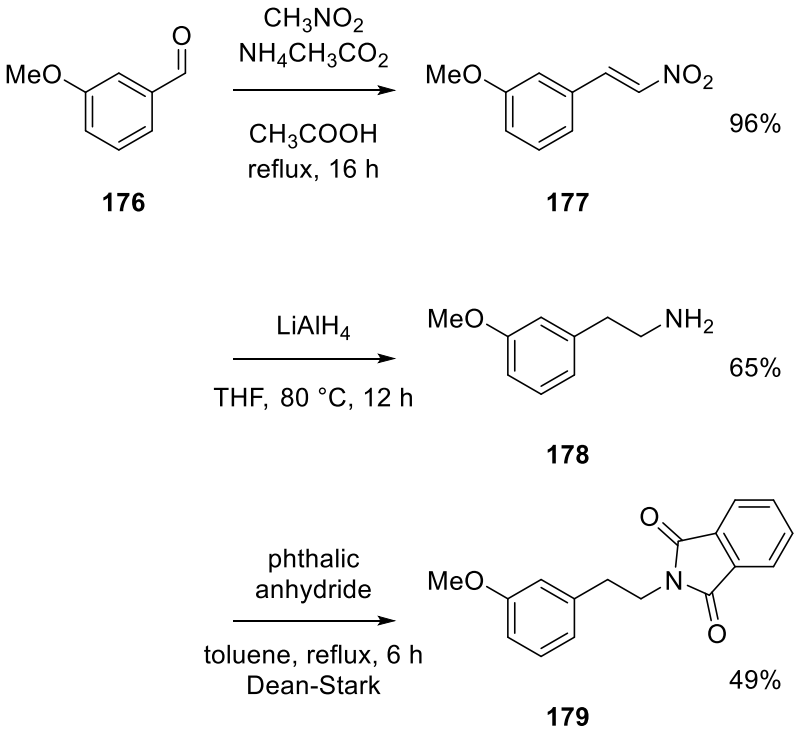

Scheme 81: Successful synthesis strategy for the preparation of protected *m*-tyramine 179, precursor to diaryliodonium salts for the preparation of 6-[^{18}F]fluoro-*m*-tyramine

The Henry reaction allowed for near quantitative conversion of commercially available benzaldehyde **176** to the corresponding β-nitrostyrene **177**, affording the product as a pale yellow solid without the need for any additional purification.[358,359] Also known as the 'nitro-aldol' reaction, this very useful C-C bonding forming reaction proved to be a convenient method of installing the required length side-chain, with an *in situ* dehydration, utilising the buffer system generated by combining ammonium acetate and acetic acid to provide the synthetically useful nitroalkene **177**.

Treatment of **177** with lithium aluminium hydride afforded phenylethylamine **178** *via* complete reduction of the nitroalkenyl moiety, although conversion to the hydrochloride salt afforded a cleaner product, immediate use of free amine **178** proved to be the most convenient substrate for subsequent conversion and further purification was deemed unnecessary.

At this stage it was decided to employ a phthalimidyl protection strategy, selected for its particularly high robustness under a variety of conditions and complimentary to the sturdiness of the methoxy protected phenol moiety. Although deprotection of

these groups requires harsh conditions (e.g. H_2NNH_2), typically not compatible with radiosynthetic equipment, for this work they provided a clear method of ensuring diaryliodonium salt stability.[360] In addition, it was believed that doubly protecting the amine functionality within an extendedly conjugated system would drastically reduce the nucleophilicity of the amine, hence reducing the risk of homo-attack on the highly electrophilic diaryliodonium salt product, which could bring about the formation of a neutral cyclic species (Figure 58).

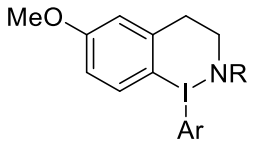

Figure 58: Neutral cyclic iodine (III) species which could potentially be formed if the *m*-tyramine amine is not doubly protected, particularly because of the optimum ring size afforded.

Initial efforts in producing **179** from phenylethylamine **178** and phthalic anhydride proved challenging, as both very poor conversions coupled with challenging purification resulted in exceptionally poor yields (0—25%). A number of small modifications were trialled, including the addition of 3 Å molecular sieves into the reaction mixture, alternative solvents and use of Dean-Stark apparatus,[361] of these, use of the latter followed by recrystallization from acetone:ethanol (1:9) proved to be the most successful method, although yields were still limited to 49%.

As with previous preparations of diaryliodonium salts, it was considered that the non-participating ring (n.p.r.) could be varied to control selectivity through relative electronics of the resulting protected *m*-tyramine diaryliodonium salt and hence three different aryliodobis(acetate)s, prepared as previously discussed (Section 2.5), were utilised in the preparation of diaryliodonium salts **180**, **181** and **182** (Scheme 82).

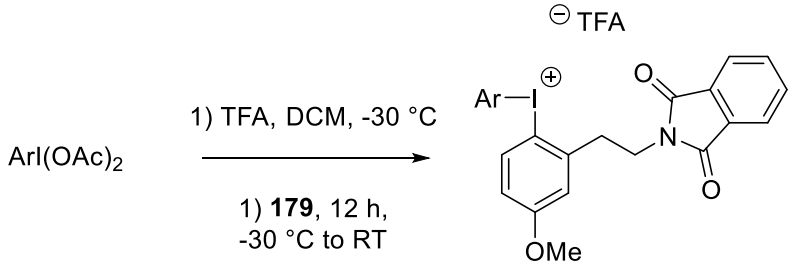

133, Ar = 2-thienyl
134, Ar = 4-anisyl
135, Ar = 2-anisyl

180, Ar = 2-thienyl, 0%
(observed but not isolated)
181, Ar = 4-anisyl, 20%
182, Ar = 2-anisyl, 17%

Scheme 82: Preparation of diaryliodonium trifluoroacetates 180-182 for the production of 6-[^{18}F]fluoro-*m*-tyramine using aryliodobis(acetate)s as λ^3-iodane precursor reagents

As anticipated, direct reaction of aryliodobis(acetate)s **133**-**135** with electron-rich arene **179** proved to be poor in all cases, in particular, isolation of diaryliodonium salt **180** could not be achieved *via* this route. Formation of a diaryliodonium species corresponding to **180** was observed by ^{1}H-NMR (doublet above 8.0 ppm consistent to previously observed protons *ortho*- to the iodine centre) of the crude reaction mixture, however, recrystallization failed to yield the desired product. Multiple attempts at column chromatography of crude reaction mixtures of **180** also failed to afford the product, presumably as a result of diaryliodonium salt instability as an artefact of the high electron density of both aryl substituents attached to the iodine centre as well as over exposure of the sensitive material to heat, light, solvent, silica, *etc*.

This direct method of diaryliodonium salt formation did, however, successfully afford both **181** and **182** *via* recystallisation from DCM:ether:petrol, with material amounts sufficient for the subsequent [$^{18/19}$F]fluorination experiments. Numerous efforts were also made to produce crystals of **181** and **182** of suitable quality for x-ray crystallography including *via* slow vapour diffusion as discussed in Section 2.7, however, only sufficiently large crystals of **181** were obtained and on crystallographic analysis the structure still exhibited substantial disorder (Figure 59).

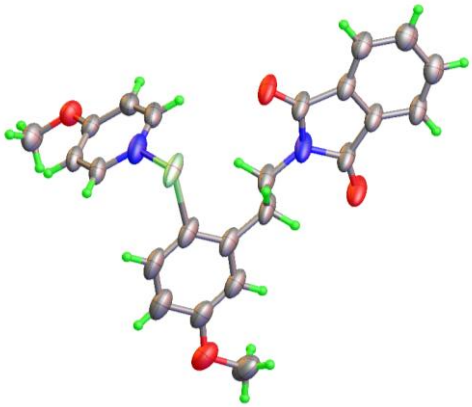

Figure 59: Attempted x-ray crystallography of diaryliodonium salt 181 afforded the above disordered structure.

Despite the inability to obtain high quality x-ray crystal structure date of diaryliodonium salts **181** and **182**, the other supporting data (^{1}H-NMR, ^{13}C-NMR, HR-MS, elemental analysis) validated successful preparation of both targets. This encouraging result not only confirms the varied substrate scope of this method of diaryliodonium salts, but also two valuable diaryliodonium salt precursors have been afforded, useful for the preparation of 6-[^{18}F]fluoro-*m*-tyramine. Given the small amounts of material needed for [$^{18/19}$F]fluorination studies, attempts to optimise the preparation of **180**—**182** *via* incorporation of yield-improving arylstannane functionality was deemed unnecessary, but could be attempted in future work.

4.2 [^{19}F]Fluorination of 6-Fluoro-*m*-tyramine Precursors

As with the diaryliodonium salts designed for 4-[^{18}F]fluorophenol (Chapter 2), initial fluorination work on diaryliodonium salts **181** and **182** was conducted using 'cold' [^{19}F]fluoride, to again assess the selectivity profile of each diaryliodonium salt under our artificial fluorination conditions, whilst monitoring the reaction progress by ^{1}H- and ^{19}F-NMR in real-time. As before, each diaryliodonium salt was dissolved in deuterated DMF before the addition of caesium fluoride and the reaction mixtures were heated up to 140 °C, heated in 20 °C increments every 30 min, whilst monitoring the change in the ^{1}H- and ^{19}F-NMR spectra (Scheme 83).

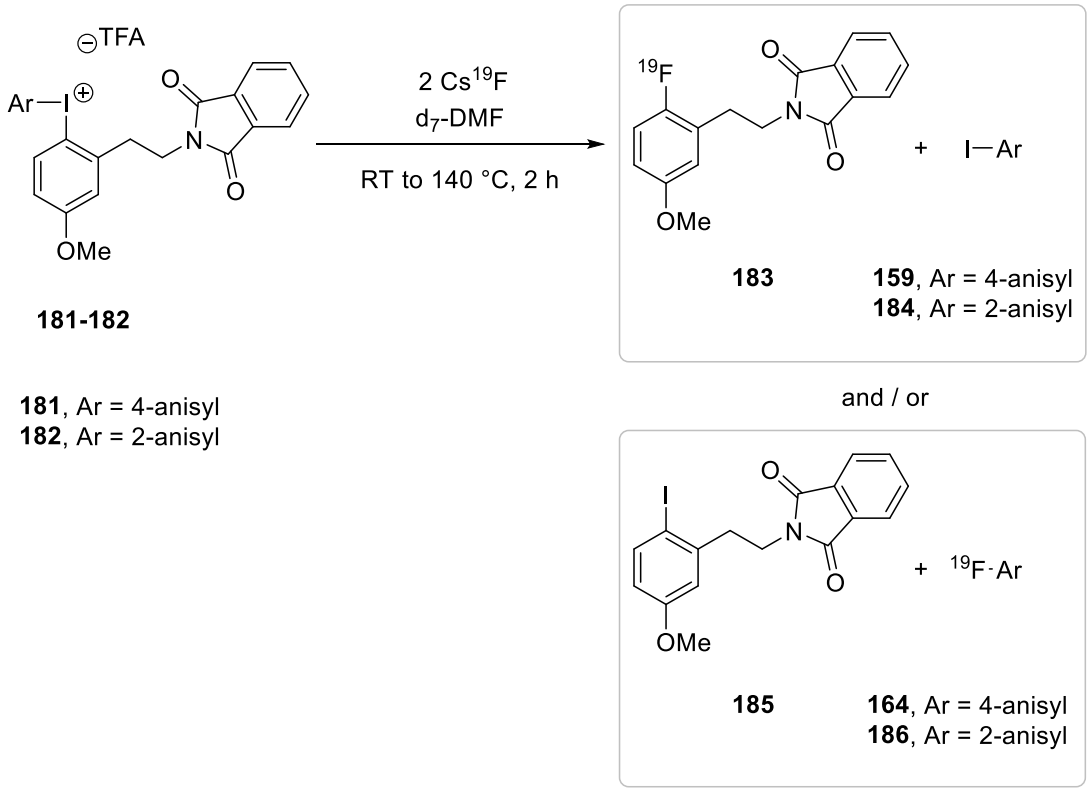

Scheme 83: Dynamic ^{1}H- and ^{19}F-NMR [^{19}F]fluorination study with diaryliodonium salts 181-182, highlighting the potential fluoro- and iodoarene products

As before, the identities of fluoroarene products were elucidated by adding an authentic sample of the relevant fluoroarenes to the complete reaction mixture, then re-analysing the mixture *via* ^{1}H- and ^{19}F-NMR with the expectation of seeing the corresponding peaks increase in intensity. Samples of protected 6-fluoro-*m*-tyramine **183**, 4-fluoroanisole **164** (expected to be seen for the fluorination of **181**) and 2-fluoroanisole **186** (expected to be seen for the fluorination of **182**) were available for product validation. Fortunately, the formation only two fluoroarene products were observed during [^{19}F]fluorination reactions of both **181** and **182**, making analysis of the [^{19}F]fluoroarene products straight forward (Figure 60 and Figure 61).

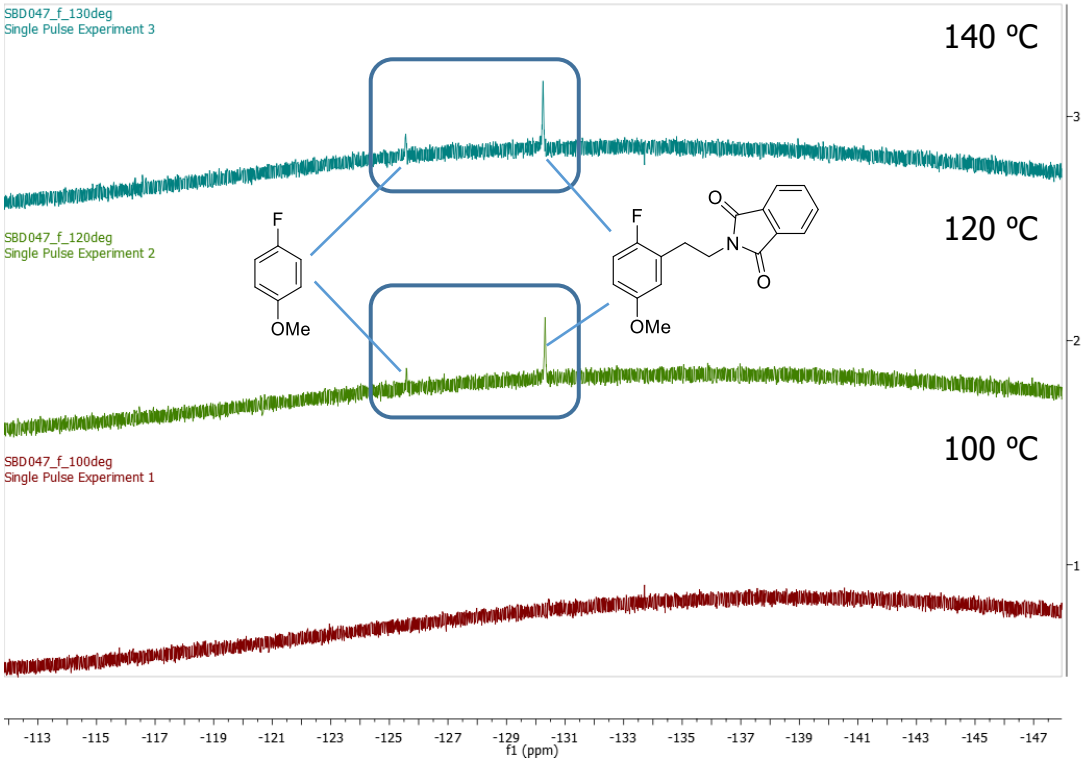

Figure 60: Dynamic ^{19}F-NMR experiment following the fluorination of 2-(2-(3-Methoxyphenethyl)isoindoline-1,3-dione)(4-methoxyphenyl)iodonium trifluoroacetates 181.

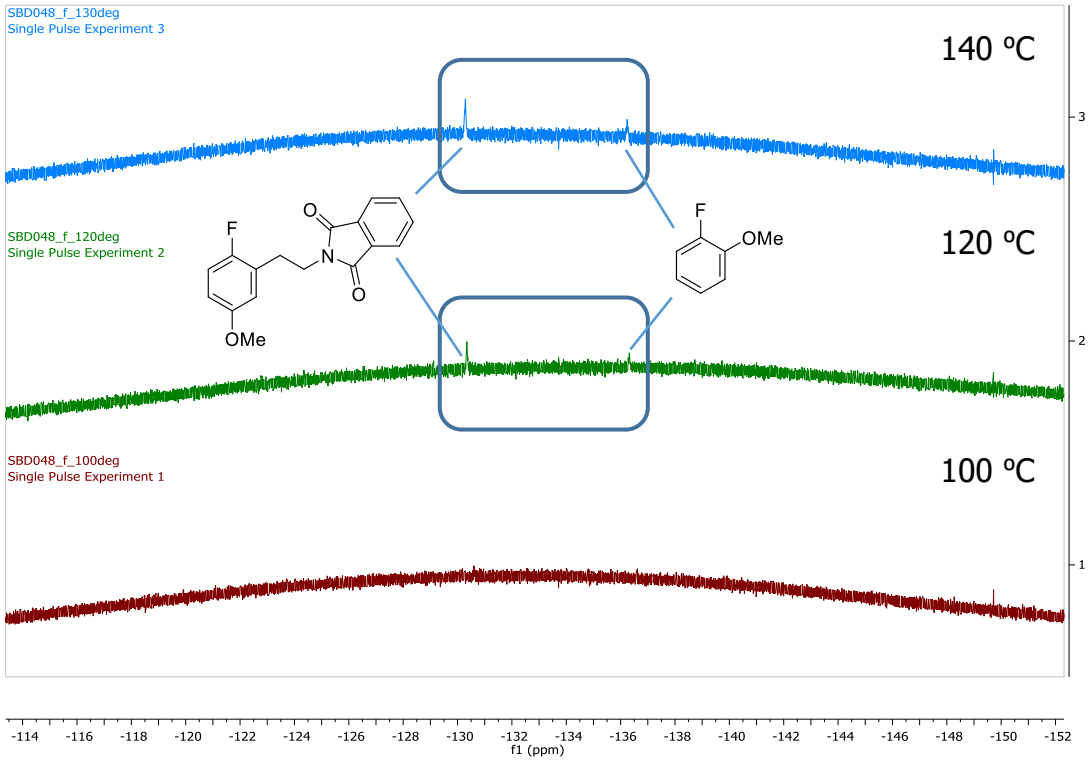

Figure 61: Dynamic ^{19}F-NMR experiment following the fluorination of 2-(2-(3-Methoxyphenethyl)isoindoline-1,3-dione)(2-methoxyphenyl)iodonium trifluoroacetates 181.

The dynamic [^{19}F]fluorination experiments portrayed by the ^{19}F-NMR spectra above demonstrate some interesting selectivity outcomes for the reactions of **181** and **182** with caesium fluoride. In both cases it appears that fluorination was heavily directed towards formation of protected 6-fluoro-*m*-tyramine species **183**, caused by the so-called *ortho*-effect, discussed in Section 2.2.1, not surprising given the electron-density exhibited by the target ring *versus* the n.p.r. Here, congestion around the axial positions of fluorination transition state promotes occupation of the pseudo-equatorial by the arene bearing the most sterically demanding, and hence this species sees preferential fluorination.

As with the [^{19}F]fluorination studies discussed earlier, the material yield of these conversions under these reactions conditions is very low, therefore the experiments are used to purely assess the selectivity profile observed for the [^{19}F]fluorination of each diaryliodonium salt. This is distinctly similar to the [^{18}F]fluorination of diaryliodonium salts discussed herein, since RCY and material yield are independent of one another, and it is the RCY that is most important in radiochemical transformations.

The table below (Table 14) summaries the findings of the above dynamic [^{19}F]fluorination studies and provides approximate selectivity ratios determined by integration of the above ^{19}F-NMR peaks, as well as corresponding shifts for the [^{19}F]fluoroarene products detected.

Precursor	Fluorinated Products	Selectivity	^{19}F-NMR Shift
181	**protected 6-fluoro-*m*-tyramine 183**	**80%**	**-130.3 ppm**
	4-fluoroanisole **164**	20%	-125.6 ppm
182	protected 6-fluoro-*m*-tyramine **183**	75%	-130.3 ppm
	2-fluoroanisole **186**	25%	-135.3 ppm

Table 14: Summary of dynamic [^{19}F]fluorination experiments on [^{18}F]fluoro-*m*-tyramine precursor diaryliodonium salts 181 and 182, including ^{19}F-NMR shifts and approximate selectivity profiles of the [^{19}F]fluoroarene products

It was anticipated that diaryliodonium salt **182** would provide a poor substrate for the preparation of **186**, given that both aryl substituents on iodine not only hold similar electron-rich quality, but also both bear functionality in the *ortho* position. Interestingly however, Table 14 highlights the lack of dissimilarity between the [^{19}F]fluorination selectivity profiles of **181** and **182**, despite this potentially poor 2-anisyl n.p.r. on precursor **182**. Seemingly the markedly bulkier functionality in the *ortho* position of target ring system heavily outweighs the effect of the ortho-methoxy group on the n.p.r. of diaryliodonium salt **182**. However, this only considers a monomeric model, where the extremities of the side chain are too distant to cause influence, whereas consideration of a dimeric model may see the side chain functionality providing additional interactions to neighbouring diaryliodonium salts.

This positive outcome demonstrates how the *ortho*-effect can be exploited to override the disadvantages associated with the fluorination of diaryliodonium salts bearing two electron-rich arene substituents, a potentially invaluable tool for the fluorination of other [^{18}F]fluoroarenes bearing steric bulk in the *ortho*- position, such as [^{18}F]FDOPA. Although the ortho-effect has been studied for simple diaryliodonium salts previously,[98,169] the application of *ortho*- substituted aromatics within diaryliodonium salts here fortifies the understanding of this advantageous effect and how it can provide highly selective late-stage radiofluorination of electron-rich arenes bearing extended functionality.

4.3 [^{18}F]Fluorination of 6-Fluoro-*m*-tyramine Precursors

Chapter 3 describes the numerous benefits associated with microfluidic radiofluorination, as well as certain features specific to [^{18}F]fluorination of diaryliodonium salts, such as the ability to operate radiolabelling within a closed system, providing access to higher than normal temperatures where RCYs are maximised. Similarly, the work therein also demonstrated how [^{18}F]fluorination reactions of electron-rich diaryliodonium salts benefit from reaching elevated temperatures rapidly to avoid decomposition of the sensitive precursor during prolonged heating, again another feature supplied by microfluidics.

Despite these key benefits, simple-to-operate batch-based radiosynthesis platforms remain more popular than microfluidic systems within the PET community,[362] particularly within the clinical setting[329] where radiosynthesis is still often conducted by non-chemically trained personnel and hence procedures are designed to be as simple as possible. Batch-based systems allow for the routine production of larger scale quantities (both in terms of material quantity and radioactivity) of fluorine-18 labelled tracers and ligands, which permits transportation of the PET imaging agent to a distance location, or does splitting between multiple patients. However, to achieve optimal [^{18}F]fluorination conditions on batch platforms, prior development on research grade microfluidic systems may be beneficial, followed by translation of those optimised parameters to the batch based system of choice, which can be complicated given the intrinsic differences between the radiosynthesis methods.

A collaborative project with radiochemists at Edinburgh University Clinical Research Imaging centre (CRIC)[363] provided the opportunity to conduct [^{18}F]fluorination of electron-rich diaryliodonium salts within a batch radiolabelling platform, namely the GE TRACERlab FX FN platform (Figure 62, left),[364] developed specifically for nucleophilic substitution with [^{18}F]fluoride. GE have developed a number of batch-based systems based around this model, encompassing electrophilic [^{18}F]F_2 fluorination chemistry, carbon-11 labelling and systems intended for immediate clinical application utilising pre-developed, robust protocols, such as the GE FASTlab (Figure 62, right).

Figure 62: Batch based radiosynthesis platforms, the GE TRACERlab FX FN platform for research purposes (left)[364] and the GE FASTlab platform designed for routine multi-tracer production of radiopharmaceuticals for clinical application (right)[365]

In this pilot study, we aimed to trial the [^{18}F]fluorination of diaryliodonium salt precursors to 6-[^{18}F]fluoro-*m*-tyramine, namely precursor **181** prepared in Section 4.2, to primarily investigate the translatability of diaryliodonium salt fluorination chemistry to the batch-based system, as well as to develop understanding of how the dominating the *ortho*-effect is outside of microfluidic radiofluorination. It is important to recall that [^{18}F]fluorination *via* batch-based synthesis was always likely to yield limited results compared to the findings from microfluidic radiofluorination, given the lack of a closed system environment and hence temperatures above 130 °C could not be accessed.

The precursor diaryliodonium salt **181** was loaded into the GE TRACERlab FX FN platform, dissolved in a mixture of anhydrous DMF and anhydrous diglyme. The precursor was then transferred to the reaction vessel along with GE cyclotron produced [^{18}F]fluoride, dried and re-administered as [^{18}F]KF.K_{222} in anhydrous DMF, following which the reaction mixture was heated to 155 °C for 30 min before being transferred to a semi-preparative radio-HPLC system for analysis of the reaction mixture (Figure 63).

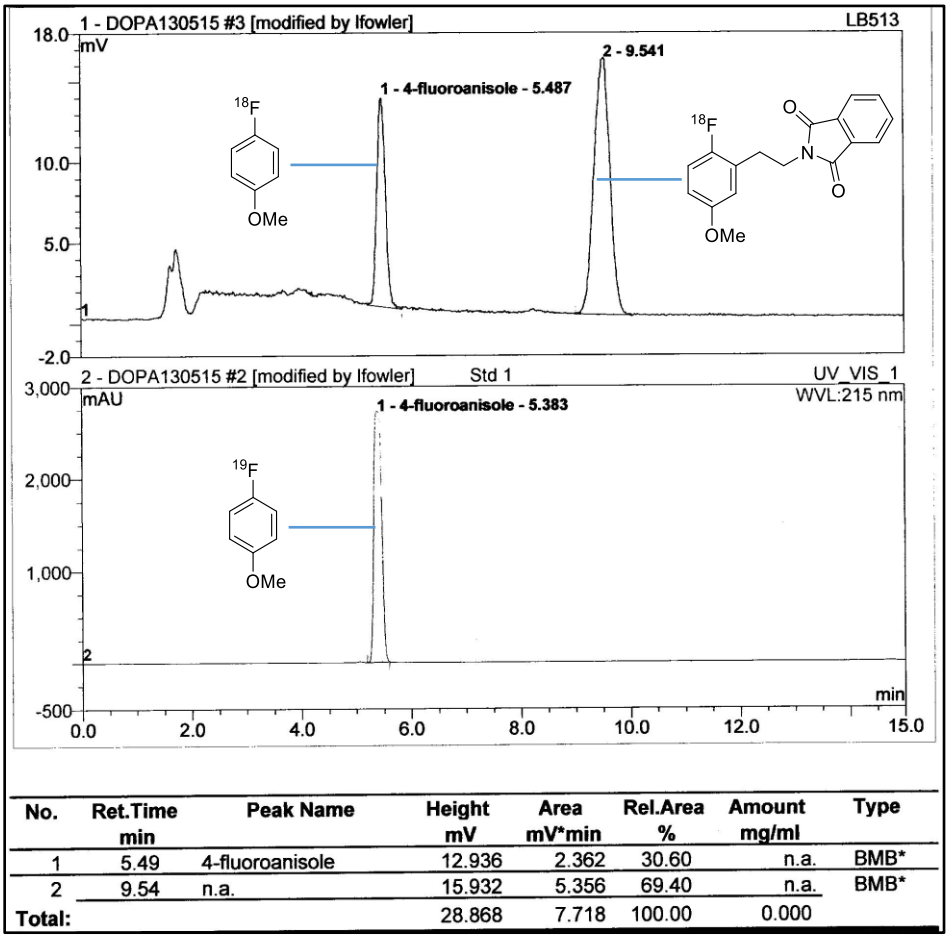

No.	Ret.Time min	Peak Name	Height mV	Area mV*min	Rel.Area %	Amount mg/ml	Type
1	5.49	4-fluoroanisole	12.936	2.362	30.60	n.a.	BMB*
2	9.54	n.a.	15.932	5.356	69.40	n.a.	BMB*
Total:			28.868	7.718	100.00	0.000	

Figure 63: UV/radio-HPLC chromatograms of the [^{18}F]fluorination of diaryliodonium salt 181 providing formation of protected 6-[^{18}F]fluoro-*m*-tyramine [^{18}F]183 , using a batch-based radiosynthesis platform (GE TRACERlab FX FN).

Although extensive testing and parameter alterations were not conducted, the pilot [^{18}F]fluorination of diaryliodonium salt **181** using the batch reactor platform proved highly successful, formation of the desired protected 6-[^{18}F]fluoro-*m*-tyramine species **[^{18}F]183** was achieved with high selectivity for target arene over the [^{18}F]fluorination of the n.p.r., over three [^{18}F]fluorination runs an average RCY of 66 % (s = 4.66, non-decay corrected) was achieved. Most importantly, this demonstrates the translatability of diaryliodonium salts as precursors to electron-rich [^{18}F]fluoroarenes, given that platform translation proved to be relatively straight forward in this case. This bodes well for further development of electron-rich diaryliodonium salt precursors, since they can be applied to both microfluidic radiosynthesis platforms as well as the commonly seen batch-based systems, thus supporting simpler conversion to the preferred clinical format. However, the benefits

provided by microfluidic systems should not be overlooked and as the development of more hybrid microfluidic, batch-scale systems continues it is likely that radiochemists will look to utilising the advantages offered by microfluidic systems for clinically licensed fluorine-18 labelled targets.

4.4 Chapter 4 Summary

Chapter 4 demonstrates the potential application of diaryliodonium salt precursors for the preparation of dopaminergic system imaging agent 6-[^{18}F]fluoro-*m*-tyramine, which also presents itself as a derivative of high valued target [^{18}F]FDOPA. Here the strategy for producing electron-rich diaryliodonium salts was adapted to permit the formation of a series of, to the author's knowledge, previously unreported protected *m*-tyramine diaryliodonium trifluoroacetates, providing a distinct advantage over previous efforts involving low SA electrophilic [^{18}F]F_2 fluorination chemistry. [^{19}F]Fluorination studies on these precursors exposed how valuable manipulation of the *ortho*-effect can be for driving [^{19}F]fluorination towards the target ring system, and preliminary [^{18}F]fluorination using batch reactor system demonstrated the high level of translatability held by diaryliodonium salts of this type, drastically improving the chances of clinical application.

5 Diaryliodonium Routes to [^{18}F]FDOPA

Chapter 4 exemplifies how diaryliodonium salts can provide precursors for late-stage radiofluorination allowing access to n.c.a. electron-rich [^{18}F]fluoroarenes produced as complete radiopharmaceuticals; herein we aim to extend that methodology to 3,4-dihydroxy-6-[^{18}F]fluoro-L-phenylalanine ([^{18}F]FDOPA), a highly valuable dopaminergic system imaging agent that still lacks a robust and reliable nucleophilic route to production. The multiple labile protic functionalities on the molecule, as well as the inclusion of function-critical stereocentre and a need for highly regiospecific fluorine-18 incorporation make radiolabelling this small molecule a challenge (Figure 64).

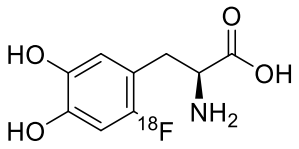

Figure 64: Structure of 3,4-dihydroxy-6-[^{18}F]fluoro-L-phenylalanine ([^{18}F]FDOPA)

Investigations into suitable protecting groups that supply compatibility with the [^{18}F]fluorination conditions and accommodate the conditions required for diaryliodonium salt formation is required, as is a simple and crucially very fast method for complete deprotection in order to maintain a high RCY. As with the production of 6-[^{18}F]fluoro-*m*-tyramine, precursor design should also consider the current trends and formats in the production of fluorine-18 labelled imaging agents and as such, translation of the diaryliodonium salt precursor into a format compatible with a 'plug and play' cassette is also explored.

5.1 Introduction to [^{18}F]FDOPA

2-[^{18}F]fluoro-2-deoxy-D-glucose ([^{18}F]FDG) has seen extensive application in the PET imaging of a wide number of cancers, allowing for detailed identification of malignant

tissue and accurate assignment of stage and restage tumours.[366] Even with continued development into other fluorine-18 labelled radiopharmaceuticals, more than 90% of all clinical PET scans are still conducted with [^{18}F]FDG, despite the huge scope for PET imaging using alternative radiotracers and radioligands (Figure 65).[367] This setback in PET imaging agent diversity can, in part, be attributed to poor translation of successful PET tracers and ligands from bespoke R&D PET imaging studies to robust and widely accepted formats; although radiochemistry developers are constantly striving to bring successful pre-clinical candidates to market using simple-to-operate multi-tracer radiosynthesis platforms.[365]

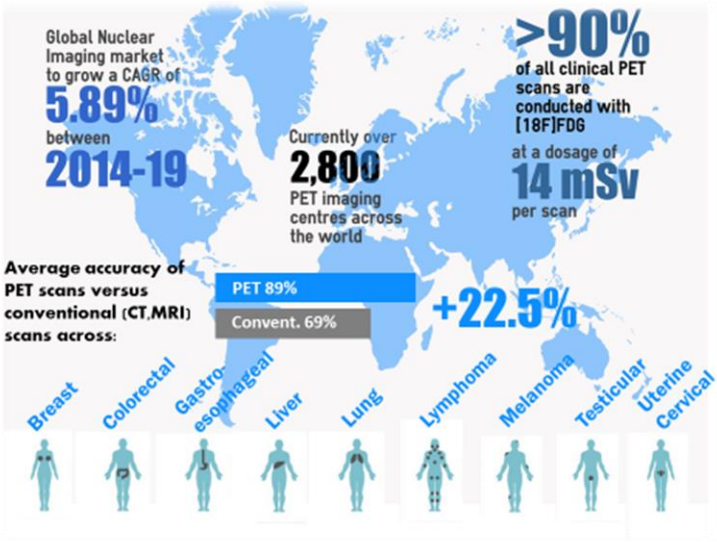

Figure 65: Infographic describing the importance of [^{18}F]FDG in oncological PET, as well as other facts related to the clinical applications of fluorine-18 labelled PET imaging agents.[367]

However, for many applications, the high uptake of [^{18}F]FDG exhibited by energetically demanding tissue, such as the brain, heart, regions of inflammation and other heavily glycolytic processes often renders the radiotracer unsuitable for identification of abnormalities in these regions. [^{18}F]FDOPA is widely regarded as a versatile yet highly selective radiotracer for the evaluation of presynaptic dopaminergic function, which holds influence over a number of diseases and conditions, making [^{18}F]FDOPA a highly desirable tool for clinicians across the globe.

Good understanding of the un-labelled derivative, L-3,4-dihydroxyphenylalanine (L-DOPA), has seen therapeutic application of the L-tyrosine derivative for the treatment

of Parkinson's disease (PD) for over 40 years.[368] As a precursor to the integral neurotransmitter dopamine (as well as norepinephrine and epinephrine), administration of L-DOPA sees the molecule cross the blood-brain-barrier and raises dopamine concentrations as it is metabolised by aromatic L-amino acid decarboxylase, aiding patients with dopamine deficiency such as those suffering from Parkinsonian symptoms or dopamine-responsive dystonia.[369]

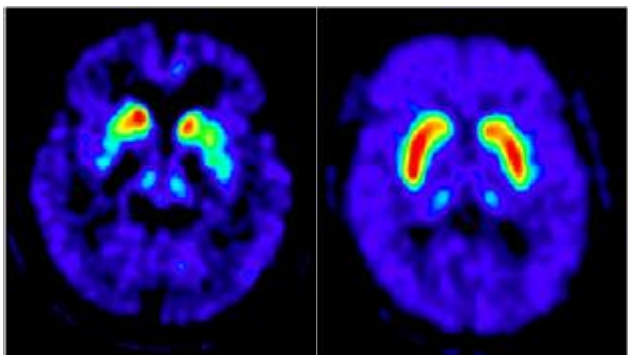

Figure 66: [^{18}F]FDOPA PET scans highlighting the loss of dopamine storage capacity in the putamen of a patient with Parkinson's disease (left) *versus* normal dopamine distribution within a healthy brain (right)

Initial efforts into the incorporation of fluorine-18 into L-DOPA sought to use the radiotracer to image the underlying pathophysiology of PD (Figure 66) and related central motor disorders, however, continued exploration into other uses of [^{18}F]FDOPA over the last 15 years has unveiled the ever expanding spectrum of applications the radiotracer can be benefit.[370] Amongst these new emerging uses, the most frequently researched is the imaging of neuroendocrine tumours (NETs),[371] a collective of cancers including pancreatic β-cell hyperplasia, pheochromocytoma, carcinoid tumours and medullary thyroid cancers (MTCs); [372,373] as well other related diseases such as hyperinsulinism, cerebral gliomas and bronchopulmonary cancer.[374]

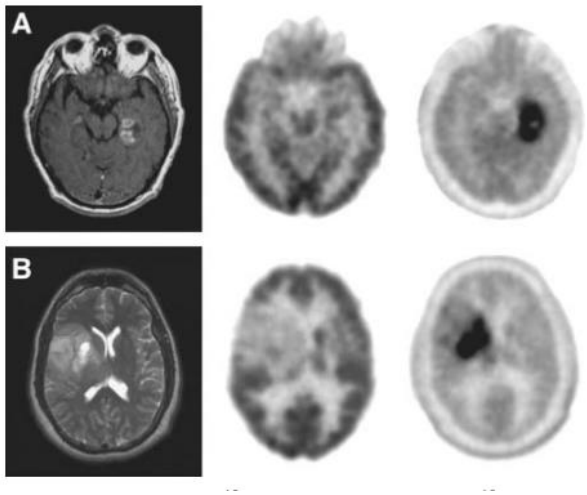

Figure 67: A demonstration of the superior sensitivity offered by [^{18}F]FDOPA PET (right) over [^{18}F]FDG PET (middle) and MRI (left) for newly diagnosed tumours of (A) glioblastoma and (B) grade II oligodendroglioma[374]

As shown in above (Figure 67) imaging of gliomas using [^{18}F]FDOPA benefits from high tumour-to-background ratio and high sensitivity, which is crucial when seeking to image non-aggressive metastatic cancers like NETs and gliomas.[375] For many of the tumour types under the NET umbrella, [^{18}F]FDOPA affords a very similar mode of action, as depicted below (Figure 68), whereby the uptake of [^{18}F]FDOPA is mediated by the sodium-independent large amino acid transporter (LAT1) protein. [^{18}F]FDOPA then undergoes metabolism facilitated by L-amino acid decarboxylase (AADC), affording [^{18}F]fluorodopamine, which no longer being able to pass out of the cell membrane provides a cellular retention mechanism and helps promote successful PET imaging. After the metabolite is transported into neurosecretory vesicles *via* a vesicular mono-amine transported, further metabolism mediated by dopamine-β-hydroxylase affords [^{18}F]fluoro-norepinephrine.[375]

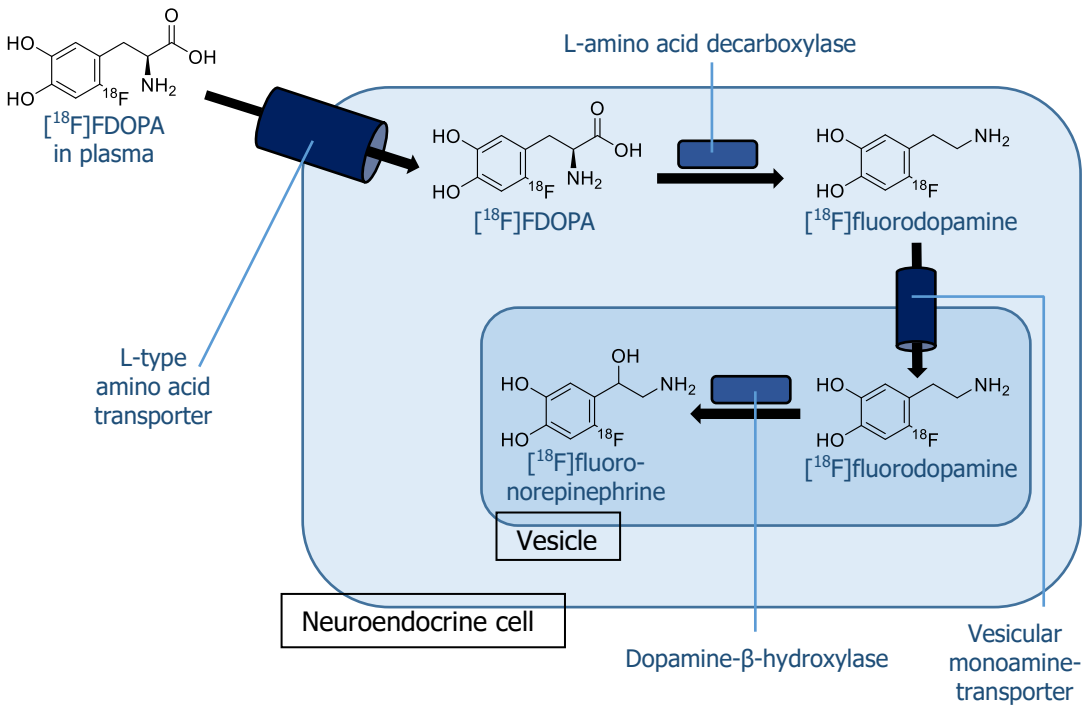

Figure 68: Schematic representation of the uptake mechanism of [^{18}F]FDOPA in neuroendocrine cells[375]

In essence, uptake of [^{18}F]FDG increases as tumour aggressiveness increases, making the radiotracer invaluable for rapid diagnosis of life threatening cancers, however, radiolabelled amino acids like [^{18}F]FDOPA hold particular value in imaging slower metastasising cancer types.[372] Whilst the mortality rate of patients suffering from NETs is relatively low, patients can experience serious detriments to their health when afflicted by NETs over extended periods of time; and the last 30 years have seen a 500% increase in the incidence of NETs, hence a reliable route to diagnosis, through non-invasive PET imaging is very much required.

5.2 Current Routes to [^{18}F]FDOPA

The ever increasing demand for a robust method of [^{18}F]FDOPA production has brought considerable attention to the preparation of this challenging fluorine-18 labelled target, and hence there are a number of diverse approaches known, however, all of which come with limitations that potentially hinder their application in the clinical setting. Traditional routes utilise electrophilic [^{18}F]F_2 or reagents derived

from [^{18}F]F_2 to achieve late-stage radiofluorination of a protected precursor, but are as expected, limited by the inherently low SA associated with carrier added [^{18}F]F_2. Unselective direct electrophilic [^{18}F]fluorination with [^{18}F]F_2 provides a mixture of regioisomers that are difficult to separate quickly,[376,377] hence subsequent efforts focussed on the incorporation of much more efficient directing metal groups (Scheme 84).

Cleavage of the carbon-silicon bond of precursor **187** to afford **188** and subsequently [^{18}F]FDOPA was first conducted by Diksic and co-workers, although benefitting from the omission of any toxic organometallic precursors, the resulting RCY and SA were relatively poor.[378] Note the use of Freon-11 (CCl_3F) in this radiosynthesis as an inert and easily removable solvent, ideal for electrophilic [^{18}F]fluorination chemistry, however, later work that found that substitution of the environmentally damaging chlorofluorocarbon for deuterated solvents afforded better results,[379] as applied for the [^{18}F]fluorination of precursor **189**. The [^{18}F]fluorodestannylation approach to [^{18}F]FDOPA *via* **190** has received more attention than alternative demetallation methods largely because of the improved conversion, affording typically higher RCYs (Scheme 84).[380] However, use of more nucleophilic trimethylstannylarene precursors rather than less toxic trialkylstannylarenes presents unfavourable toxicity concerns.

Organomercury[381] **191** and organosilver[122] **193** precursors have also been utilised to achieve highly selective radiosynthesis of [^{18}F]FDOPA, but similarly suffer from poor-modest yields, low SAs and are also relatively toxic in character, which again hampers adoption of such precursors by clinical radiopharmacies.

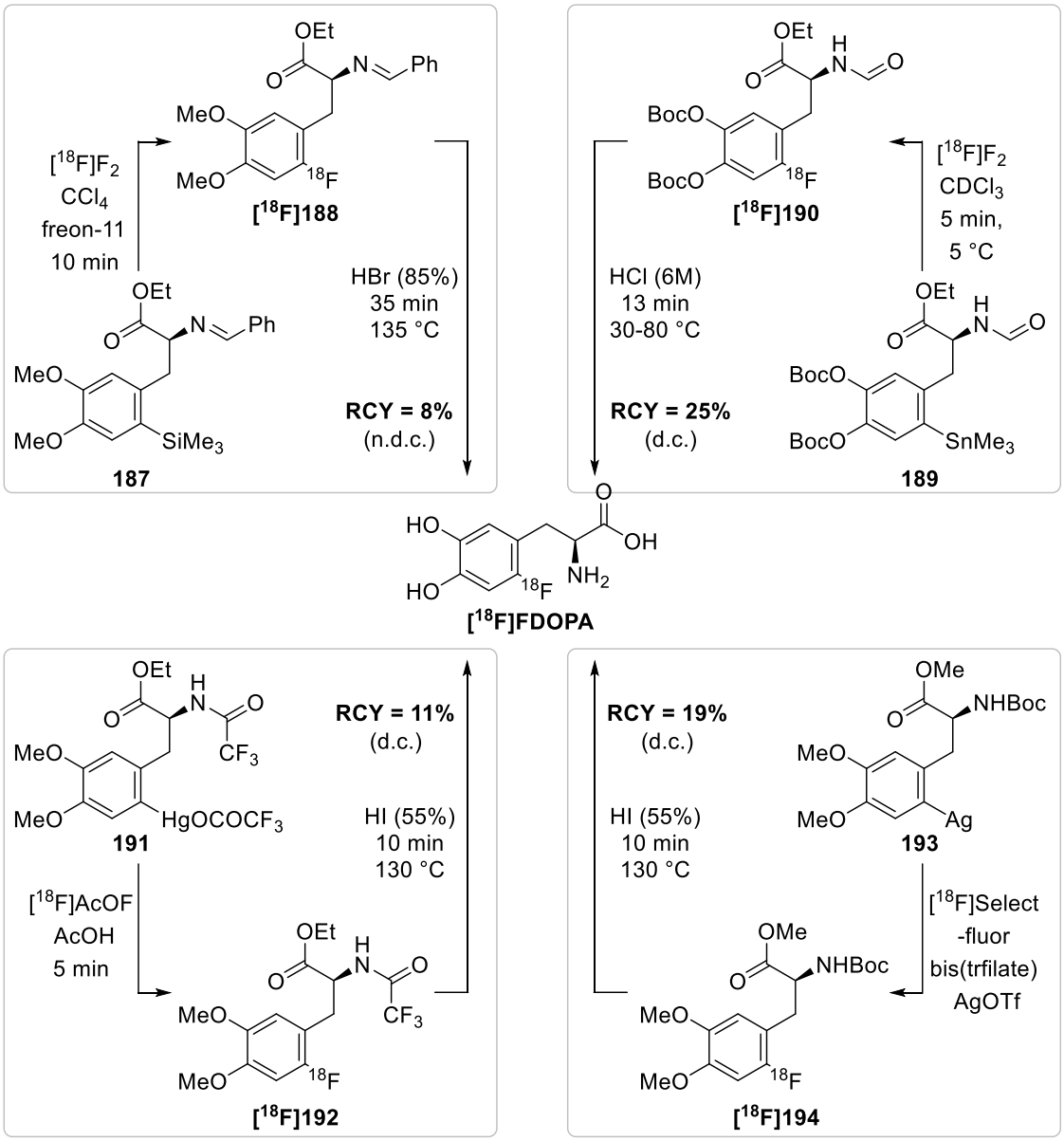

Scheme 84: Electrophilic routes to [^{18}F]FDOPA involving [^{18}F]fluorodemetallation of protected precursors

Isotopic exchange using nucleophilic [^{18}F]fluoride has also been utilised in the preparation of [^{18}F]FDOPA in attempts to capitalise on the improved SA offered by [^{18}F]fluoride, as demonstrated by the radiosynthesis developed by Wagner *et al.* (Scheme 85).[382] This three-step, one-pot protocol benefitted from the use of n.c.a. [^{18}F]fluoride, as reflected by an improved SA (1.2–2.5 GBq/μmol), whilst achieving enantiomeric purity of 99% yet a modest RCY of 22%, as limited by the incorporation method.

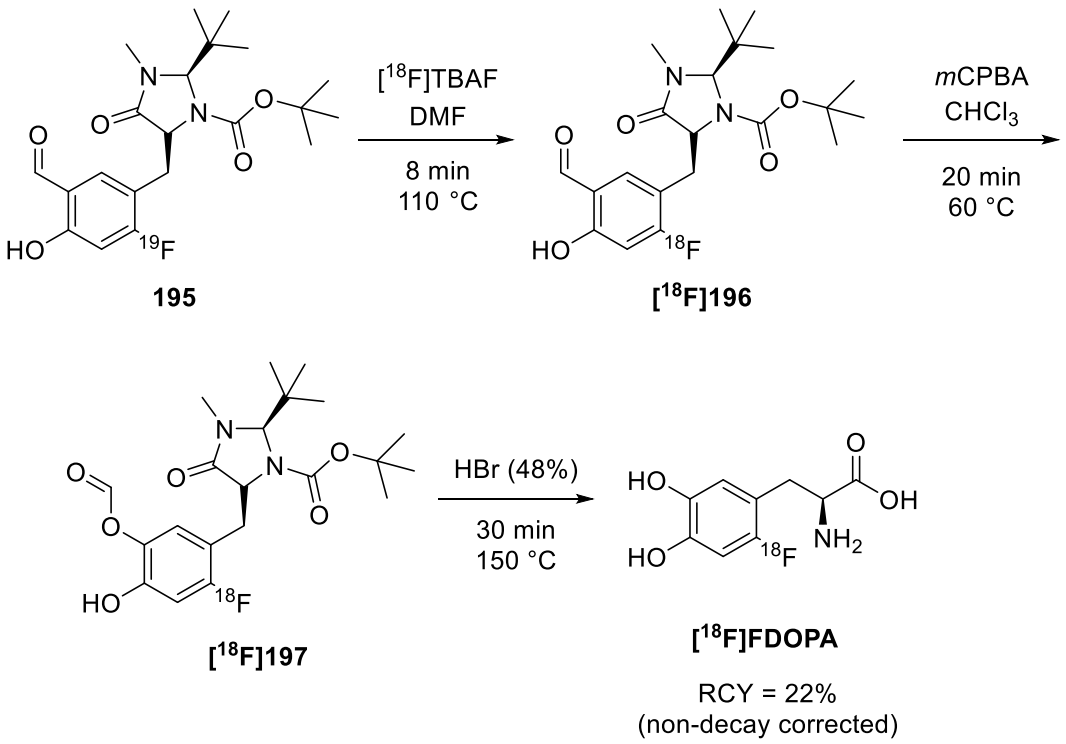

Scheme 85: Radiosynthesis of [^{18}F]FDOPA *via* isotopic exchange of 195 using nucleophilic [^{18}F]fluoride

A number of poorly effective attempts at producing [^{18}F]FDOPA from enantiomerically pure chiral precursors or chiral auxillaries have been attempted, however they are typically limited to very low RCY (5-10%) and hence have limited application.[383,384] More effectively, efforts have been taken to install fluorine-18 into simple, protected arenes bearing electron-withdrawing functionality *ortho*- to the fluorination site *via* S_NAr chemistry using [^{18}F]fluoride, hence needing multiple post-radiofluorination steps to convert the electron-withdrawing moiety into the required chiral DOPA side chain, usually by way of chiral phase transfer catalyst[385,386,387] or *via* an enzymatic route.[388] The later has been shown to provide access to [^{18}F]FDOPA from simple [^{18}F]fluoroarenes like **[^{18}F]201** in a single step, a conversion of particular significance to the work discussed in Chapters 2 and 3 (Scheme 86).[389] Despite the poor RCY achieved for this preparation, Kaneko *et al*. were able to achieve an exceptionally high SA of >200 GBq/μmol and presumably an enantiomeric excess of 100% given the enzymatic control of the reaction.[389]

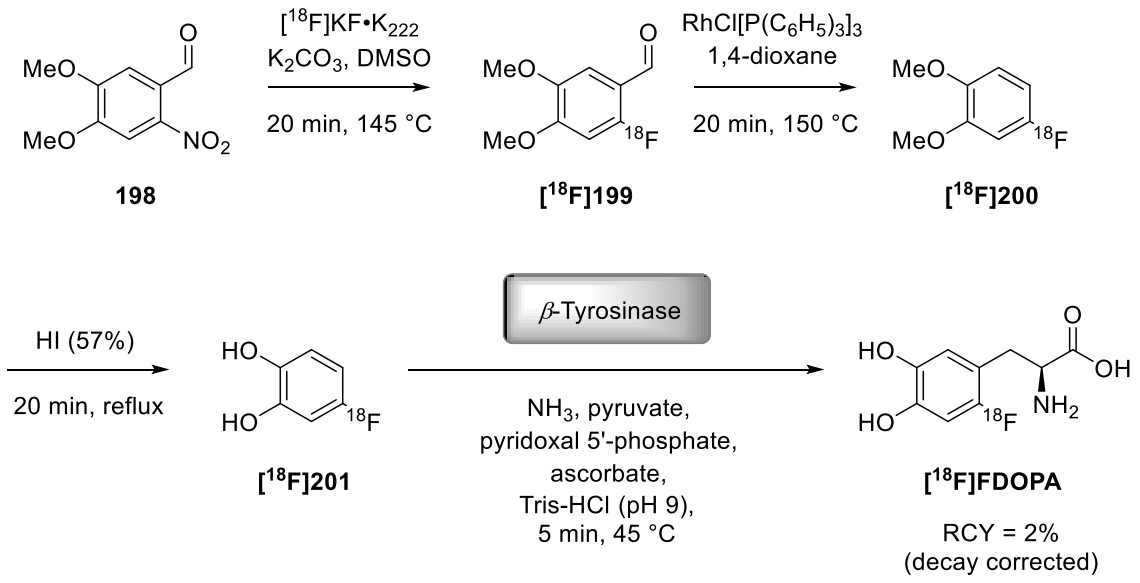

Scheme 86: Radiosynthesis of [^{18}F]FDOPA using enzymatic installation of the side functionality

Optimised asymmetric routes to [^{18}F]FDOPA have proven to be capable of affording excellent enantiomeric purity as well as drastically improved SA (>720 Gq/μmol) *versus* electrophilic routes, such as the recent work by Lemaire and co-workers (Scheme 87).[390] This elegant approach represents one of the currently the most refined routes to [^{18}F]FDOPA *via* automated radiosynthesis and with use of an optimised chiral phase-transfer catalyst, However, as seen previously the extended post-radiofluorination chemistry limits the product RCY. Other very similar automated production kits for [^{18}F]FDOPA have been developed by Trasis Pharmacy Instruments,[391] and Neptis.[392]

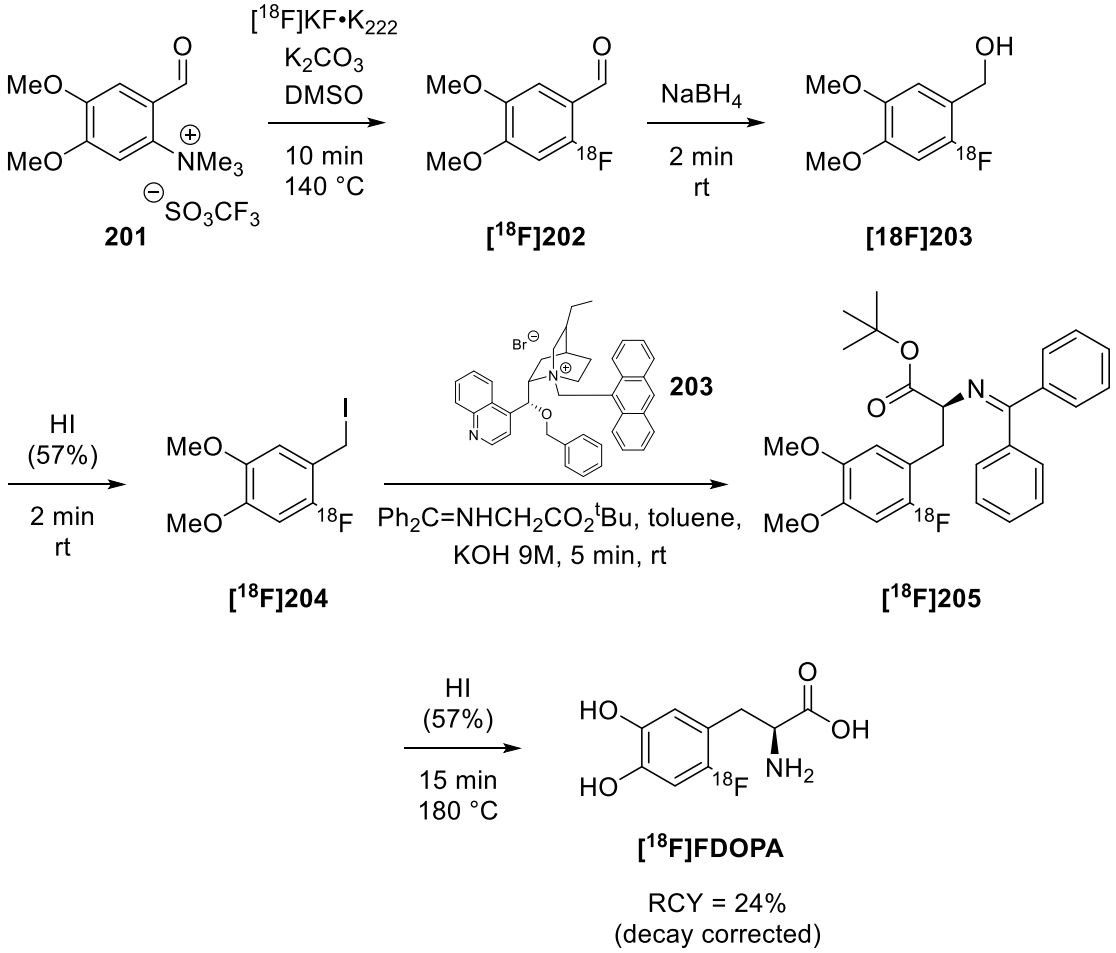

Scheme 87: Automated radiosynthesis of [^{18}F]FDOPA using a chiral phase-transfer catalyst 203

Recently, other more creative routes to [^{18}F]FDOPA have also been developed, for example, the work by Brady and co-workers[393] utilised solid-supported precursor **206** to improve the efficiency of the electrophilic radiofluorination discussed earlier, the procedure utilises a simultaneous [^{18}F]fluorination and cleavage mechanism to afford **[^{18}F]207** whilst retaining all toxic organostannane species on the resin (Scheme 88).[393]

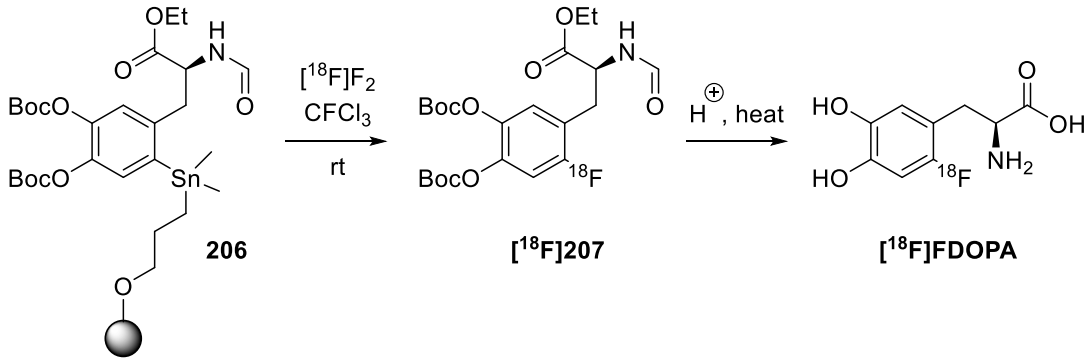

Scheme 88: Preparation of [^{18}F]FDOPA *via* a solid-supported precursor (RCY not provided)

As discussed in Section 1.6.2.4, metal mediated nucleophilic [^{18}F]fluorination routes can provide access to electron-rich [^{18}F]fluoroarenes which are otherwise unachievable by S_NAr chemistry, and methods involving copper catalysed [^{18}F]fluorination of pinacol-derived aryl boronic esters (Scheme 89),[394] as well as nickel-mediated oxidative [^{18}F]fluorination (Scheme 90)[176] have been utilised to prepare [^{18}F]FDOPA.

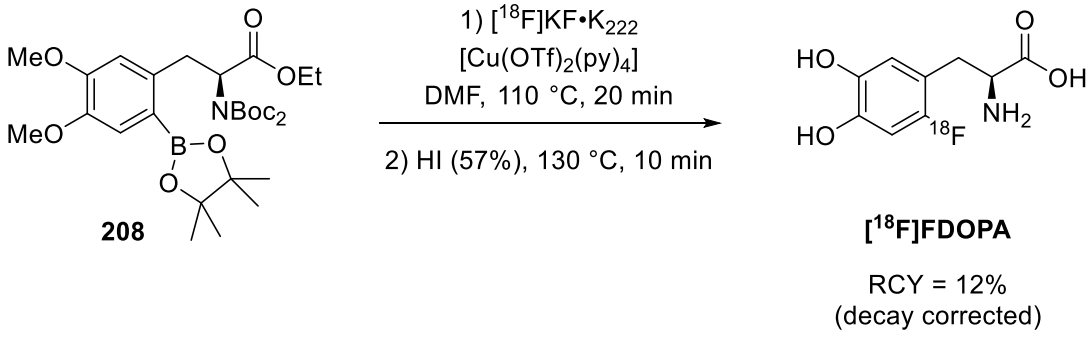

Scheme 89: Preparation of [^{18}F]FDOPA *via* copper-mediated nucleophilic [^{18}F]fluorination of a protected pinacol-derived boronic ester precursor

In this approach, Tredwell and co-workers implement successful enantioselective (ee > 99%) preparation of [^{18}F]FDOPA with a rapid two-step radiofluorination of simple to prepare precursor, using high SA [^{18}F]fluoride.[394] However, no RCY was reported for the production of [^{18}F]FDOPA and the use of a potentially toxic copper catalyst in the penultimate step of preparation potentially negates scope of the process in medical applications.

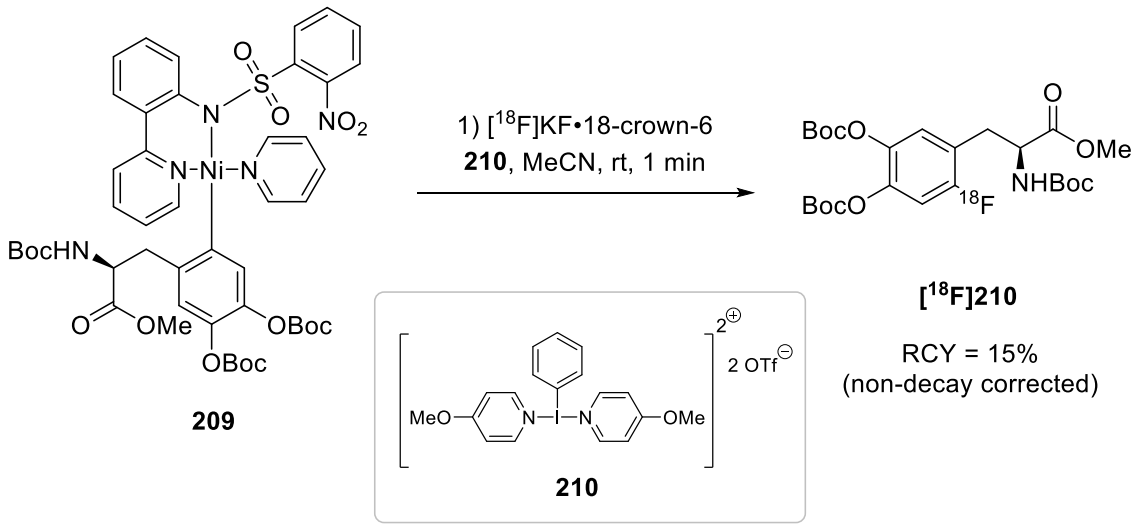

Scheme 90: Preparation of protected-[^{18}F]FDOPA *via* nickel-mediated oxidative [^{18}F]fluorination

The above method for [^{18}F]FDOPA, developed by the Ritter research group provides an interesting new approach to the preparation of the high value target, utilising aqueous [^{18}F]fluoride, *i.e.* removal of any lengthy drying time, as well as an intricate nickel based precursor and λ^3-iodane oxidant to afford ultrafast [^{18}F]fluorination.[176] Despite these benefits, their reported modest RCY omits the essential subsequent deprotection reaction to afford [^{18}F]FDOPA and hence the RCY is likely to suffer further. Other disadvantages include the extended organometallic synthesis required for the preparation of precursor **209**, that has yet to be repeated by another research entity, as well as the high likelihood of protolysis of the Ni-C bond, resulting in the formation of the protio-derivative of **210**, which may very difficult to separate from **[^{18}F]210**.

[^{18}F]Fluorination of a protected DOPA iodonium ylid precursor **213** has demonstrated potential as a high yielding route to the [^{18}F]fluoroarene. It has been shown that on reaction with [^{18}F]fluoride in a polar aprotic, the ylid directs [^{18}F]fluorination towards the aryl substituent (Scheme 91),[395] however again this method comes with a distinct limitation. Preparation of the precursor iodonium ylid requires the potentially challenging preparation of λ^3-iodane **212**, an oxidation that in practise can be difficult to conduct in the presence of multiple sensitive functionality as with **211**. As with the routes involving complex organometallic precursors described earlier,

reproducibility in the preparation of elaborate aryliodonium ylid precursors like **213** may also prove to become a challenge in practice.

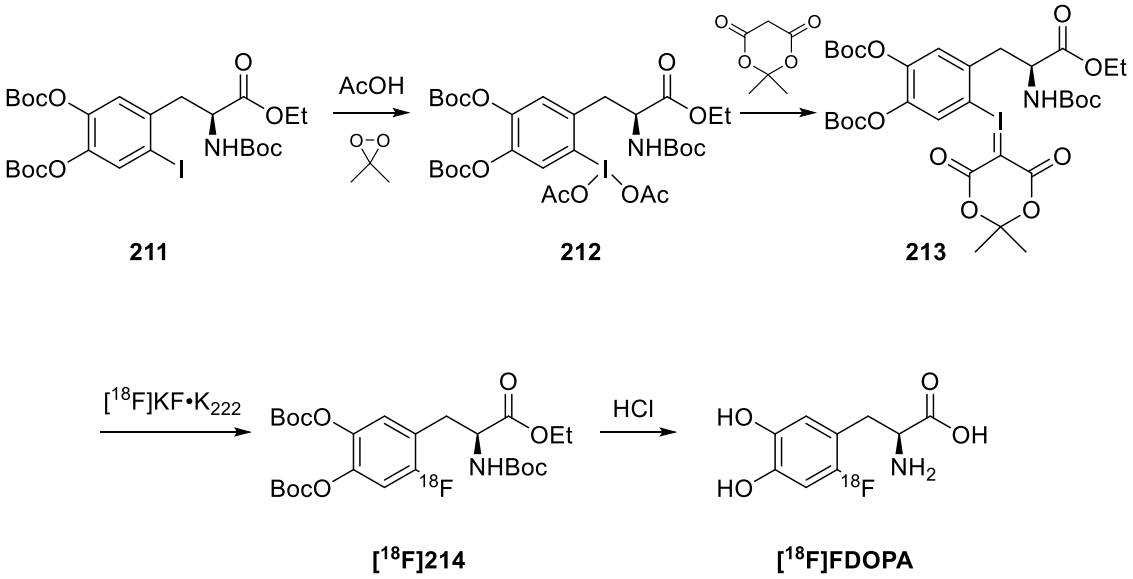

Scheme 91: Preparation of [^{18}F]FDOPA *via* an iodonium ylid precursor (RCY not provided)

Scott and co-workers have also developed an interesting diaryliodonium salt precursor based strategy that utilises a mesityl n.p.r. in the presence of a copper catalyst which results in inversion of the usual [^{18}F]fluorination regiochemistry.[396] Unlike typical [^{18}F]fluorinations of diaryliodonium salts bearing sterically hindered aromatic components, the addition of a copper catalyst not only reduced the required reaction temperature but also inverted the radiofluorination selectivity, yielding preferred [^{18}F]fluorination of the arene bearing less *ortho*- bulk. The group applied this approach to a wide range of electron-poor and electron-rich targets, including a protected [^{18}F]FDOPA substrate (Scheme 92), however, as with the related strategies described earlier, widespread adoption of this approach may still be hindered by the challenge of preparing electron-rich diaryliodonium salt precursors.

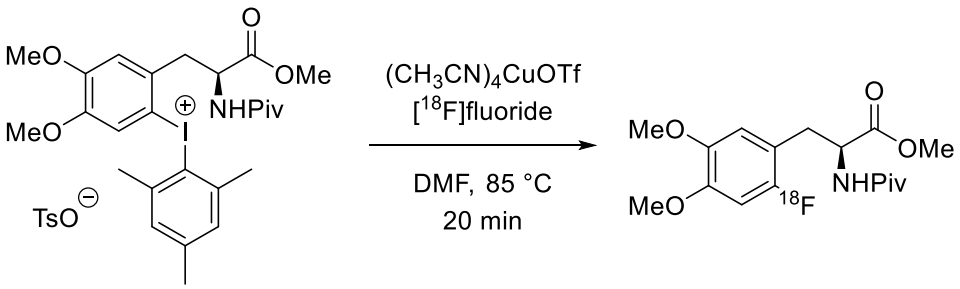

215 **[^{18}F]216**

RCY = 17%
(non-decay corrected)

Scheme 92: Preparation of a protected [^{18}]FDOPA species *via* copper-catalysed [^{18}F]fluorination of a (mesityl)(aryl)iodonium salt precursor

5.3 [^{18}F]FDOPA Diaryliodonium Salt Precursor Strategy

The former section provides a short review of the existing strategies for the radiosynthesis of [^{18}F]FDOPA, as well as the concerns that limit the application of each method for use in routine clinical production. This section describes efforts in designing a diaryliodonium salt precursor suitable for late-stage radiofluorination using n.c.a. [^{18}F]fluoride to afford [^{18}F]FDOPA in high RCYs and high SA, *via* a clinically viable format.

Prior chapters have demonstrated how the diaryliodonium salt approach ensures complete regioselectivity on [$^{18/19}$F]fluorination, an essential criterion for the preparation of [^{18}F]FDOPA, as *in vivo* studies has shown that alternative regioisomers of 6-[^{18}F]FDOPA exhibit accelerated *O*-methylation and hence installation of fluorine-18 into the 6-position of [^{18}F]FDOPA to ensure prolonged *in vivo* stability is absolutely crucial.[397] Similarly, enantiomeric purity is also essential and hence chirality should be incorporated into the molecule well before radiofluorination. The ideal [^{18}F]FDOPA diaryliodonium salt precursor should also allow for rapid, global deprotection, without requiring any further transformations to reach the target radiotracer (Scheme 93).

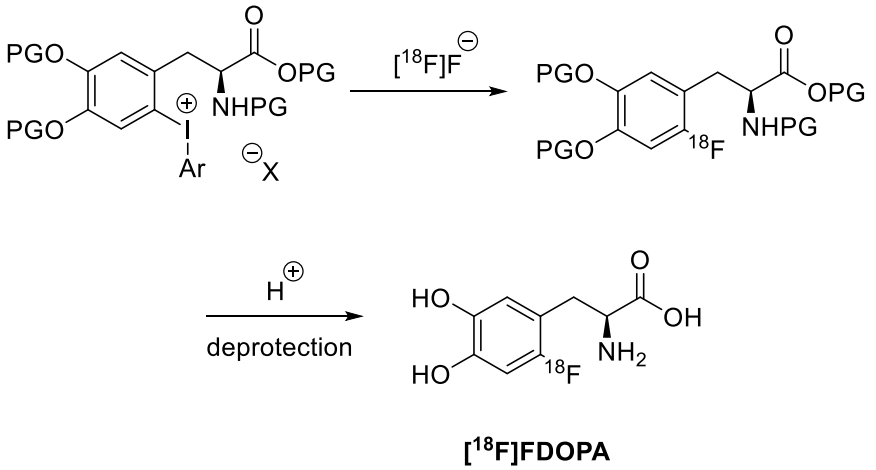

[^{18}F]FDOPA

Scheme 93: Planned radiosynthesis of [^{18}F]FDOPA *via* a diaryliodonium salt and global deprotection strategy

This planned approach should be generate a number of key benefits: a high RCY as a result of late-stage radiofluorination; high SA attributed to the use of n.c.a [^{18}F]fluoride; and the sole post-radiofluorination step should afford high product purity, high radiochemical purity and simpler purification. This route also avoids use of any toxic organometallic precursors or catalysts within the radiosynthesis, aiding the likelihood of clinical approval. In addition, this two-step approach (radiofluorination followed by acid hydrolysis deprotection) mimics the radiosynthesis of the most commonly prepared PET tracer in use, [^{18}F]FDG (Scheme 94).

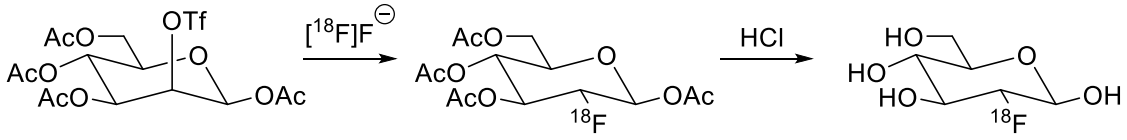

217 **[^{18}F]218** **[^{18}F]FDG**

Scheme 94: Typical radiosynthesis of [^{18}F]FDG, involving two step (radiofluorination and acid hydrolysis deprotection) approach

As mentioned before, adapting to suit current trends in clinical radiopharmaceutical production appears to the best manner for improving the success of a radiotracer production method, hence why developing a protocol for [^{18}F]FDOPA radiosynthesis that is similar to current protocols used to prepare the world's leading PET radiotracer is a wise strategy.

As part of this rationale, a collaborative project was initiated with Advanced Biomarker Technologies (ABT) (the manufacturers of the compact cyclotron used for [^{18}F]fluoride production discussed in Chapter 3) to develop a means to produce an operator-friendly route to [^{18}F]FDOPA, based around the synthesis cassette approach. It was noted that whilst synthesis cassettes are currently available for [^{18}F]FDG, [^{18}F]NaF for bone/skeletal imaging, [^{18}F]FMISO for imaging hypoxic cells and proliferation tracer [^{18}F]FLT,[398] but not for [^{18}F]FDOPA, representing a clear avenue for commercial viability. Such synthesis cassettes are usually intended for use with specific synthesis platforms, like the GE FASTlab Multi-Tracer Platform mentioned in Chapter 4, or the ABT Chemistry Production Module (CPM) (Figure 69).

Figure 69: The ABT Chemistry Production Module (CPM), a self-shielded radiosynthesis platform developed for cassette-based radiotracer production[399]

Conceptualisation of a [^{18}F]FDOPA dose synthesis card (DSC), compatible with the above system, involved translating the knowledge and understanding on diaryliodonium salt [^{18}F]fluorination chemistry developed in the prior chapters into a format suitable to this application. Reagents to be used within the cassette are purchased as miniature GMP-grade samples which can be stored within the synthesis platform, whereas diaryliodonium salt precursors will require freezer storage to ensure long-life. In this chapter efforts were made to yield a diaryliodonium salt precursor to [^{18}F]FDOPA that exhibits some bench-stability. Chapter 4 has already validated that batch-based radiosynthesis with diaryliodonium salts precursors is certainly viable, hence that being a simpler and cheaper approach than microfluidics

will be utilised here, but future iterations of a [^{18}F]FDOPA DSC could include a microfluidic reaction coil or chip.

Minimising the complexity of components within the DSC is also imperative for ensuring the device is as small, as cheap and as robust as possible, so to facilitate this fluidic control will be dictated entirely the CPM, by fitting the back of the DSC with nitrogen/vacuum ports for fluid manipulation (Figure 70, A). Of course to guarantee that the device remains sterile during transport, these ports, as well as the [^{18}F]fluoride entry port must remained sealed, until the DSC is inserted into the CPM, by way of one-way flow valves. On-device purification (Figure 70, B) and formulation (Figure 70, C) is also essential to maintain a rapid, stream-lined process, thus the inclusion of silica (or other sorbent material) SPE cartridges are also required, there is also potential to lyophilise the required reagents within the appropriate channels (Figure 70, D) to again benefit the speed and smoothness of radiotracer production.

For the radiosynthesis itself, the reaction vessel (if to be conducted as a one-pot preparation, otherwise two separate reaction vessels will be necessary) will need to protrude from the bottom of the DSC (Figure 70, E), so that it fits within a CPM miniature heating mantle. Finally, extraction of the purified and formulated [^{18}F]FDOPA product directly into a sterile Luer-Lok syringe (Figure 70, F) will allow easy administration of the product to the multiple QC analyses that are required and ultimately delivery of the tracer to the patient.

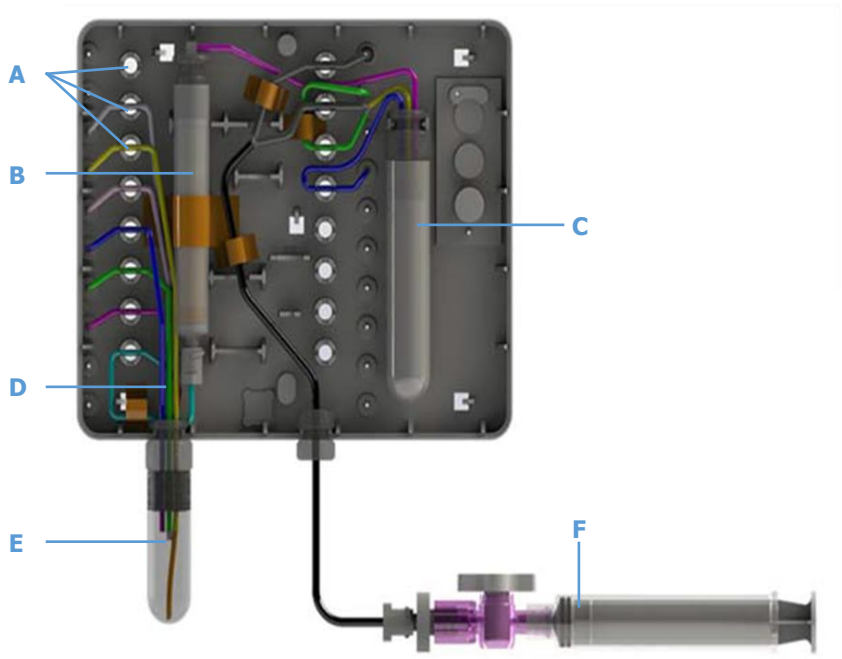

Figure 70: Concept design for a [^{18}F]FDOPA production cassette using a diaryliodonium salt precursor to provide late-stage radiofluorination as part of a two-step, one-pot protocol. A = nitrogen/vacuum ports, B = SPE cartridge for product purification, C = formulation SPE cartridge, D = potentially reagents, including diaryliodonium salt precursor could be lyophilised within the device channels, E = reaction vessel, F = product extraction into sterile Luer-Lok syringe

Synthesis cassettes like the [^{18}F]FDOPA DSC design above are intended for single dose-single patient application, and hence are produced as sealed, sterile devices, negating the need for an expensive and difficult to maintain grade A clean room; instead a lower grade clean room can be utilised (as per EU GMP classifications).[400] One of the major benefits provided by single-dose single-patient radiosynthesis is that micro-scaling of the cassette allows easy and safe disposal of the cartridge once radiotracer production is compete, as well as eliminating the risk of reagent cross-contamination.

5.4 Initial Challenges in [^{18}F]FDOPA Diaryliodonium Salt Development

It was initially conceived that diaryliodonium salt precursors to [^{18}F]FDOPA could be prepared as per the protocol utilised in Chapter 4, whereby a protected electron-rich arene could be reacted with an activated aryliodobis(acetate) to prepare the target diaryliodonium salt, without the need for activating groups, such trialkylstannane or

boronic acid functionality. Given that L-DOPA is commonly prescribed for the treatment of Parkinson's Disease, the compound is commercially available with at high enantiomeric purity (> 98%, Sigma Aldrich), making it a logical starting material for the preparation of the following protected derivatives.

Protecting groups were selected based on their ease of deprotection and the toxicity of their by-products on deprotection, as well as expected simplicity of removing these by-products from the product FDOPA. The Boc protecting group is commonly utilised for protection of the amine and catechol functionality of the molecule because of the scope for rapid deprotection using hydrochloric acid (6M), as seen with previous electrophilic and nucleophilic routes to [^{18}F]FDOPA.[393,395] Whereas the more robust protecting groups, such as the methyl or benzyl functionalities are commonly cleaved with hydrogen bromide (58%) or hydrogen iodide (57%) in a short amount of time.[378,381]

Preparation of initial protected DOPA derivatives commenced with protection of the carboxylic acid functionality by treatment with thionyl chloride in methanol or ethanol to afford the corresponding DOPA methyl/ethyl ester, followed by protection of the amine functionality *via* Boc or trityl protecting groups with Boc anhydride or trityl chloride respectively, utilising trimethylamine to deprotonate the amine in both cases. Finally the catechol functionality was protected either by benzylation with benzyl bromide and potassium carbonate, or *via* Boc protection again utilising trimethylamine, Boc anhydride with prolonged heating to afford protected DOPA derivatives **219**—**224** (Figure 71).

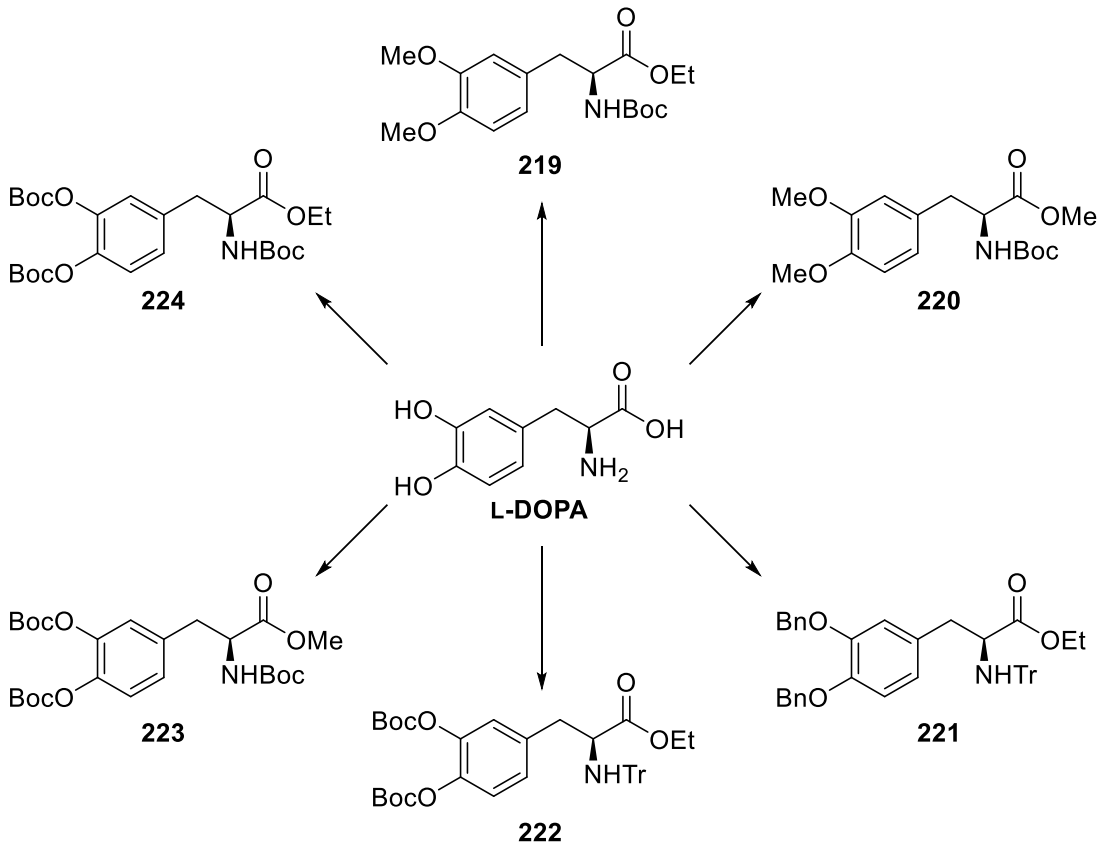

Figure 71: Conversion of commercially available L-DOPA into six protected DOPA derivatives, prepared by the author and/or prepared within the research group.

The substrates **219**—**224** were then utilised in a series of pilot experiments (0.25 mmol), with the intention of validating their application for the preparation of a DOPA diaryliodonium salt precursor. Here three aryliodobis(acetate)s were selected for the scoping study based on their varying electron-density, phenyliodo bis(acetate) **132**, 2-thienyliodo bis(acetate) **133** and 4-anisyliodo bis(acetate) **134**, prepared as described in Section 2.5. Activation of aryliodobis(acetate) reagents was realised using trifluoroacetic acid as per standard method (Section 2.7) as well as trifluoromethanesulfonic (triflic) acid to provide more forcing conditions through formation of a potentially more activated λ^3-iodane species (Scheme 95).

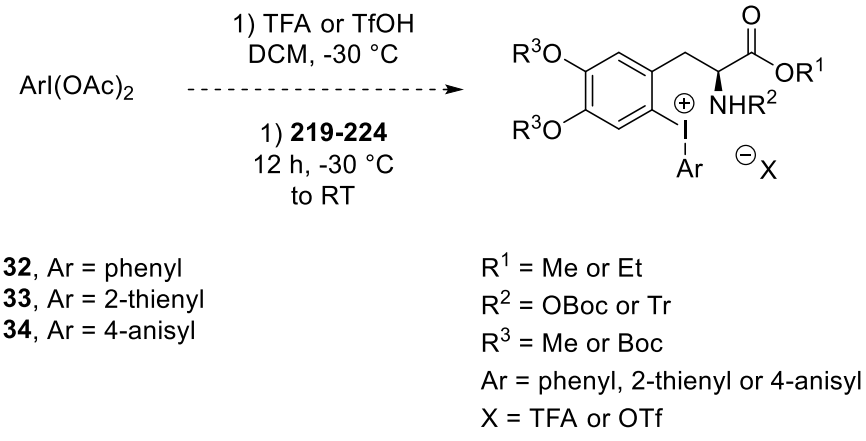

Scheme 95: Pilot reactions to scope potential of [^{18}F]FDOPA diaryliodonium salt formation under the selected conditions

Across this scoping study reactions were monitored by TLC and ^{1}H-NMR of the crude reaction mixture, where diaryliodonium salt formation was apparent (evident by the formation of ^{1}H-NMR aromatic peaks exceeding 8.0 ppm) product extraction was attempted as per the standard method (Section 2.7), by recrystallisation from DCM/diethyl ether/petrol or *via* column chromatography on SiO_2 with 4% methanol in petrol.

		Protected DOPA Derivative					
ArI(OAc)$_2$	**Acid**	**219**	**220**	**221**	**222**	**223**	**224**
Phenyl (132)	TFA	**Ar2I$^+$X$^-$ 132**	**132**	**132**	**132**	**132**	**Ar2I$^+$X$^-$**
Phenyl (132)	TfOH	-	**132**	**132**	-	-	-
2-thienyl (133)	TFA	**Ar2I$^+$X$^-$**	**Ar2I$^+$X$^-$**	-	-	-	**Ar2I$^+$X$^-$ 133**
2-thienyl (133)	TfOH	-	-	-	-	-	-
4-anisyl (134)	TFA	**Ar2I$^+$X$^-$ 134**	**Ar2I$^+$X$^-$ 134**	-	-	**Ar2I$^+$X$^-$ 134**	**Ar2I$^+$X$^-$ 134**
4-anisyl (134)	TfOH	**134**	-	-	-	-	-

Table 15: Pilot experiments for the formation of [^{18}F]FDOPA diaryliodonium salt precursors. Ar2I$^+$X$^-$ indicates observation of an apparent diaryliodonium salt species in the reaction mixture as monitored by ^{1}H-NMR, compound numbers indicates observation of the aryliodobis(acetate) starting material and - signifies the observation of a crude mixture of products

The pilot study highlighted the unsuitability of employing triflic acid for activation of the aryliodobis(acetate) precursors, presumably formation of the corresponding aryliodo bis(trfliate)s does occur but the resulting diaryliodonium triflate decomposes after formation. Another apparent trend seen is that the trityl protection strategy fails to endure the reaction conditions, since no product diaryliodonium was observed for the reactions of **221** and **222**, an unsurprising observation given the acid sensitivity of the trityl functionality.

Electron-rich protected DOPA derivatives **219**, **220**, **223** and **224** all appeared to afford, albeit very small, amounts of a diaryliodonium salt species, as detected by the formation of ^{1}H-NMR peaks clearly above 8.0 ppm, however no distinct preferences for n.p.r. was seen across the pilot study.

Reactions that appeared to yield some diaryliodonium salt product were then completed on a larger scale (≥5 mmol), however, all attempts to isolate a product diaryliodonium salt *via* this method of preparation failed to yield any of the desired product and on some occasions the protected DOPA arene starting material could be recovered. This outcome was possibly as a result of product instability and/or because the quantity of product formed was miniscule, making extraction of that material from a crude variety of compounds very challenging. It was considered that progression from the 6-fluoro-*m*-tyramine diaryliodonium salt to FDOPA diaryliodonium salt target was perhaps too large a step to take immediately, so development of an intermediate target, a diaryliodonium salt precursor for 6-[^{18}F]fluorodopamine was undertaken.

5.5 Diaryliodonium Salt Precursor to 6-[^{18}F]Fluorodopamine

Preparation of a diaryliodonium salt precursor to 6-[^{18}F]fluorodopamine not only provides a stepping stone to the high demand [^{18}F]FDOPA diaryliodonium salt target, but [^{18}F]fluoroarene is also a highly desirable PET tracer in itself, and currently the same issues involved with [^{18}F]FDOPA production exist for 6-[^{18}F]fluorodopamine. 6-[^{18}F]Fluorodopamine has previously been used for a number of *in vivo* PET imaging studies including imaging of cardiac sympathetic innervation,[401] scanning for localisation of pheochromocytoma,[402] and imaging brown adipose tissue (brown fat),

another hallmark of pheochromocytoma (Figure 72);[403] however, many potential applications of the radiotracer are limited by its inability to cross the blood-brain-barrier, hence the need for [^{18}F]FDOPA.

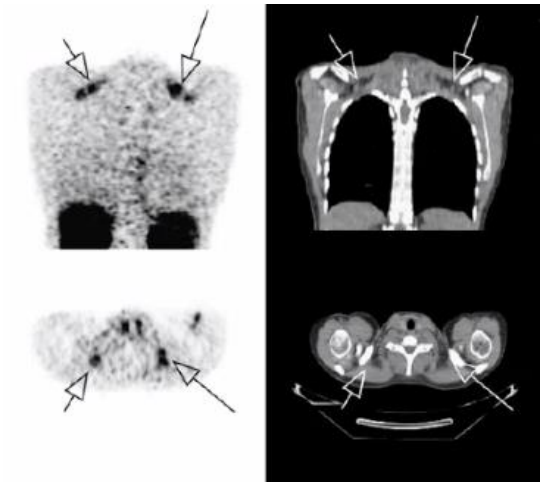

Figure 72: PET image of patient with pheochromocytoma exhibiting uptake of 6-[^{18}F]fluorodopamine uptake in the superclavicular brown fat (left) and the corresponding CT image (right)

Preparation of the 6-[^{18}F]fluoro-*m*-tyramine diaryliodonium salt precursor **181** was achieved through the reaction defined by Scheme 96 (in a yield of 20%), thus it was presumed that the 6-[^{18}F]fluorodopamine could be prepared by the same route (Scheme 97), given that the sole difference between electron-rich arenes **179** and **225** was an additional methoxy group, *meta* to the iodination position.

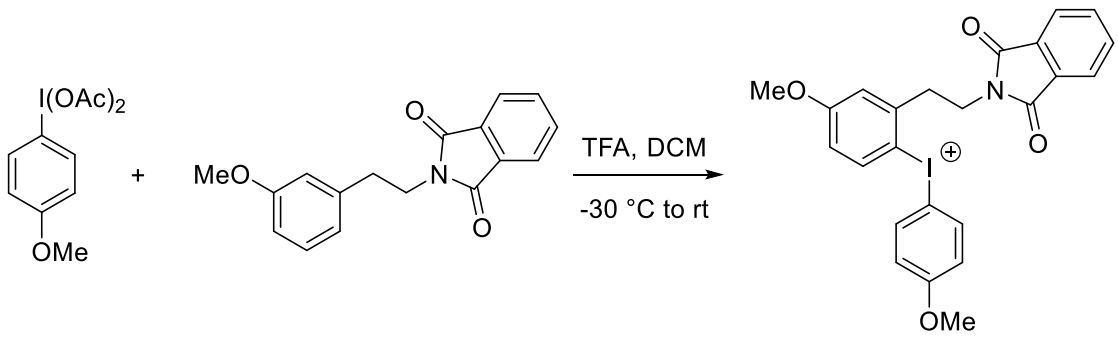

134 **179** **181**

Scheme 96: Preparation of 6-[^{18}F]fluoro-*m*-tyramine diaryliodonium salt precursor 181 through the reaction of 134 and 179, facilitated by a ligand exchange of aryliodobis(acetate)

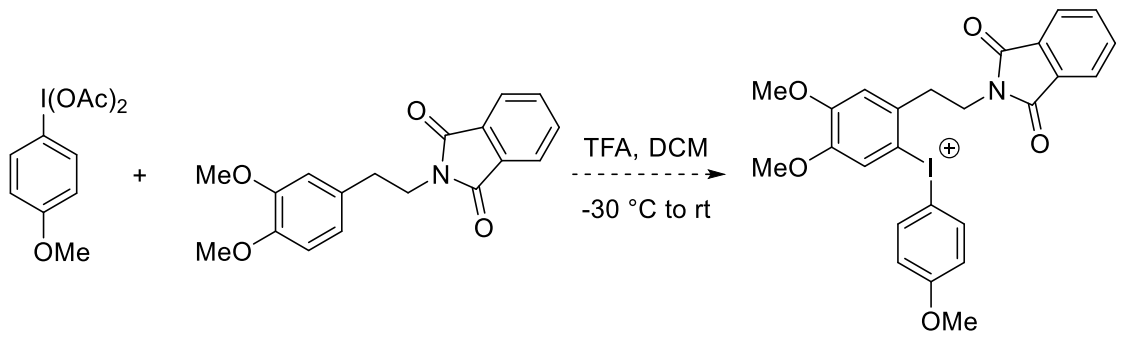

134 **225** **226**

Scheme 97: Attempted preparation of 6-[^{18}F]fluorodopamine diaryliodonium salt precursor 226 through the reaction of 134 and 224, facilitated by a ligand exchange of aryliodobis(acetate). Protected dopamine derivative 225 was prepared by the same means as 179

Despite multiple attempts at preparing diaryliodonium salt **226** *via* this route (Scheme 97), no product was obtained, and hence installation of a halogen in the 6-position was required in order to convert electron-rich arene **224** into the corresponding arylstannane compound. Here iodine was installed *via* a very convenient method that utilises silica powder, iron (III) nitrate nonahydrate and iodine to afford iodination in good yields,[404] and the subsequent stannylation was best achieved through palladium catalysed means (Scheme 98). Note that this iodination method was also utilised to afford clean iodination of 2,4,6-trimthylbenzene and of benzylphenyl ether to yield iodinated products **138** and **242**, which were utilised in Chapter 2.

Then the target 6-[^{18}F]fluorodopamine diaryliodonium salt **226** was successfully afforded by reaction of arylstannane **228** and aryliodobis(acetate) **134** (Scheme 99) as per the method discussed in Section 2.7.

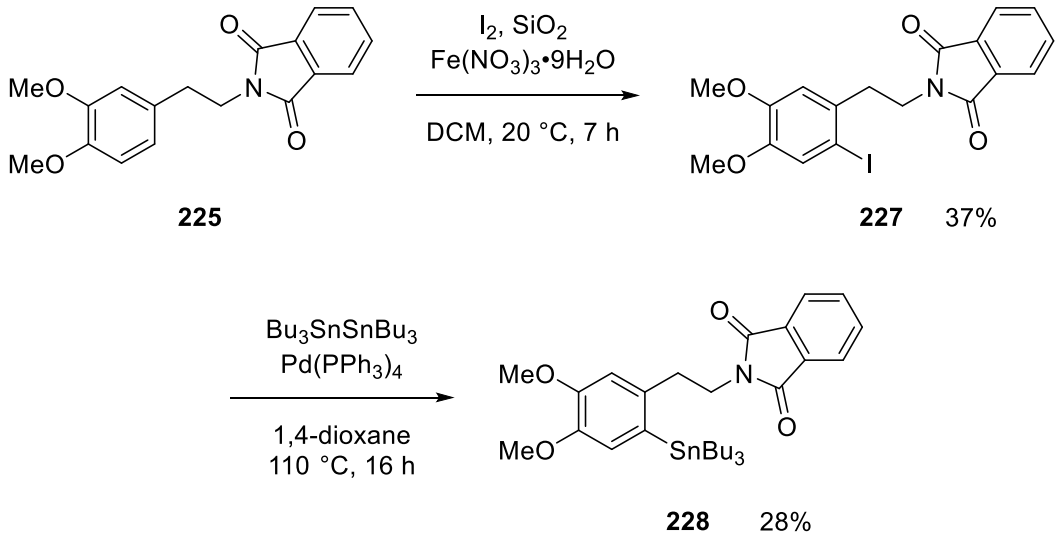

Scheme 98: Preparation of arylstannane 228 *via* iodination of electron-rich arene 225 and palladium catalysed stannylation of the resulting iodoarene 227

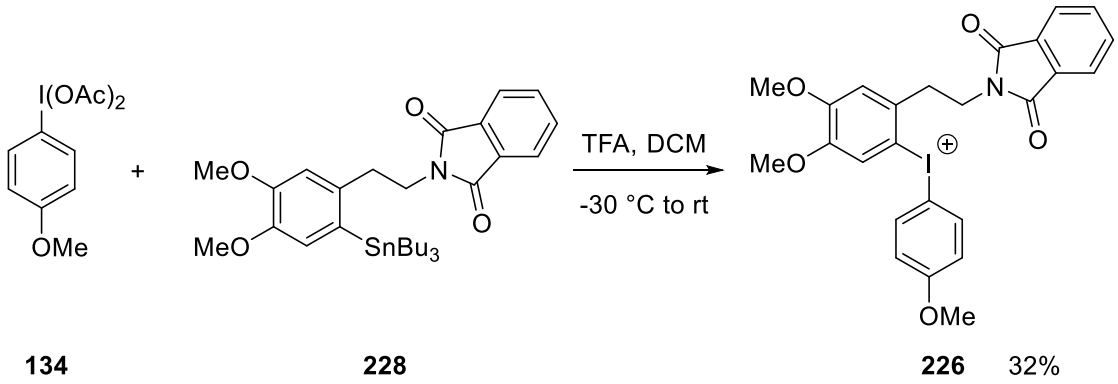

Scheme 99: Preparation of 6-[^{18}F]fluorodopamine diaryliodonium salt precursor 226 by reaction of arylstannane 228 and aryliodobis(acetate) 134

The ^{1}H-NMR spectrum for diaryliodonium salt **226** (Figure 73) highlighted an interesting observation, the proton environment *ortho*- to the diaryliodonium salt *ipso*-carbon, whilst were still notably more downfield than the corresponding iodoarene (**227**) did not exhibit the expected downfield shift of over 8.0 ppm, normally representative of diaryliodonium salt formation. Other supporting data (^{13}C-NMR, HR-MS and elemental analysis) was in agreement of the expected characterisation for diaryliodonium salt **226**. This disagreement with traditional interpretations is most likely an artefact of the increased electron-density of the diaryliodonium salt centre by the increased electron-rich nature of the target arene substituent.

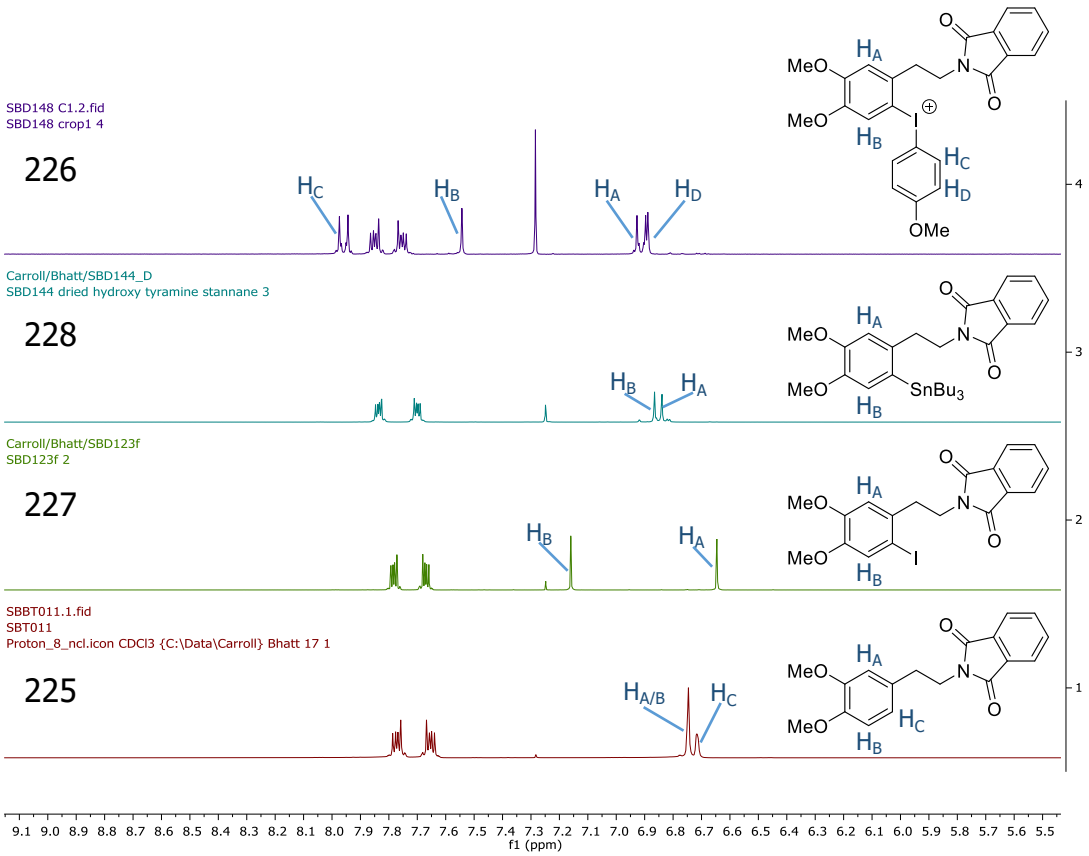

Figure 73: ^{1}H-NMR of aromatic protons for the conversion of protected dopamine 225 up to 6-[^{18}F]fluorodopamine diaryliodonium salt 226, validating the successful preparation of the target λ^{3}-iodane

Successful preparation of 6-[^{18}F]fluorodopamine diaryliodonium salt precursor **226** *via* this method demonstrates that preparation of diaryliodonium salts bearing multiple electron-rich substituents is best achieved by the above method (Scheme 99), whereby attack on the electrophilic diaryliodonium salt centre is directed by the arylstannane functionality of the electron-rich arene substrate. Hence to reach a diaryliodonium salt precursor to [^{18}F]FDOPA a route involving arylstannane preparation will be required.

5.6 Redesign of the [^{18}F]FDOPA Diaryliodonium Salt

It was planned that late-stage incorporation of iodine could be achieved using the protected DOPA arenes **219**—**224** prepared in Section 5.4, however despite trialling a variety of iodination procedures[404,405,406] **229** could not be obtained.

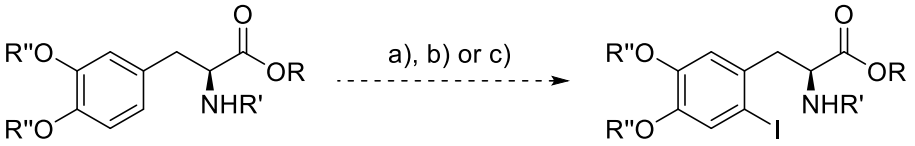

219-224 **229**

R = Me or Et
R' = OBoc or Tr
R" = Me or Boc
Ar = phenyl, 2-thienyl or 4-anisyl
X = TFA or OTf

a) I_2, SiO2, $Fe(NO_3)_3 \cdot 9H_2O$, DCM, rt, 2-16 h
b) I_2, $AgCO_2F_3$, $CHCl_3$, rt, 14 h
c) I_2, phenyliodo bis(trifluoroacetate), DCM,.rt, 16 h

It was decided that early halogenation of L-DOPA would provide a better route to substrates like **230**, and preparation of a bromo-arene would be preferred over the corresponding iodo-arene, given the difference in their relative Ar-X bond dissociation energies (346 and 240 kJ/mol respectively),[407] bromoarenes should provide more stable precursors; a valuable characteristic given that further steps were required before stannylation could be conducted.

In addition, initial work on the stannylation of electron-rich aryl halides (as discussed in Section 2.6) described how preparation of arylstannane reagents from bromoarenes rather than iodoarenes reduced the risk of homo-coupling and generally afforded superior yields. Hence, the new strategy for [^{18}F]FDOPA precursor development was conducted as follows (Scheme 100), *via* direct bromination of L-DOPA with bromine in acetic acid, followed immediately by conversion to the corresponding methyl ester **230** by treatment with thionyl chloride in methanol.[408]

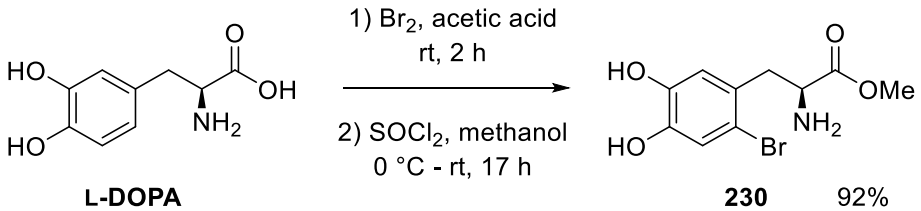

L-DOPA **230** 92%

Scheme 100: preparation of bromo-DOPA methyl ester 230 from L-DOPA

Further protection of the L-DOPA derivative was achieved through sequential Boc protection, as **230** was treated with trimethylamine and Boc anhydride in degassed methanol at room temperature for 15 h.[408] Validation of successful Boc protection of the amine group was then conducted on the intermediate before Boc protection of the catechol functionality, again using trimethylamine and Boc anhydride but with heating at 80 °C in anhydrous toluene for 7 h,[176] to afford protection DOPA derivative **231**. Simultaneous Boc protection of both the amine and catechol functionalities was attempted, but afforded a poorer yield, hence a step-wise protection method was preferred (Scheme 101).

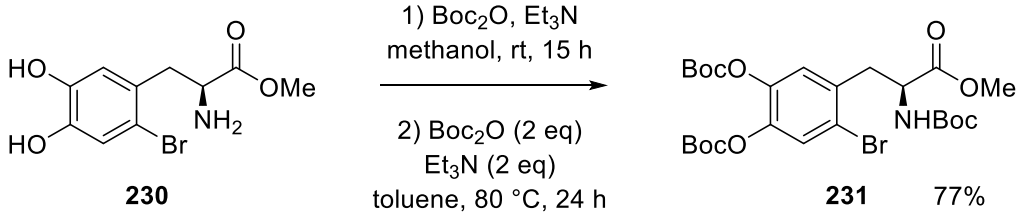

230 **231** 77%

Scheme 101: Sequential Boc protection of aryl bromide 230 to afford protected aryl bromide 231

In a bid to optimise conversion of protected DOPA bromide **231** to an arylstannane species (Scheme 102), a number of reaction conditions and catalyst systems were screened (Table 16). Preparation of the preferred tributylstannyl derivative **232**, could not be achieved in synthetically useful yields, and hence the more reactive but toxic trimethylstannyl derivative **233** was utilised as the arylstannyl substrate of choice for [^{18}F]FDOPA diaryliodonium salt preparation.

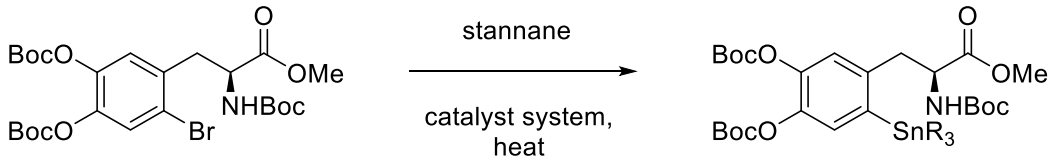

231

232, R = Bu
233, R = Me

Scheme 102: preparation arylstannanes 232 and 233 through catalysed stannylation of 231

Entry	Catalyst system	Stannane	Reaction conditions	Yield
1	Zn, $CoBr_2$, allyl chloride	Bu_3SnCl	MeCN, 50 °C, 8 h	0%[1]
2	$PdCl_2(PPh_3)_2$ (10 mol%)	$Bu_3SnSnBu_3$	1,4-Dioxane, 100 °C, 16 h	0%[2]
3	$Pd(PPh_3)_4$ (10 mol%)	$Bu_3SnSnBu_3$	1,4-Dioxane, 100 °C, 16 h	0%[2]
4	$Pd(PPh_3)_4$ (20 mol%)	$Bu_3SnSnBu_3$	1,4-Dioxane, 100 °C, LiCl, 16 h	6%
5	$(\eta^3\text{- } C_3H_5)_2Pd_2Cl_2$ (20 mol%)	$Bu_3SnSnBu_3$	1,4-Dioxane, 100 °C, LiCl, 16 h	3%
6	$Pd(PPh_3)_4$ (20 mol%)	$Me_3SnSnMe_3$	1,4-Dioxane, 100 °C, LiCl, 16 h	15%
7	$(\eta^3\text{- } C_3H_5)_2Pd_2Cl_2$ (20 mol%)	$Me_3SnSnMe_3$	1,4-Dioxane, 100 °C, LiCl, 16 h	34%

Table 16: Optimisation of reaction conditions, catalyst type and catalyst loading for the preparation of protected DOPA arylstannanes 232 and 233. [1]decomposition of starting material, [2]starting material recovered

Although optimisation of arylstannane preparations failed to achieve a high yielding process, literature examples also see yields limits to <40% for the preparation of very similar protected DOPA arylstannanes. Despite the inefficiency of the catalytic conversion, apparent by the very high catalyst loading required for successful formation of **232**/**233**, sufficient material was available for attempted preparation of [^{18}F]FDOPA diaryliodonium salt **234**. However, despite use of the more reactive trimethylstannyl derivative **233**, observation of the iconic doublet peaks corresponding to the protons *ortho* to the diaryliodonium salt centre (7.9 ppm) in the ^{1}H-NMR of the crude reaction mixture and multiple attempts at the preparation of **234**, no pure product could be isolated by this method (Scheme 103), although 5-10% of the diaryliodonium salt was visible in the ^{1}H-NMR of the reaction mixture.

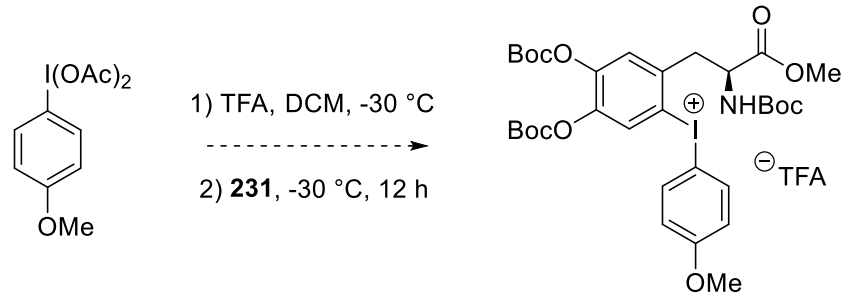

134 **234**

Scheme 103: Attempted preparation of [^{18}F]FDOPA diaryliodonium salt 234

Here, preparation of a diaryliodonium trifluoroacetate designed to yield [^{18}F]FDOPA was not afforded with the protection strategies described above, although further study into this work as well further protecting group screening was required to develop a better understanding of this challenge.

Shortly after conducting the experiments described above, Wirth and co-workers published a similar route to diaryliodonium salts for the production of [^{18}F]FDOPA, however they prepared the their diaryliodonium salts with tosylate counter-ion, before performing a counter-ion exchange conversion to afford diaryliodonium bromides.[409] However, when reacted with tetramethylammonium fluoride as part of a 'cold' [^{19}F]fluorination study, these precursors afforded very poor chemical yields; similarly, when Wirth *et al*. conducted [^{18}F]fluorination on leading precursor **235** using a batch-based synthesis platform, they afforded a RCY of <1%, indicating a concern in their diaryliodonium salt strategy, potentially as a result of the use of a more nucleophilic counter-ion.

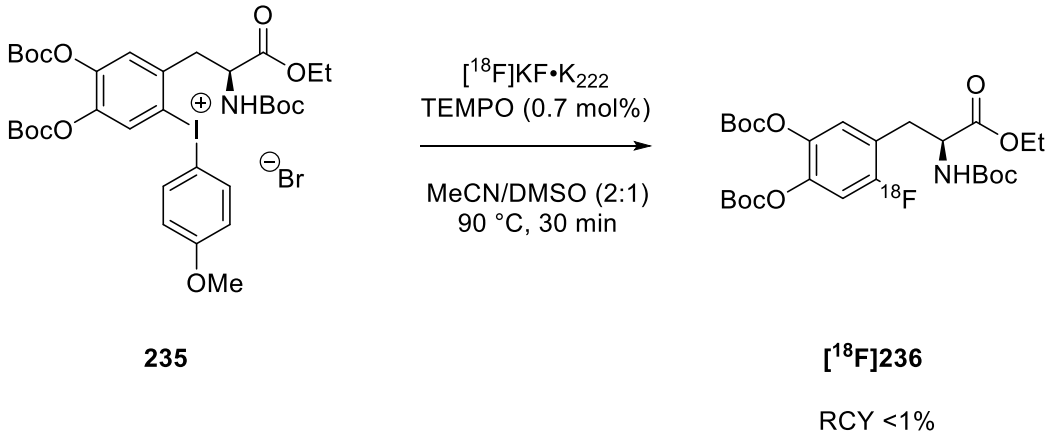

235 **[^{18}F]236**

RCY <1%

Scheme 104: Preparation of protected [^{18}F]FDOPA 234 by [^{18}F]fluorination of diaryliodonium salt 233, usiing an automated Eckert & Zeigler batch radiosynthesis system.

This result does, at least, provide proof of principle in the diaryliodonium salt approach to [^{18}F]FDOPA production, however, it is clear that much refinement in the choice of counter-ion, [^{18}F]fluorination conditions and, most crucially, the choice of protecting groups is required if a robust strategy for [^{18}F]FDOPA is to be realised. Drawing from conclusions provided by Chapters 2 and 3, radiofluorination of **235** may well have benefitted from [^{18}F]fluorination utilising a microfluidic platform, such as our bespoke set-up described in Chapter 3 and given that it was observed that prolonged heating of diaryliodonium salts leads to precursor decomposition, and that [^{18}F]fluorination conducted by rapid heating to 190° greatly improves the radiolabelling process, given that the above reaction was only conducted at 90 °C.

Also included in the aforementioned publication from Wirth and co-workers,[409] is a short assessment on some alternative protecting group approaches, in particular, the preparation of diaryliodonium salts with doubly protected amine functionality. Here they prepared di-Boc-amine and *N*-phthalimidyl derivatives of **235**, as conducted in the preparation of 6-[^{18}F]fluoro-m-tyramine (Chapter 4) and 6-[^{18}F]fluorodopamine diaryliodonium salts, which has scope for nucleophilic attack on the nearby, highly electrophilic diaryliodonium salt centre. However, on [^{18}F]fluorination of these diaryliodonium bromides bearing amine di-protection they observed no/very little [^{18}F]FDOPA production.

It was speculated that the large steric bulk associated with the phthalimidyl and di-Boc protecting group strategies may be hindering attack on the λ^3-iodane centre,

despite [^{18}F]fluoride requiring relatively very little space to approach the electrophilic iodine centre. Given, this postulation we expected a DOPA diaryliodonium salt bearing a doubly protected amine group to exhibit high stability *versus* mono-protected amine diaryliodonium salt derivatives. Hence we sought to prepare a diaryliodonium salt designed for [^{18}F]FDOPA production that utilises a more compact strategy for doubly protecting the molecule's amine functionality. Similarly, we aimed to utilise more electron-withdrawing protecting groups for protection of the catecholic functionality, by way of benzoyl protection, in a bid to reduce the overall electron-density of the target ring system (versus benzyl protected derivatives), potentially providing a more balanced and stable diaryliodonium salt, as well as improving the [^{18}F]fluorination selectivity of that ring system over the n.p.r.

Our adapted [^{18}F]FDOPA diaryliodonium salt synthesis route was planned and implemented as shown below (Scheme 105), utilising the pre-prepared brominated DOPA methyl ester **230** followed by succinimidyl protection of the amino group to yield **237**, followed by benzoyl protection and stannylation to yield arylstannane **239**.

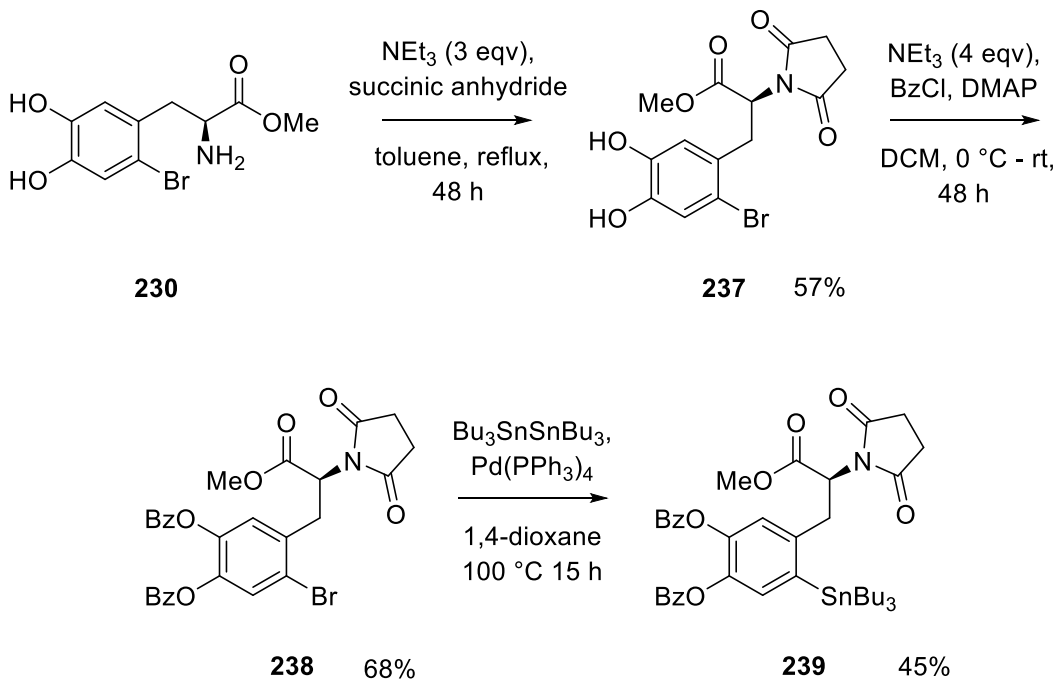

Scheme 105: Preparation of alternatively protected DOPA arylstannane 237

However, as with the previous efforts of diaryliodonium salt formation from protected DOPA arylstannanes and aryliodobis(acetate)s, the target diaryliodonium trifluoroacetate **240** was not isolated (Scheme 106). A white powder was obtained through crystallisation of the reaction mixture, which was later identified as the corresponding iodoarene, which suggests that diaryliodonium salt **240** was formed, but then underwent decomposition to afford aryliodide **241** (Figure 74) *in situ*.

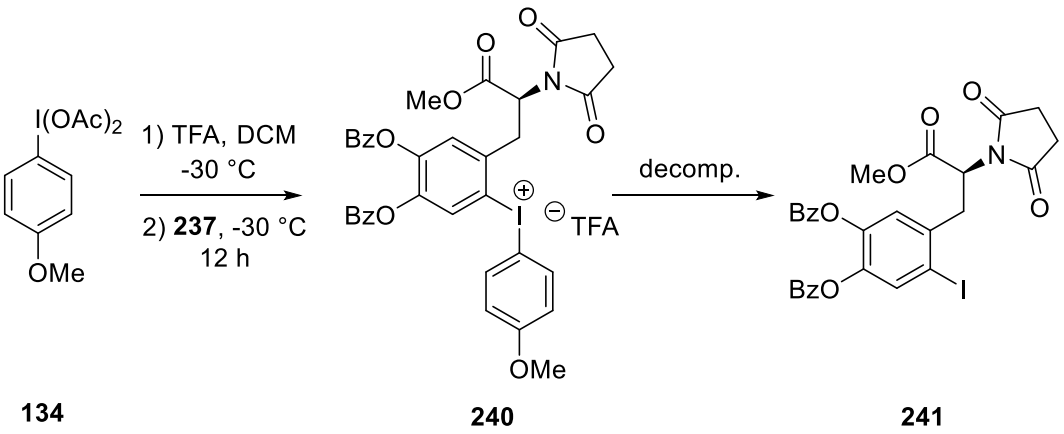

Scheme 106: Attempted preparation of [^{18}F]FDOPA diaryliodonium salt 240

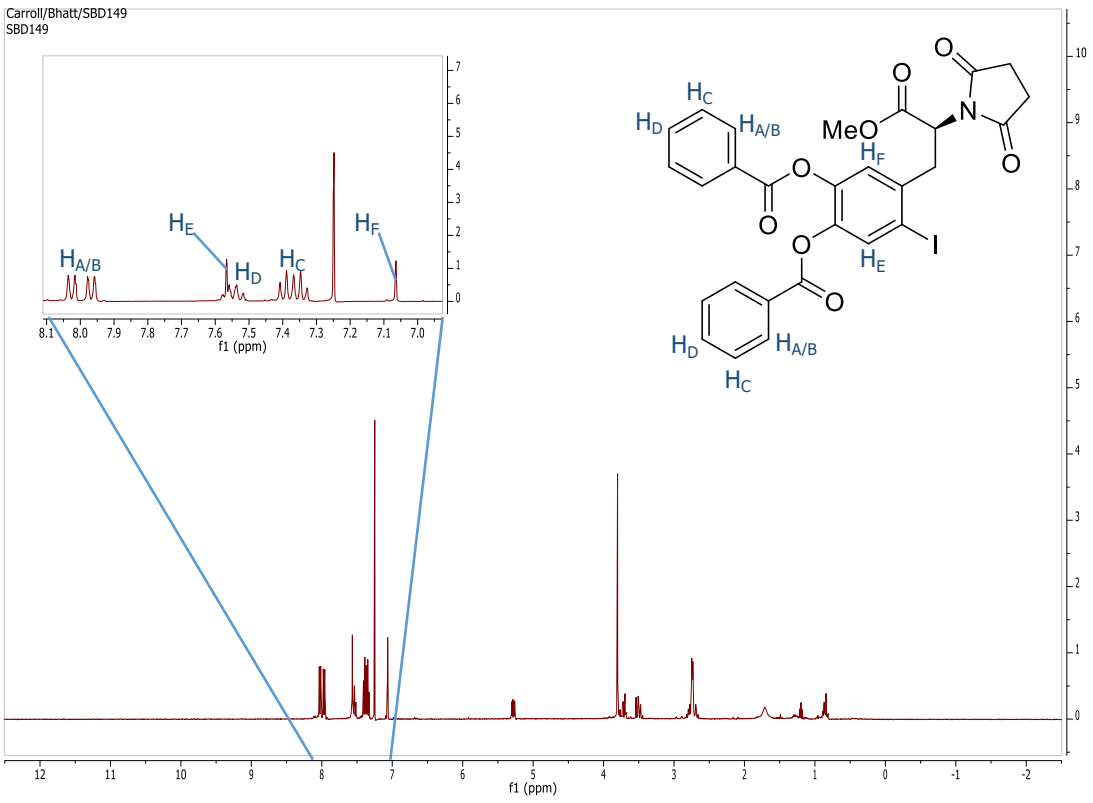

Figure 74: ^{1}H-NMR of iodoarene by-product 241 formed during the attempted preparation diaryliodonium salt 240, with the aromatic region expanded for clarity

Unfortunately this signifies the challenge in the preparation of a diaryliodonium trifluoroacetate precursor to [^{18}F]FDOPA, with the a protection suite that allows for rapid, global deprotection. These findings, as well as the elucidation of by-product **241** do validate that preparation of a [^{18}F]FDOPA diaryliodonium salt is attainable, but further refinement in protection group chemistry, counter-ion choice and method may be required in order to achieve the target precursor molecule.

5.4 Chapter 5 Summary

This chapter sought to develop a route to a diaryliodonium salt precursor designed to yield [^{18}F]FDOPA when reacted with n.c.a. [^{18}F]fluoride, with a specific protecting group array that allowed for rapid, global deprotection to yield the radiotracer in high RCYs and SA. This precursor was intended for use within a bespoke radiosynthesis cassette to be developed by ABT, providing an easy-to-operate two-step procedure for the production of [^{18}F]FDOPA, suitable for use within a clinical setting.

Although a suitably stable diaryliodonium salt precursor to [^{18}F]FDOPA has yet to be identified, although valuable insight was gained on potential routes to the target diaryliodonium salt, as well as a new diaryliodonium salt route to 6-[^{18}F]fluorodopamine, a valuable PET imaging agent with multiple applications within cancer imaging. In this preparation it was validated that the use of directing functionality, such the tributylstannyl moiety was essential for regioselective preparation of diaryliodonium salts that include arenes bearing multiple electron-donating functionality.

7 Conclusions and Further Work

The work herein has provided several key conclusions that benefit the development of diaryliodonium salts as precursors to electron-rich [^{18}F]fluoroarenes:

- A robust and versatile method for the preparation of electron-rich diaryliodonium trifluoroacetates has been developed and was utilised to prepare a series of precursors to 4-[^{18}F]fluorophenol, a valuable prosthetic group for macromolecule labelling.
- Dynamic [^{19}F]fluorination experiments using these diaryliodonium salt precursors allowed for provisional assessment of the protecting groups and non-participating rings employed for each precursor, with the observed selectivity profiles supporting the understanding of the process.
- Radiofluorination of lead candidate diaryliodonium salts for the production of 4-[^{18}F]fluorophenol were carried out with cyclotron produced n.c.a. [^{18}F]fluoride, exploiting microfluidics to achieve excellent RCYs for [^{18}F]fluorination of the target ring.
- Superiority of the hypernucleofuge strategy provided by diaryliodonium salts for the late-stage radiofluorination of electron-rich arenes *versus* traditional approaches was confirmed.
- The diaryliodonium salt precursor methodology was extended to the production of radiotracer 6-[^{18}F]fluoro-*m*-tyramine, which exhibited excellent selectivity for the target ring system as a result of a combination of the "*ortho*-effect" and electronic control on [$^{18/19}$F]fluorination. In addition, [^{18}F]fluorination of 6-[^{18}F]fluoro-*m*-tyramine diaryliodonium salt precursors was successfully conducted on a batch-based radiosynthesis platform, demonstrating the translatability of the [^{18}F]fluorination approach.
- A potential route to 6-[^{18}F]fluorodopamine, another valuable radiotracer was also developed through the preparation of diaryliodonium salt precursors, further demonstrating the wide scope for electron-rich [^{18}F]fluoroarene production exhibited by diaryliodonium salts.
- Investigations into the preparation of a diaryliodonium salt precursor to [^{18}F]FDOPA have provided key information on the functionality of protecting

groups, n.p.r.s and counter-ions, and their associated compatibility with the conditions of the various steps in the process, this should lead to a robust, viable precursor.

- In this, we have also considered the requirements for incorporation of a [^{18}F]FDOPA diaryliodonium salt precursor into a disposable, single-dose synthesis card, for a rapid and clinically compatible route to routine [^{18}F]FDOPA production.

To complete optimisation of diaryliodonium salt structures and radiofluorination conditions, further work should entail use of diaryliodonium salt precursors for batch production of 4-[^{18}F]fluorophenol, including removal of protecting groups, to allow for prosthetic group labelling macromolecules and ultimately an imaging study.

Further radiofluorination of 6-[^{18}F]fluoro-*m*-tyramine should be conducted to further validate the diaryliodonium salt strategy in this application, similarly, batch and microfluidic [^{18}F]fluorination of diaryliodonium salt precursors to 6-[^{18}F]fluorodopamine should be completed, given the high value of this radiotracer target.

A full and comprehensive combined protecting group and n.p.r. study for the preparation of diaryliodonium salt precursors to [^{18}F]FDOPA requires investigation to bring this important imaging agent into routine clinical use. Here efforts must focus on retaining a protection array that affords the required stability and selectivity, but also allows for rapid global deprotection, and ideally the precursor should be compatible with the automated reaction platforms currently in use and also, ultimately, integrated into a single-dose production cartridge, like the concept design described herein.

9 Experimental

All manipulations involving air-sensitive materials were carried out using standard Schlenk line techniques under a nitrogen atmosphere, using oven dried glassware.[410] Anhydrous DCM and MeCN were prepared by refluxing over CaH_2, whereas anhydrous toluene, THF and ether were prepared by refluxing over sodium, using benzophenone as an indicator. ^{1}H and ^{13}C NMR spectra were recorded on a Bruker 300 MHz, JEOL 400 MHz, or a JEOL 500 MHz spectrometer at room temperature. ^{1}H and ^{13}C shifts were relative to tetramethylsilane (external standard). ^{19}F spectra were recorded on either a JEOL 400 MHz, or a JEOL 500 MHz spectrometer at room temperature with ^{19}F shifts relative to $CFCl_3$ (external standard). Thin-layer chromatography was carried out on aluminum sheets pre-coated with silica gel 60F 254, and performed using Merck Kieselgel 60. Melting points were determined with a Gallenkamp MF-370 and are uncorrected. Automated flash chromatography was performed using a Varian IntelliFlash 971-FP discovery scale flash purification system. Mass spectrometry data was obtained from the EPSRC National Mass Spectrometry Service Centre, Swansea and microanalysis data was obtained from the London Metropolitan University Elemental Analysis Service and Medac Ltd.

9.1 Phenyliodobis(acetate) (132)[261,412]

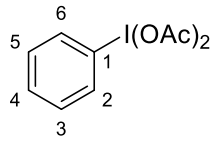

Iodobenzene (12.2 g, 60 mmol) was added to a solution of acetic acid (600 mL) at 45 °C. Sodium perborate tetrahydrate (92.3 g, 600 mmol) was added sequentially over 1 hour. The solution was stirred at this temperature for a further 4–5.5 hours before the addition of cold water (500 mL) at which point the solution was allowed to cool to room temperature. The product was washed with water (500 mL), extracted into DCM (3 × 500 mL) and the organic layers concentrated *in vacuo*. Subsequent crystallisation was induced though addition of ether/petrol to give the product as a white crystalline solid (13.7 g, 42.6 mmol, 71%). Mp 149-151 °C (from DCM-ether-petrol) (lit.[412] mp 161.1-162.2 °C); IR ν_{max}/cm^{-1} (neat) 1646, 1574, 1486, 1351,

1288, 1249, 1189; ^{1}H-NMR (300 MHz, $CDCl_3$) δ 8.10 (2H, dd, H2/H6 J = 9.1 Hz), 7.61 (1H, t, H4 J = 7.2 Hz), 7.51 (2H, t_{app}, H3/H5 J = 7.0 Hz), 2.02 (6H, s, OAc); ^{13}C-NMR (75 MHz, $CDCl_3$) 176.4 (CO), 135.0 (C2/C6), 131.7 (C4), 131.0 (C3/C5), 121.6 (C1), 20.4 (OAc). HR-MS (ESI) found: $[M+Na]^+$, 344.9598. $C_{10}H_{11}INaO_4$ requires 344.9600.

9.2 2-Thienyliodobis(acetate) (133)[255,411]

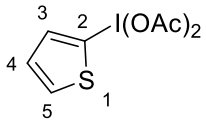

Product prepared according to procedure outlined for **132.** Product **133** was obtained by crystallisation from DCM/ether/petrol followed by suction filtration to afford a pale yellow crystalline solid (6.30 g, 19.2 mmol, 32%). Mp 120-123 °C (from DCM-ether-petrol) (lit.[411] mp 120-122 °C from $CHCl_3$-hexane); IR ν_{max}/cm^{-1} (neat) 3114, 1638, 1387, 1365, 1271, 1226, 1049, 1010; ^{1}H-NMR (300 MHz, $CDCl_3$) δ 7.80 (1H, dd, H5 J = 3. Hz, J = 1.3 Hz), 7.66 (1H, dd, H3 J = 5.4 Hz, J = 1.2 Hz), 7.15 (1H, dd, H4 J = 5.4 Hz, J = 1.2 Hz), 2.04 (6H, s, OAc); ^{13}C-NMR (100 MHz, $CDCl_3$) δ 177.3 (CO), 139.6, 135.4, 129.0, 106.3 (C1), 20.5 (OAc); HR-MS (NSI positive) found: $M+Na^+$, 350.9155. $C_8H_9IO_4SNa^+$ requires 350.9158; Anal. Calcd. for $C_8H_9IO_4S$: C, 29.28; H, 2.76. Found: C, 29.32; H, 2.69.

9.3 4-Methoxyphenyliodobis(acetate) (134)[255,412]

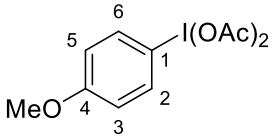

Product prepared according to procedure outlined for **132.** Product **134** was obtained by crystallisation from DCM/ether/petrol followed by suction filtration to afford a white crystalline solid (12.25 g, 34.8 mmol, 58%). Mp 91-93 °C (from DCM-ether-petrol) (lit.[412] mp 92.4-96 °C); IR ν_{max}/cm^{-1} (neat) 1639, 1582, 1570, 1490,

1291, 1251, 1182; ^{1}H-NMR (400 MHz, $CDCl_3$) δ 8.00 (2H, d, H2/H6 J = 9.0 Hz), 6.95 (2H, d, C3/C5 J = 9.1 Hz), 3.85 (3H, s, OMe), 1.99 (6H, s, OAc); ^{13}C-NMR (100 MHz, $CDCl_3$) δ 176.5 (CO), 162.3 (C4), 137.2, 116.7, 111.7 (C1), 55.7 (OMe), 20.5 (OAc); HR-MS (NSI positive) found: $[M+Na]^+$, 374.9701. $C_{11}H_{13}IO_5Na^+$ requires 374.9705; Anal. Calcd. for $C_8H_9IO_4S$: C, 37.52; H, 3.72. Found: C, 37.60; H, 3.66.

9.4 2-Methoxyphenyliodobis(acetate) (135)[255,412]

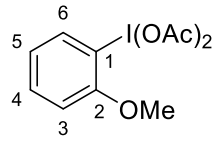

Product prepared according to procedure outlined for **132.** Product **135** was obtained by crystallisation from DCM/ether/petrol followed by suction filtration to afford a white crystalline solid (11.20 g, 31.8 mmol, 53%). Mp 144-146 °C (from DCM-ether-petrol) (lit.[412] mp 146.9-150.1 °C from $CHCl_3$-hexane); IR ν_{max}/cm^{-1} (neat) 1639, 1478, 1432, 1267, 1049; ^{1}H NMR (300 MHz, $CDCl_3$) δ 8.15 (1 H, dd, H6 J = 7.9, 1.5 Hz), 7.60 (1H, dt_{app}, J = 7.3, 1.4 Hz), 7.17 (1H, d, H3 J = 8.4 Hz), 7.04 (1H, dt_{app}, J = 7.7, 1.2 Hz), 3.99 (3H, s, OMe), 1.97 (6H, s, OAc); ^{13}C-NMR (75 MHz, $CDCl_3$) δ 176.6 (CO), 156.3 (C2), 137.8, 134.5, 122.8, 113.5 (C1), 112.0, 56.9 (OMe), 20.4 (OAc); HR-MS (NSI positive) found: $[M+Na]^+$, 374.9710. $C_{11}H_{13}IO_5Na^+$ requires 374.9705; Anal. Calcd. for $C_{11}H_{13}IO_5$: C, 37.52; H, 3.72. Found: C, 37.69; H, 3.76.

9.5 4-Methylphenyliodobis(acetate) (136)[261,412]

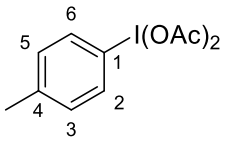

Product prepared according to procedure outlined for **132.** Product **136** was obtained by crystallisation from DCM/ether/petrol followed by suction filtration to afford a white crystalline solid (13.31 g, 39.6 mmol, 66%). Mp 108-110 °C (from

DCM-ether-petrol) (lit.[412] mp 106-110 °C from $CHCl_3$-hexane); IR v_{max}/cm^{-1} (neat) 2931, 1646, 1583, 1427, 1363, 1266, 1213, 1187, 1045, 1004; ^{1}H-NMR (300 MHz, $CDCl_3$) δ 7.97 (2H, d, H2/H6 J = 8.3), 7.29 (2H, d, H3/H5 J = 7.5), 2.44 (3H, s, *p*-Me), 1.99 (6H, s, OAc); ^{13}C-NMR (75 MHz, $CDCl_3$) δ 176.3 (CO), 142.7 (C4), 135.0, 131.8, 118.4 (C1), 21.5 (*p*-Me), 20.4 (OAc); HR-MS (NSI positive) found: $[M+Na]^+$, 358.9758. $C_{11}H_{13}IO_4Na^+$ requires 358.9756; Anal. Calcd. for $C_{11}H_{13}IO_4$: C, 37.52; H, 3.72. Found: C, 37.20; H, 3.99.

9.6 2,4,6-Trimethylphenyliodobis(acetate) (137)[261,412]

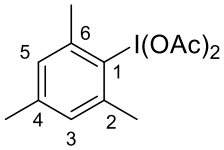

Product prepared according to procedure outlined for **132.** Product **137** was obtained by crystallisation from DCM/ether/petrol followed by suction filtration to afford a white crystalline solid (12.45 g, 34.2 mmol, 57%). Mp 163-166 °C (from DCM-ether-petrol) (lit.[412] mp 160-163 °C from $CHCl_3$-hexane); IR v_{max}/cm^{-1} (neat) 2927, 1644, 1446, 1367, 1264, 1010, 999; ^{1}H-NMR (300 MHz, $CDCl_3$) δ 7.11 (2H, s, H3/H5), 2.72 (6H, s, *o*-Me), 2.37 (3H, s, *p*-Me), 1.97 (6H, s, OAc). ^{13}C-NMR (75 MHz, $CDCl_3$) δ 176.4 (CO), 143.2 (C4), 141.3 (C2/C6), 129.7 (C1), 129.0 (C3/C8), 26.7 (*o*-Me), 21.2 (*p*-Me), 20.3 (OAc); HR-MS (NSI positive) found: $[M+Na]^+$, 387.0070. $C_{13}H_{17}INaO_4^+$ requires 387.0069; Anal. Calcd. for $C_{13}H_{17}IO_4$: C, 42.87; H, 4.71. Found: C, 42.79; H, 4.62.

9.7 4-(Benzyloxy)phenyliodobis(acetate) (166)[221]

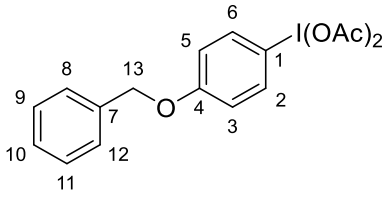

Product prepared according to procedure outlined for **132.** Product **166** was obtained by crystallisation from DCM/ether/petrol followed by suction filtration to afford a white crystalline solid (1.33 g, 3.1 mmol, 32%). Mp 111-112 °C (from DCM-ether-petrol) (lit.[221] mp 113 °C from EtOAc/Ac_2O); IR ν_{max}/cm^{-1} (neat) 1641, 1584, 1571, 1490, 1290, 1253, 1181; ^{1}H-NMR (400 MHz, $CDCl_3$) δ 7.99 (2H, d, H2/H6 J = 9.1), 7.43 – 7.34 (5H, m,), 7.02 (2H, d, H3/H5 J = 9.2), 5.10 (2H, s, CH_2), 1.98 (6 H, s, OAc). ^{13}C-NMR (100 MHz, $CDCl_3$) δ 176.5 (CO), 161.0 (C4), 137.2, 135.9, 135.5, 128.9, 128.5, 127.6, 117.5 (C1), 117.3, 70.5 (CH_2), 20.5 (OAc); HR-MS (NSI positive) found: $[M+Na]^+$, 451.0006. $C_{17}H_{17}IO_5Na^+$ requires 451.0013; Anal. Calcd. for $C_{17}H_{17}IO_5$: C, 47.68; H, 4.00. Found: C, 47.81; H, 4.04.

9.8 4-(Benzyloxy)-1-iodobenzene (140)[413,414]

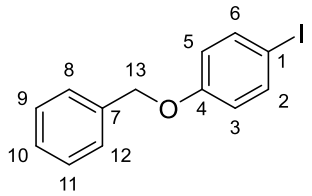

To a solution of 4-iodophenol (6.60 g, 30 mmol) in acetone (200 mL) were added potassium carbonate (20.71 g, 149.87 mmol) and benzyl bromide (2.97 mL, 4.27 g, 25.00 mmol) and the reaction mixture was heated under reflux for 16 h. The white reaction mixture was then allowed to cool to room temperature before being filtered to through filter paper and the solvent was removed under reduced pressure. The resulting yellow crude material was re-dissolved in diethyl ether (50 mL), washed with water (300 mL) and with brine (100 mL) before being extracted with diethyl ether (3×50 mL), dried with $MgSO_4$ and concentrated *in vacuo.* Purification by column chromatography on SiO_2, eluting with petrol, then 1:9 ethyl acetate:petrol) gave the product as a white solid (8.47 g, 27.32 mmol, 91%). Mp 61-63 °C (from ethyl acetate-petrol) (lit.[413] mp 62-63 °C from DCM); IR ν_{max}/cm^{-1} (neat) 1599, 1120, 973; ^{1}H-NMR (400 MHz, $CDCl_3$) δ 7.54 (2H, d, H2/H6 J = 8.6), 7.44 – 7.29 (5H, m, H8-H12), 6.74 (2H, d, H3/H5 J = 8.9), 5.02 (2H, s, CH_2); ^{13}C-NMR (100 MHz, $CDCl_3$) δ 158.7 (C4), 138.3 (C2/C6), 136.6, 128.7, 128.2, 127.5, 117.4 (C3/C5), 83.1 (C1),

70.1 (CH_2); HR-MS (ESI positive) found: $[M+H]^+$, 309.9925. $C_{13}H_{12}IO^+$ requires 309.9932.

9.9 4-(Benzyloxy)-1-bromobenzene (141)[413,414]

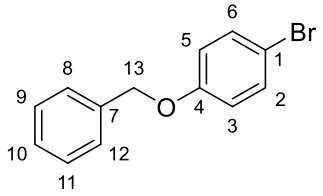

Product prepared according to procedure outlined for **140.** The product was obtained as in previous example, however purification by column chromatography on SiO_2 (1:8 ethyl acetate:petrol) afforded a white solid (4.76 g, 18.1 mmol, 94%). Mp 58-59 °C (from ethyl acetate-petrol) (lit.[414] mp 59-60 °C from ethyl acetate-hexane); IR ν_{max}/cm^{-1} (neat) 3058, 1853, 1587, 1487, 1289, 1248, 1170, 1070, 1041, 1026; ^{1}H-NMR (400 MHz, $CDCl_3$) δ 7.39 (2H, d, H2/H6 J = 7.4), 7.37 – 7.30 (5H, m), 6.85 (2H, d, H3/H5 J = 8.9), 5.03 (2H, s, CH_2). ^{13}C-NMR (100 MHz, $CDCl_3$) δ 158.8 (C4), 132.7 (C2/C6), 136.7, 129.8, 128.2, 127.55, 118.4 (C3/C5), 115.4 (C1), 70.2 (CH2); HR-MS (ESI positive) found: $[M+H]^+$, 262.0174. $C_{13}H_{12}BrO^+$ requires 262.0176

9.10 4-Iodophenyl acetate (142)[415,416]

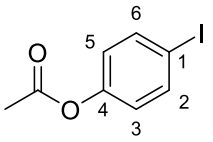

To a solution of 4-iodophenol (8.40 g, 38.16 mmol) in DCM was added trimethylamine (6.11 mL, 4.44 g, 43.85 mmol), followed by the portion wise addition of acetyl chloride (2.72 mL, 3.00 g, 38.16 mmol) at room temperature. After stirring at room temperature for 14 h the reaction mixture was poured into distilled water (100 mL), the organic layer was then washed with 5% aqueous NaOH (100 mL), distilled water (50 mL) and dried with $MgSO_4$. The solvent was removed *in vacuo* to yield a crude oil, which following purification by column chromatography on SiO_2

(1:19 ethyl acetate:petrol) afforded a white solid (9.21 g, 35.18 mmol, 92%). Mp 31–33 °C (from ethyl acetate-petrol) (lit.[415] mp 32–32.5 °C from water-methanol); IR v_{max} /cm^{-1} (neat) 3089, 1760, 1597, 1481, 1432, 1393, 1372, 1294, 1271, 1197, 1164, 1098, 1054, 1010, 942, 915, 837, 791, 705, 671; ^{1}H-NMR (400 MHz, $CDCl_3$) δ 7.66 (2H, d, H2/H6 J = 8.8), 6.84 (2H, d, H3/H5 J = 8.8), 2.27 (3H, s, OAc); ^{13}C-NMR (100 MHz, $CDCl_3$) δ 169.2 (CO), 150.6 (C4), 138.6, 123.9, 90.0 (C1), 21.2 (CH_3); HR-MS (ESI positive) found: $[M+H]^+$, 261.9499. $C_8H_8IO_2^+$ requires 261.9503

9.11 4-Bromophenyl acetate (143)[415]

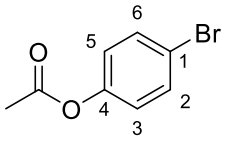

Product prepared according to procedure outlined for **142**. Product was obtained as in previous examples, however purification was achieved by distillation to afford the product as a colourless oil. (2.60 g, 12.1 mmol, 79%). R_f 0.40 (1:4 ethyl acetate:petrol); IR v_{max}/cm^{-1} (neat) 1760, 1486, 1370, 1196, 1068, 1011, 909, 843, 674; ^{1}H-NMR (400 MHz, $CDCl_3$) δ 7.47 (2H, d, H2/H6 J = 8.7), 6.97 (2H, d, H3/H5 J = 8.8), 2.28 (3H, s, OAc); ^{13}C-NMR (100 MHz, $CDCl_3$) δ 169.2 (CO), 149.8 (C4), 132.6, 123.5, 119.0 (C1), 21.2 (CH_3); HR-MS (ESI positive) found: $[M+H]^+$, 213.9645. $C_8H_8BrO_2^+$ requires 213.9649.

9.12 4-(Benzyloxy)-1-fluorobenzene (157)[416]

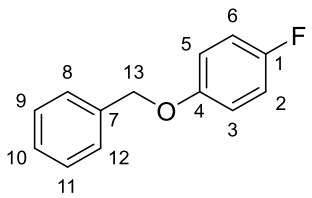

Product prepared according to procedure outlined for **140**. The product was obtained as in previous examples however purification was achieved by column chromatography on SiO_2 (petrol) to afford a crystalline white solid (0.53 g, 2.6 mmol,

79%). Mp 51-53 °C (from ethyl acetate-petrol) (lit.[416] mp 49-50 °C from diethyl ether-pentane); IR ν_{max}/cm^{-1} (neat) 3064, 3052, 3040, 3036, 2888, 2856, 1598, 1502, 1451, 1248, 1197; ^{1}H-NMR (400 MHz, $CDCl_3$) δ 7.45 – 7.28 (5H, m, H8-H12), 6.96 (2H, t_{app}, H3/H5 J = 8.7), 6.92 – 6.88 (2H, t_{app}), 5.02 (2 H, s, CH_2); ^{13}C-NMR (100 MHz, $CDCl_3$) δ 158.6 (C1), 154.9 (C4), 136.9 (C7), 128.7, 128.1, 127.6, 116.0, 115.8, 70.7 (CH_2); HR-MS (APCI corona positive) found: $[M-H]^+$, 201.0710. $C_{13}H_{10}FO^+$ requires 201.0710; Anal. Calcd. for $C_{13}H_{11}FO$: C, 77.30; H, 5.49. Found: C, 77.45; H, 5.58.

9.13 4-(Benzyloxy)-1-tributylstannylbenzene (146)[318,319,320]

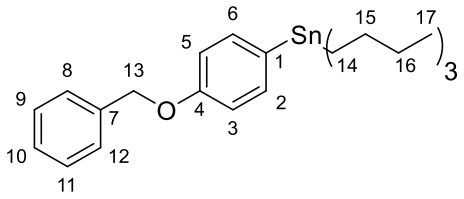

A flask was charged with zinc dust (11.09 g, 169.20 mmol), followed by anhydrous MeCN (100 mL) and the dropwise addition of trifluoroacetic acid (1.53 mL, 2.36 g, 20.71 mmol). After 5 minutes of stirring at room temperature, under nitrogen, cobalt dibromide (2.56 g, 11.70 mmol) was added, affording an immediate colour change from grey to blue. After a further 5 minutes of stirring at room temperature, allyl chloride (2.70 mL, 2.62 g, 34.22 mmol) was injected into the reaction vessel and the mixture was left to stir for a further 10 min. To the resultant red reaction mixture was then added 4-(benzyloxy)-1-iodobenzene (27.90 g, 90.00 mmol), followed immediately by tri-*n*-butylstannyl chloride (22.45 mL, 40.14 g, 123.30 mmol) and the reaction mixture was heated to 50 °C and monitored by TLC (5:95 diethyl ether:petrol) until all of the starting material had been consumed. After which the reaction mixture was allowed to cool to room temperature, poured into aqueous saturated ammonium chloride (80 mL) and extracted with diethyl ether (3 x 70 mL). The combined organic fractions were dried with $MgSO_4$, filtered and concentrated *in vacuo* to afford a crude yellow/orange oil. Purification by column chromatography on SiO_2 (petrol, then 10:90 diethyl ether:petrol) or alternatively by flash reverse phase chromatography (MeCN) which afforded the colourless oil product (32.38 g, 68.42

mmol, 86 %). R_f 0.68 (5:95 diethyl ether:petol); ^{1}H-NMR (400 MHz, $CDCl_3$) δ 7.44 (2H, d, H2/H6 J = 7.8), 7.41 – 7.30 (5H, m, Ph), 6.98 (2H, dd, H3/H5 J = 8.5), 5.05 (2H, s, H13), 1.57 – 1.48 (6H, m, H16), 1.37 – 1.26 (6H, m, H15), 1.02 (6H, t, H14 J = 8.3), 0.88 (9H, t, H17 J = 7.3); ^{13}C-NMR (100 MHz, $CDCl_3$) δ 159.1 (C4), 137.6 (C2/C6), 137.3 (C7), 132.5, 128.7, 128.0, 127.6, 114.9 (C3/C5), 69.8 (C13), 29.2 (C15), 27.5 (C16), 13.8 (C14), 9.7 (C17); HR-MS (ESI positive) found: $[M+H]^+$, 473.1921. $C_{25}H_{37}OSn^+$ requires 473.1914; Anal. Calcd. for $C_{25}H_{38}OSn$: C, 64.44; H, 8.09. Found: C, 64.50; H, 8.11.

9.14 4-(Acetoxy)-1-tributylstannylbenzene (147)[318,319,320]

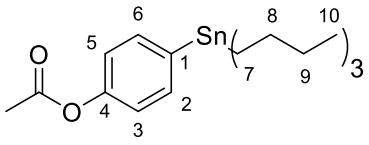

Product prepared according to procedure outlined for **146** The product was obtained as in previous examples with purification by column chromatography on SiO_2 (petrol, then 10:90 diethyl ether:petrol) which afforded the colourless oil product (6.18 g, 14.53 mmol, 61 %). R_f 0.62 (5:95 diethyl ether:petol); ^{1}H-NMR (400 MHz, $CDCl_3$) δ 7.47 (2H, d, H2/H6 J = 7.6), 7.05 (2H, d, H3/H5 J = 8.3), 2.28 (3H, s, OAc), 1.62 – 1.49 (6H, m, H9), 1.39 – 1.28 (6H, m, H8), 1.09 – 1.02 (6H, m, H7), 0.90 (9H, t, H10 J = 7.3); ^{13}C-NMR (100 MHz, $CDCl_3$) δ 169.7 (CO), 150.9 (C4), 139.3 (C1), 137.5 (C2/C6), 121.2 (C3/C5), 29.2 (C8), 27.5 (C9), 21.3 (C7), 13.8 (C10), 9.7 ($COCH_3$); HR-MS (ESI positive) found: $[M+H]^+$, 425.1567. $C_{20}H_{33}O_2Sn^+$ requires 425.1579. Anal. Calcd. for $C_{20}H_{34}O_2Sn$: C, 56.50; H, 8.06. Found: C, 56.52; H, 8.12.

9.15 4-(Methoxy)-1-tributylstannylbenzene (148)[318,319,320]

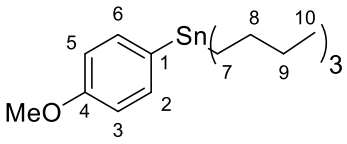

Product prepared according to procedure outlined for **146** The product was obtained as in previous examples with purification by flash reverse phase chromatography (MeCN) which afforded the colourless oil product (8.81 g, 22.17 mmol, 91 %). R_f 0.67 (5:95 diethyl ether:petol); ^{1}H-NMR (300 MHz, $CDCl_3$) δ 7.40 (2H, d, H2/H6 J = 8.5), 6.93 (2H, d, H3/H5 J = 8.5), 3.83 (3H, s, OMe), 1.62 – 1.49 (6H, m, H9), 1.35 (6H, sx, H8 J = 7.2), 1.09 – 1.01 (6H, m, H7), 0.91 (9 H, t, H10 J = 7.3); ^{13}C-NMR (100 MHz, $CDCl_3$) δ 159.7 (C4), 137.6 (C2/C6), 132.1 (C1), 114.0 (C3/C5), 55.0 (OMe), 29.2 (C8), 27.5 (C9), 13.8 (C7), 9.7 (C10); HR-MS (ESI positive) found: $[M+H]^+$, 397.1861. $C_{19}H_{33}OSn^+$ requires 397.1872. Anal. Calcd. for $C_{19}H_{34}OSn$: C, 57.46; H, 8.63. Found: C, 56.49; H, 8.59.

9.16 (3,4,5-trimethoxy)-1-tributylstannylbenzene (169)[318,319,320]

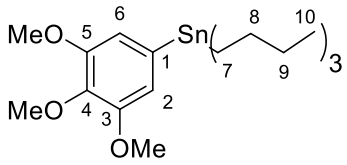

Product prepared according to procedure outlined for **146**. The product was obtained as in previous examples with purification by column chromatography on SiO_2 (petrol, then 10:90 diethyl ether:petrol) which afforded the colourless oil product (3.76 g, 8.22 mmol, 34 %). R_f 0.58 (5:95 diethyl ether:petol); ^{1}H-NMR (400 MHz, $CDCl_3$) δ 6.63 (2H, s, H2/H6), 3.86 (6H, s, *m*-OMe, *m*-OMe), 3.83 (3H, s, *p*-OMe), 1.59 – 1.49 (6H, m, H9), 1.33 (6H, sx, H8 J = 14.4, 7.3), 1.08 – 1.01 (6H, m, H7), 0.88 (9H, t, H10 J = 7.3); ^{13}C-NMR (100 MHz, $CDCl_3$) δ 153.0 (C3/C5), 138.3 (C4), 136.8 (C1), 112.8 (C2/C6), 60.9 (*p*-OMe), 56.2 (*m*-OMe, *m*-OMe), 29.2 (C8), 27.5 (C9), 13.8 (C7), 9.9 (C10); HR-MS (ESI positive) found: $[M+H]^+$, 344.0445. $C_{13}H_{21}O_3Sn^+$ requires 344.0440.

9.17 (4-(Benzyloxy)phenyl)(4-methoxyphenyl)iodonium trifluoroacetate (149)

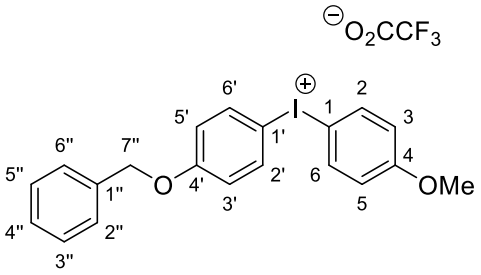

4-Methoxyphenyliodobis(acetate) (**134**) (2.32 g, 6.60 mmol) was dissolved in DCM (40 mL). The solution was cooled to -30 °C. TFA (1.01 mL, 13.2 mmol) was added dropwise, the yellow solution was stirred at -30 °C for 30 minutes, followed by 1 hour stirring at room temperature. The reaction mixture was then re-cooled to -30 °C, 4-(benzyloxy)-1-tributylstannylbenzene (**146**) (3.12 g, 6.60 mmol) was added, and stirred for 30 minutes. The reaction was warmed to room temperature and stirred overnight. The solvent was removed in vacuo, affording a yellow oil, which was crystallised from DCM/petrol/ether to given the crude product as an off-white powder. (1.99 g, 3.76 mmol, 57%). Mp 149-151 °C (from DCM-ether-petrol); IR v_{max}/cm^{-1} (neat) 3056, 3031, 1589, 1579, 1276, 1009; ^{1}H-NMR (400 MHz, $CDCl_3$) δ 7.81 (2H, d, H2'/H6' J = 3.3), 7.79 (2H, d, H2/H6 J = 9.2), 7.39 – 7.32 (5H, m), 6.95 (2 H, d, H3/H5 J = 9.2), 6.89 (2 H, d, H3'/H5' J = 3.3), 5.05 (2 H, s, C7''), 3.81 (3 H, s, OMe); ^{13}C-NMR (100 MHz, $CDCl_3$) δ 162.5 (C4), 161.6 (C4'), 136.4 (C1''), 136.3 (C2/C6/C2'/C6'), 135.6, 128.9, 128.6, 127.6, 118.4 (C1'), 117.7 (C1), 70.5 (C7''), 55.7 (OMe); HR-MS (NSI positive) found: $[M]^+$, 417.0339. $C_{20}H_{18}IO_2^+$ requires 417.0346; Anal. Calcd. for $C_{22}H_{18}F_3IO_4$: C, 49.83; H, 4.42. Found: C, 50.09; H, 3.52.

9.18 (4-(Benzyloxy)phenyl)(2-thienyl)iodonium trifluoroacetate (150)

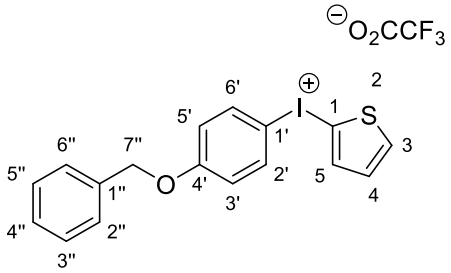

Product prepared according to procedure outlined for **149**. Product **150** was obtained by crystallisation from DCM/ether/petrol followed by suction filtration to afford a white crystalline solid (1.06 g, 2.10 mmol, 52%). Mp 162-164 °C (from

DCM-ether-petrol); IR v_{max}/cm^{-1} (neat) 3044, 3021, 2861, 1600, 1584, 1301, 1013; ^{1}H-NMR (400 MHz, $CDCl_3$) δ 7.88 (2H, d, H2′/H6′ J = 9.1), 7.66 (1H, d, H3 J = 4.9), 7.58 (1H, d, H5 J = 6.4), 7.40 – 7.31 (5H, m), 7.05 (1H, dd, H4 J = 5.3, 3.8), 6.95 (2H, d, C3′/H5′ J = 9.1), 5.04 (2H, s, C7″); ^{13}C-NMR (100 MHz, $CDCl_3$) δ 161.5 (C1′), 136.0 (C1″), 135.5 (C2′/C6′), 129.8, 128.9, 128.6, 127.6, 118.4 (C3′/C5′), 109.7 (C1′), 70.6 (C7″); HR-MS (NSI positive) found: $[M]^+$, 392.9801. $C_{17}H_{14}IOS^+$ requires 492.9805; Anal. Calcd. for $C_{19}H_{14}F_3IO_3S$: C, 45.10; H, 2.79. Found: C, 45.23; H, 2.90.

9.19 (4-(Benzyloxy)phenyl)(phenyl)iodonium trifluoroacetate (151)

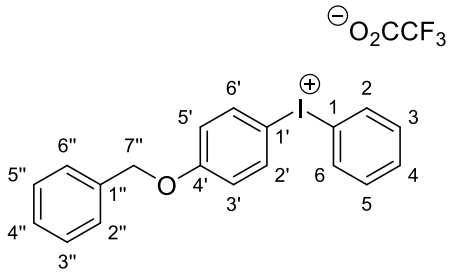

Product prepared according to procedure outlined for **149**. Product **151** was obtained by crystallisation from DCM/ether/petrol followed by suction filtration to afford a white crystalline solid (1.87 g, 3.74 mmol, 68%). Mp 156-157 °C (from DCM-ether-petrol); IR v_{max}/cm^{-1} (neat) 3012, 2799, 1596, 1584, 1204, 1057, 1022; ^{1}H-NMR (400 MHz, $CDCl_3$) δ 7.92 (2H, d, H2′/H6′ J = 8.4), 7.87 (2H, d, H2/H6 J = 9.1), 7.60 – 7.51 (1H, m, H4), 7.47 – 7.42 (2H, m, H3/H5), 7.43 – 7.35 (5H, m), 7.00 (2H, d, H3′/H5′ J = 8.4), 5.09 (2 H, s, H7″); ^{13}C-NMR (100 MHz, $CDCl_3$) δ 161.5 (C4′), 137.8 (C1″), 136.7 (C2′/C6′), 135.4 (C2/C6), 132.3, 132.1, 129.1, 128.7, 128.4, 118.7 (C1), 117.7 (C1′), 106.3 (C3′/C5′), 70.2 (C7″); HR-MS (NSI positive) found: $[M]^+$, 387.0240. $C_{19}H_{16}IO^+$ requires 387.0236; Anal. Calcd. for $C_{21}H_{16}F_3IO_3$: C, 50.42; H, 3.22. Found: C, 50.50; H, 3.29.

9.20 (4-(Acetoxy)phenyl)(4-methoxyphenyl)iodonium trifluoroacetate (152)

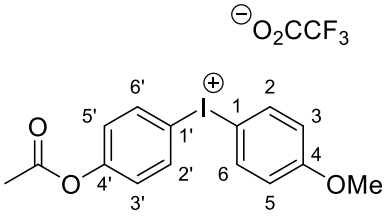

Product prepared according to procedure outlined for **149**. Product **152** was obtained by crystallisation from DCM/ether/petrol followed by suction filtration to afford a white crystalline solid (0.95 g, 1.98 mmol, 41%). Mp 147-149 °C (from DCM-ether-petrol); IR v_{max}/cm^{-1} (neat) 3070, 3023, 2956, 1702, 1423, 1403, 1130; ^{1}H-NMR (400 MHz, $CDCl_3$) δ 7.89 (2H, d, H2/H6 J = 8.9), 7.85 (2H, d, H2′/H6′ J = 9.2), 7.11 (2H, d, H3′/H5′ J = 9.2), 6.88 (2H, d, H3/H5 J = 8.9), 3.80 (3H, s, OMe), 2.28 (3H, s, OAc); ^{13}C-NMR (100 MHz, $CDCl_3$) δ 168.7 (CO), 162.6 (C4), 153.2 (C4′), 137.1 (C2/C6), 135.8 (C2′/C6′), 125.1 (C3′/C5′), 117.7 (C3/C5), 112.4 (C1′), 105.2 (C1), 55.7 (OMe), 21.2; HR-MS (NSI positive) found: $[M]^+$, 369.040. $C_{15}H_{15}IO_3^+$ requires 369.0036; Anal. Calcd. for $C_{17}H_{14}F_3IO_5$: C, 42.34; H, 2.93. Found: C, 42.34; H, 2.82.

9.21 (4-(Acetoxy)phenyl)(2-thienyl)iodonium trifluoroacetate (153)

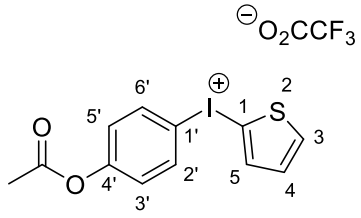

Product prepared according to procedure outlined for **149**. Product **154** was obtained by crystallisation from DCM/ether/petrol followed by suction filtration to afford a white crystalline solid (1.33 g, 2.90 mmol, 33%). Mp 138-140 °C (from DCM-ether-petrol); IR v_{max}/cm^{-1} (neat) 3067, 3021, 2970, 1714, 1419, 1240; ^{1}H-NMR (400 MHz, $CDCl_3$) δ 7.96 (2H, d, H2′/H6′ J = 9.0), 7.71 (1H, dd, H3 J = 3.8, 1.2), 7.60 (1H, dd, H5 J = 5.3, 1.2), 7.14 (2H, d, H3′/H5′ J = 9.0), 7.06 (1H, dd, J = 5.3, 3.8), 2.28 (3H, s, OAc); ^{13}C-NMR (100 MHz, $CDCl_3$) δ 168.6 (CO), 153.2 (C4′), 140.1 (C3), 136.3 (C1), 135.2 (C2′/C6′), 129.8 (C4), 125.1 (C3′/C5′), 115.3 (C1′), 21.2; HR-MS (NSI positive) found: $[M]^+$, 344.9441. $C_{12}H_{10}IO_2S^+$ requires 344.9441; Anal. Calcd. for $C_{14}H_{10}F_3IO_4S$: C, 36.70; H, 2.93. Found: C, 36.77; H, 2.36.

9.22 Bis(4-(benzyoxyl)phenyl)iodonium trifluoroacetate (155)

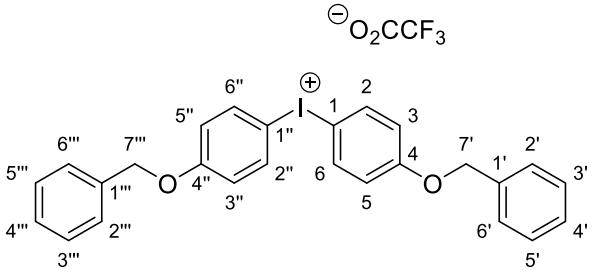

Product prepared according to procedure outlined for **149**. Product **155** was obtained by crystallisation from DCM/ether/petrol followed by suction filtration to afford a white crystalline solid (2.75 g, 4.54 mmol, 23%). Mp 156-157 °C (from DCM-ether-petrol); IR ν_{max}/cm^{-1} (neat) 3054, 3016, 2960, 2201, 1429, 1268, 1211; ^{1}H-NMR (400 MHz, $CDCl_3$) δ 7.80 (4H, d, H2/H6/H2″/H6″ J = 9.1), 7.41 – 7.29 (10H, m), 6.96 (4H, d, H3/H5/H3″/H5″ J = 9.1), 5.05 (4H, s); ^{13}C-NMR (100 MHz, $CDCl_3$) δ 161.7 (C4/C4″), 136.4 (C2/C6/C2″/C6″), 135.6 (C1′/C1‴), 128.9, 128.6, 127.6, 118.5 (C3/C5/C3′/C5′), 105.5 (C1/C1″), 70.5 (C7′/C7‴); HR-MS (NSI positive) found: $[M]^+$, 493.0645. $C_{26}H_{22}IO_2^+$ requires 493.0659; Anal. Calcd. for $C_{28}H_{22}F_3IO_4$: C, 55.46; H, 3.66. Found: C, 55.37; H, 3.74.

9.23 (4-(Benzyloxy)phenyl)(3,4,5-trimethoxyphenyl)iodonium trifluoroacetate (170)

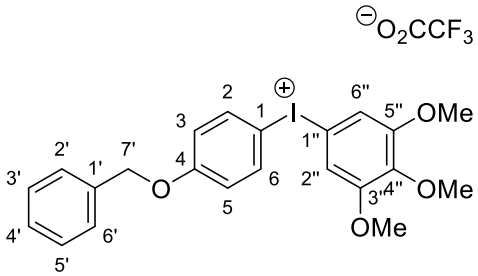

Product prepared according to procedure outlined for **149**. Product **170** was obtained by crystallisation from DCM/ether/petrol followed by suction filtration to afford a white crystalline solid (1.20 g, 2.04 mmol, 16%). Mp 158-159 °C (from DCM-ether-petrol); IR ν_{max}/cm^{-1} (neat) 3099, 2971, 2966, 2954, 2210, 1423, 1261,

1210; ^{1}H-NMR (400 MHz, $CDCl_3$) δ 7.85 (2H, d, H2/H6 J = 9.1), 7.40 – 7.32 (5H, m), 7.09 (2H, s H2′/H6′), 6.99 (2 H, d, H3/H5 J = 9.1), 5.07 (2H, s, H7″), 3.83 (3H, s, *p*-OMe), 3.80 (6H, s, *m*-OMe); ^{13}C-NMR (100 MHz, $CDCl_3$) δ 155.0 (C4), 136.8 (C3″/C5″), 135.6 (C4″), 128.9, 128.6, 127.6, 118.5 (C1″), 112.0 (C1), 108.9 (C2/C5), 105.3 (C2/C6′), 70.5 (C7″), 61.1 (*p*-OMe), 56.7 (*m*-OMe); HR-MS (NSI positive) found: $[M]^+$, 477.0621. $C_{22}H_{22}IO_4^+$ requires 477.0624; Anal. Calcd. for $C_{24}H_{22}F_3IO_6$: C, 48.83; H, 3.76. Found: C, 48.79; H, 3.74.

9.24 1-Methoxy-3-(2-nitrovinyl)benzene (177)[417,418]

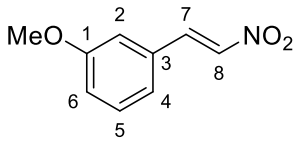

To a stirred solution of 3-methoxybenzaldehyde (1.77g, 13 mmol) and ammonium acetate (1.08g, 14 mmol) was added glacial acetic acid (200 mL) was treated with nitrostyrene (1.53 g, 25 mmol), and the mixture was heated to 110 °C for 4 h. The resulting dark green solution was cooled, diluted with cold water (500 mL) and the green precipitate was collected. Crystallisation from chloroform-hexane (1:1) afforded the product as a yellow solid 1.86 g 10.4 mmol, 80%). Mp 91-93 °C (from chloroform-hexane) (lit.[417] mp 91-92 °C from ethanol); IR ν_{max}/cm^{-1} (neat) 3110, 1634, 1578, 1509; ^{1}H-NMR (400 MHz, $CDCl_3$) δ 7.96 (1H, d, H8 J = 13.7), 7.56 (1H, d, H7 J = 13.6), 7.36 (1H, dd, H5 J = 9.0, 7.6), 7.25 (1H, s, H2), 7.16 – 7.11 (1H, m, H4), 7.03 (1H, dd, H6 J = 4.5, 2.3), 3.84 (3H, s, OMe); ^{13}C-NMR (100 MHz, $CDCl_3$) δ 160.2 (C1), 139.12 (C7), 137.4 (C8), 131.34 (C3), 130.5 (C5), 121.8 (C4), 118.1 (C6), 114.0 (C2), 55.5 (OMe); HR-MS (ESI positive) found: $[M+H]^+$, 179.0674. $C_9H_{10}NO_3^+$ requires 179.0671.

9.25 2-(3-Methoxyphenyl)ethan-1-amine (178)[417,418]

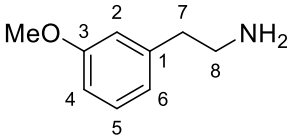

A solution of **177** (4.00 g, 22.33 mmol) in anhydrous diethyl ether (100 mL) was added dropwise to a stirred suspension of lithium aluminium hydride (1.70 g, 44.67 mmol) in anhydrous ether (100 mL) at room temperature. The mixture was stirred for 30 min after the addition was completed and treated with slow, dropwise additions of water (4.2 mL), 15% sodium hydroxide (4.2 mL), and water (12.6 mL). The mixture was filtered through a sintered glass disk (porosity m), and the filtrate was dried (sodium sulfate) and concentrated in vacuo to give a pale brown residue (2.19 g, 14.51 mmol, 65%). R_f 0.41 (15% diethyl ether:petrol); IR ν_{max}/cm^{-1} (neat) 3379, 2980, 1599, 1481, 1469, 1321, 1270, 859; ^{1}H-NMR (400 MHz, $CDCl_3$) δ 7.20 (1H, t, H5 J = 7.2), 6.82 – 6.71 (3H, m, H2/H4/H6), 3.78 (3H, s, OMe), 2.94 (3H, t, H8 J = 6.8), 2.71 (3H, t, H7 J = 6.8); ^{13}C-NMR (100 MHz, $CDCl_3$) δ 159.8 (C3), 141.4 (C1), 129.5 (C5), 121.3 (C6), 114.7 (C2), 111.5 (C4), 55.2 (OMe), 43.4 (C8), 40.1 (C7).

9.26 2-(3-Methoxyphenethyl)isoindoline-1,3-dione (179) [418,419]

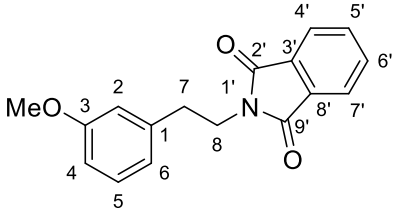

A suspension of phthalic anhydride (2.37g, 15.88 mmol) in anhydrous toluene (80 mL) in an oven dried round bottom flask fitted with Dean-Stark apparatus was heated to reflux until complete dissolution of the anhydride and no additional water was removed. To this solution was the added **178** (1.74g, 13.20 mmol) and refluxing was continued until the water evolution was completed (4 h). The reaction mixture was then concentrated *in vacao* to give a residue, purification by column chromatography on SiO_2 (20% acetone-petrol) afforded a white crystalline solid (1.82 g, 6.47 mmol, 49%). Mp 89-90 °C (from acetone-petrol) (lit.[418] mp 91 °C from diethyl ether:petrol); IR ν_{max}/cm^{-1} (neat) 2940, 1771, 1719, 1610; ^{1}H-NMR (400 MHz,

$CDCl_3$) δ 7.82 (2H, dd, H5′/H6′ J = 5.4, 3.2), 7.69 (2H, dd, H4′/H7′ J = 5.5, 3.1), 7.22 – 7.14 (1H, m, H5), 6.92 – 6.63 (3H, m, H2/H4/H6), 3.95 – 3.87 (2H, m, H8), 3.75 (3H, s, OMe), 3.00 – 2.90 (2H, m, H7); ^{13}C-NMR (100 MHz, $CDCl_3$) δ 168.3 (C2′/C9′), 159.8 (C3), 139.6 (C1), 134.0 (C3′/C5′/C6′/C8′), 132.2 (C5), 123.3 (C4′/C7′), 121.3 (C6), 114.4 (C2), 112.4 (C4), 55.3 (OMe), 39.3 (C8), 34.8 (C7); HR-MS (ESI positive) found: $[M+H]^+$, 281.1187. $C_{17}H_{16}NO_3^+$ requires 281.1192.

9.28 2-(2-(3-Methoxyphenethyl)isoindoline-1,3-dione)(4-methoxyphenyl)iodonium trifluoroacetate (181)

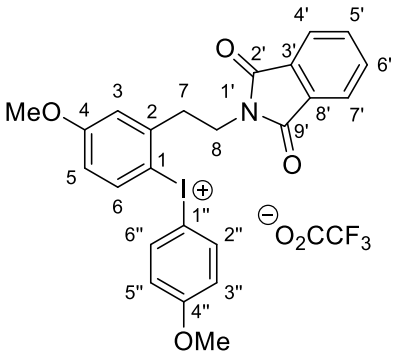

Product prepared according to procedure outlined for **149**, using **179** in the place of an arylstannane reagent. Product **181** was obtained by crystallisation from DCM/ether/petrol followed by suction filtration to afford a white crystalline solid (0.83 g, 1.32 mmol, 20%). Mp 145-146 °C (from DCM-ether-petrol); IR ν_{max}/cm^{-1} (neat) 3067, 3022, 2980, 1801, 1715, 1423, 1240, 1121; ^{1}H-NMR (400 MHz, $CDCl_3$) δ 7.98 (1H, d, H6 J = 8.8), 7.93 (2H, d, H2″/H6″ J = 9.1), 7.83 (2H, dd, H5′/H6′ J = 5.4, 3.1), 7.73 (2H, dd, H4′/H7′ J = 5.5, 3.0), 6.93 (1H, d, H5 J = 3.0), 6.88 (1H, s, H3), 6.76 (2H, dd, H3″/H5″ J = 8.9, 3.0), 3.94 – 3.86 (2H, m, H8), 3.78 (3H, s, C_6H_4-OMe), 3.76 (3H, s, OMe), 3.27 – 3.21 (2H, m, H7); ^{13}C-NMR (100 MHz, $CDCl_3$) δ 168.2 (CO), 163.1 (C4″), 153.3 (C4), 150.0 (C3), 136.8 (C2″/C6″), 135.1 (C6), 134.4 (C3′/C8′), 132.0 (C5′/C6′), 123.1 (C4′/C7′), 119.5 (C1), 118.1 (C3″/C5″), 113.7 (C6), 106.0 (C1), 101.8 (C1″), 56.2 (OMe), 55.9 (OMe), 38.0 (CH2), 36.7 (CH2); HR-MS (NSI positive) found: $[M]^+$, 514.0515. $C_{24}H_{21}INO_4^+$ requires 514.0518; Anal. Calcd. for $C_{26}H_{21}F_3INO_6$: C, 49.78; H, 3.37. Found: C, 49.80; H, 3.34.

9.29 2-(2-(3-Methoxyphenethyl)isoindoline-1,3-dione)(2-methoxyphenyl)iodonium trifluoroacetate (182)

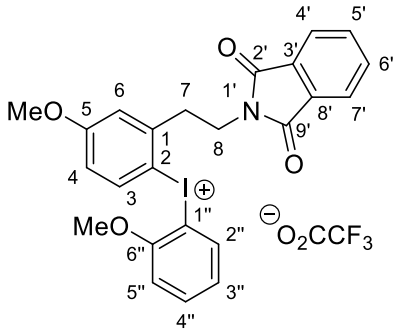

Product prepared according to procedure outlined for **149**, using **179** in the place of an arylstannane reagent. Product **182** was obtained by crystallisation from DCM/ether/petrol followed by suction filtration to afford a white crystalline solid (0.61 g, 0.98 mmol, 17%). Mp 155-157 °C (from DCM-ether-petrol); IR ν_{max}/cm^{-1} (neat) 3052, 2963, 1789, 1714, 1404, 1278, 1234, 1175; ^{1}H-NMR (300 MHz, $CDCl_3$) δ 8.06 (2H, d, H3/H2″ J = 8.9), 7.78 (4H, ddd, H4′/H5′/H6′/H7′ J = 28.6, 5.5, 3.1), 7.55 – 7.30 (2H, m, H4″/H5″), 7.08 – 7.00 (1H, m, H4), 6.96 – 6.89 (1H, m, H6), 6.82 (1 H, dd, H3″ J = 8.9, 3.0), 4.01 (3 H, s), 3.97 – 3.89 (2 H, m), 3.83 (3 H, s), 3.31 (2 H, dd, J 8.6, 6.8); ^{13}C-NMR (75 MHz, $CDCl_3$) δ 167.9 (CO), 163.2 (C6″), 143.3 (C5), 140.3 (C1), 134.1 (H3/H2″), 133.3 (C5′/C6′), 133.1 (C3′/C8′), 131.9 (C4″), 123.9 (C3″), 123.4 (C4′/C7′), 116.8 (C2), 116.2 (C1″), 112.2 (C5″), 107.5 (C4), 105.9 (C6), 56.8 (OMe), 55.7 (OMe), 37.8 (C7/C8); HR-MS (NSI positive) found: $[M]^+$, 514.0519. $C_{24}H_{21}INO_4^+$ requires 514.0515; Anal. Calcd. for $C_{26}H_{21}F_3INO_6$: C, 49.78; H, 3.37. Found: C, 49.51; H, 3.27.

9.30 2-(3,4-dimethoxyphenethyl)isoindoline-1,3-dione (225)[418]

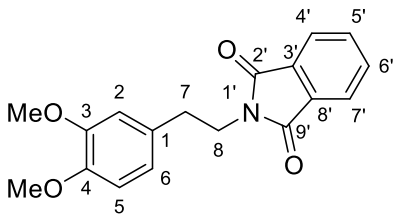

Product prepared according to procedure outlined for **179** Product was obtained by column chromatography on SiO_2 (15% ethyl acetate-petrol) affording a white crystalline solid (0.94 g, 3.01 mmol, 44%). Mp 166-168 °C (from ethyl acetate-

petrol) (lit.[418] mp 171 °C from diethyl ether:petrol); IR ν_{max}/cm^{-1} (neat) 2943, 1761, 1712, 1600; ^{1}H-NMR (300 MHz, $CDCl_3$) δ 7.71 (4H, ddd, H4′/H5′/H6′/H7′ J = 35.6, 5.5, 3.1), 6.75 (2H, m, H5/H6), 6.72 (1H, s, H2), 3.91 – 3.83 (2H, m, H8), 3.80 (3H, s, *p*-OMe), 3.78 (3H, s, *m*-OMe), 2.96 – 2.87 (2H, m, H7); ^{13}C-NMR (75 MHz, $CDCl_3$) δ 168.1 (CO), 148.8 (C3), 147.7 (C4), 133.9 (C5′/C6′), 132.0 (C3′/C8′), 130.5 (C1), 123.1 (C4′/C7′), 120.8 (C6), 111.9 (C2), 111.3 (C5), 55.8 (OMe), 55.8 (OMe), 39.3 (C8), 34.0 (C7); HR-MS (ESI positive) found: $[M+H]^+$, 311.1278. $C_{18}H_{18}NO_4^+$ requires 311.1277; Anal. Calcd. for $C_{18}H_{17}NO_4$: C, 69.44; H, 5.50; N, 4.50. Found: C, 69.31; H, 5.58; N, 4.42.

9.31 2-(2-iodo-4,5-dimethoxyphenethyl)isoindoline-1,3-dione (227)

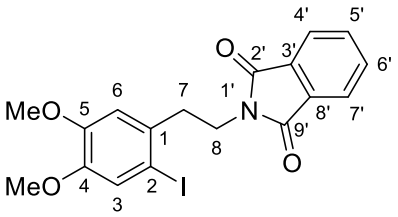

Iron nitrate nonahydrate (2.02 g, 5.0 mmol) and silica gel (2.02 g, 5.0 mmol) were ground together in a mortar and pestle to give a fine, pale yellow powder before addition to a solution of iodine (1.40 g, 6 mmol) in DCM (300 mL). The suspension was then stirred for 5 minutes before the addition **225** (3.11 g, 10.0 mmol) then stirred for 16 h at room temperature and filtered to remove any solids. The filtrate was then stirred with aqueous sodium thiosulfate (2M, 200 mL, 400 mmol) until the colour dissipated then the organic layer was separated, washed with brine (100 mL) and extracted into DCM (3 × 100 mL). The organic layers were combined, dried ($MgSO_4$) and concentrated in vacuo to give the product as a colourless crystalline solid (1.14 g, 2.6 mmol, 26 %). Mp 158–159 °C (from ethyl acetate-petrol) (lit.[419] mp 164-166 °C from methanol); ^{1}H-NMR (400 MHz, $CDCl_3$) δ 7.73 (4H, ddd, H4′/H5′/H6′/H7 J = 44.9, 5.4, 3.1), 7.16 (1H, s, H3), 6.65 (1H, s, H6), 3.89 (2H, dd, H8 J = 8.1, 6.6), 3.79 (3H, s, OMe), 3.66 (3H, s, OMe), 3.03 (2H, dd, H7 J = 8.1, 6.6); ^{13}C-NMR (100 MHz, $CDCl_3$) δ 168.2 (CO), 149.3 (C4), 148.3 (C5), 134.1 (C1), 133.2 (C3′/C8′), 132.1 (C5′/C6′), 123.3 (C4′C7′), 121.7 (C3), 112.5 (C6), 88.2 (C2), 56.1 (OMe), 55.9 (OMe), 38.8 (C8), 37.9 (C7); HR-MS (ESI positive) found: $[M+H]^+$,

437.0138. $C_{18}H_{17}INO_4^+$ requires 437.0133; Anal. Calcd. for $C_{18}H_{16}INO_4$: C, 49.45; H, 3.69; N, 3.20. Found: C, 49.34; H, 3.74; N, 3.16.

9.32 2-(4,5-dimethoxy-2-(tributylstannyl)phenethyl)isoindoline-1,3-dione (228)[176]

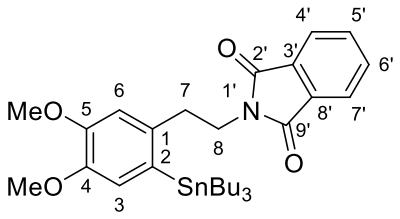

To **227** (0.74 g, 1.69 mmol) in dioxane (40 mL) at room temperature was added lithium chloride (0.359 g, 8.47 mmol), tetrakis(triphenylphosphine)palladium (0.20 g, 0.170 mmol, 10.0 mol%) and bis(trimethyltin) (1.97 g, 3.39 mmol, 2.00 equiv). After stirring for 6 hr at 100 ºC, the reaction mixture was cooled to 23 ºC and concentrated in vacuo. The residue was purified by chromatography on silica gel, eluting with 20% ethylacetate-petrol, to afford a colourless oil (0.284 g, 0.47 mmol, 28%). R_f 0.68 (20% ethyl acetate-petrol); IR ν_{max}/cm^{-1} (neat) 3331, 2980, 1736, 1346, 1590, 1468, 1434, 1354, 1046; ^{1}H-NMR (400 MHz, $CDCl_3$) δ 7.77 (4H, ddd, H4'/H5'/H6'/H7' J = 54.4, 5.4, 3.0), 6.87 (1H, s, H3), 6.84 (1H, s, H6), 3.91 – 3.86 (2H, m, H8), 3.85 (3H, s, OMe), 3.79 (3H, s, OMe), 2.96 – 2.87 (2H, m, H7), 1.57 – 1.47 (8H, m, $SnCH_2$), 1.33 (8H, h, J = 7.3), 1.16 – 1.09 (8H, m), 0.86 (9H, t, CH_3 J = 7.3); ^{13}C-NMR (100 MHz, $CDCl_3$) δ 168.2 (CO), 149.3 (C5), 147.2 (C4), 137.7 (C1), 134.0 (C2), 132.6 (C5'/C6'), 132.2 (C3'/C8'), 123.3 (C4'/C7'), 119.1 (C3), 112.0 (C6), 55.9 (OMe), 55.7 (OMe), 39.9 (C8), 37.3 (C7), 29.3 ($Sn\underline{C}H_2$), 27.5 ($SnCH_2\underline{C}H_2$), 13.8 ($\underline{C}H_3$), 10.6; HR-MS (ESI positive) found: $[M+H]^+$, 601.2266. $C_{30}H_{44}NO_4Sn^+$ requires 601.2270; Anal. Calcd. for $C_{30}H_{43}INO_4Sn$: C, 60.02; H, 7.22; N, 2.33. Found: C, 59.85; H, 7.37; N, 2.27.

9.33 (4-(5-*N*-[2-(1,2-Dimethoxy-phenyl)ethyl]-phthalimide)(2-thienyl)iodonium trifluoroacetate (226)

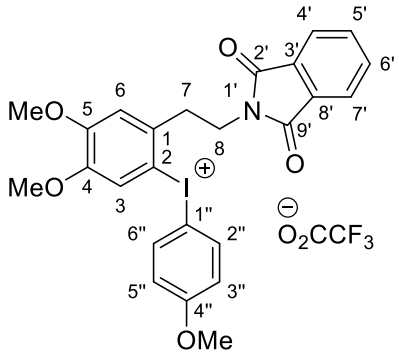

Product prepared according to procedure outlined for **149**. Product **226** was obtained by crystallisation from DCM/ether/petrol followed by suction filtration to afford a white crystalline solid (0.51 g, 0.78 mmol, 32%). Mp 166-168 °C (from DCM-ether-petrol); IR v_{max}/cm^{-1} (neat) 3071, 3022, 1821, 1728, 1425, 1321, 1119; ^{1}H-NMR (400 MHz, $CDCl_3$) δ 7.93 (2H, d, H2″/H6″ J = 8.9), 7.76 (4H, ddd, H4′/H5′/H6′/H7′ J = 37.6, 5.3, 3.0), 7.52 (1H, s, H3), 6.88 (1H, s, H6), 6.86 (2H, d, H3″/H5″ J = 3.4), 3.89 (3H, t, H8 J = 7.3), 3.87 (3H, s, OMe), 3.79 (3H, s, OMe), 3.78 (3H, s, OMe), 3.25 – 3.17 (2H, m, H7); ^{13}C-NMR (100 MHz, $CDCl_3$) δ 168.1 (CO), 162.3 (C4″), 152.6 (C5), 149.6 (C4), 136.0 (C2″/C6″), 134.3 (C5′/C6′), 134.0 (C3′/C8′), 131.9 (C1), 123.5 (C4′C7′), 119.6 (C2), 117.6 (C3), 112.9 (C3″/C5″), 109.6 (C1″), 105.4 (C6), 56.7 (OMe), 56.2 (OMe), 55.7 (OMe), 38.2 (C8), 37.1 (C7); HR-MS (NSI positive) found: $[M]^+$, 544.0612. $C_{25}H_{23}INO_5^+$ requires 544.015; HR-MS (NSI positive) found: $[M]^+$, 544.0642. $C_{25}H_{24}INO_5^+$ requires 544.0644; Anal. Calcd. for $C_{27}H_{23}F_3INO_7$: C, 49.33; H, 3.53; N, 2.13. Found: C, 49.38; H, 3.57; N, 2.18.

9.34 Methyl (S)-2-amino-3-(2-bromo-4,5- dihydroxyphenyl) propanoate (230)[408]

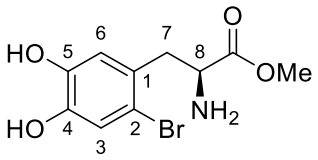

To a solution of L-3,4-dihydroxyphenylalanine (9.86 g, 50 mmol) in glacial acetic acid (250 mL) was added a solution bromine (2.80 mL, 52.5 mmol) in glacial acetic acid (50 mL) dropwise, over 1.5 h. The resulting yellow solution was then concentrated *in*

vacao to afford a yellow residue, which was then re-dissolved in methanol (200 mL) treated with thionyl chloride (20 mL) at 0 °C, then allowed to warm to room temperature before being stirred for a further 14 h. The solvent was removed in vacao to afford an amorphous yellow solid (19.22 g, quant.) as the hydrochloride/hydrobromide salt of **230** and was used without further purification. ^{1}H-NMR (300 MHz, $CDCl_3$) δ 7.12 (1H, s, H3), 6.91 (1H, s, H6), 4.22 (1H, t, H8 J = 7.2 Hz), 3.83 (3H, s, OMe), 3.22 (2H, br d, J = 7.2 Hz).

9.35 Methyl (*S*)-3-(2-bromo-4,5-bis((*tert*-butoxycarbonyl)oxy) phenyl)-2-((*tert*-butoxycarbonyl)amino)propanoate (231)[408]

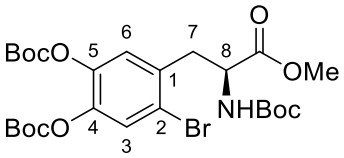

To a stirring solution of **230** (2.90 g, 10.0 mmol) in anhydrous methanol (50 mL) was added trimethylamine (1.67 mL, 12.0 mmol) followed by di-tert-butyldicarbonate (2.62 g, 12.0 mmol). The reaction was stirred at 0 °C for 2 h, followed by 15 h at room temperature. The solution was then diluted with ethyl acetate (60 mL) and washed with water (60 mL) and brine (60 mL) before being dried over $MgSO_4$. After concentration *in vacao* confirmation of a successful amine protection was confirmed by ^{1}H- and ^{13}C-NMR. The yellow residue was then re-dissolved in anhydrous toluene, to which was then added trimethylamine (3.49 mL, 25 mmol) and di-tert-butyldicarbonate (5.46 g, 25 mmol). The reaction mixture was then heated at 80 °C for 24 h. The solution was then diluted with ethyl acetate (60 mL) and washed with water (60 mL) and brine (60 mL) before being dried over $MgSO_4$ and concentrated *in vacao*. Purification by column chromatography on SiO_2 (0-20% ethyl acetate-petrol) afford the product as a colourless residue (4.55 g, 7.71 mmol, 77%). R_f 0.26 (20% ethyl acetate-petrol); ^{1}H-NMR (400 MHz, $CDCl_3$) δ 7.47 (1H, s, H3), 7.11 (1H, s, H6), 4.60 (1H, q, H8 J = 7.7), 3.69 (3H, s, OMe), 3.16 (3H, ddd, H7 J = 56.9, 13.8, 6.8), 1.52 (27 H, s, Boc); ^{13}C-NMR (100 MHz, $CDCl_3$) δ 172.2 , 155.1 (COOMe), 150.3 (Boc CO), 141.7 (C4/C5), 134.6 (C1), 127.3 (C3), 125.3 (C6), 120.8 (C2), 84.4 (Boc $C(CH_3)$), 84.2 (Boc $C(CH_3)$)(Boc $C(CH_3)$)(Boc $C(CH_3)$)(Boc $C(CH_3)$)(Boc $C(CH_3)$)(Boc $C(CH_3)$)(Boc $C(CH_3)$)(Boc $C(CH_3)$)(Boc $C(CH_3)$)(Boc $C(CH_3)$)(Boc $C(CH_3)$)(Boc C(CH3)), 80.2

(Boc C(CH3)), 53.3 (C8), 52.6 (OMe), 38.2 (C7), 28.3 (NHBoc C($\underline{C}H_3)_3$), 27.7 (OBoc C($\underline{C}H_3)_3$); HR-MS (ESI positive) found: $[M+H]^+$, 590.1542. $C_{25}H_{37}BrNO_{10}^+$ requires 590.1543; Anal. Calcd. for $C_{25}H_{36}BrNO_{10}$: C, 50.85; H, 6.15; N, 2.37. Found: C, 50.72; H, 6.29; N, 2.47.

9.36 Methyl (*S*)-3-(4,5-bis((*tert*-butoxycarbonyl)oxy)-2-(trimethylstannyl)phenyl)-2-((*tert*-butoxycarbonyl)amino)propanoate (233)[409]

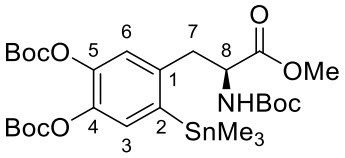

Product prepared according to procedure outlined for **228**, utilising **231** as the substrate and hexamethylditin in place of hexabutylditin. Purification by column chromatography on SiO_2 (0-60% ethyl acetate-petrol) afforded the product as a clear oil (1.56 g, 2.31 mmol, 31%). R_f 0.32 (30% ethyl acetate-petrol); IR ν_{max}/cm^{-1} (neat) 3070, 3019, 1818, 1725, 1430, 1381, 1109; ^{1}H-NMR (300 MHz, $CDCl_3$) δ 7.14 (1H, s, H3), 6.90 (1H, s, H6), 4.97 – 4.41 (1H, m, H8), 3.84 (3H, s, OMe), 3.04 (2H, td, H7 J = 15.5, 14.9, 7.2), 1.57 (27H, s, Boc), 0.34 (9H, s, $SnMe_3$, with tin satellites J^2 Sn-H = 54.8 Hz). ^{13}C-NMR (75 MHz, $CDCl_3$) δ 171.5 ($\underline{C}OOMe$), 155.1 (NH$\underline{C}OO$), 151.6 (OBoc), 151.3 (OBoc), 142.0 (C5), 138.8 (C1), 133.6 (C4), 129.4 (C3), 113.3 (C6), 83.3 (Boc), 82.0 (Boc), 79.8 (NBoc), 55.8 (H8), 54.6 (OMe), 41.2 (C7), 28.3 ($C(\underline{C}H_3)_3$), 28.0 ($C(\underline{CH}3)_3$), 27.7 ($C(\underline{CH}3)_3$), -8.0 ($SnMe_3$); HR-MS (ESI positive) found: $[M+H]^+$, 675.2128. $C_{28}H_{46}NO_{10}Sn^+$ requires 675.2130.

9.37 (*S*)-4-Bromo-5-(2-(2,5-dioxopyrrolidin-1-yl)-3-methoxy-3-oxopropyl)-1,2-phenylene dibenzoate (238)[420]

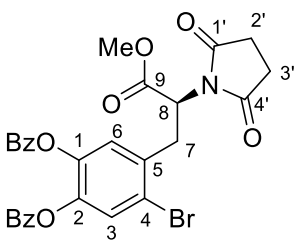

To a vigorously stirred suspension of bromo-DOPA methyl ester **230** (7.66 g, 26.41 mmol) in anhydrous toluene (200 mL) was added triethylamine (10.9 mL, 79.1 mmol) and succinic anhydride (3.17 g, 31.6 mmol) at room temperature. The reaction mixture was then stirred for 48 hours at reflux and allowed to cool to room temperature. Benzoyl chloride (15.2 mL, 65.9 mmol) and triethylamine (9.11 mL, 65.9 mmol) were added to the reaction mixture at 23 °C. The reaction mixture was stirred for 12 h at 80 °C, allowed to cool to 23 °C, and then transferred to a separating funnel. The organic layer was washed with brine (3 × 50 mL). The combined aqueous layers were extracted with ethyl acetate (50 mL). The combined organic layers were dried over magnesium sulfate, filtered, and concentrated *in vacuo*. The residue was purified by flash column chromatography on SiO_2 (0-50% ethyl acetate-petrol) to afford the title compound (5.98 g, 10.3 mmol, 39% yield) as a pale brown residue. R_f 0.24 (20% ethyl acetate-petrol); IR ν_{max}/cm^{-1} (neat) 3115, 1823, 1730, 1377, 1325, 1319; ^{1}H-NMR (400 MHz, $CDCl_3$) δ 8.00 (4H, dd, OBz J = 23.4, 6.8), 7.56 (1H, s, H3), 7.55 (2H, q, OBz J = 8.9, 8.1), 7.37 (4H, dt, OBz J = 15.8, 7.7), 7.06 (1H, s, H6), 5.28 (1H, dd, H8 J = 12.0, 4.8), 3.80 (3H, s, OMe), 3.74 – 3.46 (2H, m, H7 (ABX system)), 2.83 – 2.65 (4H, m, H2'H3'); ^{13}C-NMR (100 MHz, $CDCl_3$) δ 176.9 (CO), 168.6 (COOMe), 164.2 (COOPh), 163.9 (COOPh), 142.0 (C1), 141.6 (C2), 134.4 (C5), 134.1 (OBz), 130.3 (OBz), 130.2 (OBz), 128.7 (OBz), 128.7 (OBz), 128.3 (OBz), 127.9 (OBz), 126.4 (C3), 120.8 (C4), 53.1 (C8), 50.9 (OMe), 34.0 (C7), 28.1 (C2'/C3'); HR-MS (ESI positive) found: $[M+H]^+$, 579.0551. $C_{28}H_{23}BrNO_8^+$ requires 579.0556.

9.38 (*S*)-4-(2-(2,5-Dioxopyrrolidin-1-yl)-3-methoxy-3-oxopropyl)-5-(tributylstannyl)-1,2-phenylene dibenzoate (239)

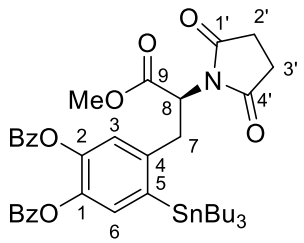

Product prepared according to procedure outlined for **228**, using arylbromide **238** as the substrate. Purification by flash column chromatography on SiO_2 (0-40% ethyl

acetate-petrol) afforded the product as a colourless oil (0.87 g, 1.1 mmol, 45%). R_f 0.32 (15% ethyl acetate-petrol); IR ν_{max}/cm^{-1} (neat) 3069, 3020, 1821, 1726, 1422, 1381, 1313. 1122; ^{1}H-NMR (400 MHz, $CCDCl_3$) δ 8.31 – 8.18 (4H, m, OBz), 7.79 (2H, q, J = 7.3), 7.61 (4H, dt, OBz, J = 12.6, 7.7), 7.49 (1H, s, H6), 7.20 (1H, s, H3), 5.56 – 5.48 (1H, m, H8), 4.04 (3H, s, OMe), 4.02 – 3.69 (2H, m, H7 (ABX system)), 2.98 (4H, q, H2'/H3' J = 2.8), 1.56 – 1.45 (8H, m, $SnCH_2$), 1.32 (8H, h, J = 7.2), 1.15 – 1.07 (8H, m), 0.85 (9H, t, CH_3 J = 7.2); ^{13}C-NMR (100 MHz, $CDCl_3$) δ 176.41 (CO), 169.2 (COOMe), 166.6 (COOPh), 165.5 (COOPh), 145.3 (C2), 144.8 (C4), 141.8 (C1), 139.9 (C5), 133.9 (OBz), 130.2 (OBz), 129.7 (OBz), 128.8 (C6), 119.3 (C3), 61.0 (C8), 51.9 (OMe), 36.5 (C7), 29.3 ($SnCH_2$), 28.1 (C2'/C3'), 27.5 ($SnCH_2CH_2$), 13.8 (CH_3), 10.6; HR-MS (ESI positive) found: $[M+H]^+$, 791.2516. $C_{40}H_{50}NO_8Sn^+$ requires 791.2519.

9.39 2,4,6-Trimethyliodobenzene (242)[421]

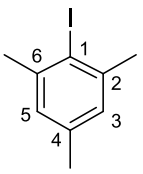

Iron nitrate nonahydrate (4.04 g, 10.0 mmol) and silica gel (4.04 g, 10.0 mmol) were ground together in a mortar and pestle to give a fine, pale yellow powder before addition to a solution of iodine (2.79 g, 11 mmol) in DCM (500 mL). The suspension was then stirred for 5 minutes before the addition mesitylene (2.40 g, 20.0 mmol) then stirred for 16 h at room temperature and filtered to remove any solids. The filtrate was then stirred with aqueous sodium thiosulfate (2M, 200 mL, 400 mmol) until the colour dissipated then the organic layer was separated, washed with brine (200 mL) and extracted into DCM (3 × 150 mL). The organic layers were combined, dried ($MgSO_4$) and concentrated in vacuo to give the product as a colourless crystalline solid (3.89 g, 15.81 mmol, 79 %). Mp 30–31 °C (from DCM) (lit.[422] mp 30 °C from ethanol); ^{1}H-NMR (400 MHz, $CDCl_3$) δ 6.89 (2H, s, H3/H5), 2.45 (6H, s, *o*-Me), 2.25 (3H, s, *p*-Me); ^{13}C-NMR (100 MHz, $CDCl_3$) δ 141.7 (C2/C6), 137.3 (C4), 127.9 (C3/C5), 104.2 (C1), 29.5 (*o*-Me), 20.6 (*p*-Me).

9.40 4-(Benzyloxy)-1-iodobenzene (138 from benzyl phenyl ether)

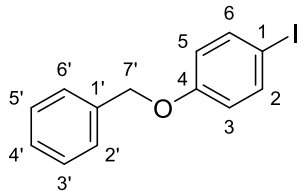

Product prepared according to procedure outlined for **242.** Purification by column chromatography on SiO_2 (15% ethyl acetate-petrol afforded the product as an off white solid concentrated (4.56 g, 14.7 mmol, 94 %). Mp 63-65 °C (from ethyl acetate-petrol) (lit.[423] mp 62-63 °C from DCM); IR ν_{max}/cm^{-1} (neat) 1600, 1270, 1123, 975; ^{1}H-NMR (400 MHz, $CDCl_3$) δ 7.54 (2H, d, H2/H6 J = 8.7), 7.45 – 7.30 (5H, m, H8-H12), 6.75 (2H, d, H3/H5 J = 8.8), 5.02 (2H, s, CH_2); ^{13}C-NMR (100 MHz, $CDCl_3$) δ 158.7 (C4), 138.3 (C2/C6), 136.6, 128.8, 128.2, 127.5, 117.4 (C3/C5), 83.2 (C1), 70.6 (CH_2).

9.41 Operation of the Advion NanoTek Microfluidic System

All radiosynthetic work conducted in-house, including the preparation and drying of [^{18}F]fluoride was performed on the Advion NanoTek Microfluidic System, operated and controlled by the NanoTek 1.4 software. The system consists of a base module (BM), concentrator module (CM), and reactor module (RM). The BM consists of two reagent cartridges (P1 and P2) used to dispense metered amounts of reactants to the microreactors for radiolabelling reactions. These cartridges comprise of a high-pressure syringe pump connected to an eight-way bridged valve supporting a looped-reservoir from which reagents are dispensed towards the microreactor. The RM consists of the isotope reagent (P3) and microreactor cartridges, as well as an eight-way distribution valve (DV) used to direct the reaction bolus to the user-desired location. P3 receives the solution of [^{18}F]fluoride (PTS-1 or PTS-2) from the CM module where it is prepared from a volume of cyclotron produced [^{18}F]fluoride in [^{18}O]H_2O. The CM module consists of a low-pressure, six-way valve reagent cartridge (CM1) and vessel chamber capable of rapid heating and evaporation of solvent. It is possible to subject the CM vessel to a combination of reduced pressure and a

positive flow of nitrogen gas allowing the [^{18}F]fluoride to be dried *via* several azeotropic distillations with MeCN.

Throughout this work, the crude reaction mixture was swept into an electronic injection valve (Smartline Valve Drive: Knauer, Germany) for direct injection onto the radio-HPLC system. The enclosed fluid paths of this tandem synthetic and analytical system ensured that the results obtained were representative of the crude reaction mixture as potential volatile products could not be lost. Operation of this valve and the initialisation of the HPLC analysis was also controlled by the NanoTek software. This software may be operated in several modes; in 'Discovery Mode' user-directed macros automate all procedures involved in the synthetic process, thereby allowing simple and rapid throughput of multiple reactions. These procedures can also be divided into their constituent parts and controlled separately within 'Manual Mode' which, therefore, allows for finer control of the system. In 'Sequence Mode' detailed macros can be written, manipulated and combined to enable extensive and complex processes to be performed with minimal user intervention. Throughout this study, user-control fluctuated between the three modes, for optimal system management.[110]

9.42 Preparation of Tetraethylammonium [^{18}F]Fluoride

Cyclotron produced, no-carrier-added [^{18}F]fluoride (5-100 mCi) in [^{18}O]H2O (1-5 mL) was adsorbed onto a pre-conditioned anion exchange resin (QMA: Waters Sep-Pak1 Light Accell Plus) before being released using a solution of K_2CO_3 (1.18 mg; 8 μmol) in MeCN/H2O (9:1 (v/v) 450 mL) (PTS-1); or $Et_4N{\cdot}HCO_3$ (3.4 mg; 17 μmol) in MeCN/H_2O (9:1 (v/v) 450 mL) (PTS-2) and into a V-vial (2 mL, Wheaton). The solutions were dried by two successive azeotropic evaporations using MeCN (450 mL) at 100 °C and under a positive flow of N_2. The [^{18}F]$Et_4N{\cdot}F$ was then dissolved in DMF (450 mL) and loaded into the storage loop (P3: 401 mL) on the microfluidic system.[110]

9.43 Radiofluorination of Diaryliodonium Salts using the Advion NanoTek Microfluidic System

Dry [^{18}F]fluoride (5-100 mCi, 450 mL DMF) and solutions of the diaryliodonium salt precursor in DMF at 10 mg/mL) were loaded into their respective storage loops (loop 3 and loop 1 respectively). Capillaries that lead from P1 and P3 to the microreactor were primed with their respective reagents. Prior to recording data several priming reaction runs were performed to confirm the integrity of the synthetic platform and the in-line analytical HPLC system. A set volume of either PTS-1 or PTS-2 (10 mL) and a variable volume of the precursor (5-20 mL: stoichiometry assessment) were dispensed into the pre-heated microreactor (130-190 °C) at pre-determined flow rates (10-30 mL/min). This is achieved by the syringes of P1 and P3, simultaneously dispensing precursor and [^{18}F]fluoride solutions (using either PTS-1 or PTS-2) from their respective loops, into the microreactor using a fixed volume of system solvent at a preset flow rate. The solutions initially mix at the entrance to the microreactor. User-operated computer software determines the reaction parameters - temperature, time and stoichiometry (P1:P3). Following completion of the reaction, P3 sweeps the crude mixture to the DV where it is directed towards the electronic injector and radio-HPLC system allowing the radiochemical yield of the process to be determined. At the start and end of each series of experiments the BM, RM, microreactor and associated transfer lines were cleaned using DMF and the CM system with acetonitrile.

HPLC methods were carried out using an Agilent 1200 HPLC system equipped with a UV absorbance detector (λ_{max} 254 nm) and a radioactivity detector (LabLogic Flow Count). The [^{18}F]fluoroarenes were not isolated and the radiochemical yield (RCY) reported relates to the amount of radioactivity of the product relative to the total radioactivity detected by radio-HPLC on analysis of the reaction mixture.[110]

10 Appendix

10.1 Crystal data and structure refinement for (4-(benzyloxy)phenyl)(4-methoxyphenyl)iodonium trifluoroacetate (149)

Table 1. Crystal data and structure refinement for mac120022.

Identification code	mac120022	
Chemical formula (moiety)	$C_{23}H_{20}F_3IO_4$	
Chemical formula (total)	$C_{23}H_{20}F_3IO_4$	
Formula weight	514.26	
Temperature	150(2) K	
Radiation, wavelength	MoKα, 0.71073 Å	
Crystal system, space group	triclinic, $P\bar{1}$	
Unit cell parameters	a = 8.6798(4) Å	α = 70.088(4)°
	b = 9.7400(4) Å	β = 80.985(4)°
	c = 13.2405(6) Å	γ = 81.327(4)°
Cell volume	1033.71(8) $Å^3$	
Z	2	
Calculated density	1.652 g/cm^3	
Absorption coefficient μ	1.595 mm^{-1}	
F(000)	508	
Crystal colour and size	colourless, 0.40 × 0.30 × 0.02 mm^3	
Reflections for cell refinement	3425 (θ range 3.0 to 28.6°)	
Data collection method	Xcalibur, Atlas, Gemini ultra thick-slice ω scans	
θ range for data collection	3.0 to 28.6°	
Index ranges	h –11 to 10, k –11 to 11, l –17 to 16	
Completeness to θ = 28.6°	81.6 %	
Reflections collected	8778	
Independent reflections	4320 (R_{int} = 0.0417)	
Reflections with $F^2>2\sigma$	3627	
Absorption correction	semi-empirical from equivalents	
Min. and max. transmission	0.5678 and 0.9688	
Structure solution	direct methods	
Refinement method	Full-matrix least-squares on F^2	
Weighting parameters a, b	0.0226, 0.0000	
Data / restraints / parameters	4320 / 0 / 291	
Final R indices [$F^2>2\sigma$]	R1 = 0.0409, wR2 = 0.0654	
R indices (all data)	R1 = 0.0563, wR2 = 0.0711	
Goodness-of-fit on F^2	1.024	
Largest and mean shift/su	0.001 and 0.000	
Largest diff. peak and hole	0.77 and –0.77 e $Å^{-3}$	

10.2 Crystal data and structure refinement for (4-(benzyloxy)phenyl)(2-thienyl)iodonium trifluoroacetate (150)

Table 1. Crystal data and structure refinement for mac12.

Identification code	mac120012	
Chemical formula (moiety)	$C_{21}H_{17}F_3INO_3S$	
Chemical formula (total)	$C_{21}H_{17}F_3INO_3S$	
Formula weight	547.32	
Temperature	150(2) K	
Radiation, wavelength	MoKα, 0.71073 Å	
Crystal system, space group	triclinic, $P\bar{1}$	
Unit cell parameters	a = 5.9984(4) Å	α = 68.019(10)°
	b = 17.5919(19) Å	β = 87.701(7)°
	c = 21.971(2) Å	γ = 83.912(7)°
Cell volume	2137.8(3) $Å^3$	
Z	4	
Calculated density	1.701 g/cm^3	
Absorption coefficient μ	1.644 mm^{-1}	
F(000)	1080	
Crystal colour and size	colourless, 0.40 × 0.30 × 0.30 mm^3	
Reflections for cell refinement	5408 (θ range 3.0 to 28.5°)	
Data collection method	Xcalibur, Atlas, Gemini ultra thick-slice ω scans	
θ range for data collection	3.0 to 26.0°	
Index ranges	h –7 to 6, k –20 to 21, l –26 to 27	
Completeness to θ = 26.0°	96.7 %	
Reflections collected	17218	
Independent reflections	8153 (R_{int} = 0.0397)	
Reflections with $F^2>2\sigma$	6983	
Absorption correction	semi-empirical from equivalents	
Min. and max. transmission	0.5593 and 0.6383	
Structure solution	direct methods	
Refinement method	Full-matrix least-squares on F^2	
Weighting parameters a, b	0.0378, 3.8934	
Data / restraints / parameters	8153 / 0 / 591	
Final R indices [$F^2>2\sigma$]	R1 = 0.0464, wR2 = 0.1029	
R indices (all data)	R1 = 0.0565, wR2 = 0.1095	
Goodness-of-fit on F^2	1.126	
Extinction coefficient	0.0001(2)	
Largest and mean shift/su	0.002 and 0.000	
Largest diff. peak and hole	2.45 and –1.04 e $Å^{-3}$	

10.3 Crystal data and structure refinement for (4-(benzyloxy)phenyl)(phenyl)iodonium trifluoroacetate (151)

Identification code	mac120001	
Chemical formula (moiety)	$C_{21}H_{16}F_3IO_3$	
Chemical formula (total)	$C_{21}H_{16}F_3IO_3$	
Formula weight	500.24	
Temperature	150(2) K	
Radiation, wavelength	MoKα, 0.71073 Å	
Crystal system, space group	triclinic, $P\bar{1}$	
Unit cell parameters	a = 9.1481(11) Å	α = 112.018(12)°
	b = 9.6626(12) Å	β = 96.244(10)°
	c = 12.4431(14) Å	γ = 100.553(10)°
Cell volume	983.3(2) $Å^3$	
Z	2	
Calculated density	1.690 g/cm^3	
Absorption coefficient μ	1.675 mm^{-1}	
F(000)	492	
Crystal colour and size	colourless, 0.40 × 0.20 × 0.04 mm^3	
Reflections for cell refinement	2404 (θ range 3.2 to 28.5°)	
Data collection method	Xcalibur, Atlas, Gemini ultra thick-slice ω scans	
θ range for data collection	3.2 to 26.0°	
Index ranges	h –11 to 10, k –9 to 11, l –14 to 15	
Completeness to θ = 26.0°	96.7 %	
Reflections collected	7074	
Independent reflections	3739 (R_{int} = 0.0597)	
Reflections with $F^2>2\sigma$	3219	
Absorption correction	semi-empirical from equivalents	
Min. and max. transmission	0.5539 and 0.9360	
Structure solution	direct methods	
Refinement method	Full-matrix least-squares on F^2	
Weighting parameters a, b	0.0560, 0.2840	
Data / restraints / parameters	3739 / 3 / 267	
Final R indices [$F^2>2\sigma$]	R1 = 0.0476, wR2 = 0.1097	
R indices (all data)	R1 = 0.0581, wR2 = 0.1214	
Goodness-of-fit on F^2	1.082	
Extinction coefficient	0.0003(7)	
Largest and mean shift/su	0.001 and 0.000	
Largest diff. peak and hole	1.66 and –1.31 e $Å^{-3}$	

10.4 Crystal data and structure refinement for (4-(acetoxy)phenyl)(4-methoxyphenyl)iodonium trifluoroacetate (152)

Identification code	mac120013	
Chemical formula (moiety)	$C_{19}H_{17}F_3INO_5$	
Chemical formula (total)	$C_{19}H_{17}F_3INO_5$	
Formula weight	523.24	
Temperature	150(2) K	
Radiation, wavelength	MoKα, 0.71073 Å	
Crystal system, space group	monoclinic, $P12_1/c1$	
Unit cell parameters	a = 10.4335(4) Å	α = 90°
	b = 11.9198(4) Å	β = 103.108(4)°
	c = 16.8661(8) Å	γ = 90°
Cell volume	2042.90(14) $Å^3$	
Z	4	
Calculated density	1.701 g/cm^3	
Absorption coefficient μ	1.624 mm^{-1}	
F(000)	1032	
Crystal colour and size	colourless, 0.45 × 0.40 × 0.40 mm^3	
Reflections for cell refinement	4854 (θ range 3.3 to 28.5°)	
Data collection method	Xcalibur, Atlas, Gemini ultra thick-slice ω scans	
θ range for data collection	3.3 to 28.5°	
Index ranges	h –13 to 9, k –12 to 15, l –21 to 19	
Completeness to θ = 25.0°	99.8 %	
Reflections collected	10253	
Independent reflections	4341 (R_{int} = 0.0234)	
Reflections with $F^2>2\sigma$	3710	
Absorption correction	semi-empirical from equivalents	
Min. and max. transmission	0.5285 and 0.5627	
Structure solution	direct methods	
Refinement method	Full-matrix least-squares on F^2	
Weighting parameters a, b	0.0219, 4.2244	
Data / restraints / parameters	4341 / 0 / 266	
Final R indices [$F^2>2\sigma$]	R1 = 0.0302, wR2 = 0.0651	
R indices (all data)	R1 = 0.0389, wR2 = 0.0717	
Goodness-of-fit on F^2	1.057	
Extinction coefficient	0.00193(15)	
Largest and mean shift/su	0.000 and 0.000	
Largest diff. peak and hole	1.26 and –0.91 e $Å^{-3}$	

10.5 [^{18}F]Fluoride Drying Macro

0 Wait Drying macro. Ensure needle is fully inserted into target water vial. Ensure QMA cartridge is loaded. Ensure all solutions are prepared and installed. Ensure all plumbing is correct.
1000 L37020000800054 L3602000300004E Set Conc 1 to 80oC
2000 /5o1V1200A6000M3000o5V1200A0M2000R Load target water
15000 /5o6V1200A6000M2000o3V1200A0R Remove target water
15000 L3702000100004D L3602000300004E Set Conc 1 to 100oC
2000 /7U2M5000U1M5000u2R Turn on the Nitrogen
10000 /5o2V1000P5000M2000go5V400D750M15000G4o2V2000A0R Add 400 uL of PTA
105000 /5M90000R Wait 100s for conc vial to dry PTA solution
100000 /5o4V1000P6000M2000o5V75D3600M2000o6V75D1200M2000o2V2000A0R Add 400 uL of MeCN (1) and flush back PTA line
75000 /5M30000R Wait 20s for conc vial to dry MeCN (1)
20000 /5o4V1000P6000M2000o6V75D3600M2000o2V2000A0R Add 400 uL of MeCN (2) and flush back PTA line
45000 /5M30000R Wait 20s for conc vial to dry MeCN (2)
20000 /7u1R Turn off the Nitrogen
2000 /3o1V2000A0M2000o8V2000A15600M2000o6V800A0R Add 325 uL of DMF
40000
/3go4V1600A19200M2000V3200A0M2000G6o8V3200A3600M2000o4V3200A0R Mix the solvent with the fluoride. Add 75 uL of DMF to flush line F

10.6 Autodiscovery Mode Operation

140000 L37020000250053 L3602000300004E Set Conc 1 to 25oC
2000 Wait End of drying macro. Pump 3 can now be prepared.
6.11.2 Autodiscovery Mode Cleaning
2000 Wait P1,2,3 reagent lines will be back-flushed. Place Reactor outlet into waste

1000
/1o1V3200A0o8A48000M1000o1A0o8A48000M1000o4V1600A0o8V3200A48000M100
0o3V100A0R P1, Clean reagent line, loop and load line
5000
/2o1V3200A0o8A48000M1000o1A0o8A48000M1000o4V1600A0o8V3200A48000M100
0o3V100A0R P2, Clean reagent line, loop and load line
2000 /7o1R Hub to Waste (A)
5000
/3o1V3200A0o8A48000M1000o1A0o8A48000M1000o4V1600A0o8V3200A24000o3V1
00A0R P3, Clean reagent line, loop and load line Sweep
1000 /6go4V600P3600M10006o2V60D3600G2R Flush APT line x2
160000 /6go4V600P3600M10006o5V60D3600G2R Flush QMA x2
160000 /6go4V600P3600M10006o6V60D3600G2R Flush line F x2
230000 /3o8V3200A24000M1000o2V100A0R P3, Sweeps reactor contents to waste

11 References

[1] W. Hollingworth, C. J. Todd, M. I. Bell, Q Arafat, S. Girling, K. R. Karia and A. K. Dixon, *Clin. Radiol.*, 2000, **55**, 825-831.
[2] J. R. Lindner, *J. Nucl. Cardiol.*, 2004, **11**, 215-221.
[3] P. K. Spiegal, *Am. J. Roentgenol.*, 1995, **164**, 241-243.
[4] K. A. Wood, P. J. Hoskin and M. I. Saunder, *Clin. Oncol.*, 2007, **19**, 237-255.
[5] S. M. Ametamey, M. Honer and P. A. Schubiger, *Chem. Rev.*, 2008, **108**, 1501-1516.
[6] P. Price and G. Laking, *Clin. Oncol.*, 2004, **16**, 172-175.
[7] L. Zhu, K. Ploessl and H. F. Kung, *Chem. Soc. Rev.*, 2014, **43**, 6683-6691.
[8] M. L. James and S. S. Gambhir, *Physiol. Rev.*, 2012, **92**, 897-965.
[9] W. H. Sweet, *New Engl. J. Med.*, 1951, **245**, 875-878.
[10] F. R. Wrenn, M. L. Good and P. Handler, *Science*, 1951, **113**, 525-527
[11] M. E. Phelps, E. J. Hoffman, N. A. Mullani, C. S. Higgins and M. M. T. Pogossian, *IEEE T. Nucl. Sci.,* 1976, **23**, 516-522.
[12] http://www.cidpusa.org/PET_Scan.html Accessed 09/01/15.
[13] S. I. Ziegler, *Nucl. Phys. A*, 2005, **752**, 679c-687c.
[14] http://www.hopkinscoloncancercenter.org/CMS/CMS_Page.aspx?CurrentUDV=59&CMS_Page_ID=FE1655FC-B16B-40A8-906E-6A68BC0EA46B Accessed 28/06/15.
[15] S. Hess, P. F. Høilund-Carlsen and A. Alavi, *Contribution of FDG to Modern Medicine, Part I, An Issue of PET Clinics*, Elsevier Health Sciences, Makati City, 2014.
[16] J. S. Welsh, *Oncologist*, 2006, **11**, 62-64
[17] C. L. Melcher, *J. Nucl. Med*, 2000, **41**, 1051-1055.
[18] P. Schotanus, *Nucl. Tracks. Rad. Meas.*, 1993, **21**, 19-22.
[19] http://eu.mouser.com/applications/medical-imaging-overview/ Accessed 01/07/15.
[20] S. E. Derenco, M. J. Weber, E. Bourret-Courchesne and M. K. Klintenberg, *Nucl. Instrum. Meth. A*, 2003, **505**, 111-117.

[21] F. Daghighian, P. Shenderov, K. S. Pentlow, M. C. Graham, B. Eshaghian, C. Melcher and J. S. Schweitzer, *IEEE T. Nucl. Sci.*, 1993, **40**, 1045-1047.
[22] B. J. Picher, H. F. Wherl and M. S. Judenhofer, *J. Nucl. Med*, 2008, **6**, 5S-28S.
[23] A. Acton, *Advances in Imaging Technology Research and Application: 2013 Edition.*
[24] S. R. Cherry, M. P. Tornai, C. S. Levin, S. Siegel and E. J. Hoffman, *IEEE T. Nucl. Sci.*, 1995, **42**, 1064-1068.
[25] S. I. Zeigler, B. J. Pichler, G. Boening, M. Rafecas, W. Pimpl, E. Lorenz, N. Schmitz and M. Schwaiger, *European J. Nucl. Med*, 2001, **28**, 136-143.
[26] R. Grazioso, N. Zhang, J. Corbeil, M. Schmand, R. Ladebeck, M. Vester, G. Schnur, W. Renz and H. Fischer, 2006, *Nucl. Instrum. Meth. A*, **569**, 301-305.
[27] R. Lecomte, J. Cadorette, S. Rodrigue, M. Bentourkia, D. Rouleau, R. Yao and P. Msaki, *IEEE Eng. Med. Biol.*, 1995, **1**, 525-526.
[28] http://depts.washington.edu/nucmed/IRL/pet_intro/intro_src/section2.html Accessed 28/06/15.
[29] T. G. Turkington, *J. Nucl. Med Technology*, 2001, **29**, 1-8.
[30] A. H. Compton, *Phys. Rev. C*, 1923, **21**, 483-502.
[31] M. Gerd and S. K. Joel, *Phys. Med. Biol.*, 2006, **51**, R117.
[32] W. A. Kalender, *Radiology*, 1990, **176**, 181-183.
[33] P. E. Kinahan, B. H. Hasegawa and T. Beyer, *Semin. Nucl. Med.*, 2003, **33**, 166-179.
[34] D. L. Bailey, D. W. Townsend, P. E. Valk and M. N. Maisey, *Positron Emission Tomography Basic Sciences*, Springer, London, 2005.
[35] N. G. Haynes, J. L. Lacy, N. Nayak, C. S. Martin, D. Dai and C. J. Mathias, *J. Nucl. Med*, 2000, 309-314.
[36] K. D. McElvany, K. T. Hopkins and M. J. Welsh, *Int. J. Appl. Radiat. Is.*, 1984, 521-524.
[37] A. W. Chao and W. Chou, *Reviews of Accelerator Science and Technology, Volume 2, Medical Applications of Accelerators*, World Scientific Publishing Co. Pte. Ltd., Singapore, 2009, 21-27.
[38] http://www3.gehealthcare.com/en/products/categories/pet-radiopharmacy/tracer_center_equipment/minitracecyclotron Accessed 09/07/15.
[39] M. M. Ter-Pogossian and P. Herscovithc, *Semin. Nucl. Med.*, 1985, **15**, 377-394.
[40] H. Ziessman, J. O'Malley and J. Thrall, *Nuclear Medicine: The Requisites*, Elsevier Saunders, Philadelphia, 4th Edition, 2013.
[41] D. O'Hagon and D. B. Harper, *J. Fluorine Chem.*, 1999, **100**, 127-133.
[42] J. Wang, M. Sánchez-Roselló, J. L. Aceňa, C. D. Pozo, A. E. Sorochinsky, S. Fustero, V. A. Soloshonok and H. Liu, *Chem. Rev.*, 2014, **114**, 2431-2506.
[43] P. Kirsch, *Modern Flouroorganic Chemistry Synthesis, Reactivity, Applications*, John Wiley and Sons ltd, Chichester, 2nd Edition, 2013.
[44] D. O'Hagan, *J. Fluorine Chem.*, 2010, **131**, 1071-1081.
[45] K. Müller, C. Faeh and F. Diederich, *Science*, 2007, **317**, 1881-1886.
[46] W. K. Hagmann, *J. Med. Chem.*, 2008, **51**, 4359-4369.
[47] C. M. Oliphant and G. M. Green, *Am. Fam. Physician*, 2002, **65**, 455-464.
[48] A. C. Altamura, A. R. Moro and M. Percudani, *Clin. Pharmacokinet.*, 1994, **26**, 201-214.
[49] R. K. Aggarwal and R. Showkathali, *Exp. Opin. Pharmacother.*, 2013, **14**, 1215-1227.
[50] P. L. McCormack, *Drugs*, 2011, **71**, 2457-2489.
[51] I. Ojima, *Fluorine in Medicinal Chemistry and Chemical Biology*, John Wiley and Sons ltd, Chichester, 2009.
[52] J. A. Dean, *Lange's Handbook of Chemistry*, McGraw-Hill, New York, 15th Edition, 1999.
[53] J. C. Kath, W. H. Brissette, M. F. Brown, M. Conklyn, A. P. DiRico, P. Dorff, R. P. Gladue, B. M. Lillie, P. D. Lira, E. N. Mairs, W. H. Martin, E. B. McElroy, M. A. McGlynn, T. J. Paradis, C. S. Poss, I. A. Stock, L. A. Tylaska and D. Zheng, *Bioorg. Med. Chem. Lett.*, 2004, **14**, 2169-2173.
[54] B. Meunier, S. P. de Visser and S. Shaik, *Chem. Rev.* 2004, **104**, 3947-3980.
[55] S. S. Batsanov, *Neorg. Mater.*, 2001, **37**, 1031-1046.
[56] B. K. Park, N. R. Kitteringham and P. M. O'Neill, *Annu. Rev. Pharmacol.* , 2001, **41**, 443-470.
[57] H.-J. Böhm, D. Banner, S. Bendels, M. Kansy, B. Kuhn, K. Müller, U. Obst-Sander and M. Stahl, *Chem. Bio. Chem*, 2004, **5**, 637-643.
[58] B. E. Smart, *J. Fluorine Chem.*, 2001, **109**, 3-11.
[59] M. Jaccaud, R. Faron, D. Devilliers and R. Romano, "*Fluorine" Ullmann's Encyclopedia of Industrial Chemistry*, Wiley-VCH, Weinheim, 2000, 381-395.
[60] P. J. Crocker, A. Mahadevan, J. L. Wiley, B. R. Martin and R. K. Razdan, *Bioorg. Med. Chem. Lett.*, 2008, **17**, 1504-1507.

[61] K. Richardson, K. Cooper, M. S. Marriott, M. H. Tarbit, P. F. Troke and P. J. Whittle, *Reviews of infectious diseases*, (suppl. 3), 1990, **12**, S267-S271.
[62] D. S. Surasi, P. Bhambhvani, J. A. Baldwin, S. E. Almodovar and J. P. O'Malley, *J. Nucl. Med Technology*, 2014, **42**, 5-13.
[63] T. Ido, C. N. Wan, V. Casella, J. S. Fowler, A. P. Wolf, M. Reivich and D. E. Kuhl, *J. Labelled Compd. Rad.*, 1978, **14**, 175-183.
[64] A. Al-Nahhas, S. Khan, A. Gogbashian, E. Banti, L. Rampin and D. Rubello, *In Vivo*, 2008, **22**, 109-144.
[65] J. Brush, K. Boyd, F. Chappell, F. Crawford, M. Dozier, E. Fenwick, J. Glanville, A. Renehan, D. Weller and M. Dunlop, *Health Technology Assessment*, 2011, **15**, 1-192.
[66] F. Dammacco, G. Rubini, C. Ferrari, A. Vacca and V. Racanelli, *Clin. Exp. Med.*, 2015, **15**, 1-18.
[67] A. Newburg, A. Alavi and M. Reivich, *Semin. Nucl. Med.*, 2002, **32**, 13-34.
[68] P. M. Rossini and G. D. Forno, *Phys. Med. Rehabil. Clin. N. Am.*, 2004, **15**, 263-306.
[69] R. Scheid, T. Lincke, R. Voltz, D. Y. Von Cramon and O. Sabri, *Arch. Neurol.*, 2004, **61**, 1785-1789.
[70] R. J. Boado, K. L. Black and W. M. Pardridge, *Mol. Brain Res.*, 1994, **27**, 51-57.
[71] E. K. Pauwels, M. J. Ribeiro, J. H. Stoot, V. R. McCready, M. Bourguignon and B. Mazière, *Nucl. Med. Biol.*, 1998, **25**, 317-322.
[72] C. Plathow and W. A. Weber, *J. Nucl. Med*, 2008, **49**, 43S-63S.
[73] R. E. Coleman, *Nucl. Med. Biol.*, 2000, **27**, 689-690.
[74] P. W. Miller, N. J. Long, R. Vilar and A. D. Gee, *Angew. Chem. Int. Edit.*, 2008, **47**, 8998-9033.
[75] R. Boellaard, M. J. O'Doherty, W. A. Weber, F. M. Mottaghy, M. N. Lonsdale, S. G. Stroobants, W. J. G. Oyen, J. Kotzerke, O. S. Hoekstra, J. Pruim, P. K. Marsden, K. Tatsch, C. J. Hoekstra, E. P. Visser, B. Arends, F. J. Verzijlbergen, J. M. Zijlstra, E. F. I. Comans, A. A. Lammertsma, A. M. Paans, A. T. Willemsen, T. Beyer, A. Bockisch, C. Schaefer-Prokop, D. Delbeke, R. P. Baum, A. Chiti and B. J. Krause, *Eur. J. Nucl. Med. Mol. Imaging*, 2010, **37**, 181-200.
[76] http://www.med.harvard.edu/JPNM/chetan/basics/basics.html Accessed 26/08/15.
[77] K. Manohar, B. R. Mittal, A. Bhattacharya, P. Malhotra and S. Varma, *Indian J. Nucl. Med*, 2013, **28**, 85-92.
[78] K. Strijckmans, *Comput. Med. Imag. Grap.*, 2001, **25**, 69-78.
[79] S. Fukumoto, *Igaku Butsuri*, 2012, **32**, 90-97.
[80] M. E. Phelps, *PET: Molecular Imaging and its Biological Applications*, Springer-Verlag, New York, 2004.
[81] E. O. Lawrence and M. S. Livingston, *Phys. Rev. C*, 1932, **40**, 19-35.
[82] F. E. Close, M. Martin and C. Sutton, *The Particle Odyssey: A Journey to the Heart of Matter*, Oxford University Press, Oxford, 2004, 84-87.
[83] http://www3.gehealthcare.com/en/Products/Categories/PET-Radiopharmacy/TRACER_Center_Equipment/PETtrace_800_Series_Cyclotron#tabs/tabEFAE0173DB5B444D832B11456DD14B5D Accessed 30/08/15.
[84] P. W. Schmor, *Proceedings of International Conference on Cyclotrons and their Applications (CYCLOTRONS 2010)*, ed. C. Petit-Jean-Genaz, Joint Accelerator Conference Website, Geneva, 2010, 419-424.
[85] R. van Grieken and M. de Bruin, *Pure Appl. Chem.*, 1994, **66**, 2513-2516.
[86] E. Rutherford, *Nature*, 1910, **84**, 430-431.
[87] R. E. Hendrick, *Radiology*, 2010, **257**, 246-253.
[88] D. J. Brenner and E. J. Hall, *New Engl. J. Med.*, 2007, **357**, 2277-2284.
[89] F. A. Cucinotta and M. Durante, *Lancet Oncol.*, 2006, **7**, 431-435.
[90] ICRP Publication 103. Ann. ICRP 37 (2-4).
[91] G. K. S. Prakash, J. Hu, M. M. Alauddin, P. S. Conti and G. A. Olah, *J. Fluorine Chem.*, 2003, **121**, 239-243.
[92] M. J. Adam and S. Jivan. *Appl. Radiat. Isotopes*, 1988, **39**, 1203–1206.
[93] V. Casella, T. Ido, A. P. Wolf, J. S. Fowler, R. R. MacGregor and T. J. Ruth, *J. Nucl. Med*, 1980, **21**, 750-757.
[94] A. Bishop, N. Satyamurthy, G. Bida and J. R. Barrio, *Nucl. Med. Biol.*, 1996, **23**, 559-565.
[95] J. Bergman and O Solin, *Nucl. Med. Biol.*, 1997, **24**, 677-683.
[96] H. Teare, E. G. Robins, E. Årstad, S. K. Luthra and V. Gourverneur, *Chem. Commun.*, 2007, 2330-2332.
[97] O. Jacobson, D. O. Kiesewetter and X. Chen, *Bioconjugate Chem.*, 2015, **26**, 1-18.
[98] H. H. Coenen, *Proceedings of Ernst Schering Foundation Symposium*, ed. G. Stock and C. Klein, Springer, London, 2007, 15-50.

[99] L. Cai, S. Lu, and V. W. Pike, *Eur. J. Org. Chem.*, 2008, 2853-2873.
[100] F. Füchtner, S. Preusche, P. Mäding, J. Zessin and J. Steinbach, *Nucl. Med.*, 2008, **47**, 116-119.
[101] E. Hess, G. Blessing, H. H. Coenen and S. M. Qaim, *Appl. Radiat. Isotopes*, 2000, **52**, 1431-1440.
[102] O. Jacobson and X. Chen, *Curr. Top. Med. Chem.*, 2010, **10**, 1048-1059.
[103] Jörgen Bergman and Olof Solin, *Nucl. Med. Biol.*, 1997, **24**, 677-683.
[104] N. Bryan, *Introduction to the Science of Medical Imaging*, Cambridge University Press, Cambridge, 2010, 202-206.
[105] http://isites.harvard.edu/fs/docs/icb.topic1050994.files/CH156_Lecture7%20Fluorine%2018. pdf Accessed 01/09/15.
[106] H. Kitano, Y. Magata, A. Tanaka, T. Mukai, Y. Kuge, K. Nagatsu, J. Konishi and H. Saji, *Annals of Nucl. Med.*, 2000, **15**, 75-78.
[107] http://www.medicalisotopes.com/display_category.php?id=2 Accessed 01/09/15.
[108] R. Alberto, K. Ortner, N. Wheatley R. Schibli and A. P. Schubiger, *J. Am. Chem. Soc.*, 2001, **121**, 3135-3136.
[109] K. Hamacher and H. H. Coenen, *Appl. Radiat. Isotopes*, 2002, **57**, 853-856.
[110] C. D. Reed, G. G. Launay and M. A. Carroll, *J. Fluorine Chem.*, 2012, **143**, 231-237.
[111] H. Sun and S. G. DiMagno, *Chem. Commun.*, 2007, 528-529.
[112] S. H. Liang, T. L. Collier, B. H. Rotstein, R. Lewis, M. Steck and N. Vasdev, *Chem. Commun.*, 2013, **49**, 8755-8757.
[113] G. Pascali, P. Watts and P. A. Salvadori, *Nucl. Med. Biol.*, 2013, **40**, 776-787.
[114] A. M. Elizarow, *Lab Chip*, 2009, **9**, 1326-1333.
[115] http://www.ezag.com/home/products/radiopharma/radiosynthesis-technology.html Accessed 21/10/15
[116] http://abt-mi.com/en/our-solutions/overview Accessed 21/10/15
[117] M. Marengo, F. Lodi, S. Magi, G. Cicoria, D. Pancaldi and S. Boschi, *Appl. Radiat. Isotopes*, 2008, **66**, 295-302.
[118] S. J. Hobson, G. G. Launay and M. A. Carroll, presented in part at *PET Chemistry UK 2013,* Newcastle-upon-Tyne, September, 2013.
[119] L. Bowden, L. Vintro, P. Mitchell, R. O'Donnell, A. Marie-Seymour, G. J. Duffy, *Appl. Radiat. Isotopes*, 2009, 67, 248-255.
[120] J. Ermert, *BioMed Research International*, Hindawi Publishing Corporation, London, 2014.
[121] Y. Gu, D. Huang, Z. Liu, J. Huang and W. Zeng, *J. Med. Chem.*, 2011, **7**, 334-344.
[122] E. L. Cole, M. N. Stewert, R. Littich, R. Hoaraue and P. J. H. Scott, *Curr. Top. Med. Chem.*, 2014, **14**, 875-900.
[123] T. Furuya, J. E. Klein and T. Ritter, *Synthesis*, 2010, 1804-1821.
[124] H. Teare, E. G. Robins, A. Kirjavainen, S. Forsback, G. Sandford, O. Solin, S. K. Luthra and V. Gouverneur, *Angew. Chem. Int. Edit.*, 2010, **49**, 6821-6824.
[125] M. M. Aladdin, *Am. J. Nucl. Med. Mol. Imaging*, 2012, **2**, 55-76.
[126] G. W. M. Visser, G. C. M. Gorree, B. J. M. Braakhuis, and J. D. M. Herscheid, *European J. Nucl. Med*, 1989, **15**, 225-229.
[127] R. E. Ehrenkaufer, J. F. Potocki and D. M. Jewett, *J. Nucl. Med*, 1984, **25**, 333-337.
[128] M. Reivich, D. Kuhl, A. Wolf, J. Greenberg, M. Phelps, T. Ido, V. Casella, J. Fowler, E. Hoffman, A. Alavi, P. Som and L. Sokoloff, *Circ. Res.*, 1979, **44**, 127-137.
[129] H. H. Coenen and S. M. Moerlein, *J. Fluorine Chem.*, 1987, **36**, 64-75.
[130] M. Speranza, C. Y. Shiue, A. P. Wolf, D. S. Wilbur and G. Angelini, *J. Fluorine Chem.*, 1985, **30**, 97-107.
[131] G. W. Visser, B. W. Halteren, J. D. Herscheid, G. A. Brinkman and A. Hoeska, *Journal of the Chemical Society, Chem. Commun.*, 1984, 655-656.
[132] H. Teare, E. G. Robins, E. Årstad, S. K. Luthra and V. Gouverneur, *Chem. Commun.*, 2007, 2330-2332.
[133] S. D. Banister, M. Kassiou and F. Dollé, *Curr. Radiopharm.*, 2010, **2**, 68-80.
[134] D. Roeda and F. Dollé, *Curr. Radiopharm.*, 2010, **3**, 81-108.
[135] H. J. Wester, *Clin. Cancer Res.*, 2007, **13**, 3470-3481.
[136] P. Ayotte, M. H. Bert and P. Marchand, *J. Chem. Phys.*, 2005, **123**, 1-8.
[137] G. Gründer, T. Siessmeier, C. Lange-Asschenfeldt, I. Vernaleken, H-G. Buchholz, P. Stoeter, A. Drzezga, H. Lüddens, F. Rösch and P. Bertenstein, *Eur. J. Nucl. Med*, 2001, **28**, 1463-1470.
[138] S. M. Moerlein, *J. Nucl. Med*, 1990, **31**, 902.
[139] L. B. Been, A. J. H. Suurmeijer, D. C. P. Cobben, P. L. Jager, H. J. Hoekstra and P. H. Elsinga, *Eur. J. Nucl. Med. Mol. Imaging*, 2004, **31**, 1659-1672.

[140] M. Pretze, F. Wuest, T. Peppel, M. Köckerling and C. Mamat, *Tetrahedron Lett.*, 2010, **51**, 6410-6414.
[141] M. R. Kilbourn, C. S. Dence, M. J. Welch, C. J. Mathias, *J. Nucl. Med*, 1987, **28**, 462-470.
[142] G. Angelini, M. Speranza, A. P. Wolf, C. Y. Shiue, J. S. Fowler and M. Watanabe, *J. Labelled Compd. Rad.*, 1984, **21**, 1223–1226
[143] H. H. Coenen, *Synthesis and Application of Isotopically Labelled Compounds*, Elsevier Publications, Amsterdam, 1989, 433–448
[144] K. Hamacher and W. Hamkens, *Appl. Radiat. Isotopes*, 1995, **46**, 911-916.
[145] M. Karramkam, F. Hinnen, Y. Bramoullé, S. Jubeau and F. Dollé, *J. Labelled Compd. Rad.*, 2002, **45**, 1103-1113.
[146] E. Blom, F. Karimi and B. Langstrom, *J. Labelled Compd. Rad.*, 2009, **52**, 504-511.
[147] M. S. Haka, M. R. Kilbourn, G. L. Watkinds and S. A. Toorongian, *J. Labelled Compd. Rad.*, 1989, **27**, 823-833.
[148] G. Angelini, M. Speranza, A. P. Wolf and C. Y. Shiue, *J. Fluorine Chem.*, 1985, **27**, 177-191.
[149] T. J. McCarthy, A. U. Sheriff, M. J. Graneto, J. J. Talley and M. J. Welsh, *COX Inhibitors*, 2002, **43**, 117-124.
[150] C. Hansch, A. Leo and R. W. Taft, *Chem. Rev.*, 1991, **91**, 165-195.
[151] F. Dollé, *Curr. Pharm. Design.*, 2005, **11**, 3321-3235.
[152] V. V. Grushin, *Accounts Chem. Res.*, 1992, **25**, 529-536.
[153] F. G. Siméon, M. T. Wendahl and V. W. Pike, *J. Med. Chem.*, 2011, **54**, 901-908.
[154] F. G. Siméon, M. T. Wendahl and V. W. Pike, *Tetrahedron Lett.*, 2010, **51**, 6034-6036.
[155] H. U. Shetty, S. S. Zoghbi, F. G. Siméon, V. M. Patterson, R. B. Innis and V. W. Pike, *J. Pharmacol. Exp. Ther.*, 2008, **327**, 727-735.
[156] T. G. Hamill, S. Krause, C. Ryan, C. Bonnefous, S. Govek, T. J. Seiders, N/D. P. Cosford, J. Roppe, T. Kamenecka, S. Patel, R. E. Gibson, S. Sanabria, K. Riffel, W. Eng, C. King, X. Yang, M. D. Green, S. S. O'Malley, R. Hargreaves and H. D. Burns, *Synapse*, 2005, **56**, 205–216
[157] O. Wallach, *J. Org. Chem.*, 1886, **235**, 233-255.
[158] G. S. Balz, *Chem. Ber.*, 1927, **60**, 1186-1190.
[159] T. J. Tewson, M. E. Raichle and M. J. Welch, *Brain Res.*, 1980, **192**, 291-295.
[160] R. J. Hicks, *Cancer Imag.*, 2004, **4**, 22-24.
[161] Y. Xing, J. Choi, J. Peng, W-Y. Lin, G. Li, P. Conti, H-R. Tseng and K. Chen, *J. Nucl. Med*, 2014, **55**, 277.
[162] S. R. Cherry, *Semin. Nucl. Med.*, 2009, **39**, 348-353.
[163] S. Chen, M. R. Javed, H. K. Kim, J. Lei, M. Lazari, G. J. Shah, R. M. van Dam, P. Y. Keng and C. J. Kim, *Lab Chip*, 2014, **14**, 902-910.
[164] L. Mu, C. R. Fischer, J. P. Holland, J. Becaud, P. A. Schubiger, R. Schibli, S. M. Ametamey, K. Graham, T. Stellfield, L. M. Dinkelborg and L. Lehmann, *Eur. J. Org. Chem.*, 2012, **5**, 889-892.
[165] J-H. Chun, C. L. Morse, F. T. Chin and V. W. Pike, *Chem. Commun.*, 2013, **49**, 2151-2153.
[166] G. J. Kienzle, G. Reischl and H-J. Machulla, *J. Labelled Compd. Rad.*, 2005, **48**, 259-273.
[167] G. Reischl, G. J. Kienzle and H-J. Machulla, *Appl. Radiat. Isotopes*, 2003, **58**, 679-683.
[168] J. P. Seibyl, W. Chen and D. H. Silverman, *Semin. Nucl. Med.*, 2007, **37**, 440-450.
[169] M. Tredwell and V. Gourverneur, *Angew. Chem. Int. Edit.*, 2012, **51**, 11426-11437.
[170] V. Gouverneur, *Nat. Chem.*, 2012, **4**, 152-154.
[171] J. R. Brandt, E. Lee, G. B. Boursalian and T. Ritter, *Chem. Sci.* , 2014, **5**, 189-179.
[172] E. Lee, A. S. Kamlett, D. C. Powers, C. N. Neumann, G. B. Boursalian, T. Furuya, D. C. Choi, J. M. Hooker and T. Ritter, *Science*, 2011, **334**, 639-642.
[173] R. Hähnel and E. Twaddle, *J. Steriod. Biochem. Mol. Biol.*, 1974, **5**, 119-122.
[174] Z. Gao, Y. H. Lim, M. Tredwell, L. Li, S. Verhoog, M. Hopkinson, W. Kaluza, T. L. Collier, J. Passchier, M. Huiban and V. Gouverneur, *Angew. Chem. Int. Edit.*, 2012, **51**, 6733-6737.
[175] Z. Gao, V. Gouverneur and B. G. Davis, *J. Am. Chem. Soc.*, 2013, **135**, 13612-13615.
[176] E. Lee, J. M. Hooker and T. Ritter, *J. Am. Chem. Soc.*, 2012, **134**, 17456-17458.
[177] V. W. Pike and F. I. Aigbirhio, *J. Chem. Soc., Chem. Commun.*, 1995, 2215-2216.
[178] E. A. Merritt and B. Olofsson, *Angew. Chem. Int. Edit.*, 2009, **48**, 9052-9070.
[179] S. Telu, J. H. Chun, F. G. Siméon, S. Lu and V. W. Pike, *Org. Biomol. Chem.*, 2011, **9**, 6629-6638.
[180] M. S. Yusubov, D. Y. Svitich, M. S. Markina and V. V. Zhdankin, *Arkivoc*, 2013, 364-395.
[181] M. R. Zhang, K. Kumata and K. Suzukhi, *Tetrahedron Lett.*, 2007, **48**, 8632-8635.
[182] L. Hadjiarapoglou, S. Spyroudis and A. Varvoglis, *J. Am. Chem. Soc.*, 1985, **107**, 7178-79.
[183] S-Z. Zhu, *Heteroatom Chem.*, 1994, **5**, 9-18.
[184] W. Kirmse, *Eur. J. Org. Chem.*, 2005, 237-260.

[185] V. V. Zhdankin, *Chem. Rev.*, 2008, **108**, 5299-5358.
[186] J. Cardinale, J. Ermert, S. Humpert and H. H. Coenen, *RSC Adv.*, 2014, **4**, 17293-17299.
[187] B. Leader, Q. J. Baca and D. E. Golan, *Nat. Rev. Drug. Discov.*, 2008, **7**, 21-39.
[188] J. M. Reichert, *Nat. Rev. Drug. Discov.*, 2003, **2**, 1304-1351.
[189] S. Aggarwal, *Nat. Biotechnol.*, 2010, **28**, 1165-1171.
[190] S. Aggarwal, *Nat. Biotechnol.*, 2012, **30**, 1191-1197.
[191] Y. Li, Z. Liu, C. W. Harwig, M. Pourghiasian, J. Lau, K. S. Lin, P. Schaffer, F. Benard, and D. M. Perrin, *Am. J. Nucl. Med. Mol. Imaging*, 2013, **3**, 57-70.
[192] Y. Li, Z. Liu, J. Lozada, M. Q. Wong, K. S. Lin, D. Yapp and D. M. Perrin, *Nucl. Med. Biol.*, 2013, **40**, 959-966.
[193] O. Jacobson, L. Zhu, Y. Ma, I. D. Weiss, X. Sun, G. Nu, D. O. Kiesewetter and X. Chen, *Bioconjugate Chem.*, 2011, **22**, 422-428.
[194] T. Kniess, M. Laube, P. Brust and J. Steinbach, *J. Med. Chem. Commun.*, 2015, **6**, 1714.
[195] E. Al-Momani, N. Malik, H. J. Machulla, S. N. Reske and C. Solbach, *J. Radioanal. Nucl. Chem.*, 2013, **295**, 2289-2294.
[196] C. Prenant, C. Cawthorne, M. Fairclough, N. Rothwell and H. Boutin, *Appl. Radiat. Isotopes*, 2010, **68**, 1721-1727.
[197] P. J. Riss, V. Ferrari, L. Brichard, P. Burke, R. Smith and F. I. Aigbirhiro, *Org. Biomol. Chem.* , 2012, **10**, 6980-6986.
[198] E. Valeur and M. Bradley, *Chem. Soc. Rev.*, 2009, **38**, 606-631.
[199] F. Wüst, C. Hultsch, R. Bergmann, B. Johannsen and T. Henle, *Appl. Radiat. Isotopes*, 2003, **59**, 43-38.
[200] G. Vaidyanathan and M. R. Zalutsky, *Bioconjugate Chem.*, 1994, **5**, 352-356.
[201] P. Mäding, F. Füchtner and F. Wüst, *Appl. Radiat. Isotopes*, 2005, **63**, 329-332.
[202] L. Lang and W. C. Eckelman, *Appl. Radiat. Isotopes*, 1997, **48**, 169-173.
[203] J. Marik and J. L. Sutcliffe, *Appl. Radiat. Isotopes*, 2007, **65**, 199-203.
[204] X. Chen, M. Tohme, R. Park, Y. Hou, J. R. Bading and P. S. Conti, *Molecular Imaging*, 2004, **3**, 96-104.
[205] T. Poethko, M. Schottelius, G. Thumshirn, U. Hersel, M. Herz, G. Henriksen, H. Kessler, M. Schwaiger and H-J. Wester, *J. Nucl. Med*, 2004, **45**, 892-902.
[206] M. S. Morrison, S. A. Ricketts, J. Barnett, A. Cuthbertson, J. Tessier and S. R. Wedge, *J. Nucl. Med*, 2009, **50**, 116-122.
[207] Y. S. Chang, J. M. Jeong, Y-S. Lee, H. W. Kim, G. B. Rai, S. J. Lee, D. S. Lee, J-K. Chung and M. C. Lee, *Bioconjugate Chem.*, 2005, **16**, 1329-1333.
[208] J. B. Downeer, T. J. McCarthy, W. B. Edwards, C. J. Anderson and M. J. Welsh, *Appl. Radiat. Isotopes*, 1997, 48, 907-916.
[209] W. Cai, X. Zhang, Y. Wu and X. Chen, *J. Nucl. Med*, 2006, **47**, 1172-1180.
[210] B. de Bruin, B. Kühnast, F. Hinnen, L. Yaouancq, M. Amessou, L. Johannes, A. Samson, R. Boisgard, B. Tavitian and F. Dollé, *Bioconjugate Chem.*, 2005, **16**, 406-420.
[211] B. Kühnast, F. Dollé, S. Terrazzino, B. Rousseau, C. Loc'h, F. Vaufrey, F. Hinnen, I. Doignon, F. Pillon, C. David, C. Crouzel and B. Tavitian, *Bioconjugate Chem.*, 2000, **11**, 627-636.
[212] D. P. Gablin, P. Garnier, S. J. Ward, N. J. Oldham, A. J. Fairbanks and B. G. Davis, *Org. Biomol. Chem.*, 2003, **1**, 3642-3644.
[213] O. Prante, J. Einsiedel, R. Haubner, P. Gmeiner, H-J. Wester, T. Kuwert and S. Maschauer, *Bioconjugate Chem.*, 2007, **18**, 254-262.
[214] K. Kettenbach, H. Schieferstein and T. L. *Ross, BioMed Research International*, Hindawi Publishing Corporation, London, 2014.
[215] D. Thonon, C. Kech, J. Paris, C. Lemaire and A. Luxen, *Bioconjugate Chem.*, 2009, **20**, 817-823.
[216] T. L. Ross, M. Honer, P. Y. H. Lam, T. L. Mindt, V. Groehn, R. Schibli, P. A. Schubiger and S. M. Ametamey, *Bioconjugate Chem.*, 2008, **19**, 2462-2470.
[217] S. Maschauer, J. Einsiedel, R. Haubner, C. Hocke, M. Ocker, H. Hübner, T. Kuwert, P. Gmeiner and O. Prante, *Angew. Chem. Int. Edit.*, 2010, **49**, 976-979.
[218] S. H. Hausner, R. D. Carpenter, N. Bauer and J. L. Sutcliffe, *Nucl. Med. Biol.*, 2013, **40**, 233-239.
[219] E. Saxon and C. Bertozzi, *Science*, 2000, **287**, 2007-2010.
[220] M. Pretze, D. Pietzsch and C. Mamat, *Molecules*, 2013, **18**, 8618-8665.
[221] T. L. Ross, J. Ermert, C. Hocke and H. H. Coenen, *J. Am. Chem. Soc.*, 2007, **129**, 8018-8025.
[222] F. R. Wüst and T. Kniess, *J. Labelled Compd. Rad.*, 2003, **46**, 699-713.
[223] B. Steiniger and F. R. Wüst, *J. Labelled Compd. Rad.*, 2006, **49**, 817-827.
[224] F. R. Wüst and T. Kniess, *J. Labelled Compd. Rad.*, 2004, **47**, 457-468.

[225] Y. Shai, K. L. Kirk, M. A. Channing, B. B. Dunn, M. A. Lesniak, R. C. Eastman, R. D. Finn, J. Roth and K. A. Jacobson, *Biochem.*, 1989, **28**, 4801-4806.
[226] L. Barre, L. Barbier and M. C. Lasne, *J. Labelled Compd. Rad.*, 1994, **35**, 167-168.
[227] T. Ludwig, J. Ermert and H. H. Coenen, *Nucl. Med. Biol.*, 2002, **29**, 255-262.
[228] T. L. Ross, J. Ermert and H. H. Coenen, *Molecules*, 2011, **16**, 7621-7626.
[229] T. Stoll, J. Ermert, S. Oya, H. F. Kung and H. H. Coenen, *J. Labelled Compd. Rad.*, 2004, **47**, 443-455.
[230] U. Mühlhausen, J. Ermert and H. H. Coenen, *J. Labelled Compd. Rad.*, 2009, **52**, 13-22.
[231] T. Ludwig, J. Ermert and H. H. Coenen, *J. Labelled Compd. Rad.*, 2001, **44**. S1-S3.
[232] P. J. Stang, *Angew. Chem. Int. Edit.*, 1992, **31**, 274-285.
[233] C. Willgerodt, Tageblatt der 58. Vers. deutscher Naturforscher u. Aertzte, Strassburg 1885.
[234] C. W. Perkins, J. C. Martin, A. J. Arduengo, W. Lau, A. Alegria and J. K. Kochi, *J. Am. Chem. Soc.*, 1980, **102**, 7753-7759.
[235] T. Wirth, M. Ochiai, A. Varvoglis, V. V. Zhdankin, G. F. Koser, H. Tohma and Y. Kita, *Hypervalent Iodine Chemistry*, Springer, London, 2003.
[236] C. Martin, *Science*, 1983, **221**, 509-514.
[237] D. B. Martin and J. C. Martin, *J. Org. Chem.*, 1983, **45**, 4155-4156.
[238] M. Frigerio, M. Santagostino and S. Sputore, *J. Org. Chem.*, 1999, **64**, 4537-4538.
[239] K. C. Nicolaou, D. L. F. Gray, T. Montagnon and S. T. Harrison, *Angew. Chem. Int. Edit.*, 2002, **41**, 996-1000.
[240] R. D. Richardson and T. Wirth, *Angew. Chem. Int. Edit.*, 2006, **45**, 4402-4404.
[241] O. A. Ptitsyna, G. G. Lyatiev, V. N. Krischchenko and O. A. Reutov, *B. Acad. Sci. USSR CH+.* 1967, 955.
[242] V. V. Zhdankin, C. M. Crittell, P. J. Stang and N. S. Zefirov, *Tetrahedron Lett.*, 1990, **31**, 4821-4824.
[243] N. S. Zefirov, V. V. Zhdankin and A. S. Kozmin, *B. Acad. Sci. USSR CH+.* 1983, 1682.
[244] V. V. Zhdankin, R. Tykwinski, B. L. Williamson, P. J. Stang and N. S. Zefirov, *Tetrahedron Lett.*, 1991, **32**, 733-734.
[245] V. V. Zhdankin, M. C. Scheuller and P. J. Stang, *Tetrahedron Lett.*, 1993, **34**, 6853-6856.
[246] R. M. Moriarty and O. Prakash, *Accounts Chem. Res.*, 1986, **19**, 224-250.
[247] M. Ochiai, K. Miyamoto, M. Shiro, T. Ozawa and K. Yamaguchi, *J. Am. Chem. Soc.*, 2003, **125**, 13006-13007.
[248] M. Achiai, K. Miyamoto, Y. Yokota, T. Suefugi and M. Shiro, *Angew. Chem. Int. Edit.*, 2005, **44**, 75-78.
[249] A. J. Edwards, *J. Chem. Soc., Dalton Trans.*, 1978, 1723-1725.
[250] T. Okuyama, T. Takino, T Sueda and M. Ochiai, *J. Am. Chem. Soc.*, 1995, **117**, 3360-3367.
[251] F. M. Beringer and R. A. Falk, *J. Chem. Soc.*, 1964, 4442-4445.
[252] M. Ochiai, *Topics in Current Chemistry, Hypervalent Iodine Chemistry, Reactivities, Properties and Structures*, Springer-Verlag, Berlin, 2003.
[253] V. V. Zhdankin, *Hypervalent Iodine Chemistry: Preparation, Structure, and Synthetic Applications of Polyvalent Iodine Compounds*, Wiley, Chicester, 2013.
[254] R. S. Berry, *The J. Chem. Phys.*, 1960, **32**, 933-938.
[255] K. M. Lancer and G. H. Wiegand, *J. Org. Chem.*, 1976, **41**, 3360-3364.
[256] Y. Yamada and M. Okawara, *Bull. Chem. Soc. Jpn.*, 1972, **45**, 2515-2519.
[257] M. A. Carroll, unpublished results.
[258] M. Ochiai, Y. Kitagawa and M. Toyonari, *Arkivoc*, 2003, 43-48.
[259] N. Jalalian and B. Olofsson, *Tetrahedron*, 2010, **66**, 5793-5800.
[260] M. A. Carroll, J. Nairne and J. L. Woodcraft, *J. Labelled Compd. Rad.*, 2007, **50**, 452-454.
[261] M. A. Carroll, J. Nairne, G. Smith and D. A. Widdowson, *J. Fluorine Chem.*, 2007, **128**, 127-132.
[262] F. M. Beringer and S. A. Galton, *J. Org. Chem.*, 1996, **31**, 1648-1651.
[263] D. J. Le Count and J. A. Reid, *J. Chem. Soc.*, 1967, **14**, 1298-1301.
[264] R. Gail, C. Hocke and H. H. Coenen, *J. Labelled Compd. Rad.*, 1997, **40**, 50-52.
[265] J. L. Neumeyer and J. G. Cannon, *J. Org. Chem.*, 1969, **26**, 4681-4682.
[266] A. Amor-Coarasa, J. Kelly, B. Hu, K. Nuemann, S. DiMagno and J. Babich, *J. Nucl. Med*, 2015, **56**, 1044.
[267] K. S. Mandap, T. Ido, Y. Kiyono, M. Kobayashi, T. G. Lohith, T. Mori, S. Kasamatsu, T. Kudo, H. Okazawa and Y. Fujibayashi, *Nucl. Med. Biol.*, 2009, **36**, 406-409.
[268] C. H. Oh, J. S. Kim and H. H. Jung, *J. Org. Chem.*, 1999, **64**, 1338-1340.
[269] M. Zhu, Y. Song and Y. Cao, *Synthesis*, 2007, 853-856.

[270] Z. Xue, D. Yang and C. Wang, *J. Orgmet. Chem.*, 2006, **261**, 247-250.
[271] F. M. Beringer, P. S. Forigione and M. D. Yudis, *Tetrahedron*, 1960, **8**, 49-63
[272] M. A. Carroll, and R. A. Wood, *Tetrahedron*, 2007, **63**, 11349-11354.
[273] J. R. Crowder, E. E. Glover, M. F. Grundon and H. X. Kaempfen, *J. Chem. Soc. (Resumed)*, 1963, 4578-4585.
[274] S-K. Kang, S-H. Lee and D. Lee, *Synlett*, 2000, 1022-1024.
[275] M. Zhu, Z. Zhou and R. Chen, *Synthesis*, 2008, 2680-2683.
[276] Y. Zhang, J. Han and Z-J. Liu, *RSC Adv.*, 2015, **5**, 25485-25488.
[277] R. J. Phipps and M. J. Gaunt, *Science*, 2009, **323**, 1593-1597.
[278] T. Kitamura, Z. Meng and Y. Fujiwara, *Tetrahedron Lett.*, 2000, **41**, 6611-6614.
[279] P. J. Stang and V. V. Zhdankin, *J. Am. Chem. Soc.*, 1993, **115**, 9808-9809.
[280] Y. Toba, *J. Photopolym. Sci. Tech.* , 2003, **16**, 115-118.
[281] J. V. Crivello, *J. Polym. Sci. A. Polym. Chem.*, 2009, **47**, 866-875.
[282] M. S. Yusubov, A. V. Maskaev and V. V. Zhdankin, *Arkivoc*, 2011, (i), 364-396.
[283] M. S. Yusubov, R. Y. Yusubova, V. N. Nemykin and V. V. Zhdankin, *J. Org. Chem.*, 2013, **78**, 3767-3773.
[284] M. S. Yusubov, G. A. Zholobova, I. L. Filimonova and K-W. Chi, *Russ. Chem. B+*, 2004, **53**, 1735-1742.
[285] P. Kazmierczak, L. Skulski and L. Kraszkiewicz, *Molecules*, 2001, **6**, 881-891.
[286] M. Iinuma, K. Moriyama and H. Togo, *Synlett*, 2012, **23**, 2663-2666.
[287] A. McKillop and D. Kemp, *Tetrahedron*, 1989, **45**, 3299-3306.
[288] T. Kitamura, K. Nagata and H. Taniguchi, *Tetrahedron Lett.*, 1995, **36**, 1081-1084.
[289] H. J. Lucas and E. R. *Org. Synth.*, 1942, **22**, 52-53.
[290] T. Dohi, M. Ito, K. Morimoto, Y. Minamitsuji, N. Takenaga and Y. Kita, *Chem. Commun.*, 2007, **40**, 4152-4154.
[291] M. A. Carroll, V. W. Pike and D. A. Widdowson, *Tetrahedron Lett.*, 2000, **41**, 5393-5396.
[292] G. F. Koser and R. H. Wettach, *J. Org. Chem.*, 1980, **45**, 1542-1543.
[293] M-R. Zhang, K. Kumata and K. Suzuki, *Tetrahedron Lett.*, 2007, **48**, 8632-8635.
[294] F. M. Beringer and R. A. Nathan, *J. Org. Chem.*, 1969, **34**, 685-689.
[295] F. M. Beringer, P. Ganis, G. Avitabile and H. Jaffe, *J. Org. Chem.*, 1972, **37**, 879.
[296] F. M. Beringer, R. A. Falk, M. Karniol, I. Lillien, G. Masulio, M. Mausner and E. Sommer, *J. Am. Chem. Soc.*, 1959, **81**, 342-351.
[297] P. J. Stang, V. V. Zhdankin, R. Tykwinski and N. S. Zefirov, *Tetrahedron Lett.*, 1991, **32**, 7497-7498.
[298] P. P. Onys'ko, T. V. Kim, O. I. Kiseleva, Y. V. Rassukana and A. A. Gakh, *J. Fluorine Chem.*, 2009, **130**, 501-504.
[299] W. Tyrra, H. Butler and D. Naumann, *J. Fluorine Chem.*, 1993, **60**, 79-83.
[300] M. D. Hossain, Y. Ikegami and T. Kitamura, *J. Org. Chem.*, 2006, **71**, 9903-9905.
[301] M. Bielawski, M. Zhu and B. Olofsson, *Adv. Synth. Cat.*, 2007, **349**, 2610-2618.
[302] J. V. Crivello and J. H. W. Lam, *J. Org. Chem.*, 1978, **43**, 3055-3058.
[303] M. Bielawski, D. Aili and B. Olofsson, *J. Org. Chem.*, 2008, **73**, 4602-4607.
[304] M. J. Peacock and D. Pletcher, *Tetrahedron Lett.*, 2000, **41**, 8995-8998.
[305] E. A. Merritt, J. Malmgren, F. J. Klinke and B. Olofsson, *Synlett*, 2009, 2277-2280.
[306] A. McKillop and W. R. Sanderson, *Tetrahedron*, 1995, **51**, 6145-6166.
[307] M. A. A. F. deC. T. Carrondo and A. C. Skapski, *Adv Crystallogr. Sect. A*, 1978, **34**, 3551-3554.
[308] L. F. Silva Jr, R. S. Vasconcelos and N. P. Lopes, *Int. J. Mass. Spectrom.*, 2008, **276**, 24-30.
[309] http://www.asynt.com/product-category/chemistry/controlled-lab-reactors/ Accessed 12/07/15
[310] X.-F. Wu, H. Neumann and M. Beller, *Chem. Rev.* (Washington, DC, U. S.), 2012, **113**, 1-35.
[311] J. K. Stille, *Angew. Chem., Int. Ed.*, 1986, **25**, 508-524.
[312] www.sigmaaldrich.com/catalog/substance/4iodophenol2200154038511?lang=en&region Accessed 09/11/15
[313] www.sigmaaldrich.com/catalog/search?term=4-bromophenol&interface=All&N=0&mode=match%20partialmax&lang=en&region=GB&focus=product Accessed 09/11/15
[314] P. K. Mandal, J. S. McMurray, *J. Org. Chem.*, **2007**, *72*, 6599-6601.
[315] B. P. Bandgar, L. S. Uppalla, A. D. Sagar and V. S. Sadavarte, *Tetrahedron Lett.*, 2001, **42**, 1163-1165.
[316] H. Azizian, C. Eaborn and A. Pidcock, *J. Orgmet. Chem.*, 1981, **215**, 49-58.
[317] T. Furuya, A. E. Strom and T. Ritter, *J. Am. Chem. Soc.*, 2009, **131**, 1662-1663.

[318] C. Gosmini and J. Périchon, *Org. Biomol. Chem.*, 2005, **3**, 216-217.
[319] I. Kazmierski, C. Gosmini, J. –M. Paris and J. Périchon, *Tett. Lett.*, 2003, **44**, 6417-6420.
[320] H. Fillon, C. Gosmini and J. Périchon, *J. Am. Chem. Soc.*, 2003, **125**, 3867-3870.
[321] A. Shah, V. W. Pike and D. A. Widdowson, *J. Chem. Soc., Perkin Trans. 1*, 1997, 2463-2465.
[322] M. Ochiai, *Top. Curr. Chem.,* 2003, **224**, 5-68.
[323] S. Martin-Santamaria, M. A. Carroll, C. M. Carroll, C. D. Carter, V. W. Pike, H. S. Rzepa and D. A. Widdowson, *Chem. Commun. (Cambridge, U. K.)*, 2000, 649-650.
[324] A. Shah, V. W. Pike and D. A. Widdowson, *J. Chem. Soc., Perkin Trans. 1*, 1998, 2043-2046.
[325] R. T. VanVleck, *J. Am. Chem. Soc.*, 1949, **71**, 3256-3257.
[326] Y. Wan, M. Alterman, M. Larhed and A. Hallberg, *J. Org. Chem.*, 2002, **67**, 6232-6235.
[327] M. Ladlow, Presentation on behalf of Uniqsis, 2013.
[328] K. S. Elvira, X. Casadevall I Solvas, R. C. R. Wootton and A. J. deMello, *Nat. Chem.*, 2013, **5**, 905-915.
[329] C. Rensch, A. Jackson, S. Lindner, R. Salvamoser, V. Samper, S. Riese, P. Bartenstein, C. Wängler and B. Wängler, *Molecules*, 2013, **18**, 7930-7956.
[330] G. Pascali, P. Watts and P. A. Salvadori, *Nucl. Med. Biol.*, 2013, **40**, 776-787.
[331] http://www.ezag.com/home/products/radiopharma/radiosynthesis-technology/modular-lab-standard.html Accessed 10/12/15
[332] A. Lebedev, R. Miraghaie, K. Kotta, C. E. Ball, J. Zhang, M. S. Buchsbaum, H. C. Kolb and A. Elizarov, *Lab. Chip.*, 2013, **13**, 136-145.
[333] M. Kroselj, A. Socan, K. Zaletel, T. Dreger, R. Knopp, T. Gmeiner and P. Kolenc Peitl, *Nucl. Med. Commun.,* 2016, **37**, 207-214.
[334] C. C. Lee, G. Sui, A. Elizarov, C. J. Shu, Y. S. Shin, A. N. Dooley, J. Huang, A. Daridon, P. yatt, D. Stout, H. C. Kolb, O. N. Witte, N. Satyamurthy, J. R. Heath, M. E. Phelps, S. R. Quake and H. R. Tseng, *Science*, 2005, **310**, 1793-1796.
[335] H. Audrain, *Angew. Chem. Int. Ed*, 2007, **46**, 1772-1775.
[336] C. Rensch, S. Lindner, R. Salvamoser, S. Leidner, C. Böld, V. Samper, D. Taylor, M. Baller, S. Riese, P. Bartenstein, C. Wängler and B. Wängler, *Lab. Chip.*, 2014, **14**, 2556-2564.
[337] J. N. Lee, C. Park and G. M. Whitesides, *Anal. Chem.*, 2003, **75**, 6544-6554.
[338] http://www.advion.com/products/nanotek/nanotek-liquid-flow-reactor/ Accessed 17/12/15
[339] *Microfluidic based microsystems*, ed. S. Kakaç, B. Kosoy, D. Li and A. Prumuanjaroenkil, Springer, Dordrecht, 2009.
[340] Y. Kikutani and T. Kitamori, *Macromol. Rapid Commun.*, 2004, **25**, 158-168.
[341] http://www.uniqsis.com/paProductsDetail.aspx?ID=ACC_MIX Accessed 18/12/15
[342] C. -Y. Lee, C. -L. Chang, Y. -N. Wang and L. -M. Fu, *Int. J. Mol. Sci.*, 2011, **12**, 3265-3287.
[343] http://www.advion.com/products/nanotek/ Accessed 19/12/15
[344] T. Collier, D. Yokell, P. Rive, R. Jackson, T. Shoup, M. Normandin, T. Brady, G. El Fakhri, S. Liang and N. Vasdev, *J. Nucl. Med.*, 2014, **55**, 1246.
[345] S. H. Liang, D. L. Yokell, R. N. Jackson, P. A. Rice, R. Callahan, K. A. Johnson, D. Alagille, G. Tamagnan, T. L. Collier and N. Vasadev, *Med. Chem. Comm.*, 2014, **5**, 432-435.
[346] A. Lebedev, R. Miraghaie, K. Kotta, C. E. Ball, J. Zhang, M. S. Buchsbaum, H. C. Kolb and A. Elizarov, *Lab Chip*, 2013, **13**, 136-145.
[347] M. A. Carroll, C. Jones and S.-L. Tang, *J. Labelled Compd. Radiopharm.*, 2007, **50**, 450-451.
[348] http://www.waters.com/waters/partDetail.htm?partNumber=WAT020545&locale=en_GB Accessed 20/12/15
[349] M. A. Carroll, G. G. Launay, C. D. Reed and S. J. Hobson, *J. Labelled Compd. Radiopharm.*, 2011, **54**, S554.
[350] R. Chirakal, G. J. Schrobilgen, G. Firnau and S. Garnett, *Appl. Radiat. Isot.*, 1991, **42**, 113-119.
[351] V. M. Lopez, C. L. Decatur, W. D. Stamer, R. M. Lynch and B. S. McKay, *PLoS Biol.*, 2008, **6**, 1861-1869.
[352] C. Nahmias, L. M. Wahl, S. Amano, M. –C. Asselin and R. Chirakal, *J. Nucl. Med.*, 2000, **41**, 1636-1641.
[353] J. T. Konkel, J. Fan, B. Jayachandran and K. L. Kirk, *J. Fluorine Chem.*, 2002, **115**, 27-32.
[354] M. Namavari, N. Satyamurthy and J. R. Barrio, *J. Labelled Compd. Radiopharm.*, 1995, **36**, 825-833.
[355] F. Claudi, M. Cardellini, G.M. Cingolani, A. Piergentili, G. Peruzzi and W. Baldinu, *J. Med. Chem.*, 1990, **33**, 2408-2412.
[356] M. Namavari, N. Satyamurthy and J. R. Barrio, *J. Fluorine Chem.*, 1995, **74**, 113-121.
[357] Y. –Z. Zu and C. Chen, *J. Labelled Compd. Radiopharm.*, 2006, **49**, 1187-1200.

[358] L. Henry, *C. R. Hebd. Seances Acad. Sci.*, 1895, **120**, 1265.
[359] P. Jakubec, D. M. Cockfield, P. S. Hynes, E. Cleator and D. J. Dixon, *Tetrahedron: Asymmetry*, 2011, **22**, 1147-1155.
[360] T. W. Green, P. G. M. Wuts, *Protective Groups in Org. Synth.*, Wiley-Interscience, New York, 1999, 564-566.
[361] E. W. Dean and D. D. Stark, *Ind. Eng. Chem.*, 1920, **12**, 486-490.
[362] R. N. Krasikova, *Current Organic Chemistry*, 2013, **17**, 2097-2107.
[363] https://clients.crfmanager.com/CRIC/Content.aspx?name=Home&type=Content&areaid=10001&oid=1 Accessed 22/12/15
[364] http://www3.gehealthcare.com/en/products/categories/pet-radiopharmacy/tracer_center_equipment/tracerlab_fx2_n Accessed 23/12/15
[365] http://www3.gehealthcare.com/en/products/categories/pet-radiopharmacy/tracer_center_equipment/fastlab Accessed 23/12/15
[366] F. Füchtner and J. Steinbach, *Appl. Radiat. Isot.*, 2003, **58**, 575-578.
[367] '*Global Nuclear Imaging Market - Growth, Trends And Forecasts (2014 - 2019)*' http://www.researchandmarkets.com/research/6n89sg/global_nuclear Accessed 12/09/15
[368] T. Simuni and H. Hurtig, *Parkinson's Disease: Diagnosis and Clinical Management*, Ed. S. A. Factor and W. J. Weiner, Demos Medical Publishing (Google eBook), 2008.
[369] Y. Hiroshima, H. Miyamoto, J. Nakamura, D. Masukawa, T. Yamamoto, H. Muraoka, M. Kamiya, N. Yamashita, T. Suzuki, S. Matsuzaki, J. Endo and Y. Goshima, *Br. J. Pharmacol*. 2014, **171**, 403-414.
[370] J. P. Seibyl, W. Chen and D. H. S. Silverman, *Semin. Nucl. Med.*, 2007, **37**, 440-450.
[371] A. Becherer, M. Szabó, G. Karanikas, P. Wunderbaldinger, P. Angelberger, M. Raderer, A. Kurtaran, R. Dudczak and K. Kletter, *J. Nucl. Med.*, 2004, **45**, 1161-1167.
[372] F. Imani, V. G. Agopian, M. S. Auerbach, M. A. Walter, F. Imani, M. R. Benz, R. A. Dumont, C. K. Lai, J. G. Czermin and M. W. Yeh, *J. Nucl. Med.*, 2009, **50**, 513-519.
[373] P. L. Jager, R. Chirakal, C. J. Marriott, A. H. Brouwers, K. P. Koopmans and K. Y. Gulenchyn, *J. Nucl. Med.*, 2008, **49**, 573-586.
[374] W. Chen, D. H. S. Silverman, S. Delaloye, J. Czernin, N. Kamdar, W. Pope, N. Satyamurthy, C. Schiepers and T. Cloughesy, *J. Nucl. Med.*, 2006, **47**, 904-911.
[375] H. Minn, S. Kauhanen, M. Seppänen and P. Nuutila, *J. Nucl. Med.*, 2009, **50**, 1915-1918.
[376] A. Luxen, M. Guillaume, W. P. Melega, V. W. Pike, O. Solin and R. Wagner, *Nucl. Med. Biol.*, 1992, **19**, 149-158.
[377] G. Firnau, R. Chirakal and E. S. Garnett, *J. Nucl. Med.*, 1984, **25**, 1228-1233.
[378] M. Diksic and S. Farrokhzad, *J. Nucl. Med.*, 1985, **26**, 1314-1318.
[379] S. Forsback, O. Eskola, J. Bergman, M. Haaparanta and O. Solin, *J. Labelled Comp. Radiopharm.*, 2009, **52**, 286-288.
[380] M. Namavari, A. Bishop, N. Satyamurthy and J. R. Barrio, *Appl. Radiat. Isot.*, 1992, **43**, 989-996.
[381] A. Luxen, M. Perlmutter, G. T. Bida, G. Van Moffaert, J. S. Cook, N. Satyamurthy, M. E. Phelps and J. R. Barrio, *Appl. Radiat. Isot.*, 1990, **41**, 275-281.
[382] E. M. Wagner, J. Ermert and H. H. Coenen, *J. Nucl. Med.*, 2009, **50**, 1724-1729.
[383] C. Lemaire, M. Guillaume, R. Cantineau, A. Plenevaux and L. Christiaens, *Appl. Radiat. Isot.*, 1991, **42**, 629-635,
[384] A. Horti, D. E. Redmond Jr. and R. Soufer, *J. Labelled. Comp. Radiopharm.*, 1995, **36**, 409-423.
[385] S. Guillouet, C. Lemaire, G. Bonmarchand, L. Zimmer and D. le Bars, *J. Labelled Comp. Radiopharm.*, 2001, **44**, S868-S870.
[386] L. Zhang, G. Tang, D. Yin. X. Tang and Y. Wang, *Appl. Radiat. Isot.*, 2002, **57**, 145-151.
[387] B. Shen, W. Ehrlichmann, M. Uebele, H. –J. Machulla and G. Reischl, *Appl. Radiat. Isot.*, 2009, **67**, 1650-1653.
[388] M. Pretze, C. Wängler and B. Wängler*, BioMed Research International*, Hindawi Publishing Corporation, London, 2014.
[389] S. Kaneko, K. Ishiwata, K. Hatano, H. Omura, K. Ito and M. Senda, *Appl. Radiat. Isot.*, 1999, **50**, 1025-1032.
[390] L. C. Libert, X. Franci, A. R. Plenevaux, T. Ooi, K. Maruoka, A. J. Luxen and C. F. Lemaire, *J. Nucl. Med.*, 2013, **54**, 1154-1161.
[391] http://www.trasis.com/download/F-Dopa_as_easy_as_FDG.pdf Accessed 02/01/16
[392] http://www.neptis-vsa.com/?s=fdopa Accessed 02/01/16
[393] *EU PAT.*, WO2003002489A2, 2003
[394] M. Tredwell, S. M. Preshlock, N. J. Taylor, S. Gruber, M. Huiban, J. Passchier, J. Mercier, C. Génicot and V. Gouverneur, *Angew. Chem. Int. Ed.*, 2014, **53**, 7751-7755.

[395] *EU PAT.*, WO2010117435, 2010
[396] N. Achiishi, A. F. Brooks, J. J. Topczewski, M. E. Rodneck, M. S. Sanford and P. J. H. Scott, *Org. Lett.*, 2014, **16**, 3224-3227.
[397] G. Firnau, S. Sood, R. Pantel and S. Garnett, *Mol. Pharmacol.*, 1981, **19**, 130-133.
[398] http://www3.gehealthcare.com/en/Products/Categories/PET-Radiopharmacy/TRACER_Center_Equipment/FastLab#tabs/tabB30E1CCCF0CD4BF3AC19CDF535C4AD87 Accessed 20/12/15
[399] http://abt-mi.com/en/assets/pdfs/White%20Paper%20-%20BG75%201.0%20Enhanced%20GMP%20-%20FDG.pdf Accessed 20/12/15
[400] http://www.cemag.us/articles/2014/03/understanding-cleanroom-classifications Accessed 20/12/15
[401] D. S. Goldsteain, G. Eisenhofer, B. D. Dunn, I. Armando, J. Lenders, E. Grossman, C. Holmes, K. L. Kirk, S. Bacharach, R. Adams, P. Herscovitch and I. J. Kopin, *J. Am. Coll. Cardiol.*, 1993, **22**, 1961-1971.
[402] K. Pacak, G. Eisenhofer, J. A. Carrasquillo, C. C. Chem, S. –T. Li and D. S. Goldstein, *Hypertension*, 2001, **38**, 3-6.
[403] M. Hadi, C. C. Chen, M. Whatley, K. Pacak and J. A. Carrasquillo, *J. Nucl. Med.*, 2007, **48**, 1077-1083.
[404] R. D. Tilve, V. M. Alexander and B. M. Khadilkar, *Tetrahedron Lett.*, 2002, **43**, 9457-9459.
[405] I. S. R. Stenhagen, A. K. Kirjavainen, S. J. Forsback, C. G. Jôrgensen, E. G. Robin, S. K. Luthra, O. SOlin and V. Gouverneur, *Chem. Commun.*, 2013, **49**, 1386-1388.
[406] J. Ruiz, Ardeo, R. Ignacio, N. Sotomayor and E. Lete, *Tetrahedron*, 2005, **61**, 3311-3324.
[407] T. S. Sheppard, *Org. Biomol. Chem.*, 2009, **7**, 1043-1052.
[408] S. Kirschbaum and H. Waldmann, *J. Org. Chem.*, 1998, **63**, 4936-4846.
[409] R. Edwards, A. D. Westwell, S. Daniels and T. Wirth, *Eur. J. Org. Chem.*, 2015, 625-630.
[410] R. J. Errington, *Advanced Practical Inorganic and Metal Organic Chemistry*, Blackie Academic and Professional, London, 1997.
[411] H.Togo, T. Nabana and K. Yamaguchi, *J. Org. Chem.*, 2000, **65**, 8391-8394.
[412] J. E. Leffler and L. J. Story, *J. Am. Chem. Soc.*, 1967, **89**, 2333-2338.
[413] F. B. Kipping and J. J. Wren, *J. Chem. Soc.*, 1957, 3246-3250.
[414] J. Nithyanandhan and N. Jayaraman, *Tetrahedron*, 2005, **61**, 11184-11191.
[415] S. R. Bull, L. C. Palmer, N. J. Fry, M. A. Greenfield, B. W. Messmore, T. J. Meade and S. I. Stupp, *J. Am. Chem. Soc.*, 2008, **130**, 2742-2743.
[416] N. Ichiishi, A. J. Canty, B. F. Yates and M. S. Sanford, *Org. Lett.*, 2013, **15**, 5134-5137.
[417] V. Gulldand, J. Chem. Soc., 1929, 1798-1801.
[418] J. Selvakumar, A. Makriyannis and C. R. Ramanathan, *Org. Miomol. Chem.*, 2010, **8**, 4056-4058.
[419] I. Osante, E. Lete and N. Sotomayor, *Tetrahedron Lett.*, 2004, **45**, 1253-1256.
[420] A. R. Mazzotti, M. G. Campbell, P. Tang, J. M. Murphy and T. Ritter, *J. Am. Chem. Soc.*, 2013, **135**, 14012-14015.
[421] T. D. Tilve, V. M. Alexander and B. M. Khadilkar, *Tetrahedron Lett.*, 2002, **43**, 9457-9459.
[422] F. Brown, J. M. A. De Bruyne and P. Gross, *J. Am. Chem. Soc.*, 1934, **56**, 1291-1293.
[423] F. B. Kipping and J. J. Wren, *J. Chem. Soc.*, 1957, 3246-3250.